JPL Publication 09-X

2008 Exoplanet Forum Report

Edited by:

P. R. Lawson, W. A. Traub and S. C. Unwin

DRAFT

National Aeronautics and
Space Administration

Jet Propulsion Laboratory
California Institute of Technology
Pasadena, California

Draft: 31 July 2008

DRAFT

This research was carried out at the Jet Propulsion Laboratory, California Institute of Technology, under a contract with the National Aeronautics and Space Administration.

Reference herein to any specific commercial product, process, or service by trade name, trademark, manufacturer, or otherwise, does not constitute or imply its endorsement by the United States Government or the Jet Propulsion Laboratory, California Institute of Technology.

Abstract

The 2008 Exoplanet Forum was organized to provide input to the Exoplanet Exploration Program from the astronomical community primarily for the purpose of technology planning. The goal was to provide long-term planning in a way that is consistent with the Exoplanet Task Force Report, and provide information to the Decadal Survey review committees that will allow them to make informed recommendations – particularly concerning technology development and technology readiness of proposed exoplanet missions.

For the 2008 Forum Meeting, groups that shared an interest in the same technology were be asked to collaborate on written contributions to the Forum. As part of their input the different groups were asked to provide 1) a list of milestones leading to technology maturity of a flagship mission; 2) a list of enabled science with current technology, and with each future milestone – leading through small and/or medium missions on to flagship missions

DRAFT

Approvals

Released by:
JPL

_____ ____

Peter R. Lawson date
Science Architect,
Exoplanet Exploration Program

Approved by:
JPL

_____ ____

Wesley A. Traub date
Chief Scientist,
Exoplanet Exploration Program

Approved by:
NASA HQ

_____ ___

Lia LaPiana date
Program Executive,
Exoplanet Exploration Program

Approved by:
JPL

_____ ___

Michael Devirian date
Manager,
Exoplanet Exploration Program

Approved by:
NASA HQ

_____ ___

Douglas Hudgins date
Program Scientist,
Exoplanet Exploration Program

Approved by:
JPL

_____ ____

Jakob van Zyl date
Director, JPL Astronomy & Physics Directorate

Approved by:
NASA HQ

_____ ___

Jon Morse date
Director,
Astronomy and Physics Division

DRAFT

Contents

ABSTRACT ..... **III**

APPROVALS ..... **V**

CONTENTS ..... **VI**

PREFACE ..... **XI**

1 EXECUTIVE SUMMARY **1**

1.1 INTRODUCTION 1
1.2 THE STATE OF EXOPLANET SCIENCE 1
1.3 PURPOSE OF THE REPORT 1
1.4 NASA'S PLANS AND CONSTRAINTS 2
1.4.1 Probe Mission Line *2*
1.4.2 Flagship Missions *2*
1.5 COMMUNITY STRATEGY 2
1.6 SUMMARY OF CHAPTER RECOMMENDATIONS 2
1.6.1 Astrometry *2*
1.6.2 Direct Optical Detection of Exoplanets *2*
Main Exoplanet Science Contribution 2
How Does Optical Imaging Complement With Other Techniques? 3
Main Technical Challenges 3
1.6.3 Direct Detection of Exoplanets with Infrared Interferometry *4*
1.6.4 Microlensing *6*
1.6.5 Radial Velocity *7*
1.6.6 Transits *8*

2 ASTROMETRY **9**

2.1 INTRODUCTION 9
2.1.1 A Micro-arcsecond Astrometry Mission *9*
Science Goals 10
Support for Micro-arcsecond Astrometry Science Other Than Exoplanets 10
Detecting and Characterizing Low Mass Planets 11
Operate as a Precurser Mission for a Future Direct Imaging Program 12
Multiplanet Systems and Planetary System Architecture 13
Micro-arcsecond Astrometry in the Context of Other Exoplanet Programs 15
Science Requirements 15
Planet Finding 15
Other Areas of Astrophysics 16
2.1.2 Other Strongly Supported Recommendations *16*
Science Goals 16
Theory 16
The Impact of Gaia 16
Detecting Large Numbers of Giant Planets 17
Lifting the Mass/Inclination Ambiguity for RV-Identified Exoplanets 19
2.1.3 Recommendations Addressed by the ExoPTF with Mixed or Ambivalent Support *19*
Astrometry at Radio Wavelengths 19
Basic Properties of Stars in Support of Exoplanet Science 20

DRAFT

Demonstrating Technology Shared With Future Imaging Missions 20
Space Astrometry Support For Microlensing 20
Astrometry with a Large-Aperture, Wide-Field Camera in Space 20
2.2 OBSERVATORY CONCEPT. 22
2.2.1 Architecture 22
SIM PlanetQuest 23
SIM-Lite 23
Planet Hunter 23
2.2.2 Performance 24
2.3 TECHNOLOGY 25
2.3.1 Past Accomplishments 25
Background 25
Previous Interferometric Astrometry Programs 26
The Hubble Space Telescope Fine Guidance Sensors (FGS) 26
The Palomar Testbed Interferometer (PTI; Colavita et al 1999) 26
The Space Interferometry Technology Development Program 28
Engineering Milestones 29
2.3.2 Future Milestones 31
Completion of Engineering Milestones 6-9 31
Developing Hardware and Software into Flight Qualifiable Components 31
Flight Software Development 31
Combining Science Payload and Spacecraft 31
Double-Blind Test of Planet Finding Capability 31
Analysis of SIM-Lite's Astrometric Capabilities 32
Completion of the PlanetHunter Strategic Mission Concept 32
Selection of Mission Concept to be Deployed 32
2.4 RESEARCH AND ANALYSIS GOALS 32
2.4.1 R&A in 2010-2020 32
2.4.2 Astrometry Beyond 2020 33
2.5 CONTRIBUTORS 34
2.6 REFERENCES 35

3 DIRECT OPTICAL IMAGING OF EXOPLANETS 39

3.1 INTRODUCTION 39
3.1.1 Science Goals and Requirements 40
Flagship-scale goals 40
Flagship-scale requirements 41
Probe-scale goals 43
Probe-scale requirements 46
3.2 OBSERVATORY CONCEPTS 47
3.2.1 Architecture scaling for internal coronagraphs 47
Ground-based telescopes 47
Suborbital environments 48
Probe-size missions 49
Flagship-size missions 49
3.2.2 Architecture scaling for external and hybrid concepts 50
External Occulters 50
Hybrid systems 51
3.2.3 Performance scaling 51
Ground-based and space parameter space 51
Scaling of exozodiacal sensitivity 52
Scaling of flight system requirements and technical maturity 54
3.2.4 Cost and risk drivers 54
3.3 TECHNOLOGY 56
3.3.1 Internal coronagraph technology 57
Coronagraph concepts 57
Optical diffraction modeling and laboratory demonstration 57
Deformable mirrors 59

DRAFT

Wavefront sensing and control algorithms 60
Coronagraph optics manufacturing 61
3.3.2 External Occulter technology 63
Optical diffraction modeling and laboratory demonstration 63
Occulter system maturation 64
Deployment 65
Formation Flying & Pointing control subsystem 66
Precision edge and scattered sun light 67
Integrated optical mechanical and thermal analysis 67
Micrometeoroids 67
Propulsion systems 68
3.3.3 Common technology 68
Telescope and mirror technology 68
Detectors 70
Precision thermal control and analysis 71
Isolation systems 71
Verification and Validation 72
3.4 RESEARCH AND ANALYSIS GOALS 72
3.5 CONTRIBUTORS 73
3.6 REFERENCES 75

4 DIRECT DETECTION OF EXOPLANETS WITH INFRARED INTERFEROMETRY 79

4.1 INTRODUCTION 79
4.1.1 Science Goals 79
4.1.2 Science Requirements 81
Planetary Detection and Characterization 81
Biomarkers and biosignatures 83
4.2 OBSERVATORY CONCEPTS 85
4.2.1 Structurally-Connected Interferometer Mission Concept 86
4.2.2 Performance 90
4.2.3 Free Flying Interferometer Concept 91
4.2.4 Performance 92
4.3 TECHNOLOGY 93
4.3.1 Accomplishments from 2000-present 93
Component and Subsystem Technology* 93
Mid-IR Spatial Filters 93
Adaptive Nulling and Achromatic Phase Shifters 94
Cryocoolers 95
Cryogenic delay lines 96
Thermal shields 96
Detector Technology 97
Integrated Modeling 98
Formation Flying Technology 98
Thrusters 98
Formation Control Testbed 99
Starlight Suppression through Nulling Interferometry 100
Planet Detection Testbed 103
4.3.2 Future Milestones 104
Small Structurally Connected Interferometer 104
Flagship Mission 105
Demonstration of Planet Detection with Chopping and Averaging (TRL 4/5) 106
Demonstration of Broadband Systematic Noise Suppression (TRL 4/5) 106
Single-Mode Filters, 6-20 microns, Demonstrated in a Cryogenic Vacuum (TRL 5) 106
Cryogenic Mid-IR Adaptive Nuller (TRL 5) 107
Planet Detection Demonstration in a Flight-like Environment (TRL 6) 107
Guidance, Navigation, & Control: Collision Avoidance, Fault Detection (TRL 5) 107
In-flight Testing of Formation Algorithms (TRL 6) 107
4.4 RESEARCH AND ANALYSIS GOALS 108
4.4.1 Ground-based Interferometry 108

DRAFT

4.4.2 Theory support *108*
4.4.3 Space-based Interferometry *109*
4.4.4 Agency Coordination and Programmatic Syngergies *109*
4.4.5 International Cooperation, Collaboration, & Partnership *109*
4.5 CONTRIBUTORS 109
4.6 REFERENCES 110

5 EXOZODIACAL DISK CHARACTERIZATION 113

5.1 INTRODUCTION 113
5.1.1 Properties of Protoplanetary and Exozodiacal Disks *114*
5.1.2 Terrestrial Planet Formation and Delivery of Volatiles *115*
5.1.3 Science Goals *116*
Obtain a better understanding of planet formation as a generic and robust process 116
Characterize the exozodiacal dust around targets for direct imaging of exoplanets 116
Use disk structure to infer the presence of unseen planets 117
5.1.4 Science Requirements for Observations of Terrestrial Planets *117*
Impact on an Optical Mission 117
Impact on an IR interferometer mission 118
5.2 CURRENT STATE OF THE FIELD 120
5.2.1 Photometry *120*
5.2.2 Disk Imaging *120*
Spitzer 121
Nulling Interferometry 121
Scattered Light Imaging 121
NIR Interferometery 124
5.2.3 Spectroscopy of Dust and Gas *125*
5.2.4 Theory and Modeling *126*
Modeling Observed Debris Disks and the Origins of Planetesimal Belts 126
Predictions for Exozodiacal Disks 127
5.3 TECHNOLOGY DEVELOPMENT AND PERFORMANCE DEMONSTRATION 130
5.3.1 Past Accomplishments *130*
5.3.2 Performance *131*
Keck Interferometer 131
LBTI 132
5.3.3 Future Developments and Milestones *133*
LBTI Milestones 133
Theory Development 134
Extremely Large Telescopes 134
A TPF Precursor Mission for Exozodiacal Dust 134
5.4 RESEARCH AND ANALYSIS GOALS 135
5.5 CONTRIBUTORS 136
5.6 REFERENCES 137

6 MICROLENSING 141

6.1 INTRODUCTION 141
6.1.1 How Microlensing Finds Planets. *142*
6.1.2 Science Goals *145*
6.1.3 Science Requirements *146*
6.2 OBSERVATORY CONCEPT 148
6.2.1 Architectures *148*
Next-Generation Ground-based Network. 148
Space-Based Microlensing Mission. 149
6.2.2 Performance *153*
Ground-based Next-Generation Network. 153
Space-based Mission: 154
Effects of Descopes on Expected Performance 156
6.3 TECHNOLOGY 156

DRAFT

6.3.1 Future Milestones *157*
6.4 RESEARCH AND ANALYSIS GOALS 158
6.4.1 Detailed Predictions for a Next-Generation Ground-based Survey *158*
6.4.2 Selection of Candidate Fields for Future Surveys *158*
6.4.3 Detailed Trade Study for a Joint Dark Energy/Microlensing Mission *158*
6.5 CONTRIBUTORS 159
6.6 REFERENCES 159

7 RADIAL VELOCITY 161

7.1 INTRODUCTION 161
7.1.1 Relevance to Space Missions *162*
7.1.2 Science Goals *165*
7.1.3 Science Requirements *166*
7.2 OBSERVATORY CONCEPTS 167
7.2.1 Architecture and Performance *168*
7.3 TECHNOLOGY 171
7.3.1 Past Accomplishments *171*
7.3.2 Future Milestones *173*
7.4 RESEARCH AND ANALYSIS GOALS 175
7.5 CONTRIBUTORS 175
7.6 REFERENCES 176

8 TRANSITS 179

8.1 INTRODUCTION 179
8.1.1 Science Enabled by Transits *180*
8.1.2 Measurement Requirements *181*
8.2 OBSERVATORY CONCEPTS 183
Performance *187*
8.3 TECHNOLOGY 189
8.4 RESEARCH AND ANALYSIS GOALS 191
8.5 CONTRIBUTORS 191
8.6 REFERENCES 191

9 MAGNETOSPHERIC EMISSION 195

9.1 INTRODUCTION 195
9.1.1 Science Goals *195*
Planetary Magnetospheric Emission 195
Magnetic Fields and Planetary Characterization 198
9.1.2 Science Requirements *199*
9.2 OBSERVATORY CONCEPT 200
9.2.1 Architecture *200*
9.2.2 Performance *201*
9.3 TECHNOLOGY 203
9.3.1 Past Accomplishments *203*
9.3.2 Future Milestones *203*
Future Ground-based Telescopes 203
Future Space Facilities 204
9.4 CONTRIBUTORS 205
9.5 REFERENCES 205

DRAFT

Preface

Our understanding of planetary systems has undergone a profound shift since 1995 when the first exoplanets were discovered. The field has been transformed from one in which extrapolation from our own Solar System has been replaced by the empirical wealth of over 300 exoplanets. The sheer variety of giant planets and planetary systems—including planets orbiting very close to the stars or on highly elliptical orbits, and resonance-locked pairs of planets—has come as a surprise. Yet these discoveries just reveal the tip of the iceberg. If our Solar System is typical, then these giant planets may be accompanied by many sibling terrestrial planets.

[More specific text to describe the 2008 Forum]

DRAFT

1 Executive Summary

Alan Dressler, Carnegie Observatories

Wesley Traub, Jet Propulsion Laboratory

1.1 Introduction

One of the most fundamental and provocative questions that can be asked is whether life exists outside of our Solar System. This question has remained a philosophical one for at least 2300 years. It is now, however, practical and feasible to seek the answer from a scientific perspective. A clear path toward answering whether we are alone in the Universe exists, and following it is the purpose of NASA's Exoplanet Exploration Program. This path involves a multidisciplinary suite of research efforts, centered on finding and characterizing exoplanets that could harbor biological activity similar to terrestrial life. .

1.2 The State of Exoplanet Science

Nearly all of the 300-plus known exoplanets have been found within the past 11 years. Of these, 94% were discovered using the radial-velocity technique, 3% by transit photometry, 2% by gravitational microlensing, 2% by direct imaging, and 2% by pulsar timing. There are about 62 ground-based and 16 space-based search programs, ongoing and future. Over the past half-decade, the discovery rate has been steady at about 30 exoplanets per year. The rate of discovery seems to be limited mainly by instrumental sensitivity, not the available number of exoplanets.

[Summary of statistics with several overview figures]

1.3 Purpose of the Report

Describe what came before: the Exoplanet Task Force and its recommendations. Summarize its conclusions.

Describe the role of the Exoplanet Exploration Program.

Describe the purpose of the document. Describe the community involvement in the Forum and how this report was drafted.

DRAFT

Describe the Decadal Survey .

1.4 NASA's Plans and Constraints

[AO for Probe-class missions, with new missions every three years. Flagship missions delayed.]

1.4.1 Probe Mission Line

[Description of what the next decade likely holds for NASA planning.]

1.4.2 Flagship Missions

[Description of what the plans had been for larger missions and the direction we would like to go to have greater science capability.]

1.5 Community Strategy

Description of what community representatives have said in the past concerning priorities for exoplanet research, as expressed through the Exoplanet Task Force recommendations. This document endorses those recommendations.

Compete for the AO Probe-class missions as NASA intends.

Endorse long-term investments in technology and precursor science that will lead toward the flagship missions eventually and will benefit Probe missions in the nearer term.

1.6 Summary of Chapter Recommendations

[Describe areas of consensus between the groups as represented by the Chapter Chairs, where applicable. Summarize the highlights of recommendations from each group in the following sections, with rationale and a forward reference to details in the text.]

[What follows are the raw inputs from the different groups, as was solicited by Wes Traub. This material is a placeholder until the Executive Summary is written.]

1.6.1 Astrometry

1.6.2 Direct Optical Detection of Exoplanets

Main Exoplanet Science Contribution

1. Probe-scale mission (1.5 m class telescope at ~$600M) starting within the next two years, for exoplanetary systems characterization that is not accessible from the ground in the same time frame:

i. Exozodiacal characterization (1 zodi at 1-3 AU) of brightness, structures and clumpiness. This is critical for future characterization of habitable Earth-size planets.

ii. Direct detection and spectral characterization (0.4 μm to 1.0 μm) of planets and planetary systems, including at least 13 known RV Giant planets. We also anticipate detection and characterization of heretofore-unknown Neptune-mass planets and Super Earths.

2. Long-term flagship mission for characterization of potentially habitable Earth-Size planets.
3. Aggressive and sustained technology development starting immediately to meet readiness by mission start, including near-space environment opportunities (rockets & balloons).
4. R&A support for developing preliminary science and maturing mission designs in particular for the definition and optimization of combined Astrometry/RV and imaging missions.

How Does Optical Imaging Complement With Other Techniques?

The Optical Imaging chapter detailed the association between astrometry or RV and imaging in space, expanding on the ExoPTF recommendations for flagship and probe-scale missions:

- Indirect methods (astrometry or radial velocities) are necessary to obtain a direct measurement of the masses, orbital parameters, and planet "addresses".
  - ❖ For a characterization-only imaging mission (i.e. if the planets are already known), the Inner Working Angle (IWA) could probably be increased, and the mission duration reduced;
  - ❖ But other driving requirements on the system, such as stability, pointing, contrast, spectral coverage and spectral resolution, remain essentially the same as for a full search-and-characterize mission.
  - ❖ Careful Design Reference Mission (DRM) development over the next several years will articulate the tradeoffs in cost and performance between imaging missions with and without astrometric precursors.
- In the short term a probe-scale direct imaging mission can be combined with existing Radial Velocities and ground-based Astrometry (PRIMA, [ref]) for the characterization of mature giant planets, Neptunes, and super Earths.
  - ❖ A probe scale will also detect and characterize exozodiacal disks, a problem ExoPTF identified as critical for future terrestrial planet imaging missions.
  - ❖ This strategy is independent from a space astrometric mission both in terms of scientific goals and timing sequence, and therefore offers an alternate and coherent program especially if an astrometric mission to detect Earth-size planets is not recommended.

Main Technical Challenges

Technical challenges for optical imaging systems are summarized in Figure 3-8 as a function of size and type (internal coronagraph & external occulters). Colors represent technology

DRAFT

risk and maturity as an indication of technology development need. Numerical values represent target performance goals for flight. Columns correspond to representative mission concepts and scales. Costs will be evaluated in the context of the ASMCS and are not available at this time.

1.6.3 Direct Detection of Exoplanets with Infrared Interferometry

A probe-scale mission (~$600M) based on a passively cooled structurally connected interferometer starting within the next two to five year (for exoplanetary systems characterization not accessible from the ground) would provide transformative science and will lay the engineering groundwork for the flagship mission with formation flying elements:

A probe-scale mission would enable an exozodiacal dust survey (<1 zodi at <1 to >4 AU) including infrared spectra to elucidate grain chemistry and evolution, disk structure, and brightness, for all TPF/Darwin stars within 30 pc of the Solar System. This is critical for future characterization of habitable Earth-size planets, as knowing which TPF/Darwin stars have the lowest amount of zodiacal dust will allow for a more efficient strategy of spectral characterization of Earth-sized planets. This information could also be used to optimize the search strategy for an astrometric mission if such a mission were delayed due to cost or technology reasons.

A probe-scale mission would enable the direct detection and spectral characterization (6.5-20 μm) of planets and planetary systems of known exoplanets. Current estimates are that more than 50 such planets can be characterized. We also expect to discover and characterize previously undetected Neptune-mass planets and Super Earths around nearby stars.

A flagship mission (such as TPF-I/Darwin) would enable the characterization of two hundred or more potentially habitable Earth-Size planets. It would be based on large passively cooled infrared telescopes and formation flying technologies. Such a mission has the highest angular resolution for planet-finding of any concepts under consideration.

We recommend aggressive and sustained technology development to meet readiness by mission start, including near-space environment opportunities (rockets & balloons).

We recommend R&A support for developing preliminary science and mission designs in particular for the definition and optimization of combined astrometry/RV and infrared imaging missions. Also R&A support for continued exozodiacal dust studies with the Keck Interferometer and the Large Binocular Telescope Interferometer.

The Direct Detection of Exoplanets with Infrared Interferometry technique is highly complementary to other techniques including radial velocity and astrometry as follows:

Indirect methods (astrometry or radial velocities) are necessary to obtain a direct measurement of the masses, orbital parameters, and stellar coordinates.

For a characterization-only or imaging/spectroscopy mission (i.e. if all the planets are already known), the Inner Working Angle (IWA) possibly could be increased, and the mission duration reduced;

Other driving requirements on the system, such as stability, pointing, contrast, spectral coverage and spectral resolution, remain essentially the same as for a full search-and-characterize mission.

A careful Design Reference Mission (DRM) performed over the next two years will be used to quantify the tradeoffs in cost and performance between direct detection infrared interferometry missions with and without astrometric precursors.

a. In the 5-10 year time frame data from a probe-scale infrared mission can be combined with existing radial velocity and ground-based astrometry planet data for the characterization of giant planets, Neptunes, and super Earths.

    i. A probe scale mission will also detect and characterize exozodiacal disks, a problem ExoPTF identified as critical for future terrestrial planet imaging missions.

    ii. This strategy is independent from a space astrometric mission both in terms of scientific goals and timing sequence, and therefore offers an alternate and coherent program especially if an astrometric mission to detect Earth-size planets is not recommended.

Technical challenges for the direct detection of exoplanets in the infrared have been listed in the chapter itself. We briefly summarize key areas for further maturation:

1. For the Probe class mission:

    a. Cryogenic testing of optical fibers for wavefront spatial filtering.

    b. It is desirable, but perhaps not essential to fabricate a cryogenic testbed of the detection system. The key issue is whether the LBTI nulling instrument is sufficiently close in design to that of the probe mission science instrument.

    c. Most of the risk has been retired because of technology developments for JWST and TPF-I/Darwin, however it is worth some investment of time and resources to under exactly what technologies can be reused or adapted and what the costs would be.

2. For the Flagship mission:

    a. Demonstration of noise suppression beyond starlight nulling. Although the demonstration of starlight suppression is almost complete at the time of writing, other techniques are needed to provide an additional factor of ~100 in noise suppression. This includes array rotation and chopping and broadband instability noise suppression. Work is well advanced for these demonstrations and is the subject of interferometer milestones 4 and 5. To bring the technology to TRL 5/6, these demonstrations should include tests in a cryogenic vacuum.

    b. A prior interferometry mission. Before proceeding to a formation flying interferometer, one could retire many of the system-level technology risks of the flagship mission to have previously flown a connected-structure interferometer mission.

    c. Space-based demonstration of formation flying with three or more satelites. Having demonstrations of coordinated satellite control, including collision avoidance maneuvers, and failsafe control algorithms would retire the major risks associated with a flagship mission.

1.6.4 Microlensing

Here are the answers to your questions for the microlensing contribution.

1. What is the main exoplanet science contribution that your technique could make during the coming decade? You might want to answer this for the case of no change from today's funding level, and also for the case of an optimistic but reasonable level of funding.

The main exoplanet science contribution that microlensing could make in the next decade is:

* The determination the demographics of planets with semimajor axes >0.5 AU, and mass greater than Mars,

* The determination the frequency of free-floating planets with mass greater than Earth.

* The determination of the frequency of Earth-mass planets in the outer habitable zone of solar-type stars in the Galactic disk and bulge.

These contributions require the launch of a 1m-class wide FOV space telescope, which can be achieved with an optimistic level of funding. This might be achieved even in the case of no change from today's funding level if the microlensing mission is paired with a JDEM mission.

Otherwise, it may be possible to achieve a subset of these contributions, namely to determine the frequency of planets with mass greater than Earth for a=1.5-5 AU, using a network of ground-based, wide FOV telescopes.

2. For the purpose of contributing to a comprehensive scientific understanding of exoplanets, how does your technique complement (or compete with) the other techniques?

For determining the demographics of planets, microlensing is almost completely complementary to Kepler, in that Kepler will determine the frequency of planets with m>M_Mars and a<~0.5 AU, and microlensing will determine the frequency of planets with m>M_Mars and a>~0.5 AU. No other technique is as sensitive as microlensing for planets beyond the snow-line, and no other technique is able to detect old, free-floating planets. Microlensing is also more sensitive to planets around low-mass stars than most techniques.

Microlensing is not sensitive to planets around nearby stars, and although a space-based microlensing mission will yield good information about the mass and distance to the host stars (and the masses of the planets), there will be limited opportunity for follow-up of the detected systems.

3. What are the main technical challenges of your technique, and what kinds of resources (time, people, money, calculations, experiments, etc.) are needed to solve these technical issues?

There are essentially no technical challenges that need to be met to achieve the science goals of the microlensing method as laid out in the chapter.

A ground-based network could be completed with the construction of a single 1-2m telescope with a wide FOV camera. The cost for such a system is likely in the range of ~$10-20M.

For one realization of a space-based microlensing mission (MPF), almost no technology development is necessary. The design heavily leverages previous missions (Spitzer, NextView, JWST), and all the components are at TRL6 or better. Most of the requirements for a space-based mission are similar to, but less stringent than, those for a JDEM mission. A

joint microlensing/JDEM mission would likely cost an additional $100-200M beyond a JDEM-only mission, and a stand-alone microlensing mission would likely cost $300M plus the cost of the launch vehicle.

1.6.5 Radial Velocity

1. What is the main exoplanet science contribution that your technique could make during the coming decade? You might want to answer this for the case of no change from today's funding level, and also for the case of an optimistic but reasonable level of funding.

The main contributions the RV technique could make in the next decade are:

* Identify suitable targets for other missions (see Question 2).

* Characterize individual planets by measuring their masses, including Earth-type planets.

* Improve our understanding of the general statistical properties of the population of planets, as related to their parent stars. This will in turn enable a better understanding of the process(es) of planet formation, migration, and evolution.

* Provide an understanding of the architecture of planetary systems, in particular those like our own Solar System with multiple planets, some of them terrestrial.

The degree to which the above can be done will depend on the level of funding.

> 2. For the purpose of contributing to a comprehensive scientific understanding of exoplanets, how does your technique complement (or compete with) the other techniques?

* RVs are an absolutely essential complement to the transit technique.

Without an accurate knowledge of the mass of a planet, the discovery is of relatively little value since it cannot be interpreted in terms of theory.

* RVs complement astrometry. They effectively reduce the number of astrometric observations needed, and strengthen the orbital solution. They also identify targets for astrometric follow-up.

* RVs can provide targets for imaging missions, and maximize their returns by enabling us to predict the optimal times of observation. Similarly for JWST.

> 3. What are the main technical challenges of your technique, and what kinds of resources (time, people, money, calculations, experiments, etc.) are needed to solve these technical issues?

Challenges are:

* Achieve a more stable wavelength reference in the optical to allowsub-m/s precision, needed to discover and characterize Earth-mass planets.

* Achieve m/s precision in the near infrared, to allow access to fainter M dwarfs. These are the prime targets for discovering Earth-mass planets in the habitable zone.

* Understand stellar jitter. This may ultimately limit our ability to discover and/or characterize Earth-mass planets. It may well be that such planets can only be discovered around the quietest stars. This means that larger samples than previously considered may need to be explored.

Resources:

DRAFT

* The main resource needed is access to telescope time. This is not strictly a "technical" resource, but it does represent the principal limitation for current Doppler searches, and is also the bottleneck for follow-up of candidate transiting planets (currently from the ground and CoRoT, soon from Kepler). It is essentially a matter of funding. Furthermore, access to telescope time affects RV precision as well, given that longer exposures are needed to average out jitter.

* Experiments are needed to make progress on stable wavelength references, both in the optical and the near infrared.

1.6.6 Transits

DRAFT

2 Astrometry

Matthew W. Muterspaugh, Tennessee State University

Angelle Tanner, Jet Propulsion Laboratory

2.1 Introduction

Astrometry is a powerful tool for detecting and characterizing exoplanet systems. Only astrometry can detect habitable earthlike planets around nearby sunlike stars while simultaneously measuring the planet masses, the most fundamental quantity for characterizing exoplanets.

The 2008 Exoplanet Forum Committee on Astrometry strongly supports the recommendations of the Exoplanet Task Force (ExoPTF) Report (ref) and those present in past Decadal Surveys. ***The Committee's highest priority is to deploy a facility for micro-arcsecond astrometry of nearby stars during the 2010-2020 decade***, with primary goals of finding earthlike planets and characterizing the structures of planetary systems. A micro-arcsecond astrometry program will support a variety of science programs outside the field of exoplanets; the Committee strongly supports a mission design that will enable these non-exoplanet related research efforts. The technology development efforts of the past few decades have provided a system architecture capable of this micro-arcsecond astrometry goal. The key technology milestones have been achieved. It is now time to deploy the facility itself.

The ExoPTF made many secondary recommendations for the role of astrometry in exoplanet studies over the next decade. These secondary science programs have more modest budgets, but make smaller contributions to the understanding of planetary systems. A number of these secondary science goals are supported by the committee, which finds that *these should be pursued, but only if doing so will not delay the deployment of the highest priority micro-arcsecond astrometry mission.*

2.1.1 A Micro-arcsecond Astrometry Mission

All the highest priority science programs considered by the astrometry committee are addressed by a single, ~5 year or longer astrometry mission capable of micro-arcsecond precisions.

On page viii of their draft report, the first recommendation the ExoPTF makes for the 6-10 year (2014-2018) timeframe is to "Lauch and operate a space based astrometric mission capable of achieving 0.2 micro-arcsec sensitivity to planet signatures around of [sic] 60-100 nearby stars." The past three decadal surveys have promoted development of a micro-arcsecond astrometric program for detecting and characterizing extrasolar planets. *The astrometry committee recommends the 2010 decadal survey continue strong promotion of a*

micro-arcsecond astrometry mission, to be deployed in the early part of the 2010-2020 decade. Those past decadal surveys resulted in strong support for technology development efforts to design such a mission. All key development milestones for an astrometric mission based on the Space Interferometry Mission (SIM) architecture (including "SIMLite" (Goullioud) and "PlanetHunter" (NASA ROSES Astrophysics Strategic Mission Concept Study, now underway)) have been accomplished, and the community is ready to capitalize on this significant investment. Further delay may waste this investment, as the current experts could be lost to other pursuits.

Mission Name	Science Topics	Planet Mass Sensitivity, 10pc	Number of Stars for Terrestrial Planet Sensitivity
SIM	Exoplanets and Astrophysics	0.5 Earths	120
SIM-Lite	Exoplanets and Astrophysics	0.7 Earths	80
PlanetHunter	Exoplanets Only	0.7 Earths	60

Science Goals

Support for Micro-arcsecond Astrometry Science Other Than Exoplanets

A potentially surprising result of an internal survey of committee members was *unanimous support for the non-Exoplanet related science that an astrometric mission will address*, despite the fact that all the scientists being surveyed work specifically in the field of exoplanets. Committee members found that this was important both for maximizing the science output and to make a major mission palatable to the astronomical community as a whole. There has been some misperception that the scope of an astrometry mission is limited to exoplanets or a few other niche topics. The committee wants to emphasize that a micro-arcsecond astrometry mission is a general purpose observatory with broad scope to a wide range of astrophysical topics.

The SIM Lite mission is a direct descendent of AIM, the astrophysics mission endorsed by the 1990 Bahcall Report, and re-confirmed by the 2000 McKee-Taylor Report. This mission was originally recommended based on its promise of addressing a wide range of problems in stellar and galactic astrophysics. Planet detection, in 1990, was posed only as an interesting possibility, rather than a major science driver.

SIM Lite, in addition to addressing the recommendations of the ExoPTF, is fully capable of performing the science laid out in the McKee-Taylor Report. Indeed, the critical importance of precision astrometry has not diminished in the intervening years. The expected ESA mission named GAIA will conduct a large astrometric survey, building on the recognized ground-breaking work of Hipparcos. As a flexibly-pointed mission capable of very high astrometric precision (4 μas positions) at faint magnitudes (V<19), SIM Lite occupies a very different parameter space from GAIA. A recent peer review of the SIM Science Team Key Projects (SIM Book, 2008) showed that with minor exceptions, the broad astrophysics case for SIM remains unsurpassed by any current or planned future mission.

The science case for SIM PlanetQuest is laid out in considerable detail in the Science Team's paper in PASP (Unwin et al. 2008). SIM Lite replaces SIM PlanetQuest as a cost-effective way to do 'precision astrophysics'. It has essentially the same accuracy as SIM PlanetQuest, but can observe approximately half the number of sources in the faint-source limit (this does not apply to the exoplanet mission, where the stars are all bright). In most cases, the Science Team is able to do the same science but a judicious re-allocation of planned observing time.

Formation and Mass Distribution of the Milky Way

Tidal tails' of dwarf spheroidal galaxies form an exquisitely sensitive tracer of the interaction history of the Galaxy, and also the detailed shape of its potential. But only if one has good 3-space positions and 3-space velocities. SIM Lite uniquely provides 2 of the 3 space velocity components in distant tails (radii > 20kpc). This technique can be extended to the Local Group (out to ~5 Mpc) through astrometry of the brightest supergiants in member galaxies, providing key data on the mass distribution and dynamics of the Local Group.

Stellar Astrophysics

Masses of stars at both ends of the main sequence are very poorly known. Many stars with mass measurements have 10% errors; not impressive for 21st century astrophysics, and insufficient to challenge models of stellar luminosity and evolution. Many 'exotic' stars such as the components of X-ray binaries have distances, masses and luminosities crudely estimated to a factor of two. These are simple, but absolutely fundamental measurements that SIM Lite can easily make.

Quasar Astrophysics

SIM Lite will probe the internal structure of quasars, in the optical, to complement the highest-resolution VLBI imaging. 30 years after the discovery of superluminal radio sources, a lot of fundamental questions about the formation and propagation of jets remain sketchy. Precision optical astrometry, while not directly resolving the quasar core, will sense variability in a waveband orders of magnitude away from the radio, and probes a regime where accelerated particle lifetimes are very short. Variability, and also a differential color shift across the optical band, is vector quantities that can be compared with other geometric and structural information in quasars.

Detecting and Characterizing Low Mass Planets

As is shown in Scargle (1982), to achieve a false alarm probability of about 1%, within a factor of two, for a number of measurements that ranges from tens to thousands, the signal to noise ratio (SNR) needed is about 5.5 to 6.0, depending slightly on the number of measurements. If σ is the one-axis RMS noise per differential measurement, N is the number of visits, and α is the amplitude of the astrometric signature that can be detected with a probability of 50%, then

$$\alpha = \mathrm{SNR} \times \sigma / N^{1/2} \qquad \text{or} \qquad N = (\mathrm{SNR} \times \sigma / \alpha)^2 .$$

For example, the Earth amplitude at 10 pc is α = 0.3 μas. For a RMS measurement uncertainty of σ = 1.4 μas, to detect an Earth with SNR = 5.5, N = 659 measurements are needed. A targeted mission with micro-arcsecond single-measurement precisions, a noise floor below 0.3 μas, and capable of targeting the closest and brightest stars is required.

Operate as a Precurser Mission for a Future Direct Imaging Program

Recent technological advancements have led us to the point where mankind might finally answer the ancient question "Are we alone?" by searching for evidence of life on planets around nearby stars. Terrestrial planets of 0.3-10 Earth masses would be most favorable to life, as heavier planets could have unfavorably thick atmospheres, and lighter ones might not have any atmosphere at all. Orbits in the range 0.85-1.6 AU around a star of solar luminosity would offer planetary temperatures compatible with liquid water. For other stellar luminosities, the "habitable zone" orbits scale roughly as the square root of the luminosity. M dwarfs are not favorable targets because habitable zones are too close to the stars for direct imaging missions of reasonable sizes. Nearby sunlike stars are preferred targets because direct imaging missions might be able to study habitable planets detected by the finder mission.

The first step is to locate suitable candidate planets. *A micro-arcsecond astrometry facility is the most feasible method for identifying candidate earthlike planets around nearby sunlike stars in the 2010-2020 decade.* The intrinsic surface jitter of stars prevents the tiny radial velocity signature (10 cm/s) of a habitable earthlike planet around a sunlike star to be detected. A direct imaging mission is inefficient for detection purposes, but will be an important tool to characterize atmospheres once planets have been identified. Only planets whose orbits are edge-on as seen from earth will transit their star, the likelihood of which is very small for planets in the habitable zones of sunlike stars; many nearby planetary systems would be missed. Other planet detection methods are not well optimized for studying nearby stars.

The second step is to obtain spectra of the planetary atmospheres, looking for signatures related to life on Earth, such as water and oxygen. The greatest challenge for the success of such a mission is the combination of the extreme contrast between and small separations of star and planet and the intrinsic faintness of the planet. The most reasonable targets for a direct imaging mission are nearby stars where this challenge is minimized (though still quite formidable). *Astrometry is well optimized for identifying low mass planets around the nearest stars, the best targets for direct imaging missions.*

The ExoPTF report states on page 55 "The most promising way to mitigate the cost of space-based direct imaging is 1) to identify targets before the direct imaging mission is flown." The astrometry committee agrees with this assessment. By first deploying an astrometric mission to find and characterize earthlike planets around nearby stars, the cost of a future direct imaging mission is greatly reduced and the scientific output greatly increased.

Where to look: Identify nearby targets

The best way to search for potentially habitable exoplanets around nearby stars is indirectly---by looking for the astrometric wobble of the star responding to the gravitational tug of the revolving planet. The minimum required single-measurement astrometric accuracy is ~1 micro-arcsecond.

The alternative---a direct search by coronographic images---is problematic. The first problem is the central obscuration, which hides large fractions of most orbits. Only for a fraction of the planet's orbit is it correctly positioned where a coronograph will detect it. The second problem is the low information rate, demanding many long exposures with rare positive results, assuming a planet is present. The third problem is the difficulty---or even impossibility---of estimating the planetary orbit from the small number of measurements

that can be obtained in the epoch of discovery, which is typically only 6 months long due to solar avoidance. Without knowing the planetary orbit, science operations become a matter of guess work, and any found planet will probably be lost.

The ExoPTF recognized these difficulties with the direct planetary search when it recommended splitting the finding and characterizing tasks between two concatenated programs, an indirect finder program and a direct characterizer program. The direct imaging mission will characterize planets found by the finder program. While the indirect finder program can stand alone and still provide valuable science content without the direct imaging program, the direct imaging mission will not have identified targets if the indirect finder is not deployed first.

When to look: Characterizing Orbits

Astrometric observations of stars hosting earthlike planets allow the orbit to be determined. The position of the planet can be predicted as a function of time. This provides a solid basis for future planning direct imaging programs, as the observing schedule can be set to look at targets when the star and planet are most optimally configured for isolating light from the planet.

The direct imaging program will operate more efficiently by only observing when the planet-star configuration is likely to produce a positive detection and spectrum of the planet. No time is wasted searching a target when the orbital configuration is poor. The technical requirements of a direct imaging mission may be reduced because it need only meet requirements for detecting planets when they are in optimal configurations.

Characterize Planets Targeted By Imaging: Masses

On page 55, the ExoPTF report finds "a capability to determine mass, specifically space-based astrometry described above, is necessary in conjunction with the direct imaging platform." The astrometry committee agrees that without this capability, the science returns of a direct imaging mission are marginalized.

The mass estimate from the orbital solution to the astrometric data from the astrometric "finder" mission is the most basic quantity in understanding the planet's characteristics. Knowledge of the planet's mass is crucial in setting the context of any spectrum of the planet's atmosphere taken by a direct imaging mission and evaluating whether the planet can support life. Only by measuring the gravitational effect of the planet on its host star can the planet mass be measured. Direct imaging and transit lightcurve observables do not provide measurements of planet mass, and model-based estimates are a poor substitute, because they require that the characteristics of exoplanets follow the patterns seen in our own Solar System.

Multiplanet Systems and Planetary System Architecture

Theoretical models of planetary system formation inevitably produce systems with multiple planets. Combined with the Doppler discovery of exoplanet systems with at least four (HD 160691) or five (55 Cnc) planets, and the eight planets in our Solar System, it is clear that we should be prepared to discover that multiple planet systems are more likely to be the rule than the exception. While the number of gas giant planets around FGK stars is beginning to be limited by Doppler detections (Cumming et al. 2008), there are only weaker constraints on Neptune-mass planets, and no constraints at all on Earth-mass planets. Using our Solar System as a guide, one expects that long-period Jupiters should be accompanied by inner terrestrial planets, and it has even been suggested that short-period, hot Jupiters

might be orbited by habitable terrestrial planets, in spite of the prior migration of the Jupiter-mass planet through the habitable zone of the star (e.g., Raymond et al. 2006). The basic theoretical expectation is that terrestrial planets should be commonplace, regardless of whether or not gas giant planets have had a chance to form (Wetherill 1996). Multiple planet systems can place strong constraints not only on the orbital stability of the entire system, but also upon the mechanisms involved in their formation and orbital evolution, and so discovering and characterizing multiple planet systems are important goals for extrasolar planet searches.

Astrometric observations provide the opportunity to measure six phase space coordinates for each planet detected. In particular, by measuring the orbit's inclination, astrometry estimates the planet-star mass ratio with no degeneracies (except for pathological geometries). On one hand, the mass of any individual planet is not particularly interesting and radial velocity surveys can measure the distribution of planet masses. However, the precise measurements of planet mass is important for understanding the dynamical state of multiple planet systems. Therefore, intensive monitoring of multiple planet systems should be one of the key science drivers for an astrometric mission.

With only radial velocities, imposing the constraint of dynamical stability can constrain the inclinations and provide upper limits for the planet masses. Unfortunately, such analyses often leave uncertainties of order ~30 degrees in inclination and a factor of ~2 in the planet masses. These uncertainties can cause even *qualitative* uncertainties in the dynamical state of the system (e.g., mode of secular evolution, being in or near a mean-motion resonance). With sufficient observations, astrometric observations have the power to resolve such degeneracies, so that dynamical modeling can constrain the formation and orbital evolution of multiple planet systems. For example, different mechanisms for eccentricity excitation make different predictions for the degree and circumstances of inclination excitation. Therefore, dynamicists look forward to astrometric measurements of the relative inclination between planets and whether this correlates with planet mass, orbital period, eccentricity, and/or presence of a binary companion.

Both the number and fraction of planets in multiple planet systems is set to increase as planet searches become sensitive to planets with lower masses and longer orbital periods. Since many, if not most, planets are members of multiple planet systems, understanding the formation and evolution of multiple planets systems is essential for understanding planet formation in general. With sufficient astrometric observations of a multiple planet system, the current planet masses and orbits can be precisely measured, so that theorists can investigate the secular orbital evolution and to gain insights into planet formation. For example, different models of planet migration and eccentricity excitation make different predictions for the secular evolution of planetary eccentricities and inclinations. Therefore, theorists look forward to astrometric observations that determine if the mode and amplitude of secular inclination evolution correlates with the mode and amplitude of secular eccentricity evolution. Searching for such a correlation could test whether certain features in the secular eccentricity evolution (previously identified by radial velocity observations) are reliable fingerprints for recognizing the outcomes of various planet formation models.

A remarkable feature of our solar system is its coplanarity. Thanks to the recent redefinition of "planet", all planets in the solar system are coplanar to within 7 degrees. If this is a general feature in most planetary systems, it is a strong observable constraint that must be matched by planetary system formation and evolution models. However, with the

coplanarity of only one system (ours) being known, it is impossible to tell how common this feature is in nature.

Studying additional multi-component solar systems will serve to expand the understanding of what a typical solar system geometry might look like, and whether the distribution of geometries even allows for "typical" to be defined. It is interesting to note that while the distribution of relative inclinations of triple stars systems is slightly biased toward coplanarity, the systems tend not to be as well aligned as the planets in our solar system.

Flexible scheduling can greatly aid the characterization of multiple planet systems. For instance, a Solar System "clone" would be recognized as especially interesting, but complex, after about two years. Such as system would easily warrant an increase in observing cadence during years 3-5.

Micro-arcsecond Astrometry in the Context of Other Exoplanet Programs

While the committee strongly supports a direct imaging after completion of a micro-arcsecond astrometric finder program, *if it comes down to choosing either one or the other, an astrometric mission is a higher priority than imaging.* The committee favors a plan of deploying an astrometric mission in the early part of the 2010-2020 decade, with a direct imaging mission be deployed at the end of the decade or early in the 2020-2030 timeframe.

The imaging mission science is marginalized without an astrometric mission. First, one doesn't know where or when to look. An imaging mission is not a viable "finder" mission; to incorporate that, the imaging mission would be much more expensive. Second, from imaging data alone, masses are unknown, and it is difficult to interpret imaging results without this. Third, astrometry is ready now. The architecture is settled and technology milestones completed. Imaging has not yet decided between nulling interferometry, external coronographs/starshades, and internal coronographs. Because imaging is at such an initial stage of development, it will not be ready to be deployed on the timescale of the next decade.

Science Requirements

Planet Finding

The Exoplanet Task Force final report recommended an astrometric mission with the capability to achieve a mission minimum detectable astrometric signature of 0.22 μas after many hundreds of measurements, derived from the desire to detect a one Earth mass planet at the inner edge of the habitable zone for a Sun-like star located at 10 pc, and having a throughput sufficient to survey 60 to 100 nearby stars to this depth during the mission lifetime in order to generate a sufficient number of candidate planets for a later direct detection mission.

These recommendations can be met by an astrometric mission capable of carrying out a roughly five-year mission while achieving the recommended astrometric precision for target stars from -1.4 Vmag through 7 Vmag that each have reference stars (typically K giants at ~1kpc) brighter than ~10 Vmag located within two degrees of the target star on the sky.

We note that the actual program undertaken by an astrometric mission would of course be informed by all prior knowledge, most notably the frequency of terrestrial planets discovered by Corot and Kepler. A flexibly pointed instrument can be adapted to maximize the science return.

Other Areas of Astrophysics

An astrometric mission only capable of meeting the recommendations for planet finding would not be capable of achieving significant strides in other areas of astrophysics as recommended by the two previous NRC astrophysics Decadal Surveys, primarily because the interesting astrometric science lies in the dim star regime out to 19 Vmag which cannot be reached by other ground or space missions. Achieving the astrophysics recommendations of the prior Decadals requires the stability to support much longer integration times than required to achieve only planet finding. Thus one of the more general purpose versions of the micro-arcsecond astrometry mission guarantees the best science return for the investment.

2.1.2 Other Strongly Supported Recommendations

Science Goals

Theory

As noted in the Report of the ExoPTF, there is a clear need to combine observational advances in detecting and characterizing exoplanets with theoretical work that supports these discoveries in several ways. The committee has focused on theoretical work of most importance for astrometric planet discoveries, as opposed to, e.g., direct detection, where the theory of exoplanetary atmospheres becomes important.

First, theoretical work on orbital dynamics is essential for determining the best fit for the exoplanet orbits, determining orbital stability over long time periods, understanding orbital resonances and how they formed, and determining the interactions in multiple planet systems where some planetary orbits are poorly constrained or completely unknown.

Second, theoretical work on planet formation mechanisms of the entire range of planets, from terrestrial planets, to ice giants, to gas giants, is necessary in order to place the exoplanet discoveries in the context of planetary system formation theories. Terrestrial planet formation is strongly influenced by gas giant planet formation and orbital evolution, so a complete theory of planet formation is needed in order to understand the formation of any one component. Theoretical models also provide testable predictions for what might be discovered, and therefore help to define the next steps in a long-term program of exoplanet discovery and exploration.

Third, understanding the extent of habitable zones around astrometric target stars will focus our attention on the best targets to search for the possible detection of habitable worlds. Recent theoretical work, e.g., has highlighted the potential of low mass, M dwarf stars as hosts for habitable worlds (Tarter et al. 2007).

The Impact of Gaia

On page 54 of the ExoPTF report, the ExoPTF finds “The European `Gaia' space mission will be a useful demonstrator of the ability to do spaceborne astrometry to find giant planets, and will contribute to the census of Jovian-mass planets around Sun-like stars.” The committee agrees Gaia is an exciting program, but finds that its existence has little impact on setting priorities for other astrometry programs because it operates in a complementary---rather than duplicate---capacity to those programs.

Gaia is a European astrometry mission with planned launch for 2011. It will achieve 100 micro-arcsecond per-measurement precisions (to V=15) on 30 million stars (and reduced

precision for up to a billion fainter stars), with each star revisited 1-250 times (typically ~90 one-dimensional measurements) over the course of the mission. It is a survey mission without capability to be pointed at a particular object, meaning the number of revisits cannot be increased for a high priority target. Gaia will saturate for very bright stars (V~6), including the stars closest to earth that are the highest priority targets when looking for earthlike planets.

The measurement precision of Gaia is insufficient to discover earthlike planets; the 100x better precision of a micro-arcsecond astrometry program is required to achieve this goal. Furthermore, the number of repeated measurements for a given target is much larger for a pointed mission (with perhaps 200-500 (two-dimensional) measurements on high priority targets), which will both improve the sensitivity to lower mass planets, and provide better coverage of a planet's orbit. Good orbital coverage is necessary to adequately characterize a planet's orbit well enough to instruct a future direct imaging mission when the best observing time will occur.

Detecting Large Numbers of Giant Planets

The discovery of the first giant exoplanet (Mayor & Queloz 1995) occurred only 13 years ago. This discovery opened up the field of exoplanet research. Currently over 250 giant exoplanets have been identified around nearby stars. These have provided initial statistics on the properties of giant planets. In order to make a substantial impact on these statistical studies, future efforts will require detection of an order of magnitude more objects.

A sub-milliarcsecond astrometric program can discover and make dynamical mass measurements for hundreds of giant exoplanets down to the mass of Jupiters. This would significantly supplement the results from the past years of RV searches, transit searches, and microlensing searches. It is worthwhile to greatly increase the numbers of planets to enable class studies with enough planets to come to conclusions about physical properties and frequencies in each of the different categories, e.g., spectral type, age, and metallicity.

MIDEX or Discovery Class Space Survey

A space-based system that is in the MIDEX or Discovery class can make a significant contribution in the area of giant exoplanets. Companions down to Neptune mass can be discovered around thousands of stars with the added precision and stability of space observations (Pravdo et al. 2007). An infrared mission in space could for the first time do a broad survey of exoplanets around low-mass and young stars. It would be complementary to Gaia both in low-mass stars that Gaia has difficulty observing, and for bright stars that could be observed with a high-dynamic range instrument but not Gaia.

An example of this class of mission is Giant Planets around M, L, and T Dwarfs in the Infrared (*GIMLI*). *GIMLI* targets low-mass systems and can thus help settle the debate over the dominant formation mechanism for EGPs (e.g., core accretion or disk instability), illuminate the differences between brown dwarfs and high mass planets, and provide a calibration of the mass-luminosity relationship for the lower end of the stellar main sequence. *GIMLI* features a 1.4-m aperture with a high-dynamic range IR instrument that performs narrow-angle astrometry with 50 μas precision. It can also accommodate a complementary coronagraph. It is sensitive to exoplanet masses down to <0.01 Jupiters, i.e., Uranus- or Neptune-masses for nearby older stars and for younger stars in the nearby star-formation regions.

Ground Based Optical Astrometry

Single-telescope ground-based astrometry has had success in discovering stellar and brown dwarf companions and measuring their dynamical masses (e.g. Pravdo et al. 2004, Pravdo, Shaklan, & Lloyd 2005, Pravdo et al. 2006), but no exoplanet has yet been astrometrically discovered. The reasons for this are simple: lack of support for observing time and lack of funding for instruments. These indirect observations have demonstrated the required sensitivity to detect large exoplanets but need a minimum of observing time for adequate time-sampling. A modest fraction, e.g. 10%, of the time currently granted to radial-velocity (RV) observations would result in the first astrometric discoveries of exoplanets.

Dynamical mass measurements could be made of >50 of the currently known exoplanets with ambiguous mass measurements (due to unknown inclination angles) with a new ground-based system featuring a detector with high dynamic range. Such an instrument could use current technology either in the visible or infrared. An infrared system would have the added advantage of opening a new region of discovery space, *viz.* exoplanets around low mass stars. Since low mass stars comprise 70% of all stars this activity would be an important component of the desired census of exoplanets. The discovery of exoplanets around low-mass stars is inadequately addressed by current programs. RV programs have demonstrated poor sensitivity to long-period (> 1 yr) planets around low-mass stars, and the detection of such planets with other techniques, e.g. transits and microlensing, has very low efficiency. An infrared camera built with existing technology, operating with adequate observing time on a large-aperture ground telescope can detect planets around many low mass stars, greatly increasing the ~10 systems that are currently known.

In a recent paper (Cameron, Britton, & Kulkarni, 2008) it was demonstrated that 100 micro-arcsecond astrometry can be achieved in few-minute observations using the Palomar 200" PALMAO adaptive optics (AO) system in K-band. The paper articulates the problem of differential AO astrometry in the face of the dominant noise source (which is correlated tilt anisoplanatism), derives its expected contribution to the astrometric uncertaintyy, developes an optimal estimation algorithm for performing astrometry, and verifies the expectations with extensive on-sky tests at Palomar and Keck. The technique achieves ~100 microarcscond precision in 2 minutes and ~100 microarcscond repeatability over 2 months. The technique is currently being used at Palomar to search for planets around mid-M-dwarfs.

The European Very Large Telescope Interferometer (VLTI) will begin commissioning the PRIMA narrow-angle differential astrometry instrument in late 2008. The most optimistic estimates predict 10-20 micro-arcsecond performance (a prototype of this technology was demonstrated at the Palomar Testbed Interferometer with ~100 micro-arcsecond repeatability (Lane et al. 2000)). This will be an excellent tool for characterizing giant planets around nearby stars, and the expected long lifetime of this program will allow it to capitalize on astrometry's increasing sensitivity with planet orbital period. The committee agrees with the ExoPTF's conclusion that, as far as ground-based observatories, there are "no other facilities that would match or exceed the performance of VLTI within the 15-year time frame" (page 101). The VLTI will operate in the near-IR, and can study objects obscured at visible wavelengths including protostars and the galactic center.

The two 10-meter Keck Telescopes have been combined as an interferometer. Project ASTRA, funded by the NSF, is building a differential astrometry module for the Keck Interferometer. The resulting astrometric precision is expected to be on the level of hundreds of micro-arcseconds. The small amount of time available for interferometry on

these large telescopes limits its impact to very specific observing programs, such as RV-identified multiplanet systems or the galactic center.

Lifting the Mass/Inclination Ambiguity for RV-Identified Exoplanets

The large majority of known exoplanets have ambiguous masses: their unknown inclination angles constrain the results to lower mass limits only. This mass ambiguity disappears in the astrometric determinations of dynamical mass, since astrometry determines the system inclination angles. Specific targets of interest where unambiguous masses are important include those with multiple planets where planet-planet interactions might become significant. The inclination ambiguity does not strongly affect statistical distributions of planet masses. However, for samples of a large number of planets it is also important to know where each of the systems lies in the parameter spaces defined by theorists. Ida et al (2004, see Figures 9 and 12) demonstrate how the knowledge of the unambiguous dynamical masses guides the development of the theory. The statistical assignment of inclination angles to many systems degrades the quality of the solutions, especially when the number of planets is limited to a small number of planets in each category of the multidimensional (spectral type, age, metallicity, etc.) parameter space.

2.1.3 Recommendations Addressed by the ExoPTF with Mixed or Ambivalent Support

Astrometry at Radio Wavelengths

Most stars are faint at radio wavelengths. A few active stars can be detected in non-thermal emmission by the VLBA. Operating at shorter wavelengths, ALMA will detect thermal emission from many main sequence stars. However, its limited resolution will restrict astrometric precisions to the milli-arcsecond level. This may be useful for the study of giant planets, but is limited in its scope. The Square Kilometer Array (SKA) will have the sensitivity required to detect main sequence stars, and the current international specifications include very long baselines that would enable astrometry at microarcsecond precisions at centimeter wavelengths. However, there is concern that any non-thermal emission, which may not be centered on the star itself, will reduce the astrometric precision, potentially to the level of hundreds of microarcseconds.

The committee generally supports radio astrometry as a useful method for exoplanet detection only if it requires a modest marginal cost to implement at existing facilities. The impact of radio astrometry on the field of exoplanets is unlikely to be substantial enough to serve as a major science driver for major new radio facilities. By itself, astrometry for exoplanet studies is not compelling enough to require that the SKA design continue to include the long baselines that would enable precision astrometry at centimeter wavelengths. Assuming that the SKA design continue to include long baselines to meet other science drivers, a program for astrometry of nearby stars would be worthwhile for the small marginal cost it would require.

The committee does promote radio astrometry as a powerful tool for science in fields other than exoplanet studies (see for example Honma et al. 2007, Hirota et al. 2007), and believes it should continue to be supported for those purposes.

Basic Properties of Stars in Support of Exoplanet Science

On page 47, the ExoPTF report states "To optimize the choice of targets and maximize the eventual scientific interpretretation of exoplanet observations, it is important to have an ongoing program to measure stellar parameters." The fractional uncertainty in an astrometrically derived exoplanet mass is at best equal to the fractional uncertainty in the host star's mass. Astrometry can contribute to constraining star masses for a range of star types by measuring the orbits of binary stars. Overall, the committee did not place high priority on developing new astrometry programs in this area. Most of the committee found that these quantities are already known well enough across the range of star types comprising the primary targets of a search for earthlike planets around nearby stars, and improving this knowledge would have a minimal impact on exoplanet science. The merits of stellar astrophysics can be separately evaluated as a science topic on its own, without playing a crucial role in the outcome of the exoplanet projects.

Similarly, the distance to a host star is required to properly characterize it and any astrometrically detected exoplanets. This will be a natural result of any astrometry program and a separate devoted effort is unnecessary. Astrometry may play a role in determining distances to planet host stars with companions detected in other manners, such as radial velocity or transits.

Demonstrating Technology Shared With Future Imaging Missions

Committee members had mixed interest in whether it is important that a space astrometry mission have a role in demonstrating technology that might be shared with a future direct imaging mission (for example, picometer metrology shared with TPF-I).

Space Astrometry Support For Microlensing

Microlensing events are a powerful tool for studying exoplanets around distant stars. The observable being used in current studies is the overall source magnification cause by the gravitational potential of the lensing object(s). The shape of the lightcurve provides information about the number of objects in a lensing system, and their relative masses.

Astrometry is a second observable that can provide additional information on the lensing system. During a microlensing event, the apparent position of the source will vary by amounts measurable by the micro-arcsecond astrometry mission.

The committee supports this as an interesting project to pursue if the design of the micro-arcsecond astrometry supports it. However, the mission design should not be altered to specifically address this program, and it should not be allowed to impact negatively the primary mission of detecting earthlike planets around nearby stars.

Astrometry with a Large-Aperture, Wide-Field Camera in Space

As an example of an alternative concept the committee considered for the sub-microarcsecond capable mission and found to be less capable in terms of astrometric performance, we examine image-plane astrometry with a giant 8m (or 16m) space telescope with a relatively large field of view (FOV) of 2 arcminutes (requiring 16k by 16k pixels for 8m, 32k by 32k for 16m). This represents a reasonable advance in technology over the < 3 arcminute FOV of WFC3 (1k by 1k to 2k by 2k pixels depending on channel) on the >3x (6x) smaller HST (the 10 degree FOV of Kepler is not diffraction limited and not applicable to the following considerations; pixelization noise in that case limits astrometric precision, and the detector-related systematic errors are larger as well, and even the 95

Megapixels in the Kepler camera is smaller than the 250-1000 Megapixels required for the concept astrometry mission).

If one considers only the photon-noise and diffraction limited SNR of the bright target star, an 8m (16m) filled-aperture telescope clearly appears to offer superior performance to a 6m baseline interferometer---both its angular resolution and collecting area are larger.

However, the real error budget contains many more terms, and in neither the interferometer nor the image plane approach does the photon-noise limited SNR of the bright target star make a significant contribution. Lacking instrumental or systematic noise sources, the dominant term becomes the photon-noise and diffraction limited SNR of the reference stars.

With smaller individual apertures, the interferometric approach has much larger field of view than even a "wide field camera" on a single giant telescope: in narrow angle mode, a SIM-based architecture uses reference stars distributed over a 2 degree field, compared to the hypothetical 2 arcminute field of a wide field image-plane camera. The area over which the interferometer can select targets is 3600x that of the wide field camera. By far, the brightest reference stars in the field contribute the most SNR to establishing a reference grid, so the number of reference stars on which astrometry is obtained is relatively negligible as long as the brightest few stars, contributing > 50% of the reference light available, are observed. For the much wider-field interferometer, the reference stars can be roughly 3600x brighter. The collecting area for an 8m (16m) filled aperture is 350x (1400x) that of the 2x30cm interferometer telescopes; and the resolution is 1.3x (2.6x) that of the 6m baseline interferometer. Overall, the interferometer SNR on reference stars (proportional to $F^{1/2}\ A^{1/2}\ /\ R$, for source brightness F, collecting area A, and resolution R) has 2.4x the SNR of the 8m and 0.6 the SNR of a 16m wide field camera.

Again, this in not likely to be the dominant term in the error budget of an image plane astrometry camera. Instead, detector systematics are likely to be a dominant error source. Assuming the camera is critically sampled (2 pixels/resolution) the focal plane will have 32,000x32,000 pixels, a CCD mosaic. The most precise astrometry with CCD cameras use single CCDs because a single piece of silicon is much more stable over a period of years than a mosaic detector. Developing a mosaic CCD whose dimensional stability over several years is at the 0.1nm (single atom) level is far beyond current technology. CCD mosaic stability aside, astrometry at the 0.2 micro-arcsecond level implies point spread fuction (PSF) fitting to within a part in 75,000 (37,500) of the 15 mas (7.5 mas) diffraction limit of the telescope. This is still over two orders of magnitude more precise PSF fitting than typically possible in modern imaging detectors such as those on HST. With current technology, the most optimistic estimates of the image-plane astrometry performance is ~50 micro-arcseconds.

Technology obstacles exist requiring a major effort to overcome current PSF fitting limitations in image plane arrays. First is inhomogeneities between detector pixels, and within the pixels themselves, introducing non-uniform responses across a pixel, making fitting below about a hundredth of a pixel impossible with current detectors and calibration methods. New manufacturing processes would be required to make detectors with uniformity 100x better than the current state of the art, and to calibrate that responsivity. Second, the variations in the differential PSF between target and reference must be stable over the timescales of interest (years). These PSF-fitting issues are mitigated in the interferometry case, where the astrometry observable is a differential interferometric delay tied directly to a laser reference, and the same detector pixels are used for target and reference. To be certain, developing the ability to fit to far below the diffraction limit is a

challenging proposition; this technology development was possible only through a decade-long effort culminating with the micro-arcsecond metrology (MAM) testbed, detailed in Section 1.2.2. It is not an efficient use of current resources to duplicate this technology development effort for the image-plane astrometry case when the interferometer-based approach is ready for deployment now. This is supported by the fact that even in the limit of systematic errors being less than that of the reference star SNR, the interferometer approach offers roughly equal astrometric precision as the much more expensive 8m (16m) filled aperture concept.

While the committee's fundamental conclusion is to support deployment of any form of a sub-micro-arcsecond precision, targeted astrometry mission capable of observing nearby stars, the committee believes the most realistic framework to achieve this is one based on the SIM technology program.

2.2 Observatory Concept.

While many programs for astrometric detection and characterization of exoplanets are supported by the committee, only the design of the highest priority, micro-arcsecond astrometry mission is considered in depth.

2.2.1 Architecture

The SIM-based architecture is mature and ready for a mission now, and is the most feasible approach to micro-arcsecond astrometry. This architecture may be realized in the form of SIM, SIM-Lite, or PlanetHunter.

A space-based mission is the most promising method of achieving micro-arcsecond level astrometric precisions. Ground based astrometric techniques must look for reference stars within the isoplanatic path, typically ~30 arcsecond. Only a very few of the nearest "best" candidates for an astrometric search for exo-Earths are double stars. Background field stars in a 30 arcsecond are typically 18-20 mag. Atmospheric noise and photon noise of the 18~20 mag reference stars limit any ground based astrometric instrument to > 10 micro-arcseconds in 1 hr of integration. Whereas a ground-based astrometric program will require 100 hours of integration to reach the 1 micro-arcsecond level, a space-based program can reach this level in a 20 minutes. A survey of the most promising 60-100 targets takes ~40% of a 5 year mission, whereas a similar ground based program would take 1500 years!

Field of view considerations favor the SIM architecture over filled-aperture space telescopes for astrometry. SIM uses reference stars up to 1 deg from the target. A space astrometric telescope would have a much smaller field and consequently would have to rely on much fainter reference stars. When the photon noise of the faint reference stars are taken into account SIM's photon limited accuracy is equivalent to a filled aperture 10m telescope with a ~10 arcmin field of view.

The science instrument considered here is a spatial interferometer, conceptually similar to Albert Michelson's interferometer on the 100-inch telescope at Mt. Wilson in 1913, and to other ground-based amplitude interferometers since that time. It collects two patches of the incoming wavefront from a star, uses a mirror on a movable delay line to apply a suitable time delay to one of the wavefront patches, and combines the patches to form an interference fringe in the pupil plane. The delay is adjusted to give the maximum visibility of the white-light interference fringe packet. The origin of the delay line is defined as its position when the axis of the instrument is perpendicular to the propagation vector of the

incoming wavefront, where the axis is the line between the pivot points of the two collecting mirrors at the ends of the instrument. The distance between these pivots is the baseline of the instrument. The angle between the instrument axis and the line of sight to the star is the arccosine of the delay divided by the baseline.

The SIM-based architecture results from twelve years of coordinated technology development and mission design. The architecture consists of one science Michelson stellar interferometer (MSI) capable of micro-arcsecond fringe determination accuracy, a guide star tracking system to determine the attitude of the instrument at the micro-arcsecond level relative to chosen guide stars (about a million times better than a typical spacecraft star tracker), and a metrology system to determine the orientation of the science interferometer baseline relative to the guide star tracking system. Supporting mission elements include: (1) an instrument data system to control the instrument and collect instrument data for return to the ground for processing, (2) a spacecraft bus to provide housekeeping services, (3) a launch vehicle to inject the flight segment into the proper orbit, (4) a mission operations system to monitor and control the flight segment, and (5) a science operations system to plan observations, reduce the science data and distribute science data to the science users.

A number of variants of the SIM-based architecture have been studied by the SIM project team, aimed at providing a full range of science/cost performance options for the science community and NASA to choose from. A brief description of these options follows.

SIM PlanetQuest

This is the most capable of the options, consisting of a 9 m science interferometer baseline and two 7.2 m MSIs to form the guide star tracking system. This mission is launched into an Earth-trailing Solar orbit (ETSO), drifting away from Earth at about 0.1 AU/year. It is launched on one of the largest EELVs (Atlas V 551 or Delta IV Heavy) and tracked by the NASA Deep Space Network (DSN). Mission operations is conducted from JPL and science operations from the Michelson Science Center (MSC) at Caltech.

SIM-Lite

There are three versions of this option that hit different cost/performance points. All have a 6 m science interferometer baseline, all have one 4.2 m MSI that serves as one of the two guide star trackers, and all have one 30 cm diameter telescope that serves as the second, lower accuracy, guide star tracker. All are launched by an EELV (Atlas V 531 class) into ETSO, are tracked by the DSN, and are operated from JPL and Caltech, the same as the full SIM PlanetQuest. Option variations result from the size of the science interferometer siderostat (50 cm or 30 cm), and the way science operations are carried out.

Planet Hunter

There are two versions of this option with different cost/performance points. Both have one 6 m science baseline that has a restricted field of regard of only 4° (vs. 15° for SIM and SIM-Lite), both have one 4.2 m guide MSI, and both have one 30 cm guide-2 telescope. Options derive from whether the mission is flown in ETSO as for SIM or in a 900 km Sun-synchronous, terminator Low Earth Orbit (LEO). LEO offers a less expensive launch vehicle, less expensive ground communication system (Faribanks, AL), and the use of magnetic torquers to dump momentum allowing longer mission lifetime but comes at the expense of requiring a large deorbit engine to clear LEO at the end of mission life and the need to spend more than 50% of mission time maneuvering to avoid Earth-shine entering the instrument.

2.2.2 Performance

The accuracy of an angle measurement is determined by the total number of photo-electrons collected in the interference fringe pattern (mainly set by the brightness of the star, the collecting area, and the integration time), the shape of the pattern (mainly set by the length of the baseline and the wavelength) and knowledge of the baseline vector (direction in 3-space and length).

The relative position of a target star with respect to its group of reference stars is determined during a "visit". "Visits" can be either short or long, depending on the measurement accuracy desired. A "short visit" is about 2200 seconds in length. In a short visit, the target star's two-dimensional location in the plane of the sky is measured with respect to a local framework defined by the average location of 4 to 5 nearby reference stars. The measurement along each axis takes half of the total, or 1100 sec.

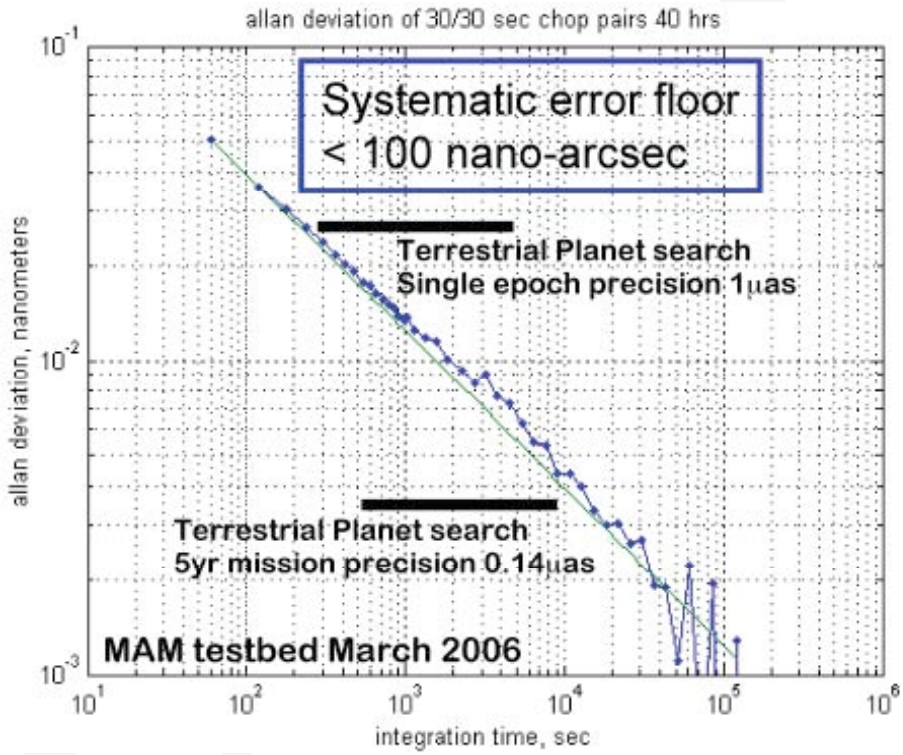

During the 1100 sec time allocated to each axis in a short visit, the angle between the target star and the baseline vector is measured to a "single-star uncertainty" of about 1.0 μas for SIM-Lite and Planet Hunter (and about 0.7 μas for SIM PlanetQuest). Likewise the angle between each of the reference stars and the baseline vector is measured, and the results combined to give the average of the reference stars, to a similar "single-star uncertainty" of about 1.0 μas (or 0.7 μas for SIM PlanetQuest). The angle between the target and reference group is the difference of these angles. The uncertainty is the "differential-measurement accuracy", which is $[(1.0\ \mu as)^2 + (1.0\ \mu as)^2]^{1/2} = 1.4\ \mu as$ along one axis (= 0.98 μas for SIM PlanetQuest).

The key to microarcsecond precision lies in the measurement process, which is doubly differential. Differential in angle, over 1 degree, and differential in time over a chop cycle of about 90 s. First-order errors are entirely eliminated.

SIM's laboratory measurements have shown that measurements are photon-noise limited to at least x = 0.035 μas. Up to 1600 (1890) 1.4 μas (1 μas) can be combined with square-root scaling laws remaining valid for SIM-Lite/PlanetHunter (SIM). The noise floor is well below the 0.3 μas signature of an Earth around a sunlike star at 10pc.

The MAM results were obtained in a test environment substantially worse than that expected for SIM on orbit. Subsystem tests, such as MAM, validate SIM through integrated models that link them. This model linkage was itself defined as a technology milestone and was subjected to rigorous peer review.

The minimum detectable planetary astrometric signature (MDAS) is the instrument noise floor (0.035 μas for SIM-Lite and Planet Hunter, 0.021 μas for SIM PlanetQuest) times the SNR needed. This is 0.21 μas for SIM-Lite and Planet Hunter and is 0.14 μas for SIM PlanetQuest.

The minimum detectable Earth-like planet mass is dependent upon the MDAS, stellar distance, stellar mass and the planet's orbit. For a one Solar mass star at 10 pc, the minimum detectable habitable-zone planet mass depends upon where the planet is in the habitable zone. SIM-Lite and Planet Hunter, can detect a 0.44 Mearth planet at the outer edge of the habitable-zone (0.29 Mearth for SIM PlanetQuest); 0.7 Mearth at a 1AU postion (0.47 Mearth for SIM PlanetQuest); and 0.85 Mearth at a the inner edge of the habitable zone (0.57 Mearth for SIM PlanetQuest).

2.3 Technology

As in the previous section, only technology related to the highest priority, micro-arcsecond astrometry mission is considered in depth, though several other programs are supported with lower priority.

2.3.1 Past Accomplishments

Background

Optical and infrared interferometry have been well developed for ground applications (e.g., NPOI, KI, VLTI, Chara, etc.), yet these facilities suffer limitations due to coherence size, angle and time imposed by the Earth's atmosphere. A challenge was put forth to convert ground-demonstrated concepts into space-capable hardware and software with sufficient reliability to enable an unattended five to ten year space based mission.

A program was begun at JPL to identify and develop the necessary technologies to enable space-based interferometry missions. This technology program was later attached to the NASA Origins Program office at JPL and then to the Space Interferometry Mission (later renamed SIM-PlanetQuest) in order to provide a more direct reference mission focus to the technology development effort.

From 1996-2005 a Technical Advisory Committee, chaired by Robert O'Donnell, worked with the technology development team to complete the focused SIM technology development program, and continues with the SIM project to review the transition of the technologies into flight-like hardware. Since 2001, a NASA-Headquarters commissioned Independent Review Team (renamed to the External Independent Readiness Board (EIRB)), has evaluated the technical progress of the program, and continue in this role as the SIM project transitions the technology into flight-like hardware.

Previous Interferometric Astrometry Programs

A number of smaller scale interferometric astrometry programs have been developed on the ground and in space to demonstrate the technologies and science for a micro-arcsecond astrometry program. These include:

The Hubble Space Telescope Fine Guidance Sensors (FGS)

While spectacularly successful at locating previously unknown companions to stars, the high-precision radial velocities provided by Doppler spectroscopy only provides a minimum mass, not the actual companion mass. While spectacularly successful at providing parallaxes for thousands of nearby stars, HIPPARCOS could not reliably provide 10% parallaxes for stars more distant than ~100pc. Astrometry with Hubble Space Telescope has provided both.

The many results from the original HST FGS astrometry observations include parallaxes of astrophysically interesting stars (Benedict et al. 2000, 2002a, 2002b, 2003, McArthur et al. 1999, 2001), a parallax for the Hyades (van Altena et al. 1997), a link between quasars and the HIPPARCOS reference frame (Hemenway et al. 1997), determination of low-mass binary star masses (Franz et al. 1998, Benedict et al. 2001), and searches for Jupiter-mass companions to Proxima Cen and Barnard's Star (Benedict et al. 1999). Suceeding those have been FGS studies have been contributing to the study of the lower main sequence mass-luminosity relationship (Henry et al. 1999), the intercomparison of dwarf novae (Harrison et al. 2004), and parallaxes of cataclysmic variables (Beuermann et al. 2003, 2004; Roelofs et al. 2007) and the Pleiades (Soderblom et al. 2005). Most recently themes have been the cosmic distance scale and extrasolar planetary systems. This includes the galactic Cepheid Period-Luminosity Relationship (PLR) ((Benedict et al. 2007)) and the determination of extrasolar planetary masses (Benedict et al. 2002c, McArthur et al. 2004, Benedict et al. 2006, Bean et al. 2007).

Regarding the cosmic distance scale, we have obtained a parallax for the Pleiades which supports the validity of modern stellar interiors modeling. We now have 10% parallaxes for ten Galactic, solar-metallicty Cepheids, resulting in a Period-Luminosity relation that provides distances to the LMC and NGC 4258.

Currently, fewer than10% of the more than 200 candidate exoplanets orbiting nearby stars have precisely determined masses. Because the most successful technique for detecting candidate exoplanets, the radial velocity method, suffers from a degeneracy between the mass and orbital inclination for most of the known exoplanet candidates, only a minimum mass, Msini, is known. FGS has provided masses for planets in these systems: GJ876, 55 Cnc, Epsiloner Eridani, and HD33636.

A preliminary indication that for the first time the degree of coplanarity of an extrasolar planetary system associated with a normal, main sequence star will be established. Beyond that, HST FGS data for similar coplanarity tests on the multiplanet systems associated with HD 128311, HD 202206, μ Ara, and ? Cep is being collected.

The Palomar Testbed Interferometer (PTI; Colavita et al 1999)

Hands-on Training

From 2002--2006 SIM sponsored an interferometry training course for Caltech graduate students and post-docs, and JPL engineers and scientists. This course introduced students to the basics of interferometry theory and practice, and included both six hours of lecture

material, and a two-night observing session for students at the Palomar Testbed Interferometer. The school lectures included both interferometry theory for both interferometric imaging and interferometric astrometry, as well as a description of preparing for observing and reducing/interpreting data. The observing sessions specifically gave students hands-on experience in preparing observing plans, preparing the interferometer for observations (students participated in nightly alignments), and in the reduction of data (e.g. homework assignments including reducing and interpreting data taken the night before).

Demonstration of Dual-star Astrometry

PTI has demonstrated an astrometric precision of <100 micro-arcseconds between the components of a bright visual binary (Lane et al 2000). PTI is a long-baseline infrared interferometer at Palomar Observatory developed under NASA funding to demonstrate technology for future ground and space interferometers. The specific experiment mentioned above used PTI in dual-star mode, where the field at each telescope was separated into two narrow fields containing the two components of the bright visual binary 61 Cyg, which were separated in declination by 26 arcsec. The interferometer incorporates two separate interferometer beam trains, including optical delay lines and fringe trackers. Laser metrology is used to measure the delay required to detect fringes, as well as to reference the two beam trains to common fiducials at each telescope.

In the experiment, half the light from one component of the binary was continually tracked by one fringe tracker. The other fringe tracker switched, one a several minute timescale, between the two components of the binary. The key observable was the laser-measured change in delay between the two components, as corrected by residual fringe tracking errors.

The experiment was conducted over a series of 7 nights in 1999. The final results to rms residuals in the measurement of declination of 97 uas, demonstrating the feasibility of high precision narrow-angle astrometry from the ground.

PHASES

The Palomar High-precision Astrometric Search for Exoplanet Systems (PHASES) at PTI is a search for giant planets orbiting closely to either star in binary star systems, with astrometric precisions at the 20 micro-arcsecond level for arcsecond-separation binaries. PHASES is motivated both by a desire to study planets in binaries and as an astrometric program developing tools and techniques for SIM.

Seven refereed journal articles have appeared based on PHASES measurements with another in preparation. PHASES science results include reporting the observational limits to planetary companions in a number of target binaries, the precision orbits of binaries and the measured physical properties of the component stars, and characterization of two triple and two quadruple star systems, including establishing the degree of system coplanarity and the physical properties of the stars.

While the 20 micro-arcsecond precision achieved by PHASES represents progress in the field of interferometric astrometry, it should be stressed that the PHASES hardware can only be applied to a very specific class of binary stars and thus represents no competition to the much more versatile micro-arcsecond astrometry mission being promoted for 2010-2020. Technology and analysis efforts are shared between the two, and the micro-arcsecond astrometry mission will benefit from the efforts of the PHASES project.

The Space Interferometry Technology Development Program

In preparation for a micro-arcsecond astrometry mission, a technology program developed and tested components based on the Goal-level performance requirements set by the previous Decadal Surveys: 4 μas wide-angle mission accuracy over the full sky and 1 μas narrow-angle single measurement accuracy over a 1° field of regard. The components were then integrated into subsystem-level testbeds that were used to verify whole branches of the error budget to ensure that there were no missing terms. Finally, system-level testbeds were developed to fully demonstrate that the components functioned as expected in a system with full complexity.

This progressive flow from components, through subsystems, to system-level testbeds occurred for two paths: (1) Real-time optical-path-difference (OPD) nanometer-level control and (2) Picometer-level-knowledge sensing. The nanometer control path verified that vibrations and spacecraft attitude control induced motions could be rejected to a level that allowed acceptable interference fringe visibility (requires better than 10 nm optical path difference stability). The picometer sensing path verified that dynamic displacements of optical elements within the instrument could be measured to a relative precision of a few picometers and absolute distances between elements could be measured to an accuracy of approximately one micron over distances to ten meters.

A complete technology plan focusing on the SIM reference mission was first formally signed by the Origins Program Office in January 1998 and updated in 2003 and signed by NASA Headquarters. Eight (8) key technology developments from this plan were identified as "Technology Gates" with specific objectives, completion dates, and review requirements (TAC and EIRB) as a means for NASA Headquarters to carefully monitor progress. *All 8 Technology Gates have been completed and met their objectives.* These eight gates and their current statuses are listed in the following table.

Technology Gate	Description	Due Date	Complete Date	Performance
1	Next generation metrology beam launcher performance at 100pm uncompensated cyclic error, 20pm/mK thermal sensitivity	8/01	8/01	Exceeded objective
2	Achieve 50dB fringe motion attenuation on STB-3 testbed (demonstrates science star tracking)	12/01	11/01	Exceeded objective
3	Demonstrate MAM Testbed performance of 150pm over its narrow angle field of regard	7/02	9/02	Exceeded objective
4	Demonstrate Kite Testbed performance at 50pm narrow angle, 300pm wide angle	7/02	10/02	Exceeded objectives
5	Demonstrate MAM Testbed performance at 4000pm wide angle	2/03	3/03	Exceeded objective
6	Benchmark MAM Testbed performance against narrow angle goal of 24pm	8/03	9/03	Exceeded objective
7	Benchmark MAM Testbed performance against wide angle goal of 280pm	2/04, 5/04*	6/04	Met objective
8	Demonstrate SIM instrument performance via testbed anchored predicts against science requirements	4/05	7/05	Met objective

Legend

pm = picometer

mK = milliKelvin

dB = decibel (50dB = factor of 300)

* NASA HQ directed a scope increase (by adding a numerical goal to what had been a benchmark Gate) and provided a 3 month extension when performance fell short

Each of the eight technology Gates developed specific test, modeling, measurement and success criteria that were reviewed by and agreed to with the TAC and EIRB prior to testing. These formed the basis for the post-test evaluation to determine whether or not the test was successful in meeting the objectives of the Technology Gate.

Numerical modeling was a central part of the SIM technology program. Numerical diffraction modeling tools were verified for picometer accuracy over the whole range (near field, mid field and far field) using a testbed specifically developed at Lockheed Martin, Sunnyvale, CA for enabling specific test case comparison to modeling predictions. Opto-mechanical modeling tools were verified at the milli-Kelvin level, again using special testbeds developed at Lockheed Martin, Sunnyvale, CA, and at JPL in Pasadena, CA. These testbed-model comparisons showed excellent agreement (better than a factor of two over the full range of test). This experience, coupled with a similar factor of two or better performance on the subsystem and system level technology testbeds, has provided confidence in the predictive power of the modeling tools used for design and evaluation of the SIM flight system.

Another outcome of the modeling effort was the verification of the full SIM error budget, which showed consistency of the interplay between the terms in the error budget and, perhaps as importantly, showed that there were no missing terms in the error budgets (which would have shown up as un-modeled errors in the subsystem and system testbeds). This is very important in reducing the risk that there will be fundamental surprises during the flight system design, development, test and operations.

The technology program was completed in July 2005 and the final closeout report was signed by NASA Headquarters in March 2006 after extensive review and discussion with the TAC and EIRB. Detailed discussion of the SIM technology program can be found in recent SPIE and IAC papers by Laskin.

Engineering Milestones

SIM continues to transition technology to flight-qualifiable hardware through a series of engineering milestones aimed at building flight-like hardware that is environmentally (when required) and performance tested to verify its capability to perform to flight requirement allocations. These flight-like hardware assemblies are called brassboards and demonstrate that flight hardware for the SIM mission can be built. Each of these Engineering Milestones are subject to the same TAC/EIRB establishment of test and success criteria prior to testing and subject, post testing, to detailed review by the TAC/EIRB against these success criteria, exactly the same process as was used for the technology program.

The nine Engineering Milestones that were established for SIM are presented in the following table, showing the five that will be completed during the Formulation phase (Phase A/B) and the four that were to be completed during the Implementation Phase (Phase C/D/E) prior to the critical design review (CDR). Of the Formulation Phase EMs, all five have been successfully completed.

Formulation Phase				
EM-1	External Metrology Beam Launcher Brassboard (meet Qual environmental and allocated picometer performance)	5/31/06	6/5/06	Exceeded Objective
EM-2	Internal Metrology Beam Launcher Brassboard (meet Qual environmental and allocated picometer performance)	4/30/06	5/3/06**	Exceeded Objective
EM-3	Metrology Source Assembly Validation (meet Qual environmental and allocated performance)	6/30/06	6/28/06	Exceeded Objective
EM-4	Spectral Calibration Development Unit (SCDU) (demo flight-traceable fringe error calibration methodology and validate model of wavelength-dependent measurement errors)	8/30/07	12/10/07	Met Objectives
EM-5	Instrument Communication H/W & S/W Architecture Demo (validate SIM's multi-processor communications system using two brassboard instrument flight computers, ring bus, and flight software version 2.0 with specific S/W functions as listed)	4/1/07	3/5/07	Met Objectives
Implementation Phase				
EM-6	Engineering Models for Metrology Fiducials (double and triple corner cubes fully meeting SIM flight requirements)	9/30/2007*	Deferred Indefinitely along with mission	
EM-7	Metrology Source Engineering Models (optical bench; fiber splitters; fiber switches; fiber distribution assembly; laser pump module: all fully meeting SIM flight performance requirements per table).	9/30/2008*		
EM-8	Instrument/Mission Performance Prediction (update Tech Gate #8 using latest hardware results).	9/30/2008*		
EM-9	Integration of S/C FSW build-1 with phase-1 of the S/C engineering model testbed (demonstrates specific S/W functions)	10/1/2008*		

* Completion dates deferred indefinitely due to FY07 NASA decision to delay SIM indefinitely.

** Actual signoff by NASA HQ delayed until 12/12/06 due to requests for additional thermal testing by the TAC and EIRB boards.

Many components have been engineered to flight-ready status. These are summarized in the following figure:

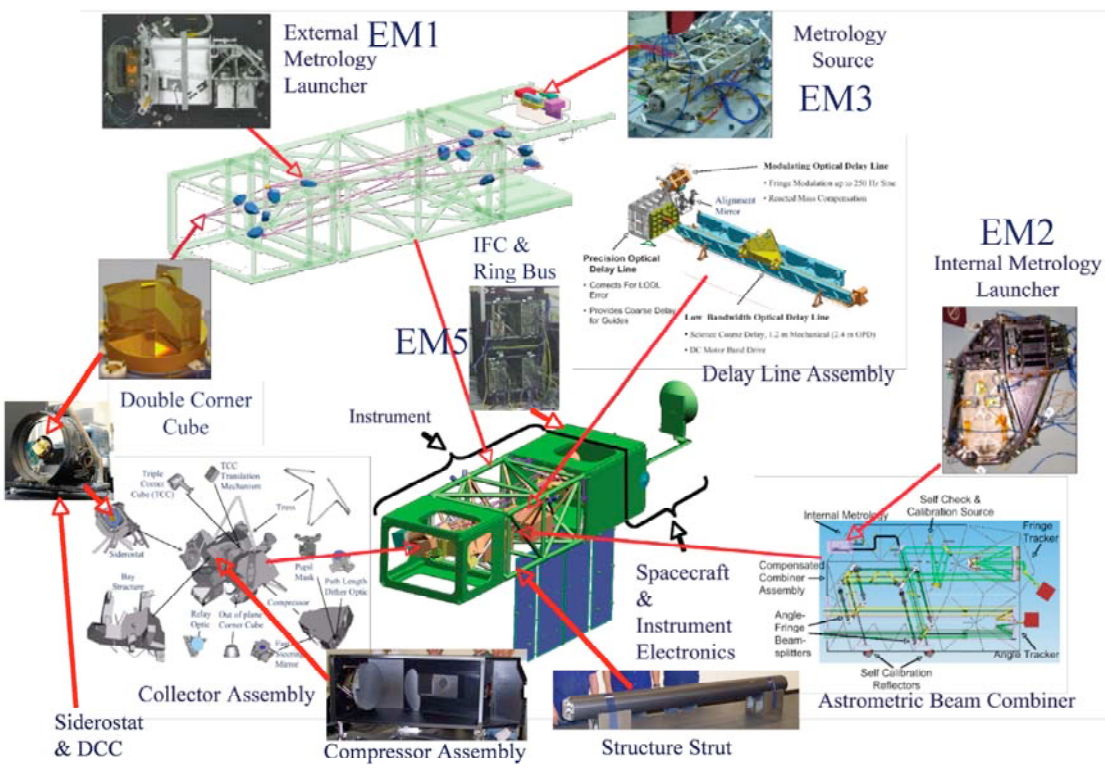

2.3.2 Future Milestones

With well over $100M invested in the development of this technology, remaining risks for a user of this technology are the usual ones that occur during the implementation of any large system (manufacturing errors, interface mismatches, personnel errors, etc.).

Completion of Engineering Milestones 6-9

The remaining Engineering Milestones will be completed as the mission moves into its implementation phase.

Developing Hardware and Software into Flight Qualifiable Components

Engineering development continues for turning the demonstrated components into flight qualifiable hardware and software. This effort has shown that, even for the most sensitive picometer-hardware, these components can be built using conventional flight hardware fabrication techniques with no degradation in performance from that of the technology demonstrations.

Flight Software Development

Technology testbeds developed for SIM have demonstrated all key algorithms for control and measurement of the instrument. The fifth engineering milestone demonstrated a distributed computing environment that supports the strict timing requirements for high-bandwidth control of hardware that is distributed over a very large structure (for example, SIM or TPFI). Processing of the SIM testbed measurements have taught the team how to process the instrument output to achieve the required measurement accuracy and precision in ways not anticipated early in the technology program, significantly relaxing hardware requirements. These data-processing lessons-learned should form the basis for ground processing for any flight interferometer.

Combining Science Payload and Spacecraft

Interactions between the spacecraft bus and the instrument are also well understood. These interactions include: vibration suppression (simple two-stage passive vibration isolation is sufficient), attitude stabilization for beam walk suppression (using the two guide interferometers as a micro-arcsecond two-axis star tracker to control the spacecraft attitude control system; about 10^6 times more accurate than a typical spacecraft star tracker), and torque feed-forward from the instrument to the spacecraft attitude control system to minimize attitude disturbances resulting from the motion of instrument siderostats and delay lines.

Double-Blind Test of Planet Finding Capability

A double-blind planet finding capability study is underway at the request of NASA SMD APD's Jon Morse. This study includes five external teams to generate model planetary systems that are consistent with what is known about planetary systems today, a simulated data generation team at Caltech, five data analysis teams (four external and one within the SIM project at JPL), an independent review/reporting team and a NASA appointed External Independent Readiness Board to oversee the entire process and advise NASA. This study will complete its first phase in August 2008 that will evaluate the capability of an astrometric planet finding mission for 48 distinct planetary system examples. Substantial

follow on work is expected that will ultimately evaluate a full mission simulation for SIM-Lite or Planet Hunter.

Analysis of SIM-Lite's Astrometric Capabilities

A RFP has been made for ~20 separate studies for what can be accomplished with SIM-Lite's astrometric capability, some of which are expected to address planet finding capability. The RFP can be found on the MSC.caltech.edu web site. Proposals are due June 13, 2008 and will result in one-year contract awards.

Completion of the PlanetHunter Strategic Mission Concept

A "PlanetHunter" Astrophysics Strategic Mission Concept Study is currently underway that will complete by March 2009. This study will include independent cost estimates of the Planet Hunter mission concept.

Selection of Mission Concept to be Deployed

SIM-based concepts are expected to be reviewed by the upcoming Astrophysics Decadal Survey. Planet Hunter and a version of SIM-Lite are expected to be presented for review.

2.4 Research and Analysis Goals

2.4.1 R&A in 2010-2020

The top science goals for astrometry related to exoplanet science in the 2010-2020 decade are:

- Detect earthlike planets in the habitable zones of nearby stars.
- Characterize earthlike planets in the habitable zones of nearby stars, including important physical quantities such as mass.
- Characterize the orbits of earthlike planets in the habitable zones of nearby stars, in preparation of a direct imaging mission, to make direct imaging more efficient.
- Characterize exoplanet systems with multiple planets, including planet-planet interactions and orbital coplanarities, quantities important in understanding the formation and evolution of planetary systems.

All are addressed by an astrometric mission capable of single measurement precisions on the scale of a micro-arcsecond or better. The committee finds the best way to achieve these goals is to deploy a space-based astrometry mission based on the SIM architecture, in the early part of the decade.

Previous decades have been spent analyzing the mission design for a micro-arcsecond astrometry mission. This decade should be spent operating such a program and analyzing the science products it returns.

The astrometry committee recommends a timeline that will obtain enough results from a micro-arcsecond astrometry mission by the end of the decade for analyzing results impacting the design of future direct imaging programs.

The astrometry committee strongly supports the non-exoplanet science programs such a mission would enable.

DRAFT

More modest astrometry programs will contribute to the understanding of giant planets, the dynamics of multiplanet systems, the variety of stars that host planets, and take advantage of the nature for astrometry to grow more sensitive to exoplanets with longer observing programs (longer period planets have larger astrometric signatures on the host star).

No science analysis effort is complete without the support of dedicated theorists. The astrometry committee recommends supporting theoretical efforts in planet formation, dynamics, and conditions for habitability.

2.4.2 Astrometry Beyond 2020

On page 28, the ExoPTF report finds that for the 11-15 year (2019-2023) timeframe "Assuming the space-borne astrometric mission described above is fielded in the second time epoch, no additional major space-based astrometric effort is envisioned in this time frame." The committee agrees with this conclusion.

Beyond the currently envisioned micro-arcsecond class astrometry mission, what roles might astrometry play in the field of exoplanets? First, longer-term monitoring of stars can capitalize on astrometry's increasing sensitivity with planet period. A many-decade survey from ground or space, such as that being initiated at the VLTI with PRIMA, will contribute to the understanding of outer planets around other stars. Second, one can consider the fundamental astrophysical limits to the astrometric technique, given an otherwise perfect instrument. A summary evaluation in comparison to the radial velocity technique is given as follows (Catanzarite, Law & Shao 2008), in regards to sensitivity to low mass planets.

From studies of our own star, as well as nearby FGK dwarfs, we expect the flux of solar-type stars to vary in a complex way over many timescales. Intensive study of the Sun's flux variability from space over that past few decades has revealed that it is (down to hourly timescales) mostly accounted for by magnetic surface features such as sunspots (dark regions) and faculae (bright regions). The evolution of sunspots and faculae introduce jitter into the Sun's centroid and radial velocity. Typical sunspot group lifetimes are about 10 days; within this coherence time, the jitter is systematic and cannot be averaged down by multiple measurements. Sunspot jitter can be considered as 'noise' in astrometric and RV measurements, and can be quantified. Using a dynamic sunspot model to match the Sun's flux variability it is found that the intrinsic jitter of the Sun's centroid is about 0.7 micro-AU per measurement for a signal with a period near one year (such as Earth in a 1 AU orbit), and the radial velocity jitter is about 0.6 m/s per measurement.

The astrometric jitter in a measurement of the Sun's angular wobble depends on distance; at 10 pc it's ~ 0.07 uas. With 100 measurements spaced farther apart than the coherence time, the jitter averages down to 0.007 uas, a factor of 5 *below* the instrumental systematic noise floor of 0.035 uas, and 40 times lower than the signature of Earth. Thus starspots, expected to be the major astrophysical contribution to noise in astrometric measurements of stars, do not pose a significant problem for detection of habitable planets around solar-type stars. On the other hand radial velocity jitter noise due to sunspots is about 7 times *higher* than the Earth's RV signal. A good detection of Earth requires averaging down the noise to 6 times *lower* than the RV signal. So sunspot jitter imposes a severe limit on the capability of the RV method to detect Earth around a star like the Sun. Even in the absence of other astrophysical and instrumental effects, it would take 35 years (1800 measurements spaced apart by more than a week) to detect Earth via RV. But stellar pulsations and granulation also introduce RV jitter in measurements of solar-type stars. The intrinsic

astrophysical noise floor for RV measurements due to all of these processes is thought to be at least 1 m/s. In the long-term, efforts to improve the astrometric precisions of focal plane arrays may make future giant space telescopes useful for precision astrometry.

2.5 Contributors

Angelle Tanner, JPL, Local Organizing Committee Astrometry Lead

G. Fritz Benedict, University of Texas, Austin

Alan Boss, Carnegie Institution

Matthew Boyce, Helios Energy Partners

Robert Brown, Space Telescope Science Institute

Geoffrey Bryden, JPL

Adam Burrows, Princeton University

Joseph Catanzarite, JPL

M. Mark Colavita, JPL

David Cole, JPL

Rolf Danner, Northrop Grumman Space Technology

Dennis Ebbets, Ball Aerospace & Technologies Corp.

Carl Gillmair, Spitzer Science Center

Sally Heap, NASA GSFC

N. Jeremy Kasdin, Princeton University

Marc Kuchner, NASA GSFC

Benjamin Lane, Charles Stark Draper Laboratory

Nicholas Law, CalTech

Charles Lillie, Northrop Grumman Space Technology

Walid Majid, JPL/CalTech

Geoff Marcy, University of California, Berkeley

James Marr, JPL

Barbara McArthur, University of Texas, Austin

Stanimir Metchev, UCLA

Jun Nishikawa, NOAJ

Charley Noecker, Ball Aerospace

Xiapei Pan, JPL

Guy Perrin, Observatoire de Paris/LESIA

Meyer Pesenson, CalTech

Steven Pravdo, JPL/CalTech

DRAFT

Stephen Rinehart, NASA

Jean Schneider, CNRS-Paris Observatory

Stuart Shaklan, JPL

Michael Shao, JPL

Wesley Traub, JPL

Stephen Unwin, JPL

Julien Woillez, W.M. Keck Observatory

2.6 References

Cameron, B., Britton, M. & Kulkarni, S., "Precision Astrometry with Adaptive Optics," submitted May 2008, [arXiv:0805.2153]

Catanzarite, J., Law N., & Shao, M., "Astrometric Detection of exo-Earths in the Presence of Stellar Noise," Proc. SPIE, 7031-91 (2008)

Cumming, A., Butler, R. P., Marcy, G. W., Vogt, S. S., Wright, J. T., and Fischer, D. A., "The Keck Planet Search: Detectability and the Minimum Mass and Orbital Period Distribution of Extrasolar Planets," PASP, 120, 531-554 (2008).

Hirota, T., et al. "Distance to Orion KL Measured with VERA," PASJ, 59, 897 (2007)

Honma, M. et al. "Astrometry of Galactic Star-Forming Region Sharpless 269 with VERA: Parallax Measurements and Constraint on Outer Rotation Curve," PASJ, 59, 889 (2007)

Ida, S. & Lin, D.N.C. "Toward a Deterministic Model of Planetary Formation. II. The Formation and Retention of Gas Giant Planets around Stars with a Range of Metallicities," ApJ, 604, 413 (2004)

Lane, B., et al. "Direct detection of pulsations of the Cepheid star ζ Gem and an independent calibration of the period-luminosity relation," Nature, 407, 485, (2000)

Mayor, M & Queloz, D. "A Jupiter-Mass Companion to a Solar-Type Star," Nature, 378, 355 (1995)

Pravdo, S.H., Shaklan, S.B., Henry, T., Benedict, G.F. "Astrometric Discovery of GJ 164B," ApJ, 617, 1323 (2004)

Pravdo, S.H., Shaklan, S.B., & Lloyd, J.P. "Astrometric Discovery of GJ 802b: In the Brown Dwarf Oasis?" ApJ, 630, 528 (2005)

Pravdo, S., Shaklan, S., Redding, D. , Serabyn, E., & Mennesson, B. 2007, "Finding Exoplanets around Old and Young Low-Mass Stars," whitepaper submitted to the AAAC Exoplanet Taskforce, (2007)

Pravdo, S. H.., Shaklan, S.B., Wiktorowicz, S.J., Kulkarni, S., Lloyd, J.P., Martinache, F., Tuthill, P.G., & Ireland, M.J. "Masses of Astrometrically Discovered and Imaged Binaries: G78-28AB and GJ 231.1BC," ApJ, 649, 389 (2006)

Raymond, S. N., Mandell, A. M., and Sigurdsson, S. "Exotic Earths: Forming Habitable Worlds with Giant Planet Migration," Science, 313, 1413-1416 (2006)

Scargle, S. D.," Studies in astronomical time series analysis. II - Statistical aspects of spectral analysis of unevenly spaced data," ApJ, 263, 835 (1982)

DRAFT

Tarter, et al. "On the Habitability of Planets Around Red Dwarf Stars, Astrobiology," 7, 30-65 (2007)

Unwin, S., et al. "Taking the Measure of the Universe: Precision Astrometry with SIM PlanetQuest", PASP, 120, 38 (2008)

Wetherill, G. W. "The Formation and Habitability of Extra-Solar Planets," Icarus, 119, 219-238. (1996)

Bean, J. L., et al. 2006a, ApJL, 653, L65

Bean, J. L. et al. 2006b, ApJ, 652, 1604

Bean, J. L. et al. 2007, AJ, 134, 749

Benedict, G. F. et al. 1998, AJ, 116, 429

Benedict, G. F. et al. 1999, AJ, 118, 1086

Benedict, G. F. et al. 2000, AJ, 119, 2382

Benedict, G. F. et al. 2001, AJ, 121, 1607

Benedict, G. F. et al. 2002a, AJ, 123, 473

Benedict, G. F., et al.. 2002b, AJ, 124, 1695

Benedict, G. F., et al. 2002c, ApJL, 581, L115

Benedict, G. F., et al. 2006, AJ, 132, 2206

Benedict, G. F., et al.. 2007, AJ, 133, 1810

Beuermann, K. et al. 2003, A&Ap, 412, 821

Beuermann, K. et al. 2004, A&Ap, 419, 291

Franz, O. G. et al. 1998, AJ, 116, 1432

Fitzpatrick, E. L. et al. 2003, ApJ, 587, 685

Fouqu´e, P., et al. 2007, ArXiv e-prints, 709, arXiv:0709.3255

Groenewegen, M. A. T. et al. 2004, A&Ap, 420, 655

Harrison, T. E. et al. 1999, ApJL, 515, L93

Harrison, T. E. et al. 2004, AJ, 127, 460

Herrnstein, J. R., et al. 1999, Nature, 400, 539

Kennicutt, R. C. et al. 1998, ApJ, 498, 181

Macri, L. M. et al. 2006, ApJ, 652, 1133

McArthur, B. et al. 1997. in Proc. 1997 HST Calibration Workshop, ed. S. Casertano, R.

Jedrzejewski, T. Keyes, and M. Stevens, STScI Publication, Baltimore, MD

McArthur, B. E. et al. 1999, ApJL, 520, L59

McArthur, B. E. et al. 2001, ApJ, 560, 907

McArthur, B. et al. 2002, The 2002 HST Calibration Workshop, Edited by Santiago Arribas,

Anton Koekemoer, and Brad Whitmore. Baltimore, MD: Space Telescope Science Institute,

DRAFT

2002, p.373

McArthur, B. E., et al. 2004, ApJL, 614, L81

McArthur, B. E. et al. 2006, The 2005 HST Calibration Workshop: Hubble After the Transition to Two-Gyro Mode, 396

McArthur, B. E., et al. 2008, in preparation

Ngeow, C.-C. et al. 2005, MNRAS, 363, 831

Perryman, M. A. C. et al. 1997, A&Ap, 323, L49

Roelofs, G. H. A. et al. 2007, ApJ, 666, 1174

Schaefer, B. E. 2007, ArXiv e-prints, 709, arXiv:0709.4531

Soderblom, D. R. et al. 2005, AJ, 129, 1616

Takeda, G.,et al. 2007, ApJS, 168, 297

Tull, R. G. 1998, Proc. SPIE, 3355, 387

Udalski, A. et al. 1999, Acta Astronomica, 49, 201

Udry, S. & Santos, N. C., 2007, Ann. Rev. Astron. & Astrophys., 45, 379.

van Altena, W. F., et al. 1997, ApJL, 486, L123

van Leeuwen, F. et al. 2007, MNRAS, 379, 723

Zaritsky, D. et al. 1994, ApJ, 420, 87

DRAFT

3 Direct Optical Imaging of Exoplanets

Chair: Rémi Soummer, AMNH

Marie Levine, JPL

3.1 Introduction

This chapter studies the direct detection and spectral characterization of extrasolar planets using optical methods: internal coronagraphs, external occulters, and hybrid systems. We build on previous reports (TPF-C STDT [ref], TPF-C Technology Plan [ref], Exoplanet Forums [ref], Exoplanet Task Force [ref]), which focused mainly on detection and characterization capabilities for a flagship mission using an internal coronagraph.

The goal is to study a range of possible mission scales, and to establish a technology plan for these missions. We identify a few relevant scales compatible with current NASA plans for a line of probe-size missions ($600M without launch vehicle) followed by a flagship (>$1B). We do not discuss details of proposed concepts, but rather present classes of mission types, where TPF-C denotes a large internal coronagraph, and TPF-O an external occulter.

The ExoPTF recommended that indirect methods (astrometry or radial velocities) are necessary to obtain a direct measurement of the masses, orbital parameters, and planet "addresses". For a characterization-only mission (i.e. if the planets are already known), the Inner Working Angle (IWA) could probably be increased, and the mission duration reduced; but other driving requirements on the system, such as stability, pointing, contrast, spectral coverage and spectral resolution, remain essentially the same as for a full search-and-characterize mission. The technology plan we propose is therefore valid in both cases.

Observing strategies and mission scales must be designed in tandem between the astrometric and imaging program. Careful Design Reference Mission (DRM) development over the next several years will articulate the tradeoffs in cost and performance between imaging missions with and without astrometric precursors.

We recognize the merits of this strategy developed by the ExoPTF, and expand on its recommendation in the short term: a probe-scale direct imaging mission can be combined with existing Radial Velocities and ground-based Astrometry (PRIMA, [ref]) for the characterization of mature giant planets, Neptunes, and super Earths. A probe scale will also detect and characterize exozodiacal disks, a problem ExoPTF identified as critical for future terrestrial planet imaging missions.

This strategy is independent from a space astrometric mission both in terms of scientific goals and timing sequence, and therefore offers an alternate and coherent program especially if an astrometric mission to detect Earth-size planets is not recommended.

DRAFT

Chapter recommendations:

1) *Probe-scale mission (1.5 m class telescope at ~$600M) starting within the next two years, for exoplanetary systems characterization that is not accessible from the ground in the same time frame:*
    a. *Exozodical characterization (1 zodi at 1-3 AU) of brightness, structures and clumpiness. This is critical for future characterization of habitable Earth-size planets.*
    b. *Direct detection and spectral characterization (0.4 μm to 1.0 μm) of planets and planetary systems, including at least 13 known RV Giant planets. We also anticipate detection and characterization of heretofore-unknown Neptune-mass planets and Super Earths.*
2) *Long-term flagship mission for characterization of potentially habitable Earth-Size planets.*
3) *Aggressive and sustained technology development starting immediately to meet readiness by mission start, including near-space environment opportunities (rockets & balloons).*
4) *R&A support for developing preliminary science and maturing mission designs in particular for the definition and optimization of combined Astrometry/RV and imaging missions.*

3.1.1 Science Goals and Requirements

Flagship-scale goals

There is no question that the direct detection of a terrestrial planet in the habitable zone of a nearby star would be of monumental importance. The various TPF study reports (e.g., Levine et al. 2005, Lunine et al. 2008), and a sizeable literature have focused on strategies for characterizing such worlds and searching for signs of life.

Earth-size planets lying inside of the habitable zone of nearby stars generally will not be massive enough to exhibit a detectable RV signal and will be too small and faint for even low-resolution spectroscopy with a small telescope, and therefore will require a flagship-size mission for their characterization. It is important to keep in mind that super-Earth size planets (~10 $M_\oplus$) can also be habitable, and recent RV results with HARPS seem to suggest that they are common (Mayor et al. 2008). Such a mission would be able to detect and characterize a large variety of planets from Earth-size to Giant planets.

The main goal is to look for the presence of O_2 and H_2O, which can be identified in Earth's spectrum with a resolution, $R = \lambda/\Delta\lambda$ of 100 (Kaltenegger 2007). This resolution should be able to identify the strong O_2 band at 0.76 μm, and H2O at 0.96 μm. Ozone (O_3), which is formed photochemicaly from O_2 in Earth's atmosphere is also an interesting biomarker but more difficult to detect in the visible. It can be detected in the infrared at 9.6 μm or in the UV at 0.25-0.32 μm. The best combination of biomarkers would be the simultaneous detection of O_2 or O_3 together with a reduced gas like CH_4, which would be undetectable in today's Earth atmosphere but was more abundant on the Proterozoic Earth (2.5-0.54 b.y. ago). CH_4 was probably even more abundant during the Archean Eon, prior to 2.5 b.y. ago, but O_2 and O_3 would have been absent at this time.

Flagship-scale requirements

The science requirements for a flagship-scale mission were set by the TPF SWG [ref] and STDT [ref] as a 95% confidence level of finding one Earth-like planet if the probability of such planets ($\eta_\oplus$) is 0.1. A careful analysis of mission completeness requires development of a comprehensive Design Reference Mission (DRM) that includes realistic observing scenarios, time constraints, photometric integration times, and multiple visits for detection and orbit characterization. For conservative estimates, an approximate mission completeness can be found as the sum of the individual completeness's for each star in the observing program. This gives the expectation value for the total number of planets found and characterized, assuming all stars have one planet drawn from the population of interest and each visit is independent and uses no prior knowledge.

It is the goal of DRM studies to analyze the mission completeness under various assumptions (single or concatenated programs), and refine the mission parameters (instrument and observing requirements). The initial performance requirements derived from these science requirements are assumed to be a contrast of 10^{-10} at an IWA=75 mas, over the spectral range, 0.5-1.0 micron, with a resolution R~100.

ExoPTF has identified two key parameters for the design of a flagship direct imaging mission: the probability of habitable planets ($\eta_\oplus$) and the level of exozodiacal light. These two parameters have a direct impact on the scale of the imaging mission: if $\eta_\oplus$ is high ($\eta_\oplus$>0.1), and if the level of exozodiacal light is smaller than 10 zodi (1 zodi is the local zodiacal light surface brightness seen from Earth), characterization with direct imaging will be within reach of a flagship mission in the near future.

The value of $\eta_\oplus$ is a main goal of the COROT and Kepler missions, and this parameter will be known within the next few years. However, the knowledge of the exozodi at a level relevant for direct imaging is currently unknown, with current ground-based sensitivity of the order of 100 zodis and future instruments (e.g. LBTI), which hope to reach 10 zodis in the infrared. A probe-size high-contrast mission has a unique capability to detect exozodiacal levels down to 1 zodi in the visible and characterize their structure.

According to the ExoPTF recommendations for the study of potentially habitable exoplanets, it is essential to combine detection and orbital characterization by an indirect technique —Astrometry or RV— with characterization using direct imaging for at least two reasons. First, only reflex motion reveals the planetary mass, which is an essential datum for understanding a planet in physical terms, and can supply the "addresses" of planets for their characterization with direct imaging. Second, indirect detection is a more thorough technique for discovering potentially habitable planets. Direct detection searches, by comparison, typically offer low completeness per search observation and seasonal search constraints (Brown et al. 2006)

However, a time-limited mission doing both detection and characterization can be optimized to produce a few detected and characterized planets, assuming high occurrence $\eta_\oplus$>0.1 (Savransky & Kasdin, 2008). In this particular DRM approach, the number of planets found and characterized does not depend strongly on $\eta_\oplus$. This is because most of the mission time is spent characterizing planets with spectroscopy and revisiting them to build an astrometric orbit.

The particular sensitivity of the mission completeness to the IWA can be used to devise a specific observing scenario for an occulter mission (Spergel 2008): a "detection mode" is

used with the starshade at larger distance and smaller wavelengths than for the "characterization mode", in order to minimize the IWA for the detection phase.

The possibility of combined missions (astrometry/RV and direct imaging) requires specific DRM studies including SNR estimations to define a matched set of missions. We introduce the problem of concatenated mission design in Figure 3-1 by showing the astrometric wobble vs. maximum separation for an Earth at the inner edge of the HZ around a qualified sample of stars within 30 pc. This figure updates Figure 11.1 in ExoPTF report by including photometric limits and restrictions of the planetary period.

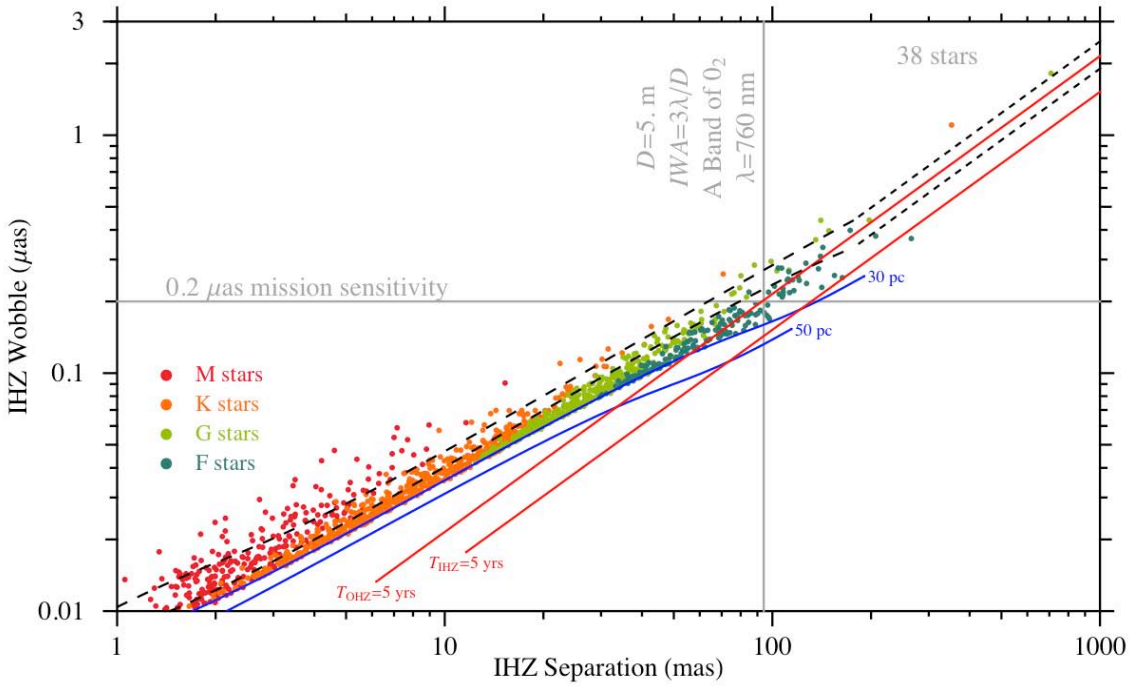

Figure 3-1: Parameter space for estimating the size of stellar samples for an astrometric finder program feeding HZ "Earths" to a coronagraphic characterizer program. (R. Brown)

The horizontal line defines the astrometric requirement (0.2 μas mission sensitivity) and a vertical line defines the IWA requirement for the imaging mission (94 mas). The other parametric assumptions in this figure include the definition of the star list (non-binary, main-sequence Hipparcos stars within 30 pc with $B–V > 0.3$), definition of the coronagraph (efficiency, bandwidth, etc.), definitions of the Inner and Outer Habitable Zones definitions (IHZ=0.82 AU, OHZ=1.6 AU), and the brightness of the exozodi (1 zodi).

For stars above the upper red line, the periods of *all* HZ orbits are less than 5 yrs and therefore formally detectable by periodogram in a 5-year astrometric search program; above the lower red line, *some* HZ periods are less than 5 years and detectable; below the lower red line, *none*. For stars above the *upper* black, dashed line, the coronagraph obtains the A-band spectrum of O_2 at 760 nm, with $R = 100$ and $SNR = 10$ in less than 10^6 sec, for *all* HZ Earths; above the *lower* black line, *some*; below the lower black line, *none*. In this case, some 38 stars are in the first quadrant, where *all* HZ Earths produce an astrometric signature of at least 0.2 μas and are resolved by the 5-m coronagraph. For 6 of 38 stars, all HZ Earths are discoverable by astrometry (period short enough) and characterizable by coronagraphy (bright enough). For 10 more stars, *some* discoverable HZ Earths are

characterizable. For 22 more stars, *some* HZ Earths are discoverable, but none of them characterizable. One star has no discoverable or characterizable HZ Earths.

A detailed study is needed to compute fractional completeness for the concatenated finder and characterizer programs, whatever the techniques. We recommend continued efforts to develop and analyze various DRM approaches, for direct and concatenated missions as initiated by ExoPTF.

Recent improvements in radial velocity techniques allow some hope of finding potentially habitable planets down to a few times Earth mass around solar-type stars. Also, alternate methods for astrometry might be possible, for example with a focal-plane wide field instrument on the direct detection mission itself.

Probe-scale goals

A small mission would be capable of characterizing at least 13 known RV-discovered planets, and could detect large terrestrial planets (~10 Earth mass) around the nearest stars. It would measure exozodiacal brightness down to the level required for Earth-size planet characterization. The ExoPTF has identified this problem as vital.

Exozodiacal dust: Hundreds of sun-like stars have been found to exhibit excess IR emission attributable to dusty circumstellar debris. The vast majority of these systems, however, remain spatially unresolved. High-resolution scattered-light images of debris disks will reveal the morphology of the disks and trace the location of the dust-producing planetesimals, but such images today are rare due to the lack of suitable high-contrast imaging systems.

Dynamical interactions of planets with residual planetesimal belts likely play a vital role in the architectures of planetary systems. Kenyon & Bromley (2004) have shown that recently formed terrestrial planets can generate copious quantities of dust in the early phases of planetary system formation. In our own solar system, Jupiter is thought to have dominated the dynamics in the early evolution of the asteroid belt. Consequently, volatile-rich planetesimals scattered towards our inner solar system may have contributed significantly to terrestrial water abundance, possibly affecting or contributing to the habitability of the early Earth.

High-resolution spatial mapping of the dusty circumstellar debris in exoplanetary systems is needed to test the generic applicability of dynamical models (Morbidelli et al. 2005) in planetary systems other than our own.

Currently deployed high contrast imaging technologies can detect only the largest, most massive, and brightest circumstellar disks, and cannot effectively probe their innermost regions (Oppenheimer et al 2008). The few images obtained to date have provided crucial insights into the formation, evolution, and architectures of exoplanetary systems; but they are just the tip of the iceberg waiting to be fully revealed. The existing sparse sample of debris disks imaged with scattered starlight represents only the youngest (10–100 Myr), or extremely anomalous, disk systems around older stars.

While holding considerable scientific interest of their own, extrasolar zodiacal disks also inhibit the detection and characterization of terrestrial planets. The ExoPTF placed a high priority on measuring exozodiacal light around target stars because levels greater than about 10 times that of the solar system will severely hamper detection of planets. Future ground-based systems (LBTI) are expected to approach this level. However, it is unsure how these measurements at 10 μm can be extrapolated to predict the zodi brightness at

visible wavelengths. A small coronagraph could survey nearby stars and provide confidence that a larger observatory would not be hampered by exozodiacal dust.

Giant planets: Characterization of extrasolar giant planets will follow a hierarchal process that begins with mass and proceeds through atmospheric temperature, composition, and further characterization of the atmosphere. Here we briefly highlight three major science questions that a probe-size mission might address.

Planet Name	M sin i	Period (d)	a (AU)	sep``	Contrast (10^{-9})
Epsilon Eridani b	1.55	2502	3.39	1.06	1.6
55 Cnc d	3.84	5218	5.77	0.43	0.6
HD 160691 c	3.10	2986	4.17	0.27	1.1
Gj 849 b	0.82	1890	2.35	0.27	3.3
HD 190360 b	1.50	2891	3.92	0.25	1.2
47 Uma c	0.46	2190	3.39	0.24	1.6
HD 154345 b	0.95	3340	4.19	0.23	1.0
Ups And d	3.95	1275	2.51	0.19	2.9
Gamma Cephei b	1.60	903	2.044	0.17	4.4
HD 62509 b	2.90	590	1.69	0.16	6.4
HD 39091 b	10.35	2064	3.29	0.16	1.7
14 Her b	4.64	1773	2.77	0.15	2.4
47 Uma b	2.60	1083	2.11	0.15	4.1
HD 89307 b	2.73	3090	4.15	0.13	1.1
HD 10647 b	0.91	1040	2.1	0.12	4.2
HD 217107 c	2.50	3352	4.41	0.12	0.9
HD 117207 b	2.06	2627	3.78	0.12	1.3
HD 70642 b	2.00	2231	3.3	0.11	1.7
HD 128311 c	3.21	919	1.76	0.11	5.9

Table 1: radial velocity planets observable with a probe-size mission

For RV-detected planets two coronagraphic images spaced in fraction of the orbital period will constrain the orbital inclination and thus the mass. This first major science goal places a requirement on the astrometric accuracy of the coronagraphic system (orientation on the sky, angular separation, and position angle of the planet with respect to the star). Table 1 lists the most accessible RV planets to direct imaging. More entries for this list will occur as RV observations continue.

Knowledge of the mass removes the foremost uncertainty in the characterization of a planet and substantially narrows the range of possible interpretations of a given spectrum. Well-characterized planets of known mass can also serve as templates for comparison with other directly detected planets for which there are no RV data.

The atmospheres of the giant planets consist of a thick envelope of hydrogen and helium with an admixture of heavy elements. The temperature determines which molecules are present in the observable atmosphere. The spectra of solar system giants are controlled by a combination of gravity, cloud thickness, and composition. The 'ice giants' (Uranus and Neptune) are blue because of their low gravity, thin clouds, and large methane abundance relative to Jupiter and Saturn. If any of these planets were warmer so that the water cloud was near the optical photosphere then the continua level would be much brighter and the molecular bands less deep. Uranus and Neptune would be less blue. Such trends are evident in the model spectra shown in Figure 3-2, which imagines moving a Jupiter progressively closer to its primary star.

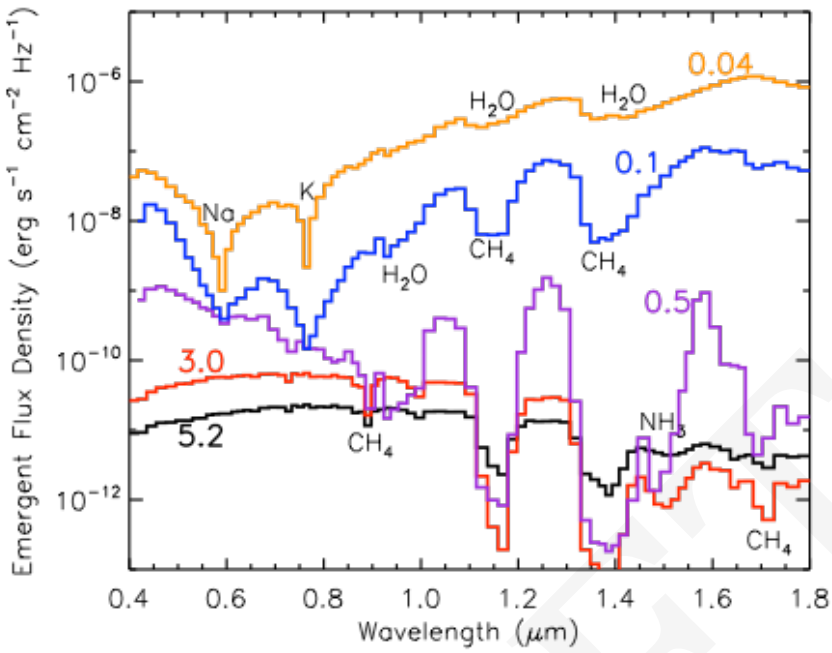

Figure 3-2: Models of progressively warmer Jupiter-mass planet at various orbital distances (labels in AU) from a solar-type star. A similar sequence would be encountered by decreasing the age and/or increasing the mass of the planet. A 4 Jupiter-mass planet would show water clouds at an age of a few Gyr. (Marley et al.)

The second high priority science goal for characterizing extrasolar giant planets would be to obtain either low-resolution spectra or filter photometry to characterize the slope and bands depths of the major absorbers. This would provide constraints on the atmospheric temperature, the presence of bright cloud layers, and given an estimate of the system age, the mass of the planet. The abundance of key absorbers, particularly methane, would provide a test of formation scenarios. For example the core accretion theory describing the formation of giant planets suggests that any massive planet will have a thick envelope of roughly nebular composition surrounding a denser core of rock and ice. Subsequent processes, including bombardment by planetesimals, can enhance the heavier elements. Observed enhancements of carbon in solar system giant planets range from ~ 3× at Jupiter to about 30× solar abundance at Uranus and Neptune. Direct collapse of Jupiter from nebular gas would not result in such a pattern of enrichment.

The third science goal should be the determination of atmospheric composition to infer whether the pattern of enrichment seen in solar system giants holds in other systems as well. The enrichment pattern might vary with the mass of the primary star, the mass of the planet, the orbital semi-major axis or other parameters. Although spectroscopy is in principle better, it may be unobtainable in reality with a small mission. The utility of very low resolution, low SNR spectra needs to be studied. One set of possible filters that might enable the science discussed above is shown in Figure 3-3. The broadband filters would constrain the overall slope while narrower filters might constrain the depths of molecular bands for bright or nearby planets.

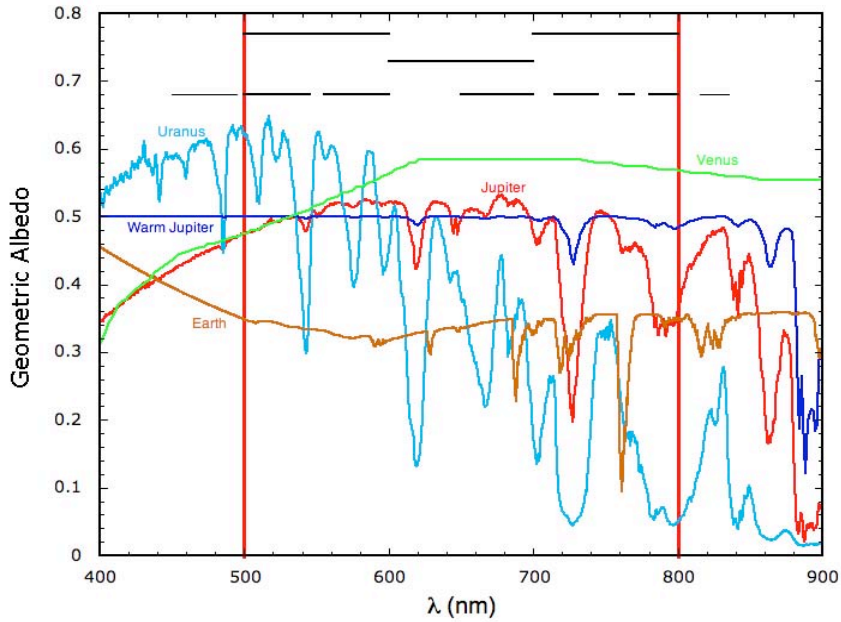

Figure 3-3: Black lines at top show some possible filter choices for a coronagraphic camera. The broad filters detect planets and constrain their spectral slope. Progressively narrower filters provide increasing levels of spectral resolution of key spectral features. (Marley et al.)

As shown in Table 1 there is a great diversity in masses and orbits among the most detectable extrasolar giant planets. By obtaining photometry in a variety of wide, medium, and (for the most favorable objects) narrow bands it will be possible to characterize rich menagerie of worlds. The resulting substantial science yield would be an important legacy of any small mission.

Super Earths: recent results from Radial Velocity with HARPS (Mayor et al. 2008) suggest that these planets are numerous. The challenge for a probe-scale telescope would be detecting and recognizing such planets. Color and absolute brightness might help to discern between, for example, a small gaseous planet, like Neptune, and a large terrestrial planet. However, this may be unreliable, because many different processes influence the color and albedo of a planet, including surface composition, altitude and thickness of clouds, molecular absorbers, and photochemical processes. The color and brightness of Earth has certainly varied over time, for example. Thus unless such a planet is found very nearby, it is likely that a small coronagraph could only obtain a "pale blue dot" image which would undoubtedly lead to calls for a more capable mission to characterize such an intriguing object. If indeed a super Earth is found nearby, a small mission could establish the presence of water vapor bands and possibly recognize water clouds, which would be of extraordinary interest. Also, if an orbit can be constructed from direct imaging, RV measurements might be able to constrain the mass knowing the orbit (Spergel, 2008).

Probe-scale requirements

A probe-scale mission can implement the general ExoPTF recommendation to combine direct and indirect methods, using the overlap between known RV planets and their discovery space. At least 13 of these planets can be characterized with a small space mission (semi-major axis >150 mas). This number of RV planets detectable with a probe-size coronagraph will increase with time as more planets are discovered. We can expect a

few tens of RV planets by the time a probe mission could be in operation. Stars with currently unconfirmed, long-term radial velocity trends would be particularly good targets for such a mission (Marcy 2007).

Ground-based astrometry with 10 μas accuracy with VLT PRIMA will also overlap with the probe-scale imaging mission parameter space, with a sensitivity for nearby (<20pc) late type stars (F-M) down to Saturn size around F stars, and sub-Uranus masses around the M stars, with orbital periods of a few years (1-5 AU) (Launhardt et al. 2005).

For Giant planets, the requirements strongly depend on the age of the objects:

Table 2 Coronagraph performance requirements for detection and characterization of giant planets

Age	Contrast	IWA	$\lambda/\Delta\lambda$	Remarks
Recently Formed	10^{-5}	0.05"	~50	Moderate NIR contrast, small IWA: distant star forming regions (e.g. Taurus).
Young (~100 MYr)	10^{-7}	0.2"	~40	NIR, next generation instruments on 8m telescopes (GPI, SPHERE)
Mature (>2GYr)	10^{-8}-10^{-10}	0.1"	~50	Goal to reach RV planets

3.2 Observatory Concepts

Over the past decade there has been a wide variety of concepts proposed to do high contrast imaging, both on the ground and in space. The architectural approaches for starlight suppression include internal coronagraphs, external occulters and a hybrid. We associate the hybrid with the external occulters, and carry only two categories, internal and external. For each, we identify the most relevant mission scales (Figure 3-4). We emphasize the synergy between direct and indirect detection programs, and consider ground-based projects, suborbital opportunities, and space observatories at the probe and flagship scales.

3.2.1 Architecture scaling for internal coronagraphs

Observatories using internal suppression rely on some version of a coronagraph (or pupil interferometer) to reduce the diffraction of the star. All the starlight enters the telescope and they thus require wavefront sensing and control with exquisite stability to eliminate speckles due to aberrations in the optics. The telescope optics can use conventional diffraction-limited optics such as the one that already exists for Hubble Space Telescope.

Ground-based telescopes

A number of large ground-based telescopes (5-8 m) are being equipped with coronagraphs and Extreme Adaptive Optics (ExAO) to achieve contrast levels of ~10^{-7} at small angles on the sky (0.2 arcsec) in the near infrared. Science goals are the detection and characterization of young giant exoplanets (10MYr -1GYr) and disks. Planets will be detectable by their thermal emission in the near infrared. Their effective temperature and composition can be inferred by comparing to models. These instruments are limited by the uncorrected atmospheric and static wavefront error residuals and by their stability. First results from these projects are expected around 2011. Future Extremely Large Telescopes (e.g. GSMT) with ExAO coronagraphs will enable similar contrasts at a smaller IWA ~30 mas

and higher contrast (~10^{-8}) at separations up to ~1 arcsec. The very small IWA will enable the study of more distant star forming regions, and improved contrast will enable the study of some reflected light Jovian planets around nearby stars. High contrast instruments on GSMT can be expected to produce results around 2020.

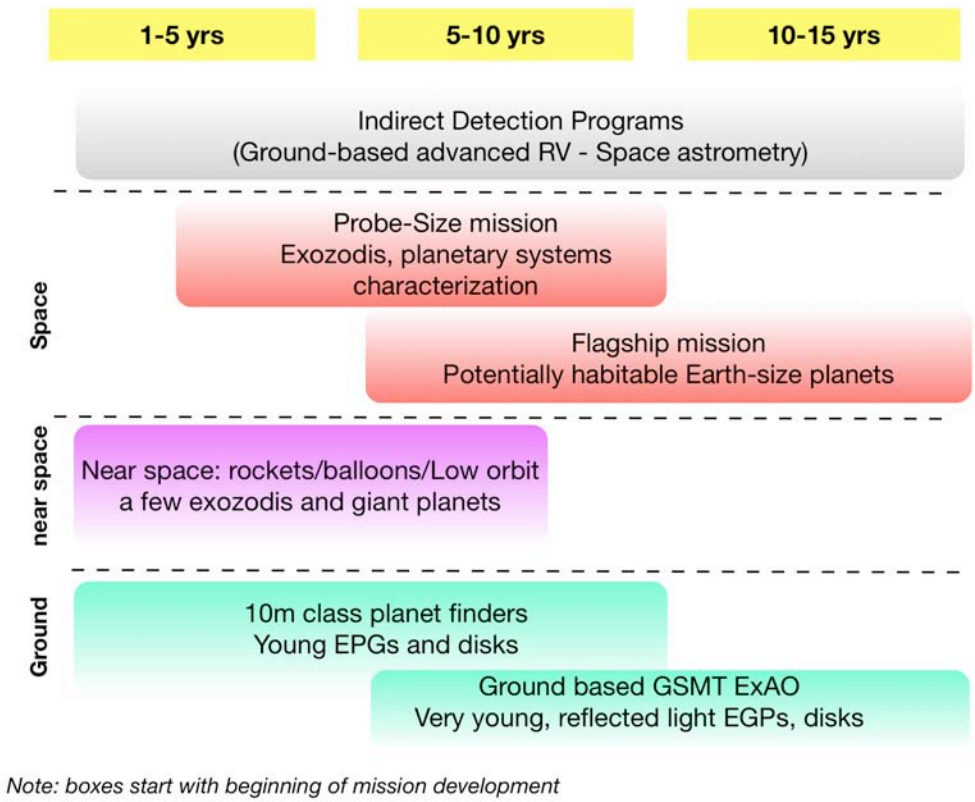

Figure 3-4 Range of relevant mission scales for direct imaging to enable a complete scientific and technological program.

Suborbital environments

Suborbital experiments with sounding rockets or balloons offer interesting possibilities for technology development and risk reduction, in order to help advance laboratory concepts to flight status. They would also be able to make observations of a few exoplanets, planet forming and exozodiacal disks.

A coronagraph instrument on a balloon-borne gondola requires the platform to be able to point at a star with stability of 1 arcsec or better (demonstrated in the lab and in flight). Lightweight telescope mirrors (0.8 to 3.0m) already exist, e.g. 3.5-m SiC primary demonstrated on Herschel. Critical requirements include internal fine-pointing capability, and minimally distorting air path near to and above the telescope (Traub & Chen 2007).

Sounding rockets can also play a role in the development of direct imaging science with 500 kg payloads, and a 600 s flight time at 400 km altitude. The payload is recovered via parachute and can be re-flown. NASA currently flies of order 10 flights each year. Plans exist to fly a 50-70 cm telescope and point it to 1-2 stellar targets (Shao et al. 2007).

Probe-size missions

The first relevant scale for space imaging missions is the "probe mission" scale (~$600M), where it becomes reasonable to consider 1.5m class telescopes and very high contrast coronagraphic instruments (10^{-9}-10^{-10}). This would allow measurements of exozodiacal disks levels, characterize mature giant planets and planetary systems known from RV, and possibly image a few super Earths around nearby stars. Because of the small telescope diameter, IWA is a critical parameter for this mission scale, which affects search completeness. The most promising coronagraph approaches suggest IWA in the 2-3 λ/D range. Active wavefront control is needed to correct optical aberrations with tight stability requirements to maintain the corrected images quality during an observation.

Flagship-size missions

The next size scale is the "flagship" class mission (>$1B) with a telescope diameter of 4 to 8 m. While this introduces new engineering challenges associated with large mirrors in space, it opens up the possibility of imaging terrestrial planets in the habitable zone of the parent star. An essential requirement for the mission scaling is the mission completeness: smaller missions (4-5 m) have a smaller set of stars available and thus a smaller number of potential planets and greater sensitivity to $\eta_{\oplus}$. They require the highest performing coronagraphs (IWA of 2-3 λ/D) and tighter stability.

A larger telescope may allow a relaxation in the IWA requirement to about 4 λ/D thus easing the complexity of the required thermal design for stability. It also opens up the search space, improves the ability to extract planets from the exozodiacal background, and improves the probability of detection. This comes, of course, at the expense of a more costly and challenging observatory.

Most of the requirements on the coronagraph instrument itself do not depend on the scale of the telescope. However, the difficulty of a larger observatory comes in the engineering challenges of testing, launching, deploying and controlling the stability of the system.

An 8 m x 3.5 m elliptical monolithic primary mirror is the largest size that can be launched with existing Delta IV heavy rocket, or 8m circular with planned Ares V. The long-term drive to study Earth-size planets at larger distances will demand breaking the barrier imposed by the Ares V launch shroud and considering even larger apertures. Large segmented mirrors are currently a major technology issue for high-contrast imaging, because of the diffraction by the segments. Specific research efforts are needed to address whether the characterization of potentially habitable planets can be achieved with large segmented telescopes. Possibilities may include coronagraph designs less sensitive to segmentation and the use of two deformable mirrors for amplitude and phase control. Non-redundant aperture masking with spatial filtering may also provide a way to get around the segment boundary (Lacour et al. 2007). External occulters would not suffer from the same limitations with a segmented aperture. However occulter size and distance scale with the telescope diameter, and studies are needed to determine whether this would be a practical solution in terms of performance, cost and science operations.

3.2.2 Architecture scaling for external and hybrid concepts

External Occulters

Observatories that use external suppression achieve high contrast by preventing the starlight from entering the telescope via an external occulter while allowing the planet light to pass. By properly designing the shape of the occulter (Cash 2006; Vanderbei et al. 2007), a deep shadow can be created at the telescope. Since no starlight enters, the need for mid-spatial frequency, high-contrast wavefront control is eliminated. The telescope can be a conventional diffraction limited one as for the internal coronagraph, however the coronagraph instrument complexity is removed. This advantage comes at the cost of a second formation flying spacecraft with a large deployable screen and the engineering challenges associated with the stringent manufacturing and deployment requirements due to volume constraints of the launch vehicle fairing.

Observatories with external occulters obey very different scaling laws. The ability to resolve close in planets is no longer a function of telescope size but rather the size and distance of the occulter (Arenberg 2006). It is also wavelength independent, as long as suppression is achieved at all bands of interest. In principal, an occulter mission can be designed at any size scale, but small-scale missions (1 to 3 m range) are considered impractical in general because the cost advantage is offset by the need for the second spacecraft. A possibility however, would be to use an existing telescope. A few studies have been carried out to try to identify such telescopes and to design occulters for them (Lo 2008). There are several challenges associated with this possibility. The existing telescope would not have a cooperative formation flying system and thus the burden would only rely on the external occulter. It may be difficult to obtain enough science time on the existing telescope to complete an adequate survey of nearby stars and specifics of the instrumentation on the telescope may be less than ideal for planet detection.

Once in the flagship cost range, all external observatory concepts are designed large enough to image earth-like planets. The telescope size is currently assumed to be 4 m in order to have the necessary resolving power in the event of large exozodiacal dust and to have the collecting area needed for the large delta-magnitude targets. Much larger telescopes (> 8 m) are not being considered here as they require even larger occulters and, for finding planets, the increased resolving power is not being used.

A 4-m telescope using an external occulter to achieve high contrast at an IWA of 72 mas requires a shade at least 50 m tip-to-tip flown at roughly 72,000 km distance. Properly designed, such a system can achieve the needed contrast over a broad band (0.4-1.1μm). The challenges are associated with meeting the tight manufacturing and deployment requirements, as well as maintaining positioning and alignment.

Occulter based missions need to slew the occulter from target to target, which introduces lag-time between observations. Efficiency of the external occulter must be carefully studied, but this may be offset by the typically higher throughput than internal coronagraphs, due to the very small number of mirrors and the absence of masks impeding the planet light (this depends on the coronagraph design too). The field of regard for observing is limited to avoid sunlight reflecting off the occulter. The occulter is restricted to a small window a few degrees across, at right angles to the sun, and the observing season is < 1 month. Adding a sun shield to allow observation to 45 deg would be a major improvement and greatly increases the likelihood of recovering planets. It also greatly relaxes the constraints on the star-to-star sequencing which can save a lot of fuel and increase observational

completeness at the same time. However, while the starshade is slewing, there is ample time for general astrophysical observations.

The starshade spacecraft maneuvers to occult target stars by using a low thrust solar electric propulsion system to maximize fuel efficiency. The expectation is that for target stars spaced on an average of 15 degrees apart on the sky, the starshade takes 8 to 13 days to slew to shadow the target star. Once the target star has been shadowed, the starshade and telescope maintain an alignment with a cross-track tolerance of 1 m during the science observation interval, which lasts anywhere between 1 to 7 days.

Hybrid systems

A recent concept combines an external occulter with an internal coronagraph, termed a "hybrid" system. Here, the occulter is designed to achieve enough suppression so that optical aberrations do not adversely impact performance, but is not intended to create all of the contrast. This suppression is estimated to be on the order of 10^{-6}. A coronagraph is then used for the remaining contrast. Such a system may have the advantage of still eliminating the need for wavefront control yet requiring a smaller occulter flown closer to the telescope. Current estimates predict a 36 m tip-to-tip occulter at only 50,000 km separation. Current studies are addressing whether proper design of such hybrid systems can relax the tight manufacturing and deployment requirements. Nevertheless, hybrids come at the expense of a slightly more complicated optical design, lower throughput, and tighter pointing and stability requirements.

3.2.3 Performance scaling

Ground-based and space parameter space

We discuss briefly the comparison between ground-based capabilities and a probe-size in space, for a projected timescale of about 15 years to demonstrate their complementarities.

Ground-based adaptive optics coronagraphs on large telescopes (VLT, Gemini), will be capable of detecting young giant planets around nearby young stars with observations starting in 2011. These instruments will be most sensitive to planets at wide separations (5 to 50 AU) and thus will not probe system architectures at smaller orbital radii.

ELTs (GSMT, E-ELT) should see first light around 2018 and high contrast instruments can be anticipated on these facilities around 2020 at the earliest. In Figure 3-4 we provide a stylized comparison of the parameter space accessible to ground-based and space instruments. A probe-size coronagraph has some overlap with an ExAO ELT for mature giant planets in reflected light, therefore extending the wavelength coverage with typically 0.4 to 1.1 μm in space and 1.0 to 2.4 μm (J-H-K bands) on the ground, and also around 3.8 μm (L') and 4.8 μm (M band).

A thirty-meter class telescope on the ground provides enough angular resolution to reach distant planet forming regions to study planet formation at moderate contrast (e.g. Taurus). A probe-size coronagraph in space offers a modest angular resolution due to its small diameter, but a very high contrast 10^{-10} opening the possibilities for characterization of faint reflected light Jovians down to super-Earths.

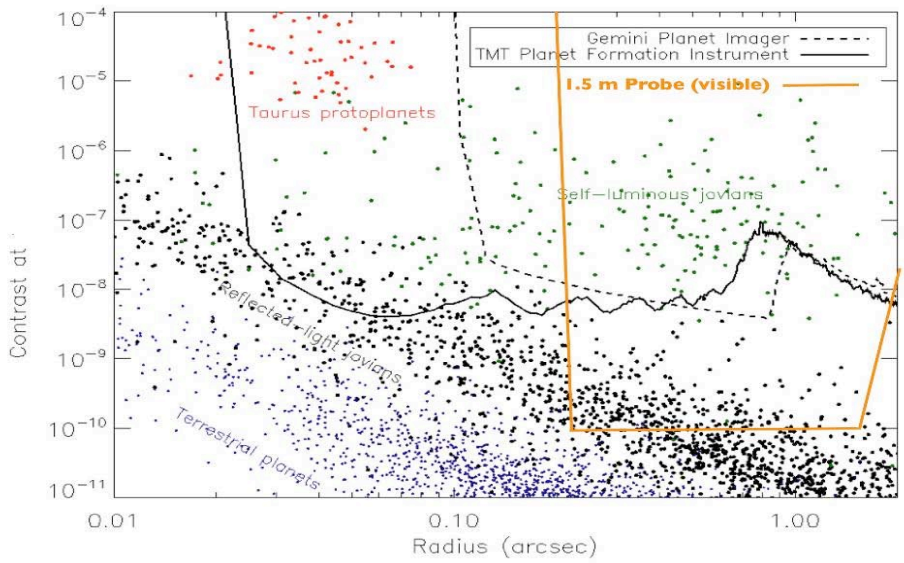

Figure 3-5: Complementarity of ground-based and space parameter spaces for the scales of missions considered in this chapter. (Macintosh et al.)

Scaling of exozodiacal sensitivity

In principle, a bright exozodi background does not make direct observations of an exoplanet impossible; it just makes the exposure time longer to reach a given SNR. In practice, however, it prohibits observations of exoplanets whose exposure times become longer than the observing season for those planets. Also, this is further complicated if the exozodi exhibits structures and clumpiness.

The parameter *EZ* defines the density of dust in the exozodi: the total exozodiacal + zodiacal background is then (2+1 *EZ*) zodis, where the factor 2 accounts for the fact that we are seeing through the whole exozodi disk, whereas we see through only half the zodiacal cloud. We assume the median of random inclinations, (60°) for all targets.

In this example, we assume a telescope 4 m in diameter, with IWA=72 mas, and capable of detecting Earth-like planets 26 mag fainter than the star (Δm= 26 mag). Brighter stars tend to have brighter exoplanets, and less luminous stars have closer-in habitable zones, where an Earth-like planet receives and reflects a greater fraction of starlight. The planet count-rate relation is affected by distance, as shown in Figure 3-6. In contrast, the exozodi count-rate is independent of distance.

With a 4m telescope and even with no exozodi, the background is as bright as Earth-sized planets orbiting stars only ~10 parsecs away. With an exozodi disk having a dust density 3 times that of the zodi, the exozodi background is ~8 times brighter than the planet. An observation of such a planetary system would be background-limited, so exposure times scale with telescope diameter, D^{-4}.

The incidence of exozodiacal light is unknown at a level below hundreds of zodis. A probe-size coronagraph would solve this issue by characterizing exozodiacal disks down to 1 zodi at 3 AU and provide the critical information needed to scale a flagship mission according to this parameter. In particular, it will bring some information about the disks structure and clumpiness, which can hamper the detection capability further. As concluded by ExoPTF, a much larger telescope may be needed if the exozodi level is high (>10 zodi). As SNR

calculation show (Figure 3-7), and it is important to keep options open, in particular in terms of technology developments discussed in this chapter.

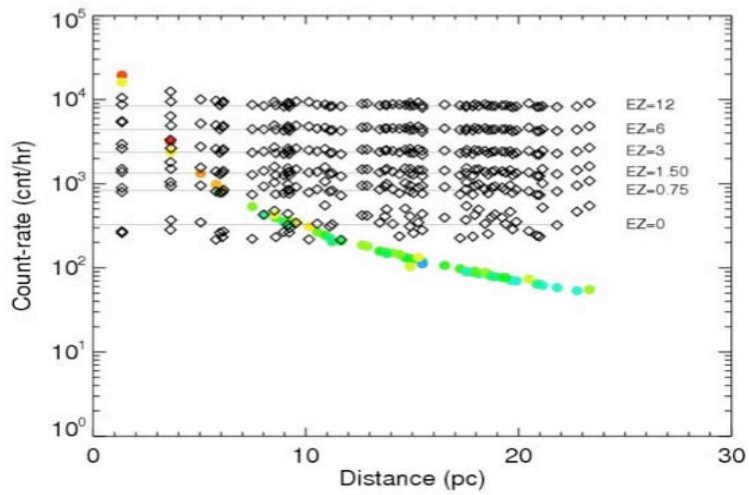

Figure 3-6: Comparison of count-rates of planets around nearby stars (colored circles) and zodi+exozodi background (black diamonds) for various levels of the exozodi dust density and a 4m telescope. Count-rates are calculated for a detection area of 3.78 pixels on a side. Blue to red means Teff=6600 to 4000 K (Heap & Linder 2008).

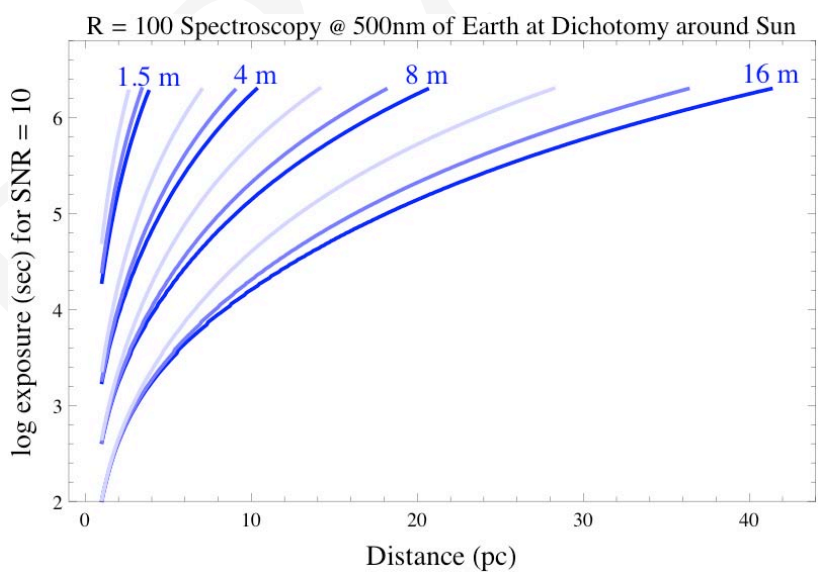

Figure 3-7: Exposure time calculations for the range of telescope sizes discussed in this chapter to achieve R=100 spectroscopy at 500nm on an Earth at dichotomy around the Sun. For each diameter, three exozodi levels are plotted, 1 zodi (Dark blue), 10 zodi (lighter blue) and 50 zodi (lightest blue).

Scaling of flight system requirements and technical maturity

The scaling of flight system requirements and technology maturity is shown in Figure 3-8 for the internal and external coronagraphs. The intent of these figures is to show how the various mission scales impact technical risk and readiness, irrespective of the merit of the science. The first column lists the main technologies of interest, with demonstration of the starlight suppression physics to flight levels being the most important. The raw contrast is defined as the ratio between the PSF brightness at the location of the planet and the PSF brightness at the PSF core. The subsequent columns correspond to representative mission concepts, and are not an exhaustive list of possibilities. Numerical values, where appropriate, represent required performance goals for flight and how they scale with mission size. Colors from green to red represent technology risk and maturity from low to very high. These are evaluated as a function of observatory size and are an indication of technology development need. Section 3.3 describes these technologies and their proposed development in more detail.

3.2.4 Cost and risk drivers

Because of constraints on the NASA budget and concerns over cost overruns of missions currently in development, providing accurate mission costs is a critical consideration for future exoplanet missions. The on-going ASMCS studies will offer a first opportunity for costing these missions, which are being categorized as either probe-scale in the $600M-700M range, without launch vehicle costs, or flagship mission for $1B or more. While the ASMCS costing exercises are not complete at this time, we can describe the rationale for the mission scales and identify the main cost drivers for each mission option.

Telescope system: Based on a multitude of past flight observatory missions, we can expect a 1.5 m class telescope system at the probe-scale cost, including instrument and a single spacecraft, while flagship missions will include systems larger than 2.5m or with multiple spacecrafts. The telescope optics will be diffraction limited and of the same quality whether they will be used for an internal coronagraph or external occulter, and thus not a discriminator. The internal coronagraph will call for an off-axis mirror.

System stability: Internal coronagraph contrast performance is very sensitive to thermal and jitter stability during a wavefront correction cycle, and this sensitivity increases as the IWA decreases, say from $4\lambda/D$ to $2\lambda/D$. This means that while a $2\lambda/D$ coronagraph can find and characterize about the same number of planets with a telescope about half the size as one operating at $4\lambda/D$, it will require at least an order of magnitude tighter requirement on pointing stability and thermal drift. One way to minimize the impact of the cost driver is to devise methods, which can sense and correct the wavefront rapidly.

Coronagraph instrument including wavefront sensing and control: This is a core element of internal coronagraphs, which is not applicable to the External Occulter (but is to the Hybrid). Cost needs to include the number of deformable mirrors and the complexity of the instrument optics. Note however that the size and complexity of the coronagraph instrument system remain essentially the same regardless of mission size.

Two or more spacecraft: This is a core element of the External Occulter and the Hybrid, which does not apply to internal coronagraphs. This entails a whole separate spacecraft system including bus, power, communications, integration & test, software etc... Furthermore, this particular application requires special propulsion systems such as ion thrusters, which add mass and complexity, as well as 25m to 50m deployable multi-layer membrane structures, formation flying metrology and alignment capabilities.

Internal Coronagraph		Ground 30m ExAO	Space 1.5m	Space 1.5m	Space 4m	Space 8m
Coronagraph Instrument Technologies	Raw Contrast at IWA *(Laboratory Demos)*	1e-7 @ 10-20% bandwidth 5 λ/D	1e-10 @ 10-20% bandwidth 4 λ/D	1e-10 @ 10-20% bandwidth 2 λ/D	1e-10 @ 10-20% bandwidth 4 λ/D	1e-10 @ 10-20% bandwidth 4 λ/D
	DMs					
	WFSC Algorithms					
	Masks					
Telescope & Mirror Technology						
Modeling Tools & Validation	Optical					
	Integrated: Opto-Thermal Mechanical					
Pointing		5 mas	0.5 mas	0.5 mas	0.5 mas	0.5 mas
Thermal Control		n/a	0.1mK	0.1mK	0.1mK	0.5 mK
Detectors						
System Verification & Validation						

External Coronagraph		1.1 m Telescope w/15 m Starshade	Existing Telescope w/ 50m Starshade	4m Telescope w/ 50m Starshade	4m Hybrid w/ 36m Starshade
Occulter Raw Contrast *(laboratory demo)*		1e-8 @ 100% bandwidth	1e-10 @ 100% bandwidth	1e-10 @ 100% bandwidth	1e-10 @ 100% bandwidth
Occulter Deployment & Tolerance	Petal Position Errors	0.5 m	0.1 m	0.1 m	0.1 m
	Shape Error	5 mm	2 mm	2 mm	2 mm
	Edge Effects	~1 cm	<1 mm	<1 mm	<1 cm
Telescope & Mirror Technology					
Modeling Tools & Validation	Optical & Scaling				
	Integrated Opto-Thermal Mechanical				
Formation Flying		±1 m	±1 m	±1 m	±0.1 m
Internal Coronagraph		N/A	N/A	N/A	1 e-4
Occulter Thermal Control		~5 K	~5 K	~ 5 K	~5 K
Detectors					
System Verification & Validation					

Figure 3-8 Summary of technologies for internal and external coronagraphs as a function of size. Columns correspond to representative mission concepts.

End-to-end verification and validation (V&V): The cost of final system testing on the ground will clearly grow as the size of the mission, and will become prohibitive (if not impossible) for a very large internal coronagraph flagship mission or for any size external occulter. V&V will then have to rely on very high fidelity models, which will be derived from extensive sub-component or sub-scale testing and model validation activities.

Thermal control: Will be a concern for either internal coronagraphs for wavefront stability (see above) or the external occulter for membrane shape.

3.3 Technology

We discuss various technologies needed, technical readiness, and we propose maturation programs for internal coronagraph, external occulter and common technologies. Past TPF activities provide significant heritage, including ongoing mission concept studies, infrastructure for coronagraph testing, and analysis tools. This technology heritage remains directly applicable to current interests in probe-scale missions and external occulters.

The current state of the art for starlight suppression technology is given in Figure 3-8 and includes all the approaches that are discussed herein. Note that many techniques have not yet had the opportunity to be tested in a precision infrastructure such as the HCIT (Trauger et al. 2007) and that future technology funds should be applied to such testing.

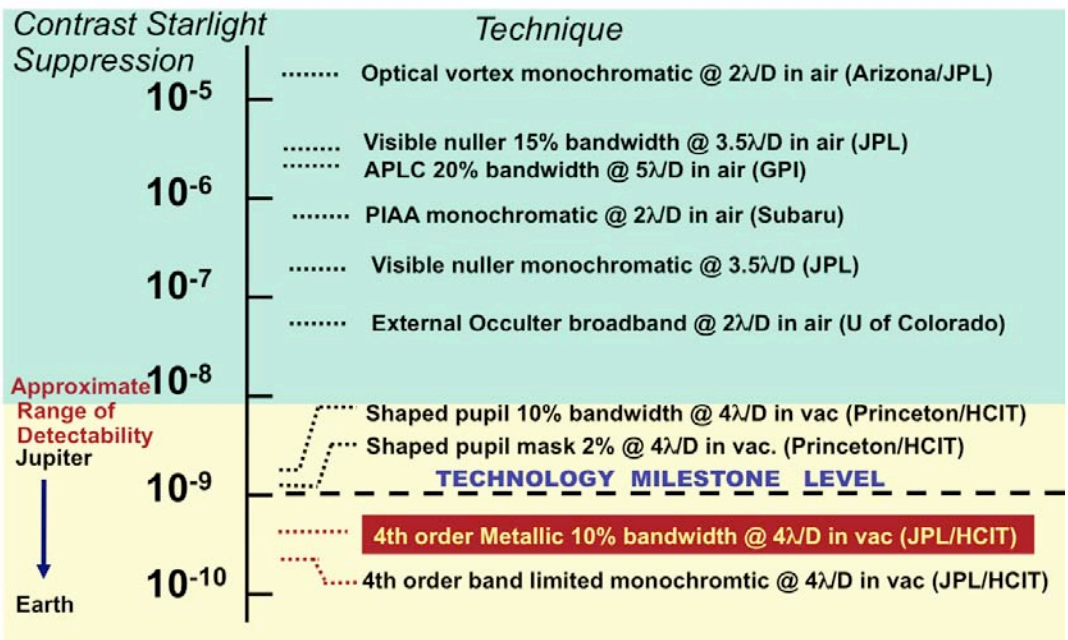

Figure 3-8: Current laboratory results

A crucial parameter in determining the scope, cost, and capabilities of a coronagraphic planet-finding mission is the IWA. Changing the IWA from 4 to 2 λ/D reduces the required telescope size and improves completeness efficiency. However, there is tremendous uncertainty in practical IWA, which is a function not just of the coronagraph architecture but complex wave-optics effects, optical bandwidth, telescope and instrument stability, etc. IWA of 4 λ/D has been demonstrated in the laboratory at performance levels nearly sufficient for detection of Earth-like planets. Many coronagraphs with IWA of 2-2.5 λ/D have been proposed but demonstrated performance is orders of magnitude worse than

theoretical limits. A similar challenge exists with external occulters for their modeling and reduced-scale laboratory demonstrations.

Resolving these questions is crucial to any decision about any future space direct-imaging mission. Significant resources should be committed to both laboratory experiments and modeling - not just simple coronagraph models, but advanced wave-optics models and integrated modeling of entire spacecraft optical systems. As recommended by the ExoPTF, a blue-ribbon panel drawn from engineering and optical-sciences communities should evaluate the status of these models and demonstrations before any mission selection is made.

3.3.1 Internal coronagraph technology

Internal coronagraphs consist of a single spacecraft. An example of mission deployment of a coronagraphic observatory is given in Figure 3-9. Specific technologies for internal coronagraphs include coronagraphic masks, Deformable Mirrors (DM) and Wavefront Sensing and Control (WFS&C). It is important to note that these coronagraph instrument technologies and their required performance goals remain essentially the same for any of the mission scales. The most detailed coronagraphic study for a space mission is the original TPF-C FB-1, which involved an eight-order band-limited mask. This concept is still a viable option for an 8 m flagship coronagraph using existing EELV launch vehicles. Studies are now looking into the opportunities offered by the Ares V.

Coronagraph concepts

A large number of coronagraphic concepts have been developed in the past few years. Several studies (e.g. STDT, Guyon et al. 2006) have detailed and compared these concepts. Coronagraphs can be organized in a few categories.

Pupil apodization: apodization can be obtained using an amplitude transmission (Shaped Pupils), or Phase Apodization Coronagraphy (Codona 2004). Another approach for pupil apodization involves pupil remapping (PIAA).

Lyot coronagraphs: these coronagraphs include a series of masks including at least a focal plane mask followed by a pupil mask (Lyot Stop). The masks can be based on amplitude (Band Limited Coronagraphs, Apodized Pupil Lyot Coronagraphs) or phase (Roddier Phase Mask, Four Quadrants Phase Mask, Optical Vortex Coronagraph).

Interferometric coronagraphs: These coronagraphs use an amplitude division interferometer to create a null from the combination of beams (Achromatic interfero-coronagraph, Visible Nulling Coronagraph).

Other techniques: In addition, several techniques have been proposed and studied to enhance coronagraphic performance or combine it with particular WFS&C schemes.

Optical diffraction modeling and laboratory demonstration

Optical diffraction technology developments depend in part on the type of coronagraph. Modeling efforts are still on going to refine the current capabilities and technology development in this area will continue in the future. Coronagraph modeling and validation is one of the required milestone defined in the TPF-C technology plan for demonstrating mission maturity.

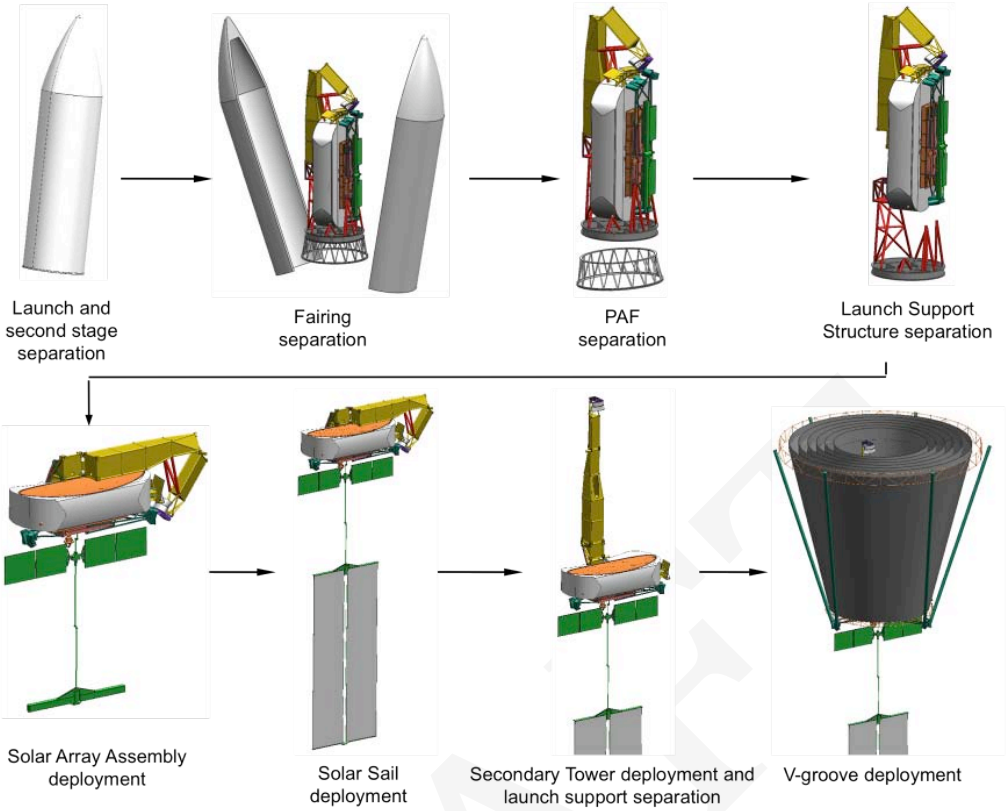

Figure 3-9: Example of deployment for a Flagship coronagraph mission. (STDT).

For Lyot coronagraphs, models are expected to work accurately down to 10^{-10} contrasts and better, but have not been fully validated. Polarization is a concern. Simulations for a Band-Limited Mask system with wavefront control have been demonstrated at the High Contrast Imaging Testbed (HCIT) (Figure 3-10) with best-achieved contrast 5.2 10^{-10} at 4 λ/D for 760-840nm (10% band).

For Shaped pupils, models are also expected to work accurately down to 10^{-10} contrasts and better. Vector propagation analysis comes into play below 10^{-9} contrasts (Ceperley et. al. 2006), but does not affect performance for apertures larger than 25mm. Tiny mask defects are important at these contrasts, however there are no theoretical showstoppers (Belikov 2007). Best contrast obtained at HCIT is 2.4 10^{-9} at 4 λ/D for 760-840nm (10%).

For phase masks (OVC, FQPM) modeling is needed to verify models to 10^{-10} contrast levels, and to integrate the models with wavefront control to investigate broadband performance with aberrations. A proof of concept has achieved 2.10^{-4} at 4 λ/D with OVC. Phase Apodization Coronagraphy has been demonstrated with on-sky observations with a mid-IR camera at Arizona (Kenworthy et al. 2007) with a contrast of 10^{-4} at 3 λ/D.

For PIAA, accurate modeling of diffractive effects between the two mirrors even with wavefront errors (Belikov et. al. 2006) has been demonstrated numerically for simple geometries and perfect pre-and post-apodizers. Propagation for more realistic cases (off-axis mirror designs, focal-to-focal PIAA, error and aberrations in the apodizers) remains an open problem at the 10^{-10} levels. Broadband wavefront control at 10^{-10} levels using two DMs has been demonstrated in numerical simulations in the case of a perfect PIAA (Pueyo 2008). Best contrast obtained is 6.7 x 10^{-7} at 2 λ/D for monochromatic light.

Ground-based coronagraphic efforts are mainly focusing on FQPM and APLCs respectively on VLT-SPHERE and Gemini Planet Imager. Both testbed results achieved similar contrast of about 10^{-5} at 6λ/D for the H-band (1.5-1.8 μm) without wavefront control (Boccaletti et al. 2008, Macintosh et al 2008) and APLC achieved 5.10^{-7} at 5λ/D at 532nm (Thomas et al. 2008).

Deformable mirrors

Deformable mirrors (DM) are a critical component of speckle suppression methodologies for all wavefront control architectures under consideration. The coronagraph application will demand more of a DM than previous applications: the DM surface needs to be positioned to less than 1 Å RMS of the desired shape, and be stable to 0.3 Å RMS for an hour. Two current technologies are viable: one made by Xinetics Inc., andthe other a MEMS device made by Boston Micromachines Corporation.

Xinetics DMs are built up from electroceramic blocks, each incorporating 1024 actuators on a 1mm pitch. These blocks can be assembled into modules covered by a single mirror facesheet and driven by a multiplexed voltage supply with 100V range and 16bits resolution for a maximum stroke of 0.2 μm.

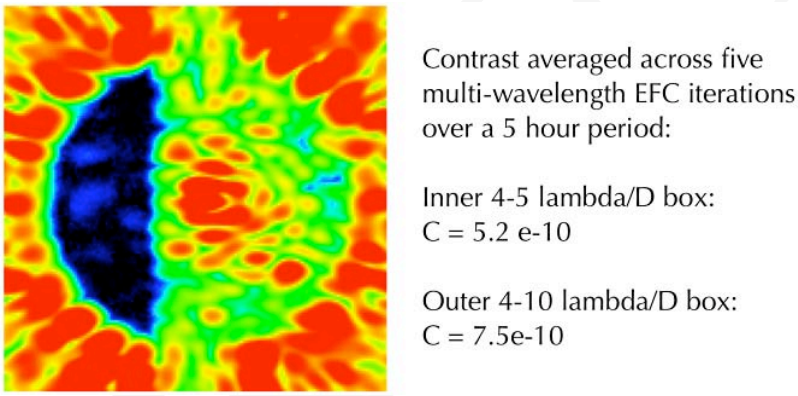

Figure 3-10: Contrast in 760-840 nm (10%) bandwidth obtained at HCIT (Moody, Gordon, Trauger, May 2008).

MEMS DMs are made of a polysilicon membrane coated with one or more metal layers for the reflective surface and actuated by 32x32 or 64x64 electrostatic actuators on the backside. Maximum stroke is about 5 μm for 250V, and fabrication reliability has increased to about one out of three devices without any dead actuators. Current developments exist to improve surface quality (bow, scalloping and print-through).

Xinetics mirrors are used at HCIT and are currently at a higher level of technology maturity than MEMS devices. However, MEMS devices are of increasing importance because of mass and cost considerations. In both cases two areas require further developments. The first is modeling of the DM this includes characterization of thermal-elastic properties for hysteresis and other non-linear mechanical phenomena, e.g. yield limits, yield properties, creep, non-isotropic material elasticity and thermal expansion. The second is the electronics, the presently are large and inefficient, a major development is required in this technology similar to what has been done for spacecraft electronics

Wavefront sensing and control algorithms

We detail below the aspects of WFS&C for space observations. Ground-based ExAO for high-contrast imaging has different sets of requirements for the compensation of the atmosphere (Macintosh et al. 2008). Technology developments are needed for the development of ExAO on large segmented apertures and for speckle reduction active methods to compensate quasi-static speckles (Wallace et al. 2006). These methods are comparable to what is studied for space, but for lower contrast.

Architecture: In principle, a single DM is sufficient to correct phase errors at all wavelengths. However, propagation-induced amplitude errors (or other amplitude errors) can only be corrected perfectly at one wavelength. Better results from a single DM and wavefront sensing in the focal plane can be obtained by minimizing the corrected intensity for several wavelengths (Figure 3-10). In broadband or for larger errors, it may not be possible to maintain the contrast performance at the 10^{-10} levels. A second DM will help dramatically broaden the band and relax the requirements (Shaklan et al. 2006). Moreover, a second DM adds redundancy to the instrument architecture.

Control: Several algorithms have been developed to control the surface of DMs for a given estimate of the field in the image plane. Current algorithms solve a simplified linear problem and iterate to solve the complete non-linear problem. The speckle-nulling algorithm proved the concept but its convergence is too slow. Faster convergence is obtained using Newton methods.

Bordé & Traub (2006) showed the mathematical formalism to tackle the problem with one DM, using energy minimization but limited in practice by the modes hidden behind the coronagraphic mask. Give'on et al (2006) generalized this formalism by recognizing that all coronagraphs were linear operators and that the problem could be regularized using standard least square techniques. This is the algorithm currently used at HCIT.

Recently Pueyo et al. (2008) proposed a variant of this regularization, with a minimization of the DM deformation while constraining the contrast below 10^{-10}. This algorithm was used numerically to show how to control two sequential DMs with both PIAA and Shaped Pupils in broadband.

Overall the problem of control with a perfect estimate has solid theoretical foundations. We recommend support for further development in this direction so that future high contrast testbeds have the hardware to operate with two DMs.

Estimation: In order to avoid non-common path errors, the estimation has to follow suppression of the bulk of the starlight. Some diversity is needed to calculate the fields from intensity measurements and several difficulties need to be considered: First, if the "sensing-exposures" are not used for science, mission efficiency is decreased. Algorithms therefore need to be optimized to use the fewest possible diversity exposures to maximize time for science. This problem has been partially tackled by Give'on et al. (2006) (pairwise estimation), Kay et al. (2007) (modified Gerchberg-Saxton) or Pueyo et al. (2008) (Hermitian properties and wavelength fit of the estimate). When the target contrast is reached, all exposures can be considered as science exposure as shown by Belikov (2007). Second, sensing involves solving an inverse problem and is therefore very sensitive to modeling errors. The model of the forward transfer function needs to be known at a level consistent with 10^{-10} contrast: we need to know the actual surface of the DMs and not just the voltage sent.

In consequence, algorithms need to have a low sensitivity to some error in the diversity, or need to be self-calibrating to adjust to slow variations in the system (DM influence functions for example). The next challenge is to design new estimation schemes that are relatively in sensitive to the system modeling, and minimize the amount of observation downtime during "sensing-exposure".

Coronagraph optics manufacturing

We organize the manufacturing technologies in four classes: binary masks, amplitude masks, phase masks, and aspheric surface polishing.

Binary Masks: These masks include Shaped Pupils, or hard-edged focal plane masks, and also the "Lyot stops" used in Lyot-style coronagraphs. The common technique used for these mask is deep reactive ion etching (DRIE). An example is given in Figure 3-11 for a series of shaped pupils manufactured at JPL Micro Devices Laboratory (MDL) on Silicon-insulator wafers. Currently, the smallest features that can be manufactured reliably are about 5 μm through the 50 μm substrate. This is sufficient for a 10^{-10} contrast Shaped Pupil 10mm or larger in size. For masks about 10mm to 30mm in size, the challenge is to develop tapered sidewalls, which has been demonstrated in the micro fabrication industry but not on shaped pupils per se. This is less of an issue if larger masks are used (>30mm).

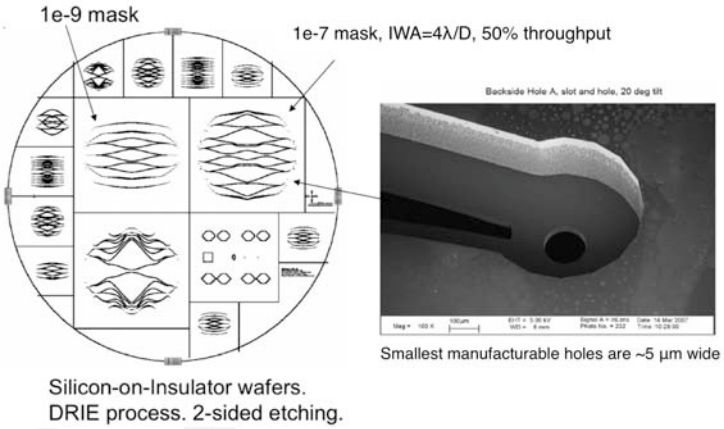

Figure 3-11: Shaped Pupils using DRIE in Silicon wafers. The inside of every closed black curve is etched out. (Princeton /JPL)

Amplitude masks: These masks include soft-edged focal plane masks (e.g. BLC), or pupil apodizations (APLC). In most cases a gray amplitude transmittance is needed, and the main difficulty is to control the amplitude and induced phase shift in broadband. The phase shift introduced by the mask can be corrected with a Deformable Mirror (DM) at one wavelength, but broadband correction is an issue. The results of Figure 3-10 have been obtained with a Nickel-deposit mask, shown in Figure 3-12. However this mask manufacturing is only possible for 1-dimensional masks.

Mask-manufacturing methods have been proposed to achieve a mostly phase neutral absorbing occulter mask, for example using a metal deposit with a profiled dielectric layer to compensate for phase changes (Moody et al 2008), or using a focused ion beam to shape dye-doped acrylic structures embedded in transparent phase-matching glass (Tolls 2005, 2006). Ion-beam machining enables 2-dimensional masks.

Another approach for amplitude masks is based on binary notch filter masks (Kuchner 2003, Balasubramanian 2005, Crepp 2006), or half-tone approaches (Vasudevan 2005, Macintosh 2008). E-beam lithography it used to write a binary pattern of blocking and transparent areas onto a substrate.

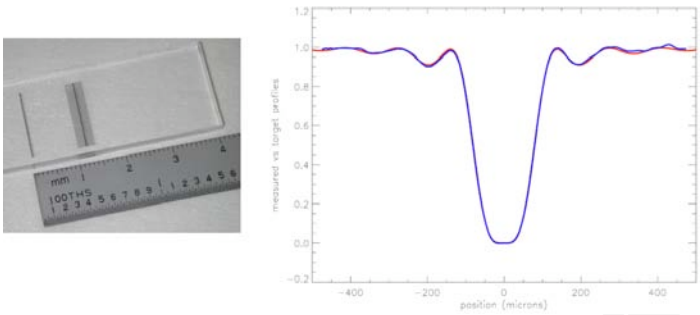

Figure 3-12: Nickel is vacuum deposited on fused silica (left), and comparison of the specified transmission profile (red) and measured (blue). This is the mask used in the result of Figure 3-10. (Moody et al. 2008)

Half-tone methods use the statistical distribution of opaque dots to achieve the desired extinction profile. These masks seem to work well in laboratory test (Tolls 2008; Thomas et al. 2008). Their maximum optical density of 5 is an issue for BLC, so they are more appropriate for pupil apodizers. A potential technology issue is due to the presence of surface plasmons when the dots have a comparable size to the wavelength. This can result in "super-transmission effects" (Genet et al. 2007) with wavelength-dependent amplitude variations. These effects can be mitigated by the optimization of the dot sizes.

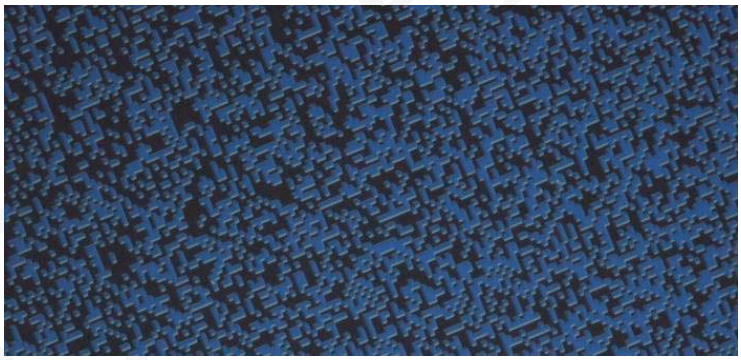

Figure 3-13: Half-tone apodizer using 2 µm black-chrome dots on glass (e-beam lithography). The apodizer is 12mm diameter. (Gemini Planet Imager, 2008)

Phase Masks: Examples of manufacturing processes are the lift-off technique to produce 4-quadrant phase masks (Riaud 2003), and more recently using half-wave plates to produce and achromatic FQPM, where four half-wave plates are assembled side-by-side (Mawet et al 2006, Boccaletti et al 2008). Phase masks for vortex coronagraphs have been manufactured using an electron beam lithographic technique (Swartzlander 2008).

Aspheric surface polishing: aspheric surfaces are needed particularly for the PIAA coronagraph. Prototype optics have been manufactured using aspheric diamond turning of both lenses and mirrors.

3.3.2 External Occulter technology

An external occulter mission consists of at least two spacecrafts: the telescope and at least one occulter or starshade. An example of a possible mission deployment is given in Figure 3-14. The telescope does not require any particularly challenging technology and we detail the technology related to the starshade itself and to formation flying.

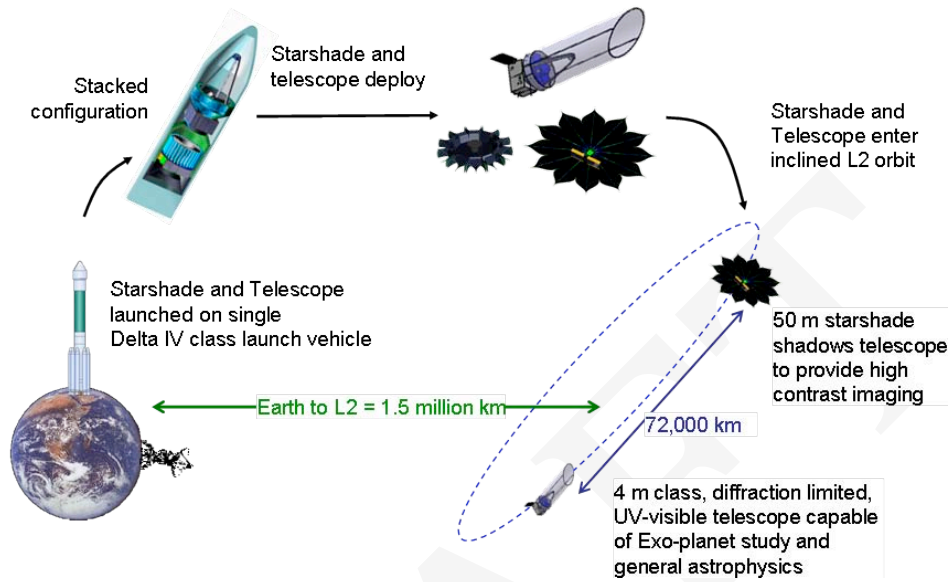

Figure 3-14: Example of a possible TPF-O mission deployment. (NWO/NGST)

The Occulter technology assessment has been subdivided into eight sub-technology areas, which are given below in order of importance. These include modeling, occulter system maturation, deployment, formation flying and pointing control subsystem, precision edge and scattered light, integrated opto-mechanical-thermal performance and analysis, micrometeoroids impacts, and propulsion systems.

Optical diffraction modeling and laboratory demonstration

Several modeling and optimization schemes for the shape of the starshade have been developed by groups at Princeton, University of Colorado, Goddard, and NGST, based on Fresnel propagation. Although modeling has not been validated at 10^{-10} contrast and will need further study, current models agree with the tests at the 5.10^{-8} level. Modeling small errors on the occulter requires non-Fourier methods that compute piecemeal propagation.

Several laboratory experiments to demonstrate the concept have started with for example small-scale (centimeter size) starshades at University of Colorado, as shown in Figure 3-15, NGST, and Princeton. Research is still needed to understand how optical and contrast performance scale from the small test articles to the full size starshade.

The main issue is that a full-size test of the system will not be possible on the ground. Engineering developments are needed as well to enable end-to-end system verification, including high-fidelity models for mechanical and thermal behavior from sub-scale or sub-component tests. The effects of gravity on such large systems further complicate ground verification. Modeling is also necessary to predict and verify, prior to launch, the alignment capability of the two spacecraft.

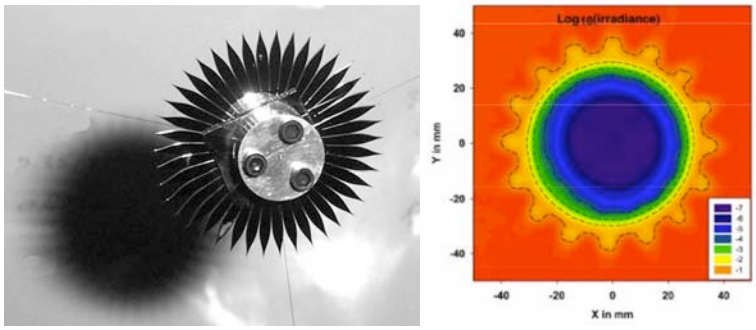

Figure 3-15: Occulter experiment using a starshade made with lithography. The contrast obtained is 5.10^{-8} with broadband sunlight (University of Colorado).

Occulter system maturation

Several approaches are possible to define the Occulter System Maturation. A proposed approach is summarized in Figure 3-16. The initial proof of concept is based on the fabrication of a single segment. This enables to define and test the large range of material properties, and the deployment and shape accuracy. A three-petal model is then fabricated and demonstrated from ambient conditions to relevant conditions of vacuum and temperature. A flow chart representation of a slightly different but compatible maturation scheme is given in Figure 3-17 detailing a technology development and test approach to reach the TRL 6 by 2012 for the starshade. This approach will validate occulter technology and system modeling on a subscale test article in ambient conditions. Should funds be available, we recommend to carry out a detailed study, with further testing in relevant environments, using a microsat or nanosat space vehicle for on-orbit demo of the complete subscale system with size 8-30m (the full scale can be up to 50m), or possibly using secondary payloads on Atlas or Delta launchers.

TRL 3 Proof of concept	TRL 4 Component level	TRL 5 Component level	TRL 6 Subscale protoflight occulter	TRL 7 Subscale protoflight occulter	TRL 8 Subscale protoflight occulter
• ~1m size • Deployment • Shape accuracy • Model development **Coupon Testings** Material properties at temperature • Mechanical • Thermophysical • Optics • Environmental stability	• Functional performance in air • 2 – 3m size, 3 petals, data on central petal • Deployment • Loads/stresses • Shape accuracy and stability • Gravity effects • Model validation • Scaling	• Functional performance in thermal vacuum • 2 – 3m size, 3 petals, data on central petal • LN2, IR • Loads/stresses • Shape accuracy and stability • Model validation • Scaling • Optics	• Functional performance in air • 8-30m size, full configuration for microsat • Deployment • Loads/stresses • Shape accuracy and stability • Gravity effects • Model validation • Scaling • Optics	• Qual/acceptance test flight article • 8-30m size, full configuration for microsat • Deployment • Loads/stresses • Temperatures • Shape accuracy and stability • Model validation • Acoustic env • Thermal vac • Optics	• On orbit demo • 8-30m size, full configuration on microsat • Deployment • Loads/stresses • Temperatures • Shape accuracy • Model validation • Formation flying • Attitude control

Figure 3-16: Occulter system maturation (Tenerelli, LM)

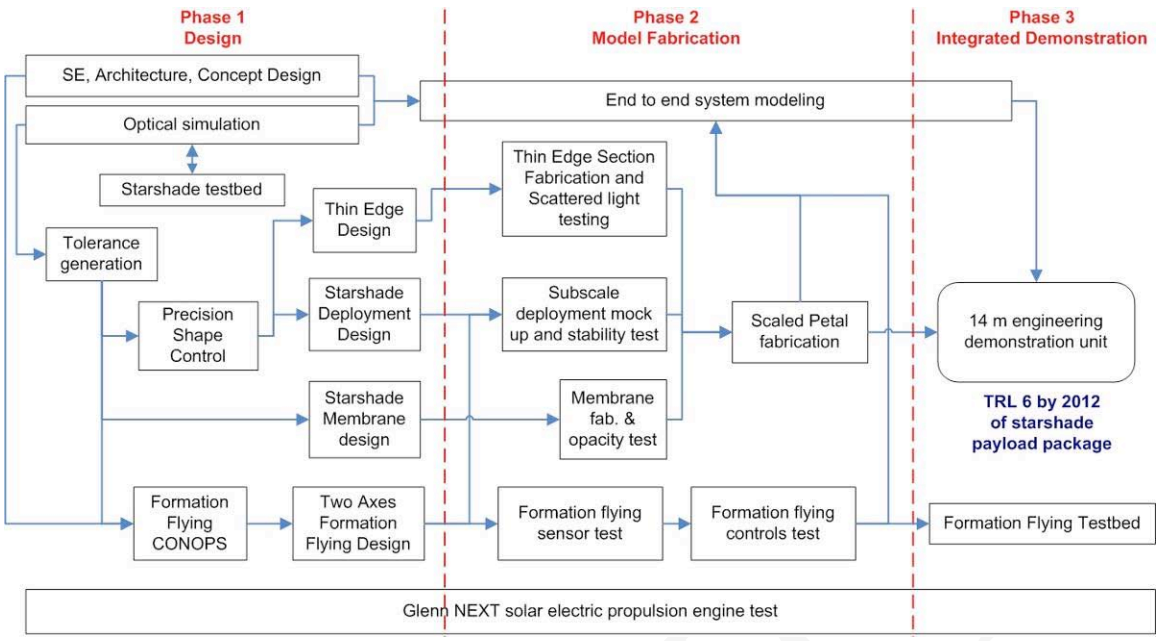

Figure 3-17: Flow chart representation of the occulter maturation (Amy Lo, NGST)

Deployment

Since available launch vehicles have fairing diameters restricted to less than 5 meters, external occulters must be folded during launch, and deployed after they reach orbit.

The technology challenges with deployment reside in how well the tip and edge figure of the occulter can be obtained since it is the outline of the deployed configuration, which will drive the ultimate contrast performance. Deployed edge accuracy is required to be about 1mm from nominal configuration (Figure 3-?). The deployment of an external occulter can possibly be accomplished a number of ways as summarized in Figure 3-18, mainly distinguishing between monolithic or hybrid deployment options.

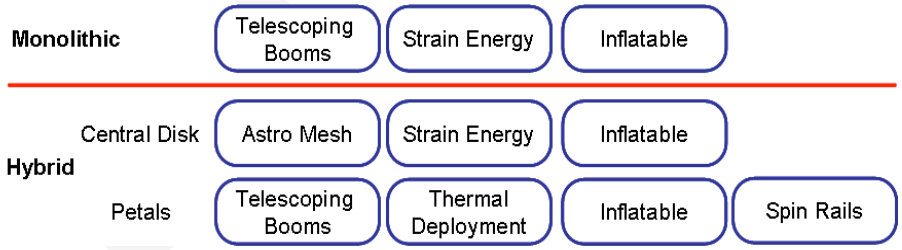

Figure 3-18: Occulted deployment trade space (Lo, NGST)

Monolithic deployment is the simplest process where the optical element is deployed via a single method as a whole structure. However, there is no simple solution for tensioning membranes as required by the shape of the occulter tip and its petals, and a separate edge support structure may be required.

Hybrid deployments allow separating the deployment of the core structure, which has relaxed requirements from the tip and edges with higher accuracy requirements. Options

include a central disk using proven deployment methods for circular structures, followed by a second stage for petal deployment.

An example of a monolithic deployment is given in Figure 3-19, where the tips of the petals are attached to the tip of the innermost of several nested telescoping booms. Each petal has its own set of stem drive and telescoping boom. The booms are nested during launch; once on orbit, a containment shield is released and the starshade fabric unfolds like an umbrella. Motor driven stem drives push out the boom segments.

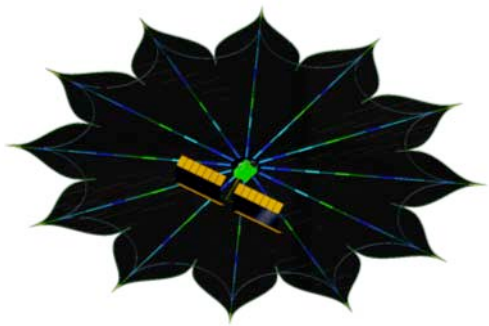

Figure 3-19: **Representative starshade and spacecraft architecture (Lo, NGST)**

Rigidizable inflatable occulters could provide an alternate deployment approach with mass advantages. A 20 m solar sail demonstrator (Figure 3-20) can provide a technology pathfinder benefitting the occulter petal system. The deployment and structural testing of the 20-meter solar sail systems was conducted in the 30 meter diameter Space Power Facility thermal-vacuum chamber at NASA Glenn Plum Brook in April though August, 2005. The mass of this solar sail is 0.25 kg/square meter.

Figure 3-20: 20m Solar Sail at NASA Plum Brook Station. (Cossapakas, L'Garde)

Formation Flying & Pointing control subsystem

The starshade must be aligned on the star for the full observation, to within a few mas. The requirements for the rigid body motion of the occulter are currently work in progress. Best estimation of the requirements is 1 m in plane and ±1 degree in tilt (Lyon et al. 2007). This tolerance is an engineering compromise between starshade size (larger shade equals looser tolerance and larger IWA) and alignment sensing capability. An angular sensor on one spacecraft can be used to measure this alignment offset. There are a few solutions for occulter acquisition and alignment maintenance during an observation. These include a three-beacon concept on the starshade (R. Lyon), or an astrometric sensor and in-shadow sensors (Noecker, 2007). For a typical 20,000-100,000 km separation, the sensor needs precision, stability, and ultimate accuracy of ~2 mas.

The pointing and control subsystem algorithms will have to consider the flexible body dynamics of the large occulter plus the much smaller deployable solar array and high gain antenna. Included in the control of the system is thruster firings, reaction wheel forces, micro-meteroid impacts, thermal deformations, which cause the center of mass and center of pressure to vary after slewing, solar wind, solar pressure and gravity gradient.

Precision edge and scattered sun light

The telescope will see the sunlit edges of the starshade as local bright spots, which can potentially overwhelm an Exo-Earth signal. A "knife-edge" treatment on the perimeter can be used to minimize the edge surface area to reduce scattering toward the telescope, an edge with a radius of curvature of 100 microns will scatter less than 30 magnitude equivalent of sunlight towards the telescope. The two associated issues are the knife edge itself, and perimeter control. Technology developments are needed to demonstrate how to maintain edge and perimeter quality during deployment and on-orbit operations with possible temperature changes through the structure from about 300K to tens of K. Additional development is needed to mitigate scattered light using highly non-reflective material on the thin edge.

Integrated optical mechanical and thermal analysis

Thermal analysis of the system can build on past experience of working with deployable membranes (e.g. JWST technology). Factors driving the accuracy of numerical solutions for thermal analysis are well known in general. However, often-neglected effects such as membrane wrinkling and material anisotropy may have significant impact on the accuracy of a thermal, mechanical and stray light prediction. It is important to develop integrated modeling capabilities which will directly analyze the sensitivities of thermal variations on system contrast to better define requirements on occulter thermal gradients and stability. Modeling tools need to be further developed to include membrane wrinkling and non-linear behaviors. These integrated models are essential for optimizing occulter designs and parameters (e.g. layer separations, material properties, etc.) and for establishing the sensitivity of performance to thermal and structural requirements.

The following example (Figure 3-21) illustrates how thermal information could be used to derive design requirements, showing the temperature profiles of the three flat layers of Kapton. In particular large temperature gradients exist for the central layer, which may induce large thermal deformations beyond required shape. Non-uniform deformations of the occulter can be mitigated for example by the use of low CTE graphite for the edge, so that the center of the starshade is allowed to expand and wrinkle without affecting performance. This example considers 1 m separation between the sheets. Shorter distances would be more favorable for thermal properties, the shortest distance being defined by micrometeoroid protection.

Micrometeoroids

Micrometeoroid impact can create tiny holes in the occulter, but a triple layer of material can be used to limit transmission of starlight (Cash et al. 2006). It is necessary to evaluate the effect of micrometeoroid impacts in terms of stray light and dynamics. The first step is to quantify the environment and determine the rate of impacts per year with mass larger than 10^{-7} g (velocity 20-50 Km/s).

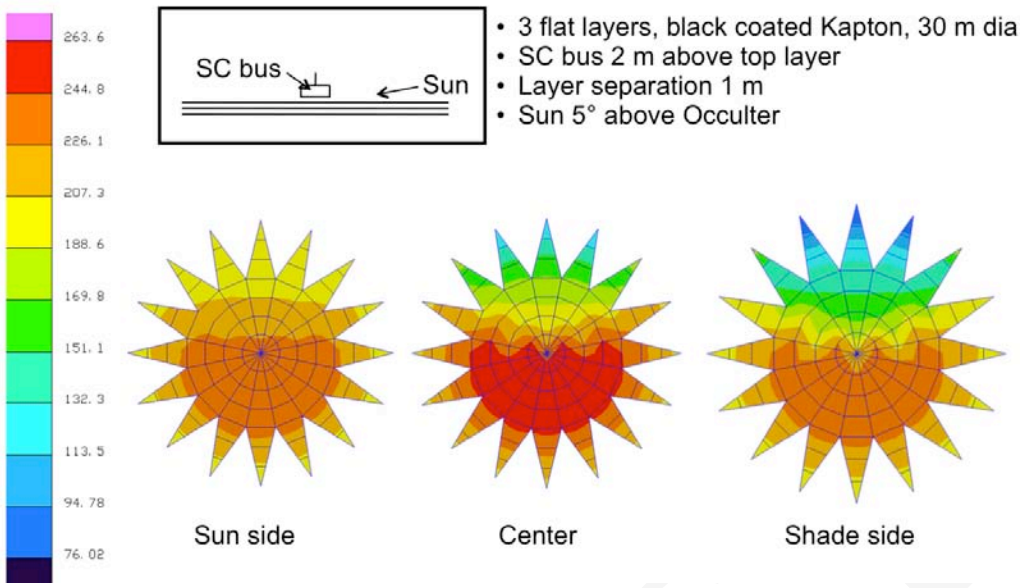

Figure 3-21: Thermal modeling of a three-layer 30m diameter Occulter (Klavins, LM)

Analysis of candidate occulter material based on JWST's shield (Si-coated Kapton) has been shown to withstand the L2 environment. Crack propagation does not seem to be an issue for Kapton, the material induced sputtering after the first layer and the membrane is not highly tensioned. However, some technology development and modeling are needed for micrometeoroid mitigation, as applied to the occulter.

Propulsion systems

Due to the large distance traveled by the starshade between observations, it is not conceivable to use conventional propulsion systems, which would require large quantities of propellant. Sustainable propulsion such as Solar Electric Propulsion is an excellent option for this application. NASA Glenn and JPL have already demonstrated this technology in 1998 on the Deep Space 1 flight mission and are involved in ongoing technology development efforts.

Two types of contamination need to be evaluated: first, the optical effect of a molecular cloud on the seeing of the telescope; second, the effect of hydrazine deposition on the occulter surfaces, which can potentially affect mechanical and thermal properties.

3.3.3 Common technology

Telescope and mirror technology

Four key metrics can be defined to allow the assessment of mirror technology (Matthews, Egerman, Wynn, ITT Space Systems Division). Their maturity is illustrated in Figure 3-22.

On-axis versus off-axis Primary Mirrors: In these systems, the primary mirror has a center hole and there is an obstructing structure that holds the secondary mirror with respect to the primary mirror. Off-axis telescope configurations are not symmetric with respect to the center of the mirror. The light is reflected to a non-obstructing secondary mirror. However, the fabrication of off-axis Primary Mirrors and telescopes has not been demonstrated at very large sizes. The most significant challenge between developing on-axis and off-axis telescopes is in the fabrication and testing of the primary mirror. Modern

optical, and opto-mechanical metrology devices (such as laser trackers) reduce the difficulty in aligning off-axis telescope systems significantly.

Passive versus Active designs: Historically, primary mirrors have been very stiff to allow the observatory to be passive in the overall implementation of the system. The primary to secondary alignments could be made infrequently by merely moving the secondary on small actuators to adjust its position. Sophisticated WFS&C schemes to control higher spatial frequency errors were not easily implemented in either software or hardware architectures. HST is an excellent example of this type of system. New technology in software, computer design, dynamic control and mirror manufacturing techniques enables the optical figure of large mirrors to be adjusted on orbit if required. These active designs are new for space-based applications, but have been demonstrated on the James Webb Space Telescope (JWST) to be feasible during ground testing. Recent advances in mirror processing technologies used in conjunction with advancements in dynamic control will enable large optics with relatively low stiffness to mass ratio passive or active primary mirrors for future systems that are not segmented.

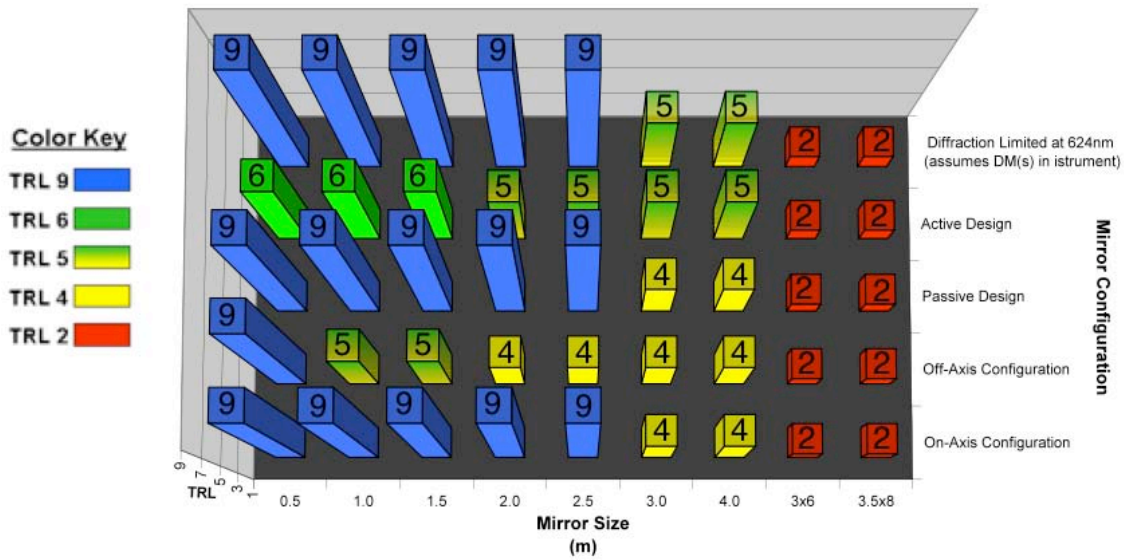

Figure 3-22 - TRL for mirror sizes and configurations. (Egerman, Matthews, ITT)

Mirror quality: the primary mirror technology for exo-earth finding coronagraphs is already in hand. Early work in coronagraph technology emphasized the need for a high-quality primary mirror with mid-spatial frequency (5-100 cycles/aperture) performance exceeding the specification of the Hubble Space Telescope. Recently it has been shown that the deformable mirrors in the coronagraph compensate for these errors and relax the optical design specifications to levels not exceeding HST (Shaklan et al. SPIE 2006). Indeed, laboratory results from JPL's HCIT show broadband performance at levels exceeding 1×10^{-9} contrast using off-the-shelf quality optics (about 1/20th wave). It is now understood that detrimental propagation effects in the optical train are most important where the beam diameter is reduced, and these effects limit the high-contrast performance (1×10^{-10} contrast) to angles of 20 – 30 cycles/aperture (about 2 arcsec for a probe-scale coronagraph mission and 0.3 arcsec for a flagship mission). The external occulter system does not suffer from these outer working angle limitations.

Size: Small optics have been manufactured in many sizes and shapes. Large space qualified primary mirror optics have traditionally been round. Large off-axis, elliptical mirrors have

been studied but nothing of any size approaching the 3-meter by 8-meter size has ever been built or qualified for space applications. The largest non-round off-axis optics for space base application that have been/are being fabricated are the ~1.4m off axis hexagonal segments manufactured during the Advanced Mirror System Demonstrator (AMSD) Program and the similarly sized and shaped segments currently being fabricated for the JWST primary mirror.

Detectors

Detectors will be a critical component of any exoplanet direct imaging mission. Whether it is an exoplanet probe or a flagship mission, it will be straining for photons because exoplanets are very faint: about 22.5 mag fainter than the star in the V band for a Jupiter-like planet, and about 25 mag fainter for an Earth-like planet. The process of dispersing the light of a faint planet over many pixels of a spectrograph will cause the read noise of a conventional detector to become a limiting factor. As shown in Figure 3-1, DRM studies suggest that for some stars, the detection can be limited by the planet flux (and not the IWA or the contrast). Detectors having high detector quantum efficiency (DQE) in the optical and near-IR (0.4-1.0 μ), low dark current, very low or no read noise (photon counting) are therefore essential.

Photon-Counting CCD's: Photon counting CCDs provide electron multiplication before their readouts, essentially eliminating their read noise (< $1e^-$). For example, a typical ExoPlanet Probe with a photon-counting CCD (zero read noise) will take only half as long to obtain a R=20 spectrum of a Jovian planet than if the CCD has a read noise 3 e-. The benefits of a photon-counting CCD are even greater for a flagship mision, where exposure times for R=70 spectroscopy of Earth-size planets are cut down by a factor of 5 (Heap, S. R. et al., 2006). This gain in ultimate sensitivity is equivalent to increasing the telescope aperture from 4 m to 6 m. The technology for the 0.4-0.7 μm region is already well in hand (Wen, Y. et al., 2006), with high-DQE photon counting detectors commercially available (e.g. E2V's L3Vision series CCDs). We recommend the continued development including pushing their DQE even higher (>0.8) and improving their radiation tolerance.

An opportunity exists to enhance the DQE in the near-IR by bringing photon-counting capabilities to p-channel CCDs. Regular p-channel CCDs already exist and have a DQE of about 0.8 at the 0.94 μm water line and at the ~0.9 μm CH_4 features. We recommend technology development to add a charge-multiplication register to the p-channel CCD, similar to what already exists for the regular (n-channel) CCD.

Low Temperature Detectors: Low temperature detectors (LTDs) are a class of photon-counting detectors that are operated at very low temperatures, typically less than 300 mK (Verhoeve, 2008). In the optical, they allow photon counting imaging spectrophotometers (the detector measures also the wavelength without the need for a spectrograph). With a LTD, every photon is counted individually and cosmic rays can be rejected extremely well because they deposit significantly more energy than an optical photon. Some LTDs are responsive to light beyond the ~1 μm cutoff of silicon CCDs. Several technologies are being developed, including doped semiconductor, Superconductive Tunnel Junctions (STJs), Transition Edge Sensors (TES), Magnetic microcalorimeters, Superconductive Quantum Interference Device (SQUID), or Microwave Kinetic Inductance Detector (MKID).

The most advanced STJ instrument (S-Cam, ESA/Estec) is 10 x 12 pixel camera with R=15 at 500nm. As long as no multiplexing scheme exists for STJs, further increase in the number of pixels will be limited.

TES arrays have been demonstrated for small size (8 x 8 pixels) and developments exist to expand the wavelength range to 0.3 – 1.7 μm. However, multiplexed read-out is not demonstrated yet with these arrays.

An advantage of MKIDs is their frequency domain multiplexing allowing large arrays to be built (Mazin et al. 2007). However, their current spectral resolution is still insufficient (R=6 demonstrated with 1000 pixels), but plans exist to develop a 25000 pixel array with R=20-50. Technology developments are needed to develop larger arrays with higher spectral resolution.

Precision thermal control and analysis

Existing thermal designs are capable of achieving sub-milli Kelvin (mK) control in benign space environments such as is offered by the Lagrangian orbits. Currently available codes and computational capability should allow the predictions of relative temperature changes to several mK's, but are not capable of absolute temperature predictions to those levels. Factors that drive the accuracy of numerical solutions are well known, alimitations in commercially available codes force the trading of numerical solution accuracy against model size and computation time. Modeling tools are available to deal with anisotropy or effects such as spectral optical properties. Effects of heat flow mechanisms that are normally neglected can be examined, e.g., the work done by thermal expansion or long-term changes in composite properties due to outgassing or radiation. Material properties uncertainties are readily addressed, even if the task of assessing these uncertainties grows rapidly when considering not only property measurement errors but also the many possible ways that such errors can be distributed throughout a complex system. Overall, there is sufficient understanding of heat transfer physics to evaluate mechanisms, check assumptions, identify uncertainties, and develop schemes for accommodating these in an end-to-end system model.

The greatest risk is in managing the sheer size of the thermal models. In particular, mapping between thermal and structural models is a known source of error as it would be necessary to have the same high fidelity discretization between the thermal and mechanical models to predict the sub-nanometer wavefronts these space applications require. However, existing commercial thermal codes are not capable of handling the same number of nodes as the large number typically used by structural models for sub-nm predictions, and so simplifying assumptions are made on the uniformity of temperatures for mapping interpolation purposes. For example, the SIM program demonstrated ±3mK accuracy in predicting the through-thickness changes in temperature gradient in a monolithic mirror, but this required a massive insulated Cu shroud in the thermal vacuum chamber to provide spatially and temporally uniform boundary conditions that could be accurately described in the thermal model. That problem simplified the configuration to be modeled in comparison with that of a large built-up primary mirror, inside a sunshade that is bound to challenge modeling fidelity, to generate relative temperature distributions accurate to 1 mK.

Isolation systems

Disturbance Free Payload: Disturbance-Free Payload (DFP) is a system architecture in which payload and spacecraft bus are separate bodies that fly in close-proximity formation, allowing precision payload control and simultaneous isolation from spacecraft disturbances. The control architecture provides isolation down to zero frequency, and sensor characteristics do not limit isolation performance. A testbed has demonstrated broadband isolation in excess of 68 dB (a factor of 2,512).

The payload and spacecraft bus have independent gravity offload systems. They are coupled through a fully controlled non-contact interface containing sensors and actuators. The payload contains fine optical-pointing sensors; the spacecraft bus contains a star tracker, three-axis fiber-optic gyros, reaction wheels and thrusters. Payload pointing stability is less than 1 micro-radian in the laboratory environment.

Two-stage isolation systems: Traditional spacecraft designs involve isolation of vibration sources via passive mechanical isolation stages – essentially compliant spring-damper systems. In order to achieve sub-mas stability with such passive systems, two stages are necessary – one stage separating the vibrating component (such as a reaction wheel assembly) from the spacecraft structure, and a second stage separating the spacecraft structure from the payload instrument. Such two-stage isolation systems are complex to integrate at the system level, require extensive mass and volume allocations, and typically require high sample rate track sensors and fast steering mirrors to reject residual disturbance that propagates to the payload. In addition it is not possible to carryout science when dumping momentum using your thruster system. However the advantage they have over the DFP system is they have flown before and have been successful. DFP is at a TRL level of 5-6 (several of the components have flown). What needs to be done is a system level environmental test of DFP.

Verification and Validation

Fundamentally the process of integration and test of large optical space borne systems (>1.1m) is no different than the process that needs to be used on any space system. Because it is impossible to perfectly reproduce space conditions on the ground, a combination of techniques must be employed to verify any space payload prior to accepting the hardware for launch. Testing is a significant part of the verification process and deserves critical attention. However, other verification techniques include analysis, demonstration, inspection, simulation and records validation are all important methods to be considered. The main point here is that the early design work of any space system should not focus on how the system will be tested prior to flight, but rather how it will be verified prior to flight.

Given that any Exoplanet Direct Imaging Mission will likely be more technically challenging than any space missions that have flown to date, a disciplined systems engineering approach must be applied to each subsystem in terms of design and verification. It is especially critical to give attention to the verification plan early on in the design process to reduce technical and programmatic risk. It is certainly preferable to have an end-to-end ground test to demonstrate optical performance of payloads on the ground. However, if the uncertainties in the test and in ground-to-orbit changes are not accommodated by design and/or operationally adjustable parameters (such as focus shift and temperature control), then such a test is meaningless. Hence, the system design must be robust and tunable on-orbit, and the verification plan must be equally robust to ensure mission success. Furthermore, advanced modeling tools and techniques will play an integral role in the verification of any Exoplanet Direct Imaging Mission. However, given the complexity we recommend further testbed demonstration to validate verification methodology and modeling accuracy/predictability for future mission concepts.

3.4 Research and Analysis Goals

Science observing and modeling support is needed in preparation of both probe-size and flagship-size missions. In particular, we can recommend efforts in the simulation of spectra for a large range of physical parameters (ages, temperature, albedo, composition, clouds,

etc.). Modeling is necessary to understand better what kind of spectra we can expect and how to use the information we can obtain from low-resolution spectra. This will also help the disambiguation of planet types for a range of physical parameters.

Ground-based observing support is needed in particular for measurements of stellar ages. It is generally believed that the exozodi should get fainter with time as the dust disk is gradually cleared out and collisions of planetesimals leading to enhanced production of dust become less frequent. However, it appears that many, perhaps the majority of TPF target stars are young (<2 Gyr). According to Barnes (2007), the median age of his sample of 70 nearby, Sun-like stars is only 1.3 Gyr. More research on stellar ages is urgently needed and may be possible through ground-based astro-seismology observations. DRM studies must be detailed, in particular for concatenated programs studies Astrometry/RV and direct imaging missions. This is of critical importance to refine the scaling of the missions and make sure that the combination of techniques offers a consistent program with matched performance.

Exozodi science is absolutely critical and support will be needed for ground-based observations with Keck Nulling Interferometer and the Large Binocular Telescope Interferometer.

3.5 Contributors

Ruslan Belikov, NASA Ames Research Center

Paul Bierden, Boston Micromachines

Anthony Boccaletti, Observatoire de Paris

Robert Brown, Space Telescope Science Institute

Chris Burrows, Metajiva

Eric Cady, Princeton University

Costas Cossapakis , L'Garde

Ian Crossfield, University of California Los Angeles

Larry Dewell, Lockheed Martin

Alan Dressler, Carnegie Institution of Washington

Robert Egerman, ITT Space Division

Tom Greene, NASA Ames Research Center

Olivier Guyon, Subaru

Sara Heap, NASA Goddard Space Flight Center

B. Jaroux, NASA Ames Research Center

Jeremy Kasdin, Princeton University

Jim Kasting, Penn State University

Matthew Kenworthy, University of Arizona

Steve Kilston, Ball Aerospace

Andy Klavins, Lockheed Martin

DRAFT

Chapter 3

John Krist, Jet Propulsion Laboratory

Benjamin Lane, Draper Laboratory

Amy Lo, Northrop Grumman Corporation

Patrick J. Lowrance, Spitzer Science Center

Rick Lyon, NASA Goddard Space Flight Center

Bruce Macintosh, Lawrence Livermore National Laboratory

Sean McCully

Mark Marley, NASA Ames Research Center

Christian Marois, Hertzberg Institute for Astrophysics

Gary Matthews, ITT Space Division

Ben Mazin, Jet Propulsion Laboratory

Charley Noecker, Ball Aerospace

Ben R. Oppenheimer, American Museum of Natural History

Nelson Pedreiro, Lockheed Martin

Aki Roberge, NASA Goddard Space Flight Center

Robert Rudd, Lawrence Livermore National Laboratory

Stephen Ridgway, National Optical Astronomy Observatories

Glenn Schneider, University of Arizona

Jean Schneider, Observatoire de Paris

Laurent Pueyo, Princeton University

Stuart Shaklan, Jet Propulsion Laboratory

Anand Sivaramakrishnan, American Museum of Natural History, Stony Brook University

David Spergel, Princeton University

Karl Stapelfeldt, Jet Propulsion Laboratory

Domenick Tenerelli, Lockheed Martin

Jason Tolomeo, Lockeed Martin

Volker Tolls, Havard-Smithonian Center For Astrophysics

John Trauger, Jet Propulsion Laboratory

Robert J. Vanderbei, Princeton University

Jeff Wynn, ITT Space Division

DRAFT

3.6 References

Arenberg, J. W., Lo, A. S., Cash, W. et al. New Worlds Occulter performance: a first look, Space Telescopes and Instrumentation I: Optical, Infrared, and Millimeter. Proceedings of the SPIE, Volume 6265, pp. 62651W (2006).

Balasubramanian, K., Wilson, D. W., Muller, R. E., et al. Thickness-dependent optical properties of metals and alloys applicable to TPF coronagraph image masks, Techniques and Instrumentation for Detection of Exoplanets III. Proceedings of the SPIE, Volume 6693, pp. 66930Z (2007).

Barnes, S. A.. Ages for Illustrative Field Stars Using Gyrochronology: Viability, Limitations, and Errors, Astrophysical Journal, 669, 1167-1189 (2007).

Belikov R., Kasdin N.J., Vanderbei R.J., "Diffraction-based Sensitivity Analysis of Apodized Pupil-Mapping Systems," ApJ Vol 652, issue 1, pp. 833-844, 11/2006.

Belikov, R., Give'on, A., Savransky, D., et al. Demonstration Of Synthetic Exo-earth Detection In The Lab With Speckle Subtraction Techniques, American Astronomical Society Meeting Abstracts, 211, 135 (2007).

Belikov, R., Kasdin, N. J., Vanderbei, R. J.. Diffraction-based Sensitivity Analysis of Apodized Pupil-mapping Systems, Astrophysical Journal, 652, 833-844 (2006).

Boccaletti, A., Abe, L., Baudrand, J., et al. Prototyping coronagraphs for exoplanet characterization with SPHERE, ArXiv e-prints, 807, arXiv:0807.0694-(2008).

Bordé;, P. J., Traub, W. A.. High-Contrast Imaging from Space: Speckle Nulling in a Low-Aberration Regime, Astrophysical Journal, 638, 488-498 (2006).

Brown, R. A.. Single-Visit Photometric and Obscurational Completeness, Astrophysical Journal, 624, 1010-1024 (2005).

Cash, W., Schindhelm, E., Arenberg, J., et al. The New Worlds Observer: using occulters to directly observe planets, Space Telescopes and Instrumentation I Proceedings of the SPIE, Volume 6265, pp. 62651V (2006).

Cash, W.. Detection of Earth-like planets around nearby stars using a petal-shaped occulter, Nature, 442, 51-53 (2006).

Ceperley, D., Neureuther, A., Miller, M., et al. Stray-light sources from pupil mask edges and mitigation techniques for the TPF Coronagraph, Modeling, Systems Engineering, and Project Management for Astronomy II. Proceedings of the SPIE, Volume 6271, pp. 62711F (2006).

Codona, J. L., Angel, R.. Imaging Extrasolar Planets by Stellar Halo Suppression in Separately Corrected Color Bands, Astrophysical Journal, 604, L117-L120 (2004).

Crepp, J. R., Ge, J., Vanden Heuvel, A. D., et al. Laboratory Testing of a Lyot Coronagraph Equipped with an Eighth-Order Notch Filter Image Mask, Astrophysical Journal, 646, 1252-1259 (2006).

Genet and Ebbesen, Nature, 445, 7123, 39, 2007

Give'On, A., Kasdin, N. J., Vanderbei, R. J., On representing and correcting wavefront errors in high-contrast imaging systems, Journal of the Optical Society of America A, 23, 1063-1073 (2006).

DRAFT

Guyon, O., Pluzhnik, E. A., Galicher, R., et al. Exoplanet Imaging with a Phase-induced Amplitude Apodization Coronagraph. I. Principle, Astrophysical Journal, 622, 744-758 (2005).

Guyon, O., Pluzhnik, E. A., Kuchner, M. J. et al. Theoretical Limits on Extrasolar Terrestrial Planet Detection with Coronagraphs, Astrophysical Journal Supplement Series, 167, 81-99 (2006).

Heap, S. R. et al. 2006, "An Integral Field Spectrograph for the Terrestrial Planet Finder Coronagraph", New Ast. Reviews, 50, 294

Kaltenegger, L., Traub, W. A., Jucks, K. W.. Spectral Evolution of an Earth-like Planet, Astrophysical Journal, 658, 598-616 (2007).

Kay, J., Kasdin, N. J., Belikov, R.. Wavefront correction in a shaped-pupil coronagraph using a Gerchberg-Saxton-based estimation scheme, Astronomical Adaptive Optics Systems and Applications III. Proceedings of the SPIE, Volume 6691, pp. 66910D (2007).

Kenworthy, M. A., Codona, J. L., Hinz, P. M., et al. First On-Sky High-Contrast Imaging with an Apodizing Phase Plate, Astrophysical Journal, 660, 762-769 (2007).

Kenyon, S. J., Bromley, B. C.. Collisional Cascades in Planetesimal Disks. II. Embedded Planets, Astronomical Journal, 127, 513-530 (2004).

Lacour, S., Thiébaut, E., Perrin, G. High dynamic range imaging with a single-mode pupil remapping system: a self-calibration algorithm for redundant interferometric arrays, Monthly Notices of the Royal Astronomical Society, 374, 832-846 (2007).

Launhardt, R.. Differential astrometry and astrometric planet searches with the VLTI., Astronomische Nachrichten, 326, 563-564 (2005).

Levine, M., Shaklan, S., Kasting, J. "Science and Technology Definition Team Report ", JPL Report D-34923 (2006)

Lo, A. S., Glassman, T., Lillie, C.. New worlds observer optical performance, UV/Optical/IR Space Telescopes: Innovative Technologies and Concepts III. Edited by MacEwen, Howard A.; Breckinridge, James B. Proceedings of the SPIE, Volume 6687, pp. 668716 (2007).

Lunine et al. 2008 Exoplanet Task Force Report

Lyon, R. G., Heap, S., Lo, A., et al. Externally occulted terrestrial planet finder coronagraph: simulations and sensitivities, UV/Optical/IR Space Telescopes: Innovative Technologies and Concepts III. Proceedings of the SPIE, Volume 6687, pp. 668719 (2007).

Macintosh, B.A., Graham, J.R., Palmer, D.W., et al. The Gemini Planet Imager: from science to design to construction. Proc of SPIE (2008)

Marcy, G.. Observed Properties of Exoplanets, In the Spirit of Bernard Lyot: The Direct Detection of Planets and Circumstellar Disks in the 21st Century, (2007).

Mawet, D., Riaud, P., Baudrand, J., et al. The four-quadrant phase-mask coronagraph: white light laboratory results with an achromatic device, Astronomy and Astrophysics, 448, 801-808 (2006).

Mayor, M., Udry, S., Lovis, et al. The HARPS search for southern extra-solar planets. XIII. A planetary system with 3 Super-Earths (4.2, 6.9, & 9.2 Earth masses), ArXiv e-prints, 806, arXiv:0806.4587-(2008).

DRAFT

Mazin, B. A., Bumble, B., Day, P. K., et al. Position sensitive x-ray spectrophotometer using microwave kinetic inductance detectors, Applied Physics Letters, 89, 222507-(2006).

Moody, D. Gordon, B. Trauger, J. "Design and demonstration of hybrid Lyot coronagraph masks for improved spectral bandwidth and throughput." Proc. SPIE 7010, 7010-139 (2008).

Morbidelli, A., Levison, H. F., Tsiganis, K., et al. Chaotic capture of Jupiter's Trojan asteroids in the early Solar System, Nature, 435, 462-465 (2005).

Noecker, M. C.. Alignment of a terrestrial planet finder starshade at 20-100 megameters, Techniques and Instrumentation for Detection of Exoplanets III. Proceedings of the SPIE, Volume 6693, pp. 669306 (2007).

Oppenheimer, B. R., Brenner, D., Hinkley, S., et al. The Solar-System-Scale Disk around AB Aurigae, Astrophysical Journal, 679, 1574-1581 (2008).

Pueyo et al. Proc of SPIE (2008)

Riaud, P., Boccaletti, A., Baudrand, J., et al. The Four-Quadrant Phase Mask Coronagraph. III. Laboratory Performance, Publications of the Astronomical Society of the Pacific, 115, 712-719 (2003).

Savransky & Kasdin, Design Reference Mission construction for planet finders Proc of SPIE (2008)

Shaklan, S. B., Green, J. J., Palacios, D. M.. The terrestrial planet finder coronagraph optical surface requirements, Space Telescopes and Instrumentation I: Optical, Infrared, and Millimeter. Edited by Mather, John C.; MacEwen, Howard A.; de Graauw, Mattheus W. M.. Proceedings of the SPIE, Volume 6265, pp. 62651I (2006)., 6265, (2006).

Shao, M., Samuel, R., Wallace, K., Levine, B.. Visible Nulling Coronagraph, In the spirit of Bernard Lyot: The Direct Detection of Planets and Circumstellar Disks in the 21st Century, (2007).

Spergel Proc of SPIE Planet detection and characterization with an occulter/telescope system (2008)

Swartzlander, G. Ford, E., Abdul-Malik, R., Astronomical demonstration of an optical vortex coronagraph Opt. Exp 10200-10207 (2008)

Thomas S., Soummer, R., Dillon, D. Testing the APLC on the LAO testbed (2008)

Tolls, V., Aziz, M., Gonsalves, R. A., et al. Study of coronagraphic techniques, Space Telescopes and Instrumentation I: Proceedings of the SPIE, Volume 6265, pp. 62653K (2006).

Traub, W. A., Chen, P.. Planetscope Precursor Experiment, American Astronomical Society Meeting Abstracts, 211, #30.06-(2007).

Trauger, J., Give'on, A., Gordon, B. et al. "Laboratory demonstrations of high contrast imaging for space coronagraphy." Proc. SPIE 6693, 66930X (2007).

Vanderbei, R. J., Cady, E., Kasdin, N. J.. Optimal Occulter Design for Finding Extrasolar Planets, Astrophysical Journal, 665, 794-798 (2007).

Vasudevan, G., Reale, M., Somerstein, S. F.. Some performance results from NIRCam's coronagraphic prototype masks, Cryogenic Optical Systems and Instruments XI. Proceedings of the SPIE, Volume 5904, pp. 66-70 (2005).

DRAFT

Verhoeve, P., J Photon counting low temperature detectors for visible to gamma ray Astrophysics Low Temp Phys 151: 675–683 (2008)

Wallace, J. K., Bartos, R., Rao, S., et al. laboratory experiment for demonstrating post-coronagraph wavefront sensing and control for extreme adaptive optics Proceedings of the SPIE, Volume 6272, pp. 62722L (2006).

Wen, Y. et al. (2006), "Individual photon-counting using e2v L3 CCD's for low background astronomical spectroscopy", SPIE 6276, 62761H

DRAFT

4 Direct Detection of Exoplanets with Infrared Interferometry

Chair: William Danchi, NASA Goddard Space Flight Center

LOC: Peter Lawson, JPL

4.1 Introduction

4.1.1 Science Goals

Advanced Imaging in the Mid-infrared: Planet Formation, Debris and Exozodiacal Disks, Warm Jupiters, Super-Earths, and Terrestrial Planet-Finding and Characterization

Advanced imaging with both high-angular resolution and high sensitivity in the mid-infrared is essential for future progress across all major fields of astronomy. Exoplanet studies particularly benefit from these capabilities. Processes occurring at 0.5 to 5 AU in protoplanetary disks are critical for the formation of giant and terrestrial planets and are best revealed by observations in the mid-infrared which is sensitive to dust emission from 100-1000K. Achieving the necessary angular resolution at these wavelengths requires long-baseline interferometry with ~100-250-m baselines to probe 1 AU scales for the nearest star-forming regions at a distance of 140 pc. Substantially more modest baselines of ~ 10-20 meters can probe solar-system scales around stars in the solar neighborhood. Thermal emission from the atmospheric and telescope(s) limits the sensitivity of ground-based observations, driving most science programs towards space platforms. Even very modest sized cooled apertures can have orders of magnitude more sensitivity in the thermal infrared than the largest ground-based telescopes currently in operation or planned.

In this chapter, we outline the scientific parameter space afforded by next generation mid-infrared interferometers, in the context of ground-based arrays, including Atacama Large Millimeter Array (ALMA), the Keck Interferometer (KeckI), Large Binocular Telescope Interferometer (LBTI), and the Very Large Telescope Interferometer (VLTI), and cooled space telescopes (*Spitzer, Herschel*, JWST). We find a mid-IR interferometer with a nulling (coronagraphic) capability on the ground and a connected-element space interferometer both enable transformative science while laying the engineering groundwork for a future "Terrestrial Planet Finder" space observatory requiring formation-flying elements.

Planet Formation *in situ*: Detailed imaging of nearby star-forming regions enable the study of planet formation *in situ.* While the next-generation millimeter-wave interferometer ALMA will lack the angular resolution to probe the terrestrial planet formation zone, mid-infrared interferometry with >250 meter baselines will be sensitive to warm dust emission within the inner few AUs of planet-forming disks. Already, the (Keck-

I) and the (VLTI) probe the dust and temperature structure around the luminous Herbig Ae stars, and T Tauri disks could be accessible from the ground with a dedicated infrared-optimized system. The study of planet formation will be revolutionized by the combination of ALMA's probe of the cold outer disk and a mid-IR interferometer's sensitivity to the warm inner disk.

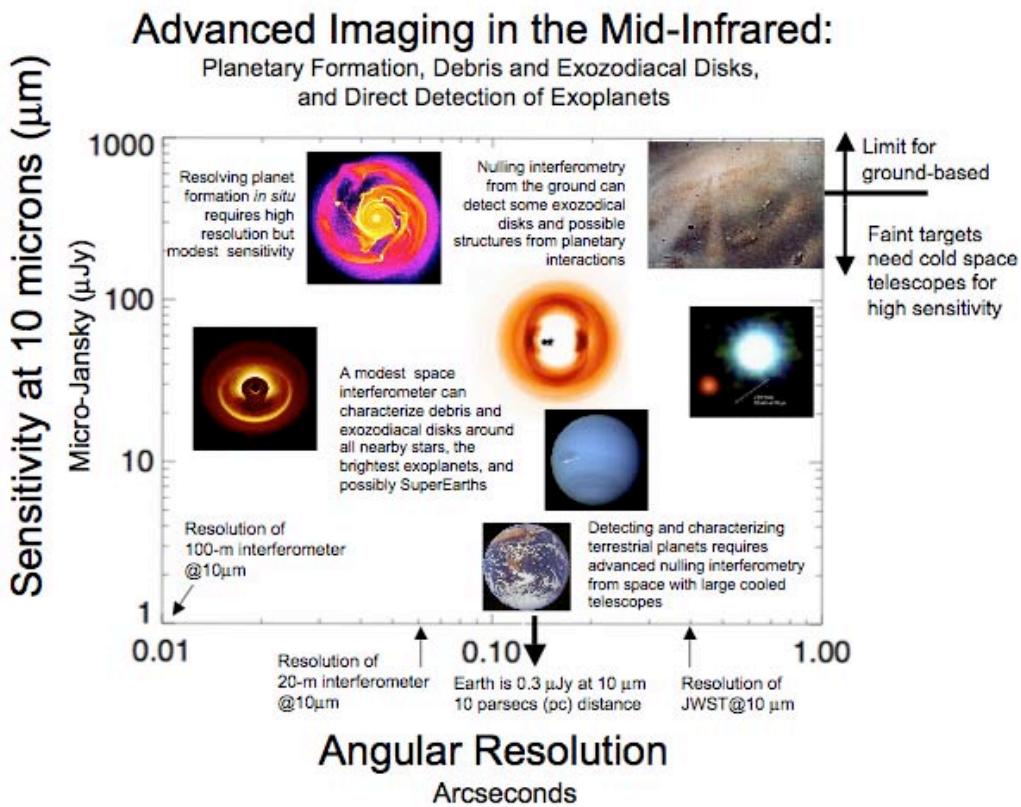

Figure 4-1. Relationship between resolution and sensitivity as it pertains to advanced imaging in the infrared for planet formation, debris and exozodial disks, and direct detection of exoplanets.

Debris and Exozodiacal Disks: The optically-thick and gas-rich disks out of which planets form are bright, dominating over the emission form the central star. As the system evolves, the dust gains grow into larger and larger bodies and the gas dissipates. Small particles of dust still pervade the system, created in collisions between planetesimals, and occasionally large collisions will produce dramatic structure in these "debris disks." Here, mid-infrared imaging in conjunction with nulling (to block out the central star), allow the spatial distribution and SED of the debris disks to be scrutinized. Ground and space-based interferometers both have important roles here, since ground systems can probe brighter debris disks with greater angular resolution (necessary to null out the star w/o nulling out the dust) and the space systems with modest ~20 m baseline can sensitively look for debris around nearby stars.

Exozodiacal disks are already under intensive study since the mid-IR emission and scattered light can mimic or hide the signal of terrestrial planets around nearby stars. Chapter XX is devoted to this crucial topic and we refer the reader to that section for further details.

Direct Detection of Exoplanets: Planned mid-infrared facilities are also designed to directly detect exoplanets using nulling interferometry. Ground-based systems can contribute as shorter wavelengths (<5 μm) but exoplanet detection in the mid-infrared (6-20 μm) is not expected to be practical since thermal emission from the warm sky and telescope swamps the faint planetary signal (except perhaps in some rare scenarios). A realistic connected-element space interferometer with up to 20 m baselines can be used to characterize the atmospheres of a large number of the currently known massive exoplanets and potentially super-Earths (Danchi et al. 2003a,b), while a more-challenging formation-flying interferometer system can be used to detect terrestrial planets and search for atmospheric biomarkers (the technical demands for terrestrial planet finding has been detailed elsewhere – TPF-I report).

4.1.2 Science Requirements

Parameter Space: Figure 4-1 shows the parameter space of spatial resolution vs. sensitivity. Using this plot, we can see the trade-offs between the high sensitivity of space vs the high angular resolution possible with ground-based work. Critically, this diagram highlights the rich and varied science goals made possible by continued incremental technical developments for advanced imaging in the mid-infrared. The full suite of capabilities will be necessary to achieve the most ambitious goal of direct detection of Earth-like planets.

Planetary Detection and Characterization

The requirement for a flagship-class mission to detect directly and characterize Earth-like planets around nearby stars implies that the missions must determine the type of a planet and characterize its gross physical properties and its main atmospheric constituents, thereby allowing an assessment of the likelihood that life or habitable conditions exist there.

Types of Stars: On astrophysical grounds, Earth-like planets are likely to be found around stars that are roughly similar to the Sun (Turnbull 2004). Therefore, target stars should include main sequence F, G, and K stars. However, M stars may also harbor habitable planets, and the nearest of these could be investigated using a high angular resolution interferometer.

Terrestrial Planets: Considering the radii and albedos (reflectivity) or effective temperatures of Solar System planets, this mission must be able to detect terrestrial planets, down to a minimum sized planet defined as having 1/2 of the Earth's surface area and the Earth's albedo. In the infrared, the minimum detectable planet would be one with an infrared emission corresponding to the surface area and optical albedo, positioned in the orbital phase space stipulated below in Figure 4-2.

Habitable Zone: The mission should search the most likely range as well as the complete range of temperatures within which life may be possible on a terrestrial-type planet. The habitable zone (HZ) is here defined as the range of semi-major axes from 0.7 to 1.5 (1.8) AU scaled by the square root of stellar luminosity (Kasting et al. 1993, Forget & Pierrehumbert 1997).

We expect planets where we will eventually find life to be small and rocky -- very similar to the Earth and although there exist other possibilities that have been theoretically explored, this idea focus the search very much towards systems like our own. Essentially all planned searches for habitable planets, focus on the so-called 'Habitable Zone' (HZ) (based on

Kasting et al. 1993), which is very loosely defined as the region around a particular star, where one would expect stable conditions for liquid water on a planetary surface. For a given planet (assuming a certain atmosphere composition and albedo) the surface temperature depends on the distance from the host star, the luminosity of the host star and the solar flux that takes the wavelength dependent intensity distribution for different stellar types into account. The topic is very complex, since many factors unrelated to stellar luminosity could work to produce conditions where water would be liquid. As an example, the Jupiter moon Europa in our Solar system is expected to have liquid water under a layer of ice, where the energy to keep it liquid originates from gravitational interactions within the Jupiter system. The detection of such habitable conditions would be extremely difficult remotely. All planned searches for habitable planets focus on the HZ, thus in principle being governed by the stellar flux. .

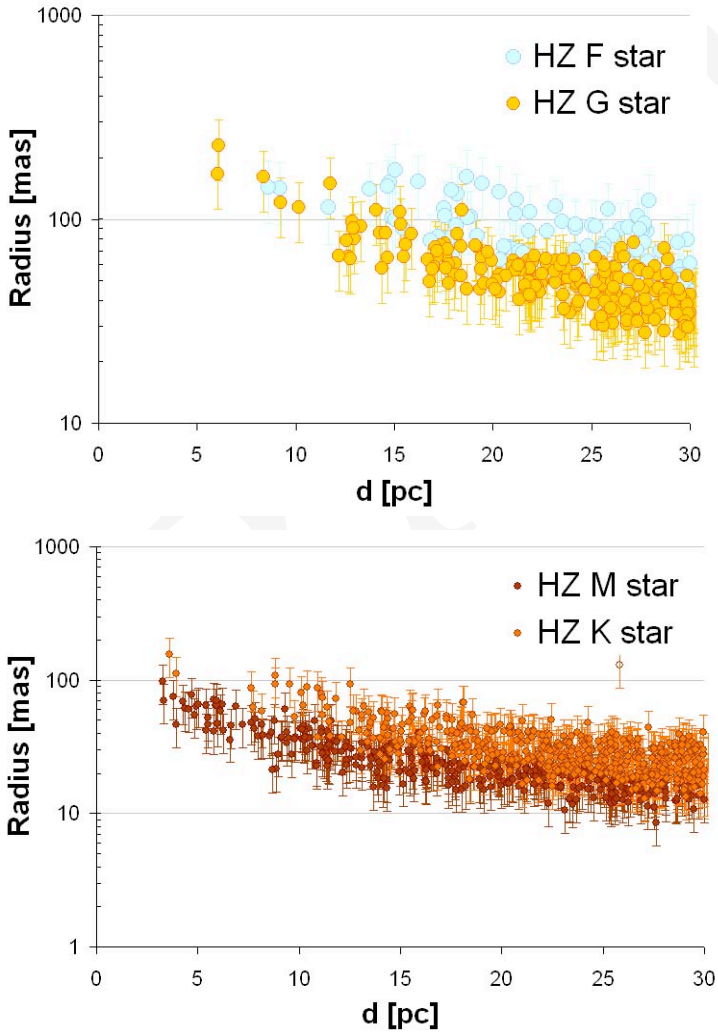

Figure 4-2. The extent of the Habitable Zone for the single main sequence stars (F,G stars on upper panel, and M, K stars on lower panel) within 30pc from the Sun (from Kaltenegger et al 2008)

The Earth-Sun intensity ratio is about 10^{-7} in the thermal infrared (~10 μm), and about 10^{-10} in the visible (~0.5 μm). In the mid-infrared (5-20 μm) thermal emission emanating from the planet is actually detected and analyzed, while at visible wavelengths (0.5-1 μm) the

reflected stellar flux is measured. The spectrum of the planet can contain signatures of atmospheric species that are important for habitability, such as CO_2 and H_2O, or resulting from biological activity (O_3, CH_4, and N_2O). Both spectral regions contain atmospheric bio-indicators: CO_2, H_2O, O_3, CH_4, and N_2O in the thermal infrared, and H_2O, O_3, O_2, CH_4 and CO_2 in the visible to near-infrared. The presence or absence of these spectral features will indicate similarities or differences with the atmospheres of terrestrial planets. Figure 4-3 displays the observed emission spectrum from the Earth in the infrared.

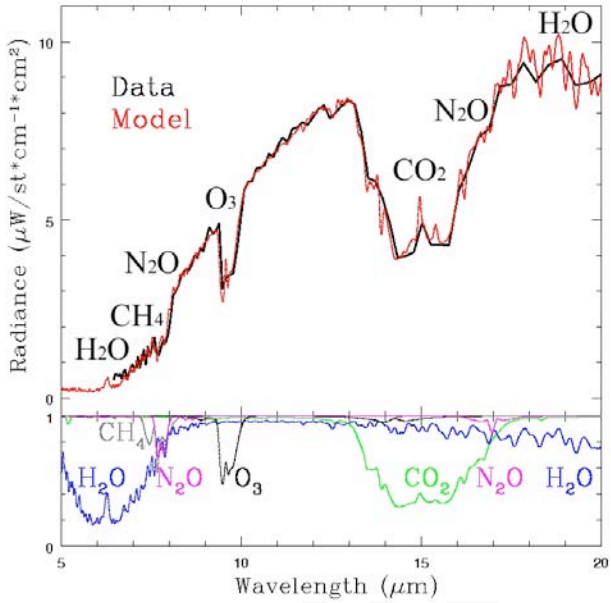

Figure 4-3. Observed emission spectrum in the infrared (Christensen & Pearl 1997) of the integrated Earth, as determined from Earthshine and space respectively. The data is shown in black, model and individual chemical feature colour (Kaltenegger et al 2007).

The search for signs of life on possibly very different planets implies that we need to gather as much information as possible in order to understand the physics and chemistry of the observed atmosphere. Knowledge of the temperature and planetary radius is crucial for the general understanding of the physical and chemical processes occurring on the planet (e.g., tectonics, water and hydrogen loss to space).

Biomarkers and biosignatures

The terms, biomarkers and biosignatures, are used here to mean detectable chemical species, or set of species, whose presence at significant abundance strongly suggests a biological origin (DesMarais et al 2002). For example, this is the case for the chemical couple CH_4+O_2. Bio-indicators are indicative of biological processes but can also be produced abiotically in significant quantities. Searches for signs of life are based on the assumption that extraterrestrial life shares fundamental physical and chemical characteristics with life on Earth, in particular that liquid water is necessary as a solvent and that such life has a carbon-based chemistry (Owen 1980; Des Marais et al. 2002). Life based on a different type of chemistry is not considered here because the vast possible life-forms produce signatures in their atmosphere that so far are unknown. Thus we assume that extraterrestrial life is similar to life on Earth in its use of the same input and output gases, that it exists out of thermodynamic equilibrium, and that it has analogs to bacteria, plants, and animals on Earth (Lovelock 1975).

Candidate biomarkers that might be detected by a instrument with low spectral resolution (Resolution < 50) include O_2, O_3, and CH_4. There are fundamental biogeochemical and thermodynamic reasons for believing that these gases should be ubiquitous byproducts of carbon-based biochemistry, even if the details of a particular alien biochemistry are significantly different than that on Earth. Production of O_2 by photosynthesis allows terrestrial plants and photosynthetic bacteria (cyanobacteria) to use abundant H_2O as the electron donor to reduce CO_2, instead of having to rely on scarce supplies of H_2 and H_2S. Oxygen and N_2O are two very promising bio-indicators. Oxygen is a chemically reactive gas. Reduced gases and oxygen have to be produced concurrently to produce quantities large enough to be detectable in disk-averaged spectra of terrestrial planet atmospheres, as they react rapidly with each other. N_2O is a biomarker in the Earth's atmosphere, being produced in abundance by life but only in trace amounts by natural processes. Although a relatively weak feature in the Earth's spectrum, it may be more pronounced in extrasolar terrestrial planet atmospheres of different composition or host star spectral type (Segura et al. 2005). Currently, efforts are ongoing to explore the plausible range of habitable planets and to improve our understanding of the detectable ways in which life modifies a planet on a global scale.

An important first step towards the exploration of terrestrial extrasolar planets will be a space mission that can detect and record low-resolution spectra of extrasolar planets. Molecules, such as O_2, O_3, CH_4 are good biomarker candidates that can be detected by a low-resolution (Resolution < 50) spectrograph. There are fundamental biogeochemical and thermodynamic reasons for believing that these gases should be ubiquitous byproducts of carbon-based biochemistry, even if the details of alien biochemistry are significantly different than the biochemistry on Earth. Note that life can also exist without producing either O_2 or CH_4. Even so, we need to understand the abiotic sources of biomarkers better, so that we can identify when it might constitute a "false positive" for life detection, when abiotic sources could produce high quantities of a species we understand as a biomarker on Earth. Further research in theoretical modeling is necessary to explore the plausible range of habitable planets and to improve our understanding of the ways in which life modifies a planet on a global scale that could be detected using astronomical techniques, such as discussed herein.

Giant Planets: The occurrence and properties of giant planets may determine the environments of terrestrial planets. The field of view and sensitivity must be sufficient to detect a giant planet with the radius and geometric albedo or effective temperature of Jupiter at 5 AU (scaled by the square root of stellar luminosity) around at least 50% of its target stars.

Exozodiacal Dust: Emission from exozodiacal dust is both a source of noise and a legitimate target of scientific interest. This mission must be able to detect planets in the presence of zodiacal clouds at levels up to a maximum of 10 times the brightness of the zodiacal cloud in the Solar System. From a science standpoint, determining and understanding the properties of the zodiacal cloud is essential to understanding the formation, evolution, and habitability of planetary systems. Thus, this mission should be able to determine the spatial and spectral distribution of zodiacal clouds with at least 0.1 times the brightness of the Solar System's zodiacal cloud.

Spectral Range and Resolution: The required spectral range for characterization of extrasolar planets will emphasize the characterization of Earth-like planets and is therefore set to 6.5 to 18 μm in the infrared. The minimum spectral resolution is 25 with a goal of 50, which would measure water (H_2O) and ozone (O_3) with 20% accuracy in the equivalent

width of the spectral feature.

Number of Stars to be Searched: To satisfy its scientific goals, this mission should detect and characterize a statistically significant sample of terrestrial planets orbiting F, G, and K stars. A sample of 150 stars within 30 pc (including a small number of nearby M stars) should suffice as a minimum requirement, provided the frequency of Earth-like planets ($\eta_{\oplus}$) is greater than about 0.1 (or one such planet in 10 stars).

Table 1. Flagship Interferometer Mission Requirement Summary	
Star Types	F, G, K, selected, nearby M, and others
Habitable Zone	0.7–1.5 (1.8) AU scaled as $L^{1/2}$ *(Note *)*
Number of Stars to Search	>150
Completeness for Each Core Star	90%
Minimum Number of Visits per Target	3
Minimum Planet Size	0.5–1.0 Earth Area
Geometric Albedo	Earth's
Spectral Range and Resolution	6.5–18 μm; R = 25 [50]
Characterization Completeness	Spectra of 50% of Detected or 10 Planets
Giant Planets	Jupiter Flux, 5 AU, 50% of Stars
Maximum Tolerable Exozodiacal Emission	10 times Solar System Zodiacal Cloud
*There are two definitions in the literature for the outer limit of the habitable zone. The first is 1.5 AU scaled to the luminosity to the ½ power based on Kasting et al. (1993). The second is 1.8 AU scaled in the same way from Forget & Pierrehumbert (1997).	

4.2 Observatory Concepts

At mid-infrared wavelengths the required angular resolution of ≤50 mas would necessitate a single telescope with a primary mirror larger than 40 m across. An interferometer is therefore a compelling choice for the overall design. The technique of nulling interferometry (Bracewell 1978) is used to suppress the on-axis light from the parent star, whose photon noise would otherwise overwhelm the light from the planet. Off-axis light is modulated by the spatial response of the interferometer: as the array is rotated, a planet produces a characteristic signal which can be deconvolved from the resultant time series (Bracewell 1978; Woolf and Angel 1998). Images of the planetary system are formed using an extension of techniques developed for radio interferometry (Lay et al. 2004).

The collecting apertures can be deployed on a single 'structurally-connected' spacecraft or on separate spacecraft that fly in formation. The former is more appropriate for a smaller mission targeting larger planets or Earth-sized planets within about 10 pc, and is a logical step towards a larger formation-flying mission with long baselines needed to detect Earth-sized planets at distances of 30 pc or greater. This, in turn, is a step towards the very large formation-flying systems that will be needed to achieve the strategic goals of life detection and planet imaging. We briefly describe concepts for both a small structurally-connected interferometer, and a larger formation-flying system.

4.2.1 Structurally-Connected Interferometer Mission Concept

An example of a small structurally connected infrared interferometer concept is the Fourier-Kelvin Stellar Interferometer (FKSI) implementation, which is a two-telescope passively cooled nulling interferometer operating between 3 and 8 μm (see Danchi et al. 2003a,b), as shown in Figure 4-4. The FKSI observatory will operate at the second Sun-Earth Lagrange point (L2) in a large amplitude Lissajious (or halo) orbit. While we have explored a range of aperture sizes for FKSI, our baseline design employs 0.5 m apertures. The telescopes employ two flat mirrors (siderostats) mounted 12.5 apart on composite support booms, minimizing alignment requirements for the beams that enter the instrument package. The booms support sunshades that allow passive cooling of the structure to 60-65K, reducing thermal noise in the telescope system to a level that is negligible compared to that from the local zodiacal cloud (zodiacal background limited performance) over most of the instrument passband.

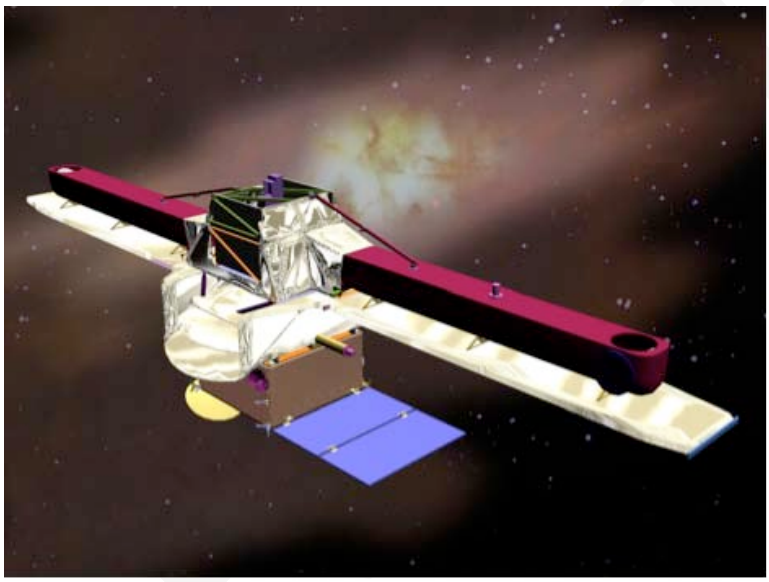

Figure 4-4. A small structually-connected interferometer mission concept. Two telescopes and passive cooling are used for observations in the 3 to 8 micron band.

The mechanical design is appropriate for the the smallest of the the Atlas V launch vehicles with a 4-m diameter fairing. The design minimizes the number of deployments. They are: (1) and (2) the two siderostats mounted on the ends of the booms, separated by 12.5 m, deployed using the well proven MILSTAR hinge technology. The booms are made from composite structures for an optimal strength to weight ratio, and the fixed sunshades are mounted to them; (3) a high-gain gimbaled S band antenna for the data downlink; (4) a solar array for power; and (5) a radiator.

A schematic diagram of the optical design is shown in Figure 5-5. There are five major subsystems in the instrument payload, which is mounted through a low mechanical frequency coupling and gamma-Al struts to the spacecraft bus. These include: (1) the boom-truss assembly which holds the siderostat mirrors and the non-deployed sunshields; (2) the main instrument module and optical bench assembly which includes a pair of off-axis parabolic mirrors for afocal beam size reduction, and also a fast steering mirror assembly to for the control of fine pointing, two optical delay lines (one to be used, the other is a spare), and two dichroic beam splitters, one for the angle tracker and fringe tracker assemblies (0.8-2.5 μm), the other for the science band of 3-8 μm; (3) the angle tracker

assembly for fine pointing; (4) the fringe tracker assembly for stabilizing the fringes for the nulling instrument assembly; and (5) the nulling instrument assembly itself.

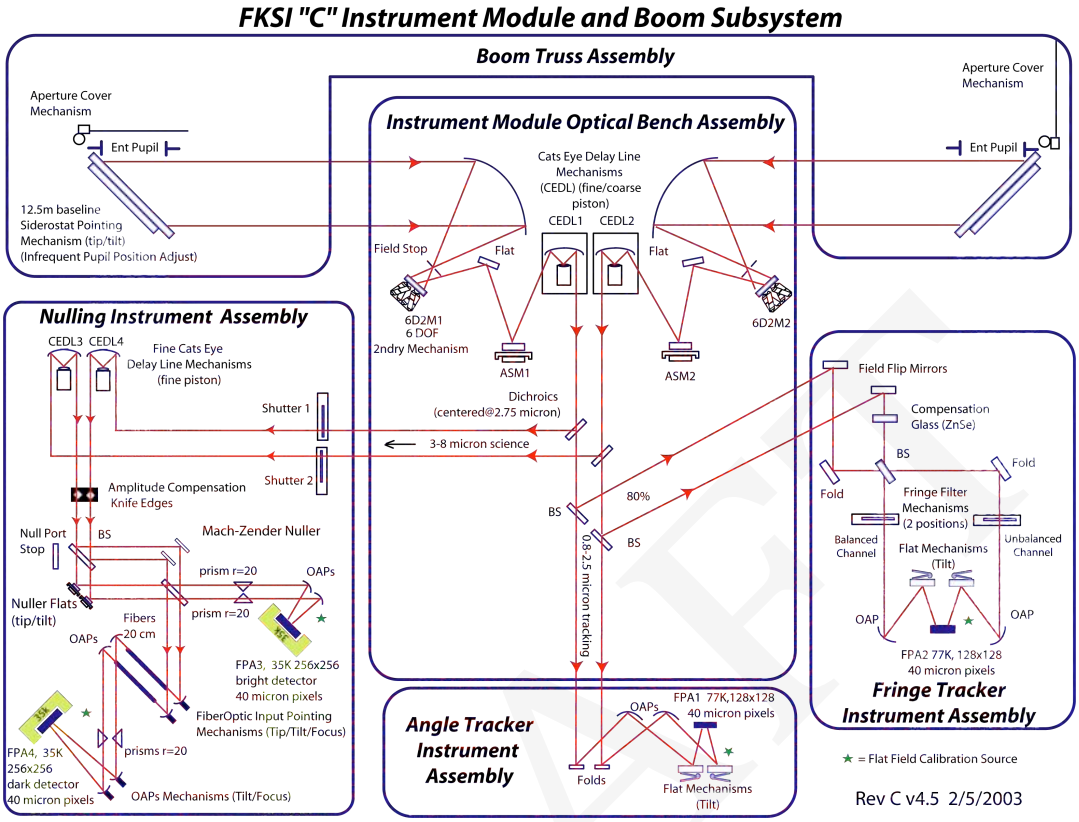

Figure 4-5. Schematic design of the boom and instrument module subsystem for FKSI. The various subassemblies are as noted in the figure.

The nulling instrument is based on a modified Mach-Zehnder beamsplitter design that maximizes the symmetry of the two beams, helping to ensure a deep null. Other elements in the system include shutters for alignment and calibration purposes, an assembly for amplitude control of the fringe null, and optical fibers for wavefront cleanup. The fibers help achieve the desired null depth with reduced tolerances on the preceding optical components (in order to reduce manufacturing costs). The dark and bright outputs are sent to their respective Focal Plane Arrays (FPAs), which could long wavelength HgCdTe arrays from Teledyne (previously Rockwell) operating at 35K, or Si:As arrays operating at 8K, based on those for the MIRI instrument on JWST. The FPAs for the fringe and angle trackers are operated at 77K and are based on the HgCdTe arrays used on the NICMOS instrument on HST. Cryogenic delay lines are used to equalize the pathlengths between the two sides of the interferometer.

Orbital Parameters	What FKSI does:
Removes sin(I) ambiguity	Measure
Planet Characteristics	
Temperature	Measure
Temperature variability due to distance changes	Measure
Planet radius	Measure
Planet mass	Estimate
Planet albedo	Cooperative
Surface gravity	Cooperative
Atmospheric and surface composition	Measure
Time variability of composition	Measure
Presence of water	Measure
Solar System Characteristics	
Influence of other planets, orbit coplanarity	Estimate
Comets, asteriods, zodiacal dust	Measure

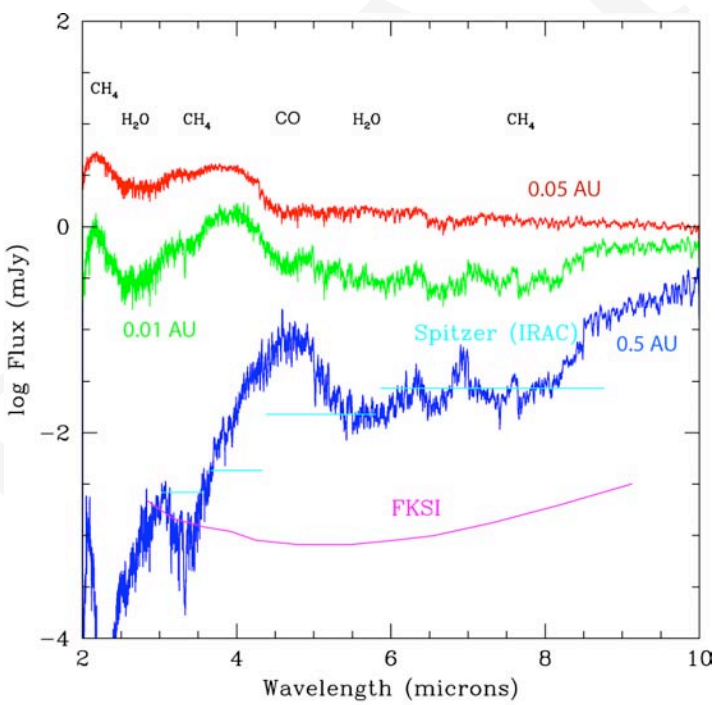

Figure 4-6. (a) Upper panel. Characteristics of exoplanets that can be measured using FKSI. (b) Lower panel. The FKSI system can measure the spectra of exoplanets with a wide range of semi-major axes

When the Instrument is in operation, it rotates slowly around the line of site to the object. In doing so, a sinusoidal signal is generated at the output of the nuller instrument, which is non-zero if there is a planet or material within the transmission pattern of the nuller. Data

from the bright port is also taken providing measurements of the visibility of the object. Simulations have been performed, both for nulling operation as well as imaging (Danchi et al. 2003a; Barry et al. 2005, 2006). Figure 4-6 left panel displays the types of measurements that are made with such as system, while the right panel shows that a small interferometer is capable of measuring the emission spectra of known exoplanets with a large range of semi-major axes.

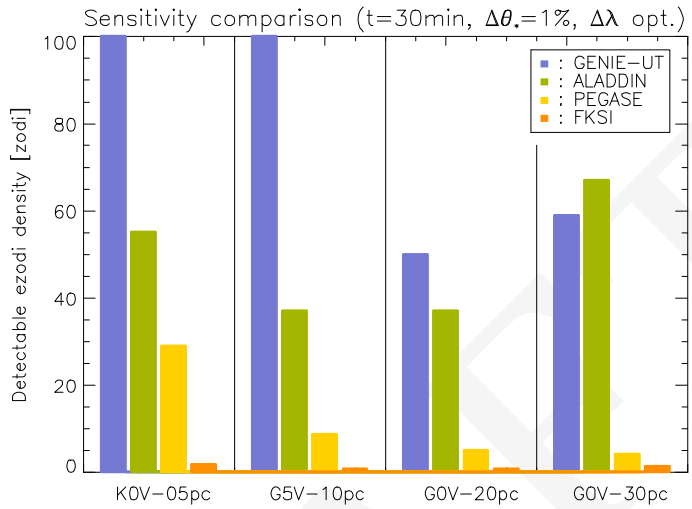

Figure 4-7. Expected performance for Pegase and FKSI compared to the ground-based instruments (for 30 min integration time and 1% uncer-tainty on the stellar angular diameters).

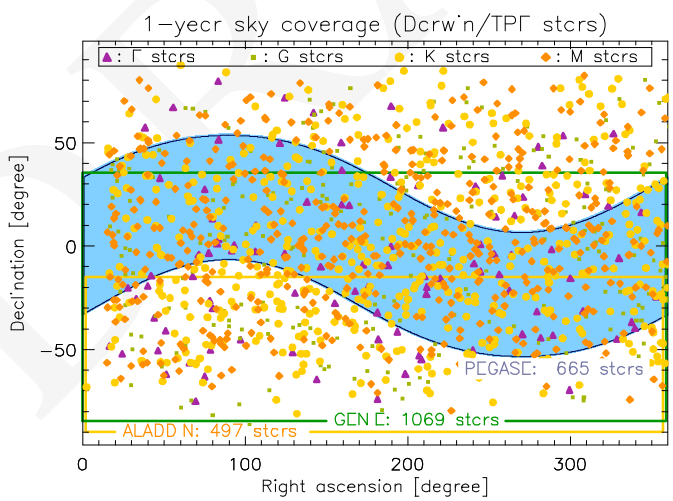

Figure 4-8. Sky coverage after 1 year of observation of GENIE (dark frame), ALADDIN (light frame) and Pegase (shaded area) shown with the Darwin/TPF all sky target catalogue. The blue-shaded area shows the sky coverage of a space-based instrument with an ecliptic latitude in the [-30°,30°] range (such as Pegase). The sky coverage of FKSI is similar to that of Pegase with an extension of 40° instead of 60°.

The concept discussed above has undergone a thorough integrated analysis and modeling study of the structure and optics to validate the design and ensure it meets requirements (Hyde et al. 2004). A major concern was the propagation of reaction-wheel disturbances from the spacecraft bus through the bus-instrument package coupling up to the boom system. Contributions to the performance error budget for the required 10^{-4} null are well understood and have been reported in Hyde et al. (2004). The null depth requirement drives the instrument performance. Other sources of noise include the Fringe Tracker (FT), the Optical Delay Line (ODL), the Attitude Control System (ACS), and the booms themselves. The boom system had lowest order modes at 5.6 and 7.3 Hz. Through this modeling and validation campaign, we were able to verify that the closed loop performance requirement could be met or exceeded at all wheel speeds from 0.1 to 100 Hz (Hyde et al. 2004).

4.2.2 Performance

Figure 4-6 (upper panel) displays a table of planetary characteristics and what can be determined using a modest nulling interferometer, such as planetary temperature, radius, mass density, albedo, surface gravity, and atmospheric composition, including the presence of water. To date, progress has been made on the physical characteristics of planets largely through transiting systems, but a small planet finding interferometer can measure the emission spectra of a large number of the non-transiting ones, as well as more precise spectra of the transiting ones.

Many molecular species, such as carbon monoxide, methane, and water vapor, have strong spectral features in the 3-8 μm region, as can be seen in Figure 4-6 (lower panel), which displays model atmospheres for extrasolar planets calculated by Seager (2005), for planets at various distances from the host star. The red curve shows the theoretical spectrum of a very hot, close-in planet at 0.05 AU, while the blue curve displays spectrum for a much cooler planet ten times further out, at 0.5 AU. Also displayed are sensitivity curves for the IRAC instrument on Spitzer (light blue) and FKSI (purple). Clearly such a mission concept has sufficient sensitivity to detect and characterize a broad range of extrasolar planets.

Initial studies with very conservative assumptions of an 8 m boom length, 140 extrasolar planets (known at that time), 120 second on-source integration time, 15 nm rms path length error, telescope temperature of 65K, and a small sunshield with a +/- 20 degree field of regard; gave ~25 detections. Currrently, there are about 250 known planets, so with those assumptions and the same detection ratio of about 18%, we expect to be able to detect and characterize about 45 exoplanets, and a larger sunshade with a field of regard of +/- 45 degrees, would approximately double this number to ~90 planets.

Recent studies of the detectability of debris disks (Defrere et al. 2008) demonstrated that the residual pathlength error for a small system like FKSI should be of the order of 2 nm rms, which would significantly increase the number. As a conservative estimate, we expect that a small system could detect (e.g. remove the sin(i) ambiguity) and characterize about 75-100 known exoplanets.

These recent studies also have shown that a small mission is ideal for the detection and characterization of exozodial and debris disks around ALL TPF candidate stars in the Solar neighborhood as seen in Figures 4-7 and 4-8. (Defrere et al. 2008). Indeed, the performance level of the FKSI system is of the order of 1 Solar System Zodi in 30 minutes of integration for a G0 star at 30 pc. With a small sunshade this system could observe of the order of 450 stars in the Solar neighborhood, and with a larger field-of-regard, such as +/- 45 degrees, the exozodis and debris disks of about 1000 stars could be studied.

If the telescopes are somewhat larger than has been discussed in some of the existing mission concepts (e.g., 1-2 m) and are somewhat cooler (e.g., < 60K) so that the system can operate at longer wavelengths, it is possible for a small infrared structurally-connected interferometer to detect and characterize super-earths and even ~50-75 earth-sized planets around the nearest stars. This is especially important now that there is evidence that lower mass planets are very common, based on the detection of the 5.5 Earth mass planet using the microlensing approach (e.g. Beaulieu et al. 2006, Gould et al. 2006).

Further studies of the capabilities of a small infrared structurally-connected interferometer are necessary to improve upon our estimates of system performance.

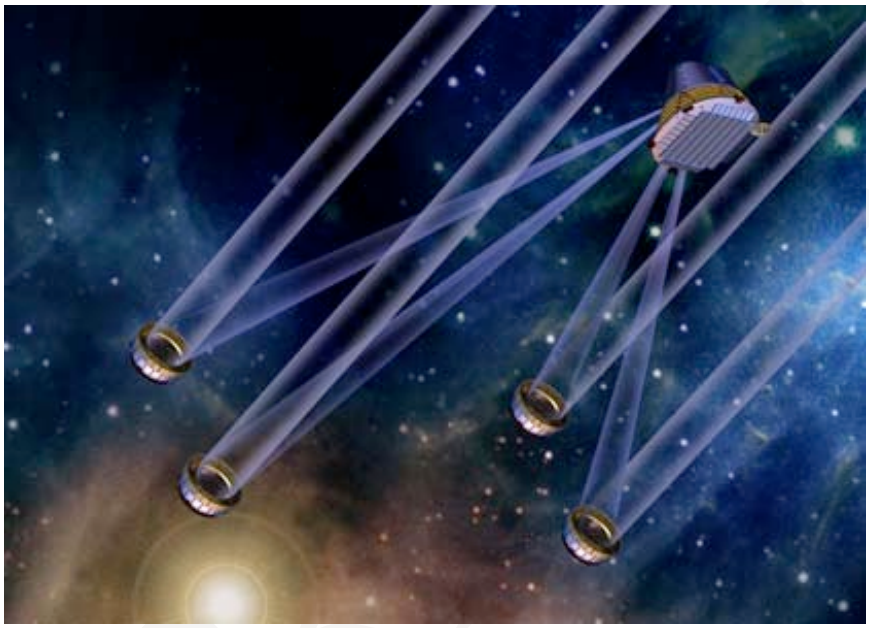

Figure 4-9: 'Emma X-Array' formation flying concept.

4.2.3 Free Flying Interferometer Concept

Figure 4-9 depicts a mission concept capable of detecting a large number of Earth-sized planets. This Emma X-Array formation-flying design is the culmination of more than a decade of study by NASA and ESA. Light from the target star is reflected from the four collector mirrors (~ 2 m diameter) and focused onto the input apertures of the combiner spacecraft approximately 1 km away. To observe a target system, the collector array is rotated slowly about the line-of-sight, using a combination of centimeter-precision formation flying and careful attitude control to maintain the pointing of the beams. The light entering the combiner passes through a series of optics (Figure 4-10) that perform beam steering and compression, delay compensation, intensity and dispersion correction (see "the Adaptive Nuller" below), pairwise beam combination with p phase shift (the nullers), cross-combination of the nulled beams, single-mode spatial filtering, and, finally, dispersion and detection of the nulled light on the science camera. The time series of output data is synthesized into an image. A key advantage of the X-Array configuration is its very high angular resolution, as illustrated by the simulated image shown in Figure 4-11.

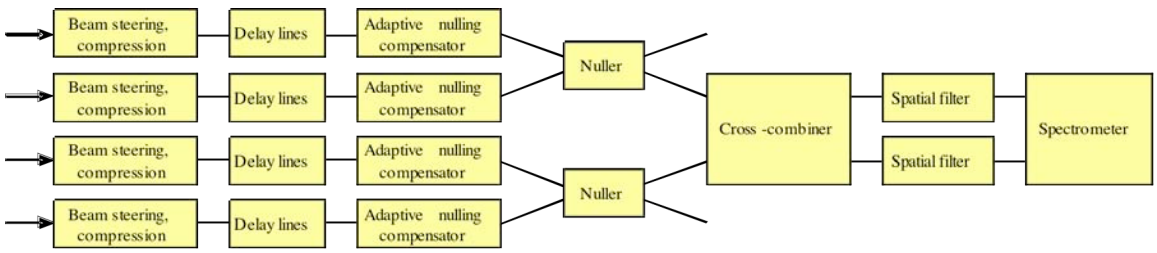

Figure 4-10: Schematic of beam combiner optics.

4.2.4 Performance

The planet-finding capability for a formation-flying Emma X-Array design is shown in Figure 4-12. A mission with 2-m diameter collectors would be capable of detecting over 100 earth-sized planets around nearby stars, primarily F, G, and K spectral type, over a period of 2 years, assuming η_{earth} = 1. The performance model is described in Lay et al. (2004) and includes the dominant sources of noise: photon noise from local zodi, exo-zodi and stellar leakage, and instability noise (Lay 2004) from fluctuations in the phasing and intensity balance within the instrument optics. Following a candidate planet detection and follow-up confirmation, a longer period of observing time is dedicated to spectroscopic characterization, using the same observing procedure as for the initial detection.

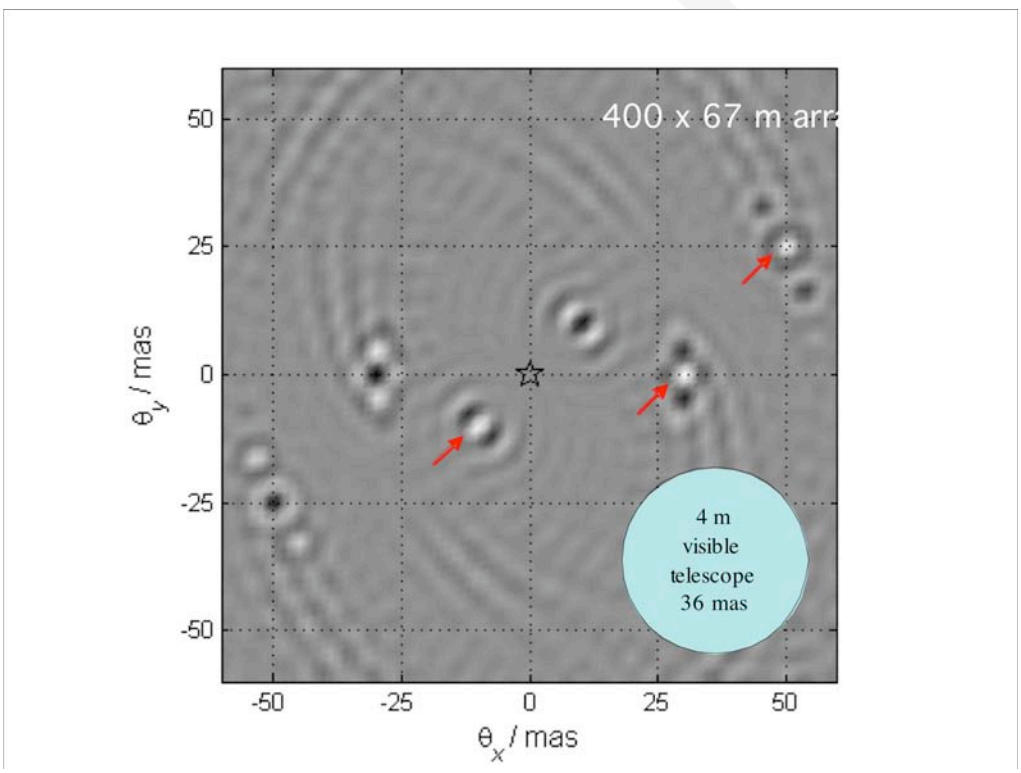

Figure 4-11: Simulated 'dirty' image from Emma X-Array, prior to deconvolution. Angular resolution is 2.5 mas. Planet locations are indicated by red arrows.

Simultaneous full resolution (R~100) spectroscopy for all objects within the field of view is a natural by-product of interferometric observing. While data from the detection and orbit determination phases should be sufficient for a coarse spectrum, a deep characterization

will require significant integration time. Detection of CO_2 for an Earth at 5 pc with 2-m collectors will require ~ 24 hours of integration (SNR of 10 relative to the continuum). The narrower ozone absorption line requires 16 days at 5 pc. For ozone at 10 pc, integration times as long as 40 days could be needed, falling to ~ 6 days with 4-m diameter collectors.

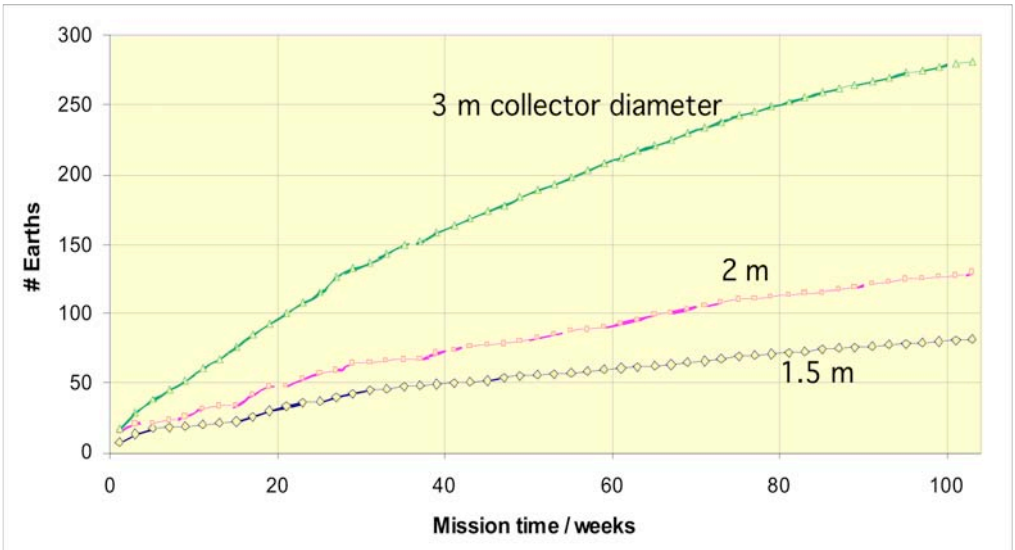

Figure 4-12: Predicted number of Earths detectable by Emma X-Array architecture as a function of elapsed mission time and collector diameter.

4.3 Technology

4.3.1 Accomplishments from 2000-present

Component and Subsystem Technology*

Mid-IR Spatial Filters

Spatial filters are an essential technology for nulling interferometry, converting complex optical aberrations in the incoming wavefronts into simple intensity and phase differences which are more readily corrected, making extremely deep nulls possible. Spatial filters may be implemented in a variety of ways, including single-mode fiber-optics made from chalcogenide glasses, metallized waveguide structures micro-machined in silicon, or through the use of photonic crystal fibers. Two types of fiber spatial filters have been successfully developed: polycrystaline silver halide fibers have been developed by Prof. Abraham Katzir at Tel Aviv University (TAU) in Israel; and chalcogenide fibers have been developed by Dr. Jas Sanghera at the Naval Research Laboratory (NRL.

The 20-cm long chalcogenide fibers developed by the Naval Research Laboratory (shown in Figure 4-13) were shown to demonstrate 30 dB rejection (a factor of 1000) of higher order modes and have an efficiency of 40%, accounting for both throughput and Fresnel losses. The transmission losses were measured to be 8 dB/m, and the fibers are usable up to a wavelength of about 11 μm. The chalcogenide fibers developed at the Naval Research

Laboratory were used successfully in the Achromatic Nulling Testbed and are currently in use in the Adaptive Nuller testbed.

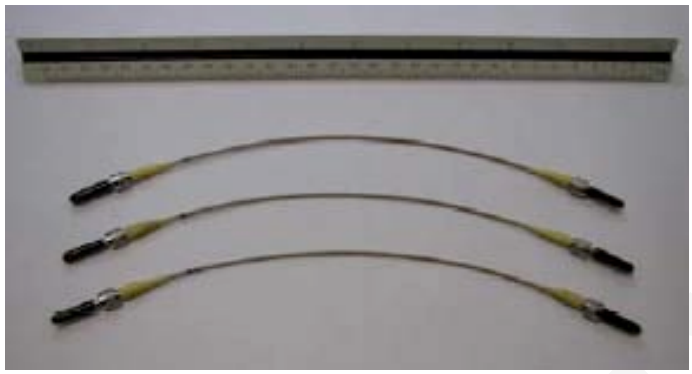

Figure 4-13: Single mode fibers for mid-infrared developed by TAU.

The 10-20 cm long silver halide fibers that were developed by Tel Aviv University were shown to demonstrate 42 dB rejection (a factor of 16,000) of higher order modes with transmission losses of 12 dB/m. This high rejection of higher-order modes was accomplished with the addition of aperturing of the output of the fibers, made possible by the physically large diameter of the fibers. Silver halide fibers should in principle be usable up to a wavelength of about 18 microns, although the lab tests at JPL were conducted only at 10 microns. This is the first time silver halide fibers were demonstrated to have single-mode behavior.

Adaptive Nulling and Achromatic Phase Shifters

The variations in amplitude and phase that may be present in the incoming wavefront must be corrected in order to achieve deep nulls at every wavelength. The Adaptive Nuller was designed to correct phase and intensity variations as a function of wavelength, in each of two linear polarizations. In principle this should allow high performance nulling interferometry, while at the same time substantially relaxing the requirements on the nulling interferometer's optical components. The goal of the testbed was to demonstrate, in a 3 μm band centered at a wavelength of 10 μm, the correction of the intensity difference to less than 0.2% rms (1 σ) between the interferometer's arms, and at the same time correct the phase difference across the band to < 5 nm rms (1 σ). This overall correction is consistent with a null depth of 1×10^{-5} (1 part in 100,000) if all other sources of null degradation can be neglected.

The Adaptive Nuller was designed to correct these variations, matching the intensity and phase between the two arms of the interferometer, as a function of wavelength, for both linear polarizations. A deformable mirror is used to adjust amplitude and phase independently in each of about 12 spectral channels. A schematic of the adaptive nuller is shown in Figure 4-15. Two prisms split the incoming light into its two linear polarization components and divided it into roughly a dozen spectral channels. The light is then focused onto a deformable mirror where the piston of each pixel independently adjusts the phase of each channel. By adjusting the angle of the reflected beam so that the beam is slightly vignetted at an exit aperture, the intensity is also controlled. The adaptive nuller uses a broadband thermal source to generate light in the 8–12 μm wavelength band.

The results of this research up until 2008 have been published by Peters et al. (2008). In March/April 2007, the testbed achieved its primary goal of demonstrating phase

compensation to better than 5 nm rms across the 8–12 μm band and intensity compensation to better than 0.2%. In June 2008 the mid-infrared Adaptive Nuller demonstrated a null depth of 1.1×10^{-5}, (93,000:1 rejection ratio), over a bandwidth of 32%.

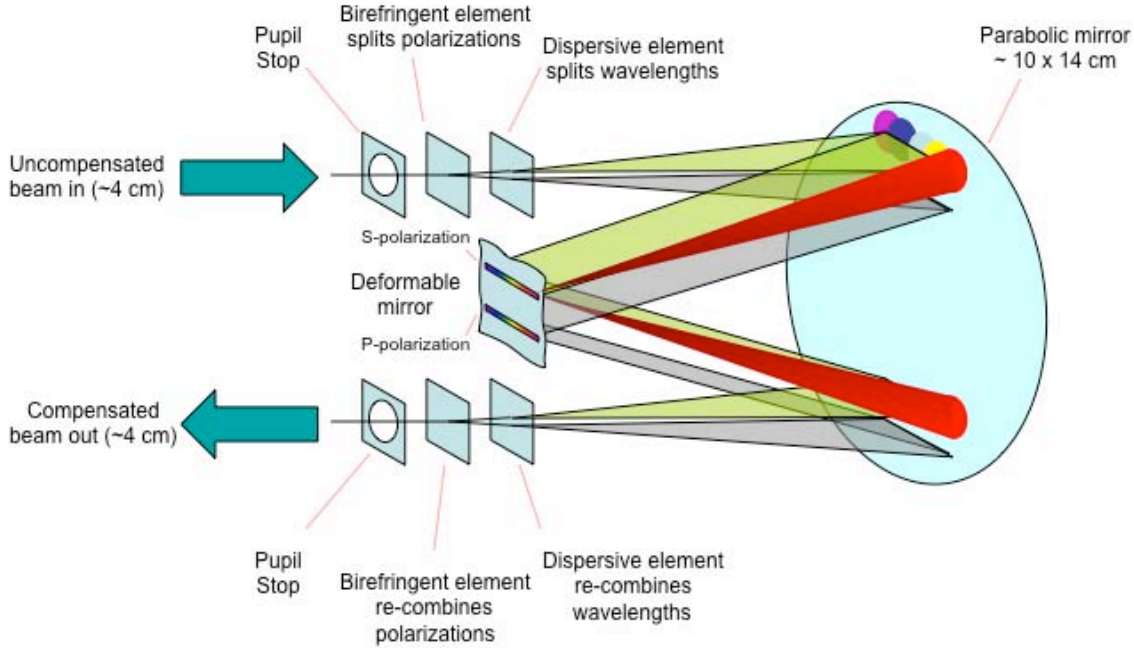

Figure 4-15. Schematic of the Adaptive Nuller. Uncompensated light that enters the device is split into two linear polarizations, and each polarizaion is treated separately then recombined. Light is dispersed and imaged onto a deformable mirror (DM). Piston of elements in the DM adjusts phase at a particular wavelength, and tilt of the same pixel adjusts relative intensity by shearing the output pupil at that wavelength.

This is the deepest broadband null ever achieved by a mid-infrared nulling interferometer, and almost attains the TPF-I flight requirement. Work is ongoing to improve the performance of the testbed to demonstrate nulls better than 1.0×10-5, as measured data sets 6 hours or more in duration.

Cryocoolers

With the Advanced Cryocooler Technology Development Program (ACTDP), the TPF-I and JWST projects have produced development model coolers that have met or exceeded their performance requirements, which are to provide ~30 mW of cooling at 6 K and ~150 mW at 18 K. This demonstrates the approach to cooling the science detector to a temperature low enough to reveal the weak planet signals. This activity is at TRL 6 (Lawson et al. 2007).

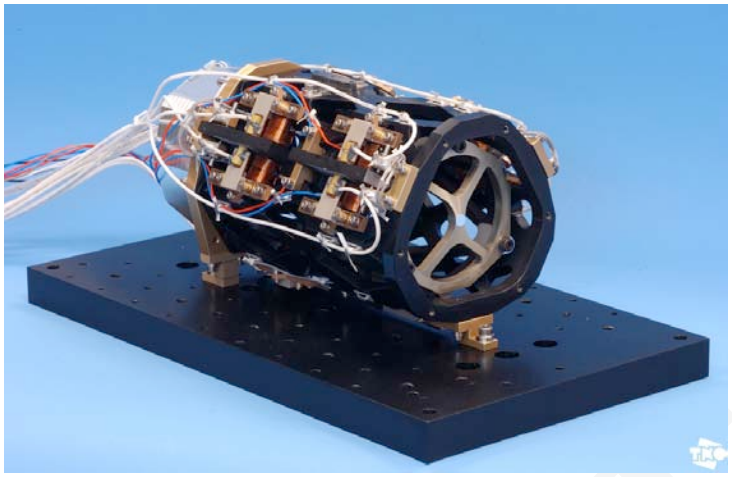

Figure 4-16. Overview of the Optical Delay Line with the outer fixed structure holding the active parts for magnetic levitation and axial motion, and the inner moving structure that includes the optical components. Courtesy ESA and TNO.

Cryogenic delay lines

The Dutch company TNO Science and Industry led a consortium that developed a compact cryogenic Optical Delay Line (ODL) for use in future space interferometry missions such as ESA's Darwin and NASA's TPF-I (Figure 4-16). The prototype delay line is representative of a flight mechanism. The ODL consists of a two-mirror cat's eye with a magnetic bearing linear guiding system. TNO and its partners have demonstrated that accurate optical path length control is possible with the use of magnetic bearings and a single stage actuation concept. Active magnetic bearings are contactless, have no friction or hysteresis, are wear free, and have low power dissipation. The design of the Darwin broadband ODL meets the ESA requirements, which are an OPD stroke of 20 mm, stability of 0.9 nm rms (with a disturbance spectrum of 3000 nm rms, < 20 mW power dissipation (2 mW with flight cabling), output beam tilt <0.24 microradians, output lateral shift < 10 microns peak-to-peak, wavefront distortion <63 nm rms at 40K, and wavelength range (0.45-20 microns). The Darwin ODL is representative of a future flight mechanism, with all materials and processes used being suitable for flight qualification. Positioning is done with a voice coil down to subnanometer precision. The verification program, including functional testing at 40 K, has been completed succesfully. This technology is at at TRL 6 (see Fridlund, C.V.M. et al. 2008).

Thermal shields

Science requirements for JWST have driven the need for a deployable, low areal-density, high thermal performance efficiency (effective emittance, e* of 10^{-4} to 10^{-5}) sunshield to passively cool the Observatory Telescope Elements and Integrated Science Instruments Module (OTE/ISIM). The thermal performance dictated the need for a sunshield consisting of multiple, space membrane layers such that the ~200 kW of the Sun's energy impinging on the sun-facing layer would be attenuated such that the heat emitted from the rear or OTE-facing membrane would be < 1W. This would enable the OTE/ISIM to operate at cryogenic temperature levels (< 50 K) and have a temperature stability of 0.1 to 0.2K over the field-of-regard pointing re-alignments.

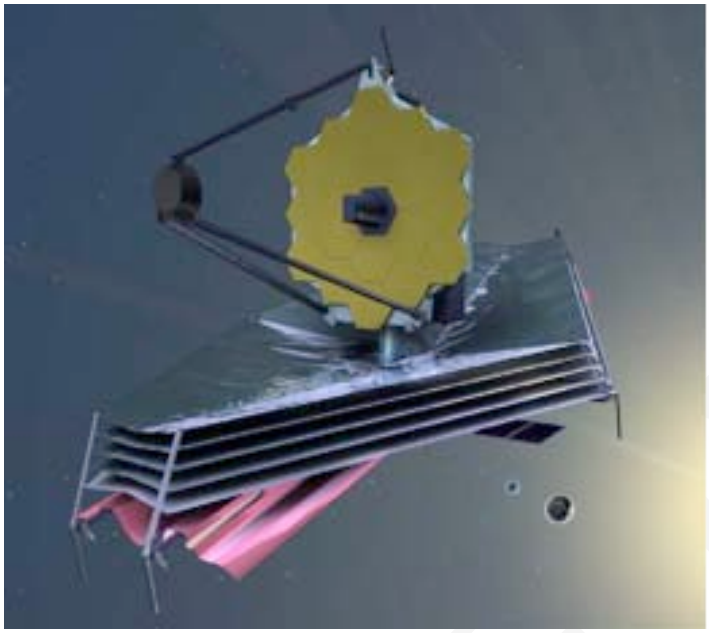

Figure 4-17. The James Webb Space Telescope. Courtesy NASA/JSWT.

Based on these top-level mission requirements a sunshield was developed employing 5 membrane layers with pitch and dihedral separation angles of 1.6 and 2 degrees, respectively. Through the use of a low solar absorptance-to-emittance ratio (α_S / ε_H) coating on the sun-facing surface (layer 1) and an infrared highly reflective coating on the majority of the other membranes' surfaces, the sun's heatload absorbed by the sun-facing membrane is reduced and the resulting infrared energy re- emitted to the other layers would be reflected laterally out the open sides of the sunshield, thus greatly attenuating the residual infrared energy emitted by the OTE/SIM-facing membrane surface (layer 5). From a variety of trade studies the Sunshield evolved into a 5-membrane system as shown in Figure 4-17 with membranes 140 to 150 m^2 in size that are supported by six spreader bar/boom assemblies and are lightly tensioned in a deployed configuration by constant-force spring-loaded catenary cable assemblies attached to the periphery of each membrane. The present sunshade design for JWST is at TRL 6 and meets the similar requirements for the flagship mission and is more than adequate for a small mission (Kurland 2007).

Detector Technology

Detectors or Sensor Chip Assemblies (SCAs) from the JWST Mid-Infrared Instrument (MIRI) have been developed by Raytheon Vision Systems (RVS) having 1024x1024 pixels fabricated from arsenic-doped silicon (Si:As) and which consist of a detector layer and a readout multiplexer. The detector structure is a back illuminated silicon substrate with an active detector layer grown on top of that, followed by a blocking layer (to minimize the dark current), and then indium bumps. The readout multiplexer is a cryogenically optimized electronic circuit chip having a source follower (transistor) for each detector pixel, which then multiplexes those pixels down to four video outputs that are read by the remaining instrument electronics. The two components of the SCAs are mated together through matching indium bumps. The required performance levels are: dark current less than 0.03 electrons per second, readout noise less than 19 electrons, and quantum efficiency >50%. These detectors have been rigorously tested and have met or exceeded these requirements for JWST, giving a TRL of 6 (Ressler 2007). These detectors meet or

exceed the requirements for both a small structurally connected interferometer mission and the flagship mission. See Figure 4-18 for an example of a complete focal plane module for the MIRI instrument on JWST.

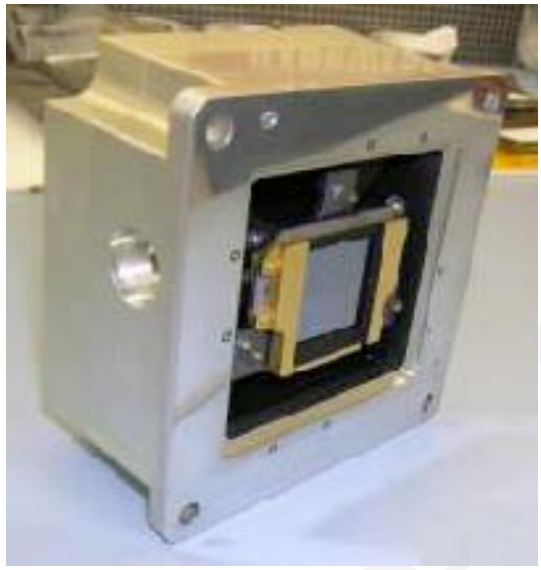

Figure 4-18. The MIRI Focal Plane Module contains the SCA, a fanout board, and the mounting structure needed to position and isolate the sensor. Courtesy NASA/JSWT.

Integrated Modeling

Observatory Simulation: Demonstrate a simulation of the flight observatory concept that models the observatory subjected to dynamic disturbances (e.g., from reaction wheels). Validate this model with experimental results from at least the Planet Detection Testbed at discrete wavelengths. Use this simulation to show that the depth and stability of the starlight null can be controlled over the entire waveband to within an order of magnitude of the limits required in flight to detect Earth-like planets, characterize their properties, and assess their habitability. This activity is at TRL 5 (Lawson et al. 2007).

Formation Flying Technology

Thrusters

Missions employing Precision Formation Flying (PFF) require propulsion capabilities that exhibit low plume contamination, high thrust precision, and high power and propellant efficiency. Ion thrusters typically deliver low-contamination plumes and high efficiency by using noble gas propellants, but conventional thrusters provide thrust levels over an order of magnitude greater than the sub-milli-Newton (mN) to mN levels needed for precision-controlled formation-flying space interferometer missions.

Figure 4-14 A MiXI microthruster

Figure 4-14 displays a miniature ion thruster, the Miniature Xenon Ion (MiXI) thruster, a new option that meets mission needs. One particularly useful characteristic of the MiXI thruster is its incredibly large thrust range that provides smooth amplitude modulated thrust in the 0.1 – 3.0 mN in the amplitude modulated mode and 0.001 – 0.1 mN of thrust in PWM mode (patent-

pending). With a minimum on-time of less than 1 ms, the MiXI thruster can provide impulse bits of less than 1 μN·s at low power levels. The PWM mode of the MiXI thruster is achieved by precision control of the thruster voltages.

Formation Control Testbed

The Formation Control Testbed (FCT) (Figure 4-16) was built to provide an end-to-end autonomous formation flying system in a ground-based laboratory. The FCT provides an environmentfor system-level demonstration and validation of formation control algorithms. The algorithms are validated using multiple floating test robots that emulate real spacecraft dynamics. The goal is to demonstrate algorithms for formation acquisition, formation maneuvering, fault-tolerant operations, as well as collision-avoidance maneuvering. (See Lawson et al. 2008 and references therein.)

The FCT is comprised of two robots with flight-like hardware and dynamics, a precision flat floor for the robots to operate on, ceiling-mounted artificial stars for robot attitude sensing and navigation, and a "ground control" room for commanding the robots and receiving telemetry. The robots and part of the flat floor are shown in Figure 4-15. The layout of the FCT emulates the environment of a formation of telescopes that is restricted to maneuvering in the same plane in space, normal to the direction of the target star.

Figure 4-15. The Formation Control Testbed (FCT). Shown here are the two robots of the FCT. Each robot carries cannisters of compressed air that allow them to float off a polished metal floor. The floor is flat to within 2 one-thousandths of an inch and spans a much larger area than shown here. The robots serve as the hardware interface and testing ground for flight software developed for space applications in formation flying. Courtesy Caltech/JPL/NASA.

To be as flight-like as possible, each robot is equipped with a typical single-spacecraft attitude control suite of reaction wheels, gyros, and a star tracker. Thrusters are also available for attitude control. Each robot has a lower translational platform and an upper attitude platform. The attitude platform is the "spacecraft" and is completely disconnected from the translational platform.

- The attitude platform/spacecraft houses the avionics, actuators, sensors, inter-robot and "ground"-to-robot wireless communication antennae, and the spacecraft

processors.

- The translational platform provides both translational and rotational degrees of freedom to the attitude platform via (i) linear air bearings (the black, circular pads at the base of each robot) that allow the entire robot to float freely on the flat floor, and (ii) a spherical air bearing at the top of the vertical stage (the black, vertical cylinders).

In 2007 the Formation Control Testbed demonstrated precision maneuvers using two robots, showing autonomous initialization, maneuvering, and operation in a collisionfree manner. The key maneuver that was demonstrated was representative of TPF-I science observations. Repeated experiments with the robots demonstrated formation rotations through greater than 90 at ten times the flight rotation rate while maintaining a relative position control to 5 cm rms. Although the achievable resolution in these experiments was limited by the noise environment of the laboratory, it was nonetheless demonstrated (through modeling) that in the relatively noise-free environment of space, the performance of these algorithms would exceed TPF-I flight requirements.

Starlight Suppression through Nulling Interferometry

The flight requirement for TPF/Darwin flight mission is to achieve a mean rejection ratio of 100,000:1 across the full science band of 6-20 microns. Laboratory work with the Adaptive Nuller has yielded mid-infrared rejection ratios of 93,000:1 nulls with bandwidths of 32% at a mean wavelength of 10 microns. These results show that at the subsystem level the nulling performance is almost at TRL 4. Moreover, these results show that the Adaptive Nuller is a viable solution to the design of achromatic phase shifters, and that the chalcogenide single-mode fibers it uses are viable in the lower wavelength range of the science band (6-12 microns). A summary of the past decade's research in nulling interferometry is given the paragraphs that follow.

Deep nulls of narrowband light have been achieved using both pupil-plane and focal plane nulling techniques and the extension of these results to broadband and randomly polarized sources is now the remaining challenge. To achieve deep nulls in an interferometer, the optical properties of the combined beams must be quite similar. The properties include intensity balance, polarization angle, polarization dispersion, and wavefront differences. Some of the requirements for the balance in these properties can be mitigated by the use of single mode spatial filtering at the detector, for example by using a single mode fiber to receive the light. The components of the optical system will introduce defects into the pristine wavefront received from the stellar source, adding wavefront deformations and polarization changes. If these defects are more or less the same in each input beam of the interferometer, the system will still be capable of nulling. For a broadband source, the effects of the defects need to be controlled across the entire nulling waveband and this requirement has been addressed with the development of the Adaptive Nuller (Peters et al. 2008) which is a system designed to correct intensity and phase differences across the band for both polarizations.

Since 1999 when Ollivier (1999) reported laser nulls of $\sim 6\times10^3$ and Serabyn (1999) reported 2×10^4, progress has been made in both null depth and bandwidth. Deep, single polarization laser nulls in the mid-infrared waveband of order 2×10^6 were reported by Martin et al (2003) and Samuele et al (2007) reported nulls of order 1×10^7 at visible wavelengths. Similarly, since Wallace et al. (2000) reported broadband nulls of 6×10^3 at 8% bandwidth, Samuele et al (2007) achieved 9×10^5 at 15% bandwidth in the visible and Peters et al (2008) have achieved 8×10^4 at 32% bandwidth in the mid-infrared. These

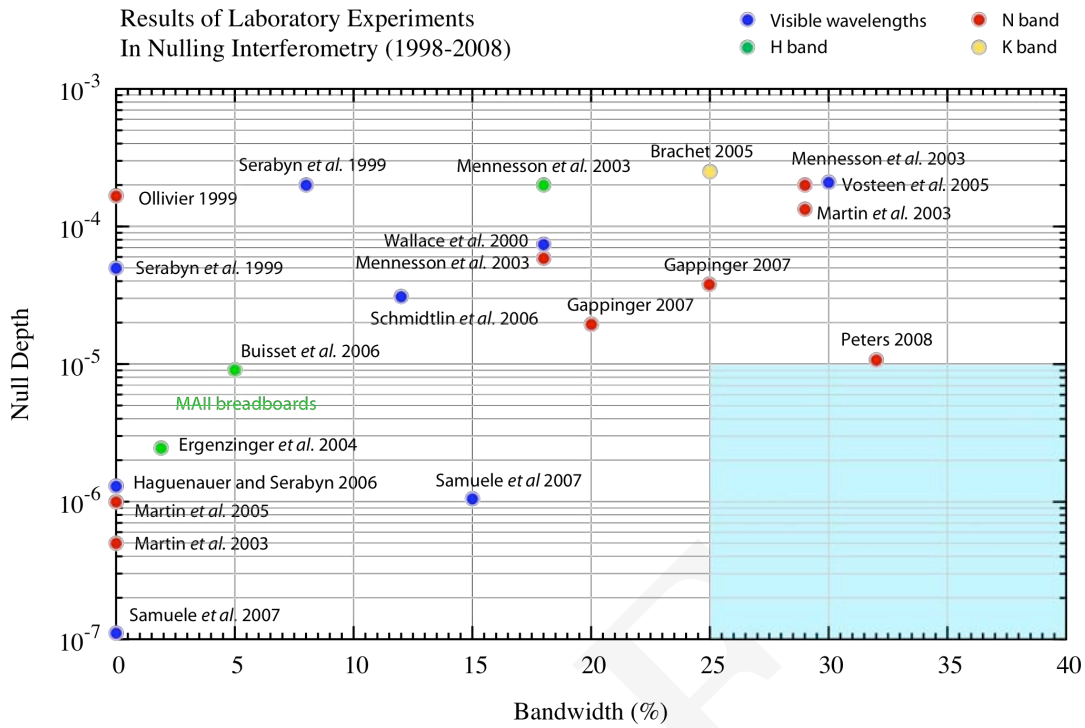

Figure 4-19: Chart of null depths achieved since 1999.

results and some others of note are included in Figure 4-19, which shows a summary of nulls (Lawson et al. 2008).

Serabyn's early nuller, known as the SIM roof-top nuller, was used for both laser and broadband nulling tests near the visible waveband. It used a geometric field inversion technique but was asymmetric in that a beamsplitter-compensator plate arrangement was used. A more symmetrical nuller (Figure 4-21) was then built for the Keck telescopes, the modified Mach-Zehnder (MMZ) nuller (Crawford et al., 2005) in which field inversion was performed outside the nuller and the beams traversed two beam splitters each, allowing symmetrical treatment (Figure 4-20).

The Keck nuller (Serabyn et al., 2004) employs two MMZ nullers to null four input beams and operates in the mid-infrared. More recently, laboratory work has used Mach-Zehnder schemes to produce symmetrical nulling systems for the Planet Detection Testbed (PDT) (Martin et al. 2006) and the Achromatic Nulling Testbed (ANT) (Gappinger et al. 2007), for example. The PDT has nulled four laser beams at 10.6 μm wavelength at the 2.5×10^{-5} level.

A somewhat different interferometric beam combination scheme has also been proposed in Europe (Wallner et al. 2004, Karlson et al. 2004). By combining beams directly on a single mode fiber, the complex interaction of the light with beamsplitter and antireflection coatings can be eliminated. Conceptually, such a beamcombiner can be both achromatic and polarization insensitive, at the cost of some optical throughput efficiency. Small scale testbeds for this type of beamcombiner are being developed and have achieved deep laser nulls of 0.9×10^{6} (Mennesson et al 2006) in the visible and broadband nulls of order 10^{4} at 18% bandwidth at J-band (Martin et al, 2008) (Figure 4-23).

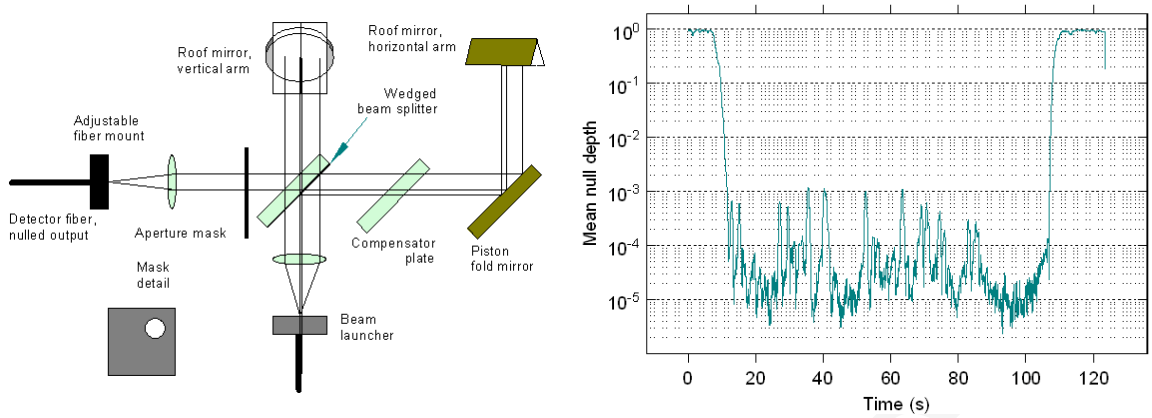

Figure 4-20: (left) SIM rooftop nuller layout, (right) laser null at 633 nm showing single polarization null depths of order 10^{-5}.

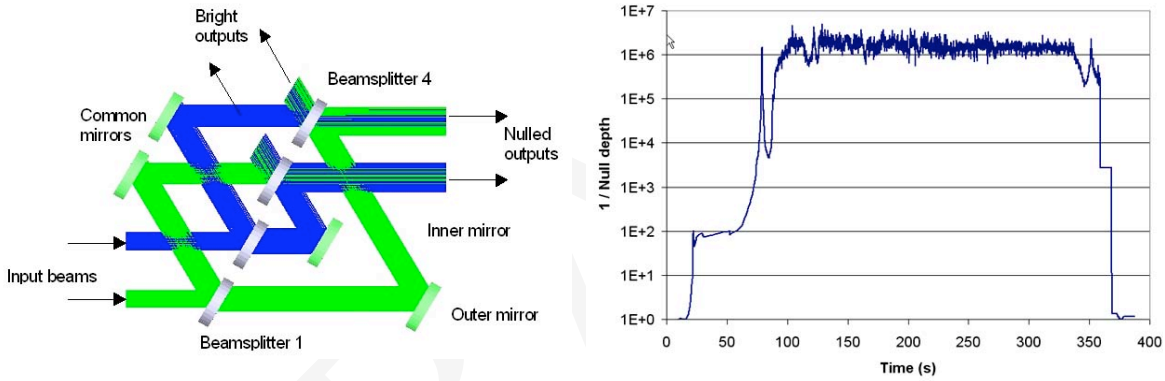

Figure 4-21: (left) MMZ nuller built for Keck telescopes, (right) single polarization laser null at 10.6 µm showing null depth of 5×10^{-7}.

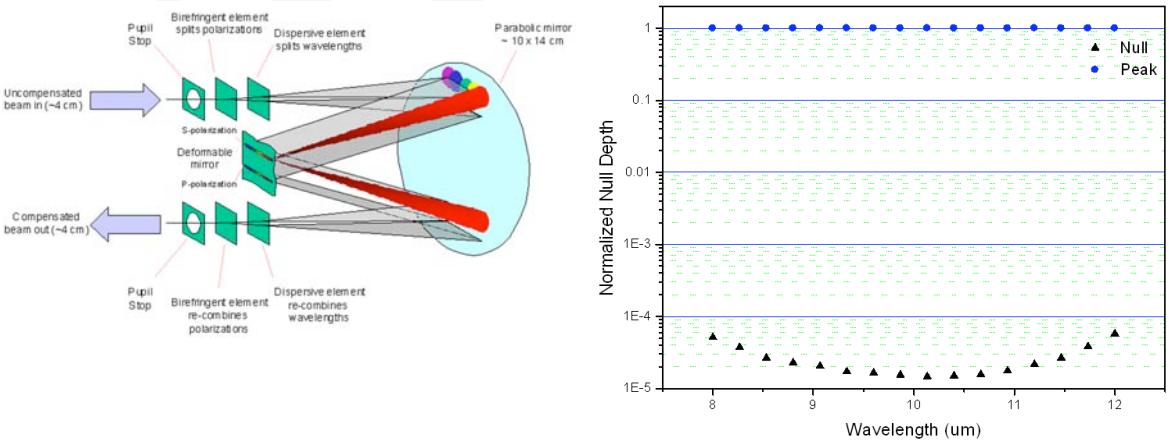

Figure 4-22: (left) compensator portion of the Adaptive Nuller, (right) unpolarized null depths across the band between 8 and 12 µm.

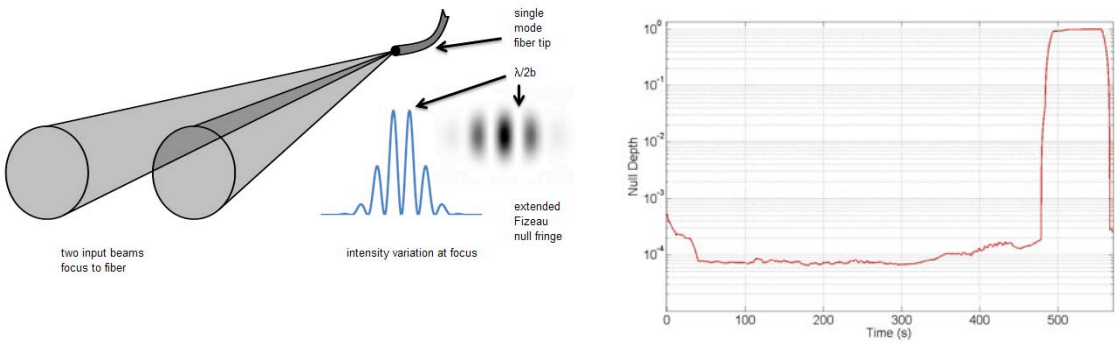

Figure 4-23: (left) concept for a nuller using a fiber beam combiner, (right) unpolarized broadband null of 18% bandwidth at 1.65 μm showing null depth better than 10^{-4}.

Planet Detection Testbed

The Planet Detection Testbed (PDT) is a breadboard system intended to demonstrate techniques that will be required for detection of exoplanets using a mid-infrared telescope array. As a breadboard system operating in a normal room environment it differs from a flight demonstration system in both its layout and in the flux levels used which are much higher than would be encountered in space. It does however embody the controls and sensors necessary for operation in space. However these differences do not affect the key goal of the testbed which is to demonstrate faint planet detection using nulling interferometry, phase chopping and averaging.

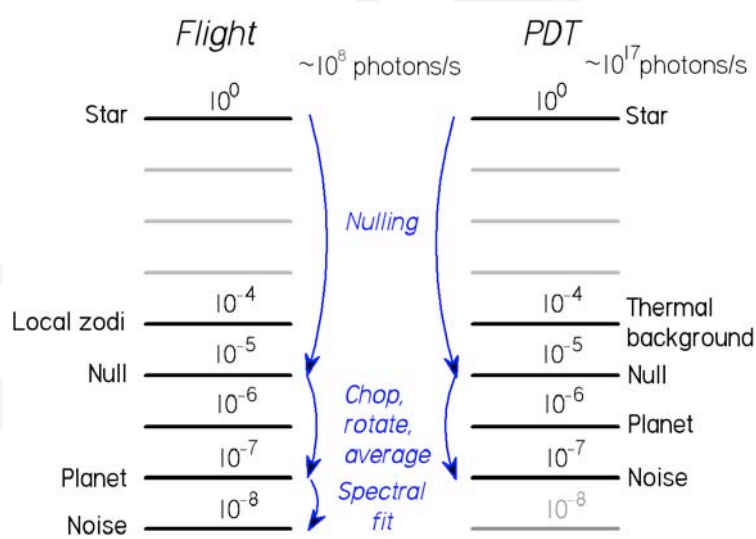

Figure 4-24: Photon rates for the planet detection process for flight and PDT

Key exoplanet detection techniques are being tested and demonstrated in the PDT. . To reach the flight goal of detection of a planet 10^7 times fainter than the parent star, a series of steps (illustrated in Figure 4-24) must be taken:

- The star's apparent intensity is reduced relative to the planet by a factor of 100,000. This is done by interferometric nulling.

- The interferometer array is rotated around the line of sight to the star to search the whole region around the star for a characteristic planet signature. In PDT this is done by controlling the optical path relationships between the planet source beams, simulating the phase changes caused by rotation of the telescope array around the line of sight to the star. During this rotation, stable nulls need to be maintained; PDT has systems and control loops analogous to those needed for flight in order to control the instability noise and maintain deep nulls.
- The planet signal is modulated against the bright radiation background. This is done using phase chopping. The combination of rotation, phase chopping and averaging over time reduces the noise level by a factor of 100 to 10^{-7} of the stellar intensity.
- The technique of spectral fitting uses correlations between null fluctuations across the spectral band to reduce the instability noise. This yields a further factor of 10 in reduction of the noise level.

Thus, the combination of these four techniques yields the necessary performance. In the current milestone the objective is to demonstrate the first three parts of this process; the stable nulling, the array (or planet) rotation and the phase chopping. At the time of writing, PDT has demonstrated detection of a planet 2 million times fainter than the star using some simplified methods. The testbed is now being prepared for faint planet detection using the first three techniques. The suppression effect achieved using these techniques in which the nulled starlight at 10^{-5} is reduced to 10^{-7} will be representative of flight performance. Validation of the fourth technique, spectral fitting, will be left to a future plan.

4.3.2 Future Milestones

Small Structurally Connected Interferometer

Table 2 displays a summary of the technical readiness levels (TRLs) of key technologies used in the small infrared structurally connected interferometer (FKSI) mission. These levels are estimated using NASA standard terminology for them (Mankin 1995).

Many of the key technological hurdles for FKSI as understood in the original studies performed by our group in 2002-2003 have been solved by NASA flagships projects, in particular, the investments in JWST and TPF-I/Darwin technologies can be directly used in the FKSI system. As of early 2007, JWST passed all of its key technology milestones, including those for cryocoolers, precision cryogenic support structures, detectors, cryogenic mirrors, and sunshades. All of these technologies can be adapted to the FKSI mission with little effort.

Key technologies unique to the FKSI mission have also benefited from NASA's investments in the Keck Interferometer Nuller system (now in operation at the Keck Observatory) and the TPF-I testbeds at JPL including the Planet Detection Testbed and the Achromatic Nuller Testbed. The broadband null depths from these testbeds are about an order of magnitude better than the requirements for the FKSI mission.

The optical fibers needed for wavefront cleanup have been fabricated and tested at room temperature as part of the TPF-I technology program. Currently two types of fibers have been tested in the laboratory and work sufficiently well for the FKSI mission, these are chalcogenide fibers fabricated at the Naval Research Laboratory (NRL) (Aggarwal & Sanghera 2002) that operate from the near- to mid-infrared, and silver halide fibers developed at Tel Aviv University that operate in the longer wavelength part of the mid-

infrared (see Ksensov et al. 2007 and references therein). A third type of fiber, a hollow glass waveguide fiber developed at Rutgers University (Harrington 2001) may also be of use. Further testing is planned, including cryogenic testing of all fibers.

Table 2. Technical Readiness Levels for Key Subsystem Components

Item	Description	TRL	Notes
1	Cryocoolers	6	Source: JWST
2	Precision cryogenic structure	6	Source: JWST
3	Detectors (near-infrared)	6	Source: HST, JWST Nircam
4	Detectors (mid-infrared)	6	Source: Spitzer IRAC, JWST MIRI
5	Cryogenic mirrors	6	Source: JWST
6	Optical fiber for mid-infrared	4	Source: TPF-I
7	Sunshade	6	Source: JWST
8	Nuller Instrument	5	Source: Keck Interferometer Nuller, TPF-I project, LBTI
9	Precision cryogenic delay line	6	Source: ESA Darwin

*Note: The requirement for the FKSI project is a null depth of 10^{-4} in a 10% bandwidth. Laboratory results with the TPF-I testbeds have exceeded this requirement by an order of magnitude (Lawson et al. 2008).

At a system level, a nuller instrument fabricated at JPL has been delivered to and is in use at the Keck Observatory. The FKSI nuller instrument is actually simpler than the Keck instrument, as the latter requires chopping out the background created by a warm telescope and sky (not needed by FKSI). Indeed the first data from the Keck Interferometer Nuller has recently been published (Barry et al. 2008). The Bracewell Infrared Nulling Cryostat (BLINC, Hinz et al. 2000) is a cryogenic nuller in use on the MMT, which has achieved significant results in studies of accretion disks around Herbig Ae/Be stars (REF).

Finally, FKSI requires a precision cryogenic delay line with a stroke of the order of a centimeter. Fortunately, commercial firms in Europe, under contract from ESA have developed such a prototype cryogenic delay line, which is at a high TRL level. This delay line has a precision of 1.3 nm and a stroke of 10 mm, which is more than adequate for a small interferometer. Also two short stroke cryogenic delay lines have been flown as part of two Michelson spectral interferometers, both of which were developed at the Goddard Space Flight Center. One was the FIRAS instrument on the COBE mission, which won a Nobel Prize in Physics for Drs. John Mather and George Smoot for cosmic microwave background research. A second has been flown successfully on the CASSINI mission, for the CIRES instrument. (REFS needed).

In summary, we note only one area where technology development is needed for a Phase A start for a small infrared structurally-connected interferometer, which is cryogenic testing of the optical fibers for wavefront cleanup.

Flagship Mission

The technology program for the Terrestrial Planet Finder Interferometer is now close to achieving all of its milestones in starlight suppression. The basic component technology for starlight suppression at mid-infrared wavelengths is now at Technology Readiness Level (TRL) 4. TRL 5 requires testing in a relevant environment, which for TPF/Darwin would be

a cryogenic vacuum near 40 K. Most research so far has been undertaken in air at room temperature. As will be discussed below, sufficient progress has now been made that the greatest advance in this area would be to proceed to brass-board designs of already successful components and subsystems, and to implement system-level cryogenic testing.

Ground-based demonstrations with the Formation Control Testbed (FCT) have shown that the Guidance, Navigation, and Control algorithms now exist to execute precision maneuvers with two telescopes (see the Milestone #2 Whitepaper and Report). Additional testing should be carried out to validate collision avoidance and fault tolerant algorithms, but the greatest advance would be to transition to space-based demonstrations in collaboration with our European colleagues.

Future technology demonstrations and their corresponding TRL are listed as follows.

Demonstration of Planet Detection with Chopping and Averaging (TRL 4/5)

Further noise suppression is required over and above broadband starlight suppression. Nulling reduces the glare of starlight to a level fainter than the warm glow of local zodical dust (around the Sun) and exo-zodiacal dust (around the target star), but the planet itself may still be 100 times fainter. The technique for detecting and characterizing planets therefore relies on several other strategies.

The first step is to suppress the response to any thermal emission that is symmetrically distributed around the star. In principle this will remove the detected glow of local and exozodiacal dust. By rotating the array and averaging the response, the planet signal can be further enhanced. The beam combiner for TPF/Darwin therefore combines two pairs of beams to null the starlight, and the beam combining system modulates the response on the sky (keeping the star nulled) by chopping back and forth between these nulled pairs. This milestone has been detailed in the Whitepaper for the Planet Detection Testbed (Martin et al. 2008).

Demonstration of Broadband Systematic Noise Suppression (TRL 4/5)

An additional step is required to suppress the noise down below the typical brightness of an Earth-like planet. After nulling and chopping, the dominant source of noise is due to residual instabilities in the null depth, which generates a white-noise of similar intensity to the planet signal. This noise can be suppressed by appropriate choice of interferometer baselines and by filtering the measured data from a complete rotation of the array. This milestone should be demonstrated by the Planet Detection Testbed in 2009.

Additional technology progress beyond this milestone would depend on cryogenic testing of components and systems.

Single-Mode Filters, 6-20 microns, Demonstrated in a Cryogenic Vacuum (TRL 5)

The single-mode fibers used in the Adaptive Nuller are made of chalcogenide material and have been demonstrated to yield 25 dB or more rejection of higher-order spatial modes, thus meeting the flight requirements (Ksendzov et al. 2007). Because this material becomes opaque at wavelengths above 12 microns, other materials must be used in the 12-20 micron wavelength band. Silver halide single-mode fibers have been demonstrated to meet flight requirements at 10 microns, and should also work well at longer wavelengths (Ksendzov et al. 2008). Although this performance is sufficient for flight, it would be greatly advantageous to improve the throughput of these devices, to test them throughout the full wavelength range they are intended for, and to test them cryogenically. Spatial filter technology would

then be at TRL 5. It would furthermore be advantageous to implement mid-infrared spatial filters and beam combiners using integrated optics, so as to reduce the risk associated with the complexity of the science instruments.

Cryogenic Mid-IR Adaptive Nuller (TRL 5)

Adaptive nulling is straightforward to generalize over the full science band, and should be demonstrated within a cryogenic vacuum, bringing the technology to TRL 5. This would necessitate the successful validation of cryogenic spatial filters and the testing of a cryogenic deformable mirror.

Planet Detection Demonstration in a Flight-like Environment (TRL 6)

Laboratory work is well advanced to demonstrate the detection of planet light with a similar system (see Figure). Simulated planets two million times fainter than a star have been detected in early trials, and the work is ongoing. Although these tests represent the full complexity of beam combination, this research is being conducted at room-temperature in air, and the noise properties of the testbed are therefore unlike those that would be met in flight. Following the completion of this work, the next step would be to build a vacuum cryogenic beam combiner with flight-like servo systems, including the brass-board components described above.

Guidance, Navigation, & Control: Collision Avoidance, Fault Detection (TRL 5)

Additional tests that could be carried out with the FCT include demonstrating new capabilities such as (1) reactive collision avoidance, (2) formation fault detection, and (3) autonomous reconfiguration and retargeting maneuvers. Also, using a real-time simulation environment, such as FAST we could demonstrate the performance with full formation-flight complexity, with five interacting spacecraft showing synchronized rotations, autonomous reconfigurations, fault detection, and collision avoidance.

In-flight Testing of Formation Algorithms (TRL 6)

National agencies in Europe are actively advancing the technology of formation flying, with flight missions starting in 2009-2014. The European Space Agency and national space agencies in Europe have a program of precursor missions to gain experience in formation flying to support XEUS and Darwin. In 2009 the Swedish Space Agency will launch the Prisma mission. This is primarily a rendezvous and docking mission, but will also test RF metrology designed for Darwin. In 2012 ESA plans to launch Proba-3, which will include optical metrology loops for sub-millimeter range control over a 30-m spacecraft separation. The French and Italian space agencies are planning to launch Simbol-X in 2014. Simbol-X is an X-ray science mission with an architecture very similar to XEUS, but with a 20-m spacecraft separation. Simbol-X should enter Phase B of development in the summer of 2008.

Although two-spacecraft precision maneuvers were demonstrated in 2007, a major goal that remains is to demonstrate robust algorithms for three or more spacecraft, such as would be used by TPF-I (Lawson et al. 2008). The opportunity no doubt exists to leverage the expertise developed for TPF-I in collaboration with our European colleagues. The greatest advance in maturing technology for formation flying would be to have a modest-scale technology mission devoted to verifying and validating guidance and control algorithms. Such in-flight testing would be made even more meaningful if it could include and the interferometric combination of starlight from separated platforms.

A ground-based facility such as the FCT should continue to provide the means to test and improve real-time formation-flying algorithms as the technology matures, even while the technology is being proven in space.

4.4 Research and Analysis Goals

4.4.1 Ground-based Interferometry

Ground-based interferometry serves critical roles in exoplanet studies. It provides a venue for development and demonstration of precision techniques including high contrast imaging and nulling, it trains the next generation of instrumentalists, and develops a community of scientists expert in their use. With the highest priority, nulling facilities should be refined and operated for the characterization of debris disks and exozodiacal light and the impact of these on direct detection missions.

Ground-based interferometry can also provide unique support to exoplanet studies. RV detections have been vetted for the possibility of stellar companions on highly inclined orbits[1]. Transit planets can be studied more precisely with direct measurement of the stellar diameters[2]. Keck and VLTI will soon offer precision narrow-angle astrometry, intermediate between HST and SIM, that will open new areas of exoplanet parameter space, and will improve the characterization of known exoplanet systems, contributing to construction of well-understood target lists for direct detection missions. Ground based interferometers will soon be capable of direct detection and study of some exoplanets (Monnier et al, 2006, SPIE 6268, 62681P).

We endorse the recommendations of the "Future Directions for Interferometry" Workshop[3] and the ReSTAR committee report[4] to continuing vigorous refinement and exploitation of existing interferometric facilities (Keck, NPOI, CHARA and MRO), widening of their accessibility for exoplanet programs, and continued development of interferometry technology and planning for a future advanced facility.

The nature of Antarctic plateau sites, intermediate between ground and space in potential, offers significant opportunities for exoplanet and exozodi studies by interferometry and coronagraphy (Kenyon et al, 2006, PASP 118, 924; Foresto et al, 2006, SPIE 6268, 94B). Balloon altitudes are also promising for high contrast imaging (Traub & Chen, 2007, BAAS 211, 30.06, Rinehart et al. 2008). Further evaluation of these opportunities should be encouraged and supported, with the expectation that they may be competitive for future implementation.

4.4.2 Theory support

In order to achieve our most ambitious goals of relating exoplanet atmospheres composition to planet formation, system evolution, surface chemistry and biology, we will require sustained support of strong astrobiology and atmospheric chemistry programs.

---

1 Baines et al, 2008, http://adsabs.harvard.edu/abs/2008arXiv0803.4131B
2 Baines er al, 2008, http://adsabs.harvard.edu/abs/2008arXiv0803.1411B
3 http://www.noao.edu/meetings/interferometry/
4 http://www.noao.edu/system/restar/files/ReSTAR_final_14jan08.pdf

4.4.3 Space-based Interferometry

Space-based interferometry serves critical roles in exoplanet studies. It provides access to a spectral range that can not be achieved from the ground and can characterize the detected planets in terms of atmospheric composition and effective temperature. Sensitive technology has already been proven for missions like JWST, SIM, and Spitzer, and within NASA's preliminary studies of TPF. With high priority, technology for nulling interferometers in space should be advanced to make the next generation spacecraft to detect and characterize the closest planets flight ready.

4.4.4 Agency Coordination and Programmatic Syngergies

The very broad scientific and public interest in exoplanets, and the direct relevance to both NASA and NSF goals, makes it an ideal topic for coordination between the agencies, and we urge NASA and NSF staff to leverage this relationship to cover the full breadth of exoplanet science and technology.

4.4.5 International Cooperation, Collaboration, & Partnership

During the past six years (2002-2008) using a NASA/ESA Letter of Agreement (LOA) allowed the US and European communities to develop a joint TPF and Darwin mission concept based on a convergence of science requirements, design studies, and shared technology goals. The relationships forged between US and European collaborators should be fostered during the next decade for further studies of small mission and flagship mission concepts. A new letter of agreement is necessary to further future collaborations.

4.5 Contributors

Olivier Absil, University of Grenoble

Rachel Akeson, Caltech, Michelson Science Center

Adrian Belu, LUAN -- University of Nice Sophia Antipolis

Mathew Boyce, Helios Energy Partners

Richard K. Barry, NASA Goddard Space Flight Center

James Breckinridge, Caltech, Jet Propulsion Laboratory

Adam Burrows, Princeton University

Christine Chen, Space Telescope Science Institute

David Cole, Caltech, Jet Propulsion Laboratory

William C. Danchi, NASA Goddard Space Flight Center

Rolf Danner, Northrop Grumman Space Technology

Peter Deroo, Caltech, Jet Propulsion Laboratory

Vincent Coude de Foresto, LESIA -- Observatoire de Paris

Denis Defrere, University of Liege

Dennis Ebbets, Ball Aerospace and Technology Corporation

Ismail D. Haugabook, Sr., Digital Technical Services

DRAFT

Charles Hanot, Caltech, Jet Propulsion Laboratory, University of Liege

Phil Hinz, Steward Observatory, University of Arizona

Kenneth J. Johnson, U. S. Naval Observatory

Lisa Kaltenegger, Harvard Smithsonian Center for Astrophysics

James Kasting, Pennsylvania State University

Matt Kenworthy, Steward Obsevatory, University of Arizona

Peter Lawson, Caltech, Jet Propulsion Laboratory

Oliver Lay, Caltech, Jet Propulsion Laboratory

Bruno Lopez, Observatoire de la Cote d'Azur

Rafael Millan-Gabet, Caltech, Michelson Science Center

Stefan Martin, Caltech, Jet Propulsion Laboratory

Dimitri Mawet, Caltech, Jet Propulsion Laboratory

John Monnier, University of Michigan

M. Charles Noecker, Ball Aerospace and Technology Corporation

Jun Nishikawa, National Astronomical Observatory of Japan (NAOJ)

Meyer Pesesen, Caltech, Jet Propulsion Laboratory

Sam Ragland, W. M. Keck Observatory

Stephen Rinehart, NASA Goddard Space Flight Center

Eugene Serabyn, Caltech, Jet Propulsion Laboratory

Mohammed Tehrani, The Aerospace Corporation

Wesley A. Traub, Caltech, Jet Propulsion Laboratory

Stephen Unwin, Caltech, Jet Propulsion Laboratory

Julien Woillez, W. M. Keck Observatory

Ming Zhao, University of Michigan

4.6 References

Barry, R.K., W. C. Danchi, M C. Koresko, et al., "High-Resolution N-Band Observations of the Nova RS Ophiuchi with the Keck Interferometer Nuller," Astrophysical Journal, (2008).)

Crawford, S. L. Colavita, M. M., Garcia, J. I., et al., "Final laboratory integration and test of the Keck Interferometer nuller," Proc SPIE, 5905, (2005).

Cockell, C.S., T. Herbst, A. Leger, et al., "Darwin – A Mission to Detect, and Search for Life on, Extrasolar Planets," Astrobiology, in press, 2008.

Danchi, W.C., Deming, D., Kuchner, M., & Seager, S. "Detection of Close-In Extrasolar Giant Planets with the Fourier-Kelvin Stellar Interferometer," Astrophysical Journal Letters, **597**, L57 (2003).

DRAFT

Danchi, W.C., Allen, R.J., Benford, et al., "The Fourier-Kelvin Stellar Interferometer," in the Proceedings "Towards Other Earths: DARWIN/TPF and the Search for Extrasolar Terrestrial Planets," Heidelberg, Germany, 22-25 April 2003 (ESA Publication SP-539, October 2003)

Danchi, W.C., Allen, Barry, R., R.J., Benford, et al., "The Fourier-Kelvin Stellar Interferometer: A Practical Interferometric Mission for Discovering and Investigating Extrasolar Giant Planets," in "New Frontiers in Stellar Interferometry," Glasgow, Scotland, Proc. SPIE, vol. 5491, 236 (2004).

Danchi, W.C., & B. Lopez, "The Fourier-Kelvin Stellar Interferometer (FKSI) -- A practical infrared space interferometer on the path to the discovery and characterization of Earth-like planets around nearby stars,", Comptes rendus - Physique (C.R. Physique), 8, 396-407 (2007).

Defrere, D., O. Absil, V. Coude du Foresto, et al. "Nulling interferometry: performance comparison between space and ground-based sites for exozodiacal disc detection," submitted to Astronomy and Astrophysics, May 2008.

Forget, F., & Pierrehumbert, R.T., "Warming early Mars with carbon dioxide clouds that scatter infrared radiation," Science, 278, 1273-1276.

Frey, B.J., R.K. Barry, W.C. Danchi, et al., "The Fourier-Kelvin Stellar Interferometer (FKSI) nulling testbed II: Closed-loop pathlength metrology and control subsystem," Proc. SPIE, vol. 6268, (2006).

Fridlund, C.V.M., Gondoin, P., Bavdaz, M. et al., "Feather-light touch all that's needed for Darwin's frictionless optics," in the website; http://www.esa.int/esaCP/SEMD3J8J50F_index_0.html, 2008.

Gappinger, R.O., Diaz, R.T., Martin, S.R., et al. "Current progress on TPF-I mid-infrared achromatic nulling at the Jet Propulsion Laboratory," Proc SPIE, 6693 (2007)

Hyde, T.T., Liu, K-C., Blaurock, C., Bolognese, J., et al. "Requirements Formulation and Dynamic Jitter Analysis for the Fourier-Kelvin Stellar Interferometer," Proc. SPIE, 5491, 553 (2004)

Karlson, A.L., Wallner, O., Armengol, J. M. P., et al., "Three telescope nuller based on multibeam injection into single-mode waveguide," Proc. SPIE, 5491, 831–841 (2004).

Kasting, J.F., Whitmire, D.P., and Reynolds, R.T., " Habitable zones around main sequence stars," Icarus, 101, 108-128 (1993).

Lawson, P.R., Lay, O. P. Martin, S. R., et al. "Terrestrial planet finder interferometer: 2006-2007 progress and plans," Proc. SPIE, 6693 (2007)

Leger, A. Herbst, T., et al., "DARWIN mission proposal to ESA". submitted 23 Jul 2007. Astrophysics, arXiv:0707.3385v1 [astro-ph].

Lopez, B., S. Wolf, S. Lagarde, P. Abraham, et al., "MATISSE: perspective of imaging in the mid-infrared at the VLTI," Proc. SPIE, 6268, 31 (2006).

Martin, S. R., Serabyn, E., Hardy, G. J., "Deep nulling of laser light in a rotational shearing interferometer," Interferometry for Optical Astronomy II, edited by W. A. Traub, Proc. SPIE 4838, 656-667 (2003)

Martin, S.R., "The flight instrument design for the Terrestrial Planet Finder Interferometer" Proc. SPIE 5905, 21-35 (2005).

Martin, S.R., "Progress in four-beam nulling: results from the Terrestrial Planet Finder Planet Detection Testbed," in 2006 IEEE Aerospace Conference, Big Sky, Montana (2006)

Martin, S. R., Szwaykowski, P., Loya, F., Liewer, F., "Progress in testing exo-planet signal extraction on the TPF-I Planet detection Testbed" Proc SPIE, 6268, (2006).

Martin, S.R., Scharf, D., Wirz, R. et al. , "TPF-Emma: concept study of a planet finding space interferometer," Proc. SPIE, 6693, 669309 (2007).

Martin, S.R., Scharf, D.P., Wirz, R., et al. "Design Study for a Planet-Finding Space Interferometer". IEEE Aerospace Conf, Big Sky, Mt, USA (2008)

Martin, S.R., Serabyn, E., Liewer, K, "The development and applications of a ground-based fiber nulling coronagraph," Proc. SPIE, 7013, (2008)

B. Mennesson; P. Haguenauer; E. Serabyn; K. Liewer "Deep broad-band infrared nulling using a single-mode fiber beam combiner and baseline rotation," Proc SPIE Vol. 6268 (2006)

Ollivier, M., Contribution à la Recherche d'Exoplanète, "Coronagraphie Interférentielle pour la Mission Darwin," Ph.D. thesis, University Paris XI (1999).

Peters, R.D., Lay, O., "Progress in deep broadband interferometric nulling with the Adaptive Nuller". Proc. SPIE, 7013, (2008)

Peters, R. D., Lay, O. P., Jeganathan, M., "Broadband phase and intensity compensation with a deformable mirror for an interferometric nuller," Appl. Opt. 47, 3920-3926 (2008).

Samuele, R., Wallace, J. K., Schmidtlin, E., Shao, M., Levine, B. M., Fregoso, S., "Experimental progress and results of a visible nulling coronagraph," 2007 IEEE Aerospace Conference, Big Sky Montana, paper 1333 (2007).

Serabyn, E., Wallace, J. K., Hardy, G. J., Schmidtlin, E. G. H., Nguyen, H. T., "Deep nulling of visible laser light," Appl. Opt. 38, 7128-7132 (1999).

Serabyn, E., Booth, A.J., Colavita, M.M, et al., "The Keck interferometer nuller: system architecture and laboratory performance," Proc SPIE, 5491, 806-815, (2004)

Wallace, K., Hardy, G., Serabyn, E., "Deep and stable interferometric nulling of broadband light with implications for observing planets around nearby stars," Nature 406, 700-702 (2000).

Wallner, O., J. M. P. Armengol, and A. L. Karlson, "Multiaxial single-mode beam combiner," Proc. SPIE 5491, 798–805 (2004)

DRAFT

5 Exozodiacal Disk Characterization

Chair: Phil Hinz, University of Arizona

LOC: Rafael Millan-Gabet, Caltech

5.1 Introduction

Characterization of the debris disks around nearby stars is an important complement to planet finding for several reasons. Primarily, the detection of debris material, especially in or close to the habitable zone is a direct indication of planet building material in this zone. In a gas-poor disk, debris material is cleared away through collisional destruction, radiation pressure, or Poynting-Robertson drag on relatively short timescales compared to those of planet formation or the planetary system itself. Therefore, the presence of dust indicates that larger parent bodies must also be located in the system. Thus, the detection of dust, in tandem with detection of the massive planets in the system allows the development of a more complete observational picture of the architecture of a planetary system. In fact, information gleaned from disk structure can be used to detect planets that would otherwise be too faint or have a mass that is too low to be detected using other techniques. Similarly, the presence of small body populations in a habitable zone could affect habitability through the frequency of large impact events. However, for the ultimate goal of detecting and characterizing an extrasolar Earthlike planet, debris disks can decrease the significance of the detection and potentially obscure the planet signal altogether.

The recently completed report by the Exo-planet Task Force made two recommendations related to dust disk detection. In the near term (1-5 years) they recommended the community "invest in a census of exozodi systems around exoplanet target stars", and in the medium term (6-10 years) that the community should "implement next generation high spatial resolution imaging techniques on ground-based telescopes: AO for direct detection of young, low-mass companions, and interferometry for disk science."

This chapter describes the state of the field and near future plans for exozodiacal dust detection and modeling. The plans described in the chapter agree sunbstantiall with that of the Exo-Planet Task Force. Based on discussion in the May 2008 Exoplanet Forum, following is the consensus set of recommendations on exozodiacal dust:

- ***NASA should continue its support of KI, LBTI, and similar efforts that will measure zodiacal dust density and morphology critical for planning future direct imaging missions***
- ***Continue studies of Exoplanet Probe class space missions that can address the density and morphology of dust in the habitable zone of nearby stars with a much higher sensitivity limit and a much larger sample of nearby systems than***

can be done with ground-based technologies.

- ***Continue the development of collisional debris disk models to complement observations, aiding in interpretation and extrapolation of such results.***

5.1.1 Properties of Protoplanetary and Exozodiacal Disks

During the collapse of dense interstellar cloud cores, conservation of angular momentum dictates the formation of a rotating disk of gas and dust around the young star. Planets grow in this circumstellar disk, interact with it, and implant their signatures on it. The discovery of such disks around nearby stars has provided the opportunity to study planet formation in real time, rather than working backward from completed or mature systems. It is now understood that planet formation is a general physical process that operated in our own young Solar System, including the transformation of interstellar organic material into pre-biotic compounds like those that gave rise to life on Earth. The older, dust-rich disks – debris disks – are also vital for efforts to image and characterize extrasolar terrestrial planets. Debris dust surrounds our Sun today (the zodiacal dust) and about 10 – 20% of nearby stars harbor a currently detectable debris disk, typically detected at a separation similar to the Sun's Kuiper belt (Beichman et al. 2006, Trilling et al. 2008, Hillenbrand et al. 2008) but the extension of these statistics to the habitable zone is not yet known. While exozodiacal dust is a major source of background flux and probably confusion in direct imaging of exoplanets, it may also provide indirect evidence of planets through dust structures caused by gravitational perturbations. The signature of the Earth may be seen in clumps within the zodiacal dust in the inner Solar System.

The current paradigm for the formation of a mature planetary system has three main phases:

- the formation of gas-giant planets like Jupiter,
- the formation of terrestrial planets, and
- the clearing of most leftover planetesimals (i.e. asteroids and comets) from the system.

This timeline is represented in Figure 1. It is during the last phase that most of the volatile content of Earth's surface was delivered by the impact of water-rich planetesimals (e.g., Morbidelli et al. 2000). Protoplanetary disks may be divided into three classes that appear to roughly correspond to each phase.

1. The youngest class is the *primordial disks*, which are composed of relatively unprocessed interstellar material left over from star formation. Primordial disks are gas-rich, as evidenced by observations of sub-mm CO emission (e.g., Thi et al. 2000); the bulk of the gas, however, is molecular hydrogen. Since giant planets are primarily composed of gas, they must form in gas-rich disks, and the primordial disks match this description. Contrary to earlier conception, these disks are apparently not quiescent or static. They are the sites of active chemistry and large-scale motions of gas, dust, and planetary bodies of all sizes through migration.
2. The next class is the *transitional disks*, which appear to be clearing material from their inner disks, but still retain optically thick, gas-rich outer disks. This relatively new class has been the focus of recent intensive study, as they provide a window on the rapid transformation from a primordial disk into a young planetary system.

3. The oldest class is the *debris disks*, which are dusty, gas-poor disks. These disks are composed of material produced by the destruction of planetesimals and contain little or no unprocessed interstellar material. Debris disks have a wide range of ages, from about 10 Myr to a few Gyr. Terrestrial planets are likely forming in the younger debris disks, while the older ones correspond to the disk-clearing phase. Dust is removed from debris disks through Poynting-Robinson drag, planetary sweeping, or radiation pressure and replenished via collisions between and evaporation of planetesimals.

A coronagraphic image of a disk from each of the three classes appears in Figure 1, which implies a very clean, orderly progression in both planet formation and disk evolution. However, the theoretical stages in planet formation may be occurring simultaneously in different parts of a disk. In addition, the different classes of disk are not cleanly separated, with apparent overlap in the age ranges of each class, indicating that stochastic processes may significantly shape the evolutionary pathways of individual systems. The relationship of this diversity of disk properties with the wide range of extrasolar planetary systems remains a topic of current study.

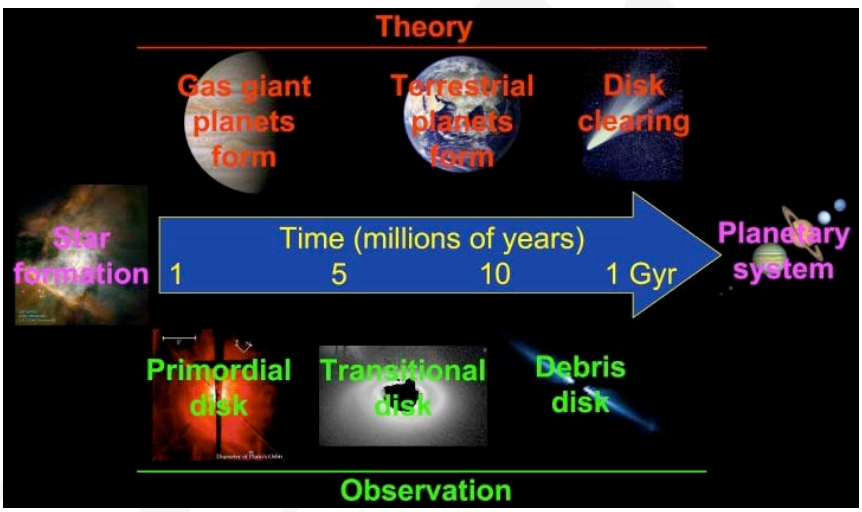

Figure 5-1. Timeline for planet formation and the evolution of circumstellar disks. Above the arrow, the main theoretical phases in planetary formation are shown. Below, the classes of circumstellar disks are identified. A coronagraphic image of an example from each class is shown; the primordial disk around AB Aurigae at left (Grady et al. 1999), the transitional disk around HD 141569A in the center (Clampin et al. 2003), and the debris disk around AU Microscopii at right (Krist et al. 2005). [Figure credit: A. Roberge, **higher quality available for final version**]

5.1.2 Terrestrial Planet Formation and Delivery of Volatiles

In order for terrestrial-sized planets to acquire large quantities of volatiles such as water, giant planets are likely required to gravitationally stir up planetesimals and inject them into the inner disk. The gas composition in a debris disk may provide information on the composition of the planetesimals producing the disk. For example, recent far-ultraviolet spectroscopy of the gas in the well-studied β Pic debris disk has shown that carbon is extremely overabundant relative to every other measured element (e.g., C/O = 18 × solar;

Roberge et al. 2006), despite the fact that the central star appears to have solar metallicity (Holweger et al. 1997). This overabundance likely reflects the composition of the parent material of the gas, which would have to be much more carbon-rich than expected based on what we know about Solar System asteroids and comets. Either the β Pic planetesimals producing the gas are selectively losing their volatile carbon compounds, or they are simply more carbon-rich overall than any Solar System planetesimal. The latter possibility has important consequences for any terrestrial planets that might be forming around β Pic and their volatile composition.

5.1.3 Science Goals

The extrasolar planetary systems already discovered show a surprising diversity in their architectures compared to our own Solar System. Studies of protoplanetary and debris disks are essential to understand the origins of this diversity and to predict what other phenomena might be observed in the future. They also affect our ability to make new discoveries, through the impact of exozodiacal dust on direct imaging and characterization of exoplanets. The primary goals of protoplanetary and debris disk studies are as follows.

Obtain a better understanding of planet formation as a generic and robust process

Planets can form around normal stars with spectral types ranging from at least late M (Butler et al. 2004) to early A (Johnson et al. 2007), around pulsars (Wolszczan & Frail 1992), and possibly even around brown dwarfs (Chauvin et al. 2004). Their birth environments are apparently also diverse, ranging from low mass star-forming regions like the Taurus cloud to energetic, high mass star-forming regions like the Orion nebula. Most planet formation models were developed to explain the Solar System itself and currently cannot explain the diversity of planets already detected. Theoretical improvements to these models are hampered by a lack of basic information on protoplanetary disks, including initial masses of the disks, typical lifetimes of disks around stars of different masses and in different stellar environments, the evolution of the gas to dust ratio, density and temperature structure, and chemical evolution. It is highly desirable that models of planet formation could be improved so that they would be able to predict the prevalence of Earth-mass planets around different types of stars including ones of varying metallicity and mass, and the predicted abundances of volatile chemicals on their surfaces, to motivate and guide future efforts to find and characterize potentially habitable exo-Earths.

Characterize the exozodiacal dust around targets for direct imaging of exoplanets

When viewed from a distance, the most conspicuous feature of the Sun's planetary system is the zodiacal dust, which is tenuous but covers a large surface area. A significant fraction of nearby stars has similar dust at much higher abundance. Emission from exozodiacal dust is likely to be the largest source of astrophysical noise in direct imaging and characterization of extrasolar planets. If the dust is too bright, the observation time needed to detect and characterize a planet becomes prohibitively long. For the TPF-C mission, the break point was estimated to be 10 times the level of dust in the Solar System (10 "zodis"). In Section 1.1.4, we present a simple prescription for the acceptable levels of exozodi as a function of telescope aperture size. In Sections 1.2 and 1.3, we discuss the current exozodi detection limits and upcoming opportunities to push down to the levels of dust relevant for direct imaging missions.

Use disk structure to infer the presence of unseen planets

While exozodiacal dust hampers direct imaging of exoplanets, it may also provide another means of indirect detection. In the Solar System, the gravitational influence of the Earth temporarily traps zodiacal dust into a ring at 1 AU, with additional clumps leading and trailing the planet (Dermott et al. 1994). Rings, clumps, and warps (or "x-patterns") have been seen in coronagraphic images of nearby debris disks (e.g. HR4796; Schneider et al. 1999, Fomalhaut; Kalas et al. 2005). Such structures are often attributed to the influence of an unseen planet orbiting in the debris disk, and may be a unique way of finding planets that are extremely difficult to detect with other indirect techniques, like young planets and planets on wide orbits. Unfortunately, we have not yet been able to associate an observed disk dust structure with a known exoplanet. Part of the problem is the difficulty of detecting planets in the currently known debris disks, which have hundreds to thousands of times more dust than the Solar System. The other part of the problem relates to the dynamical modeling used to interpret dust structures. In Section 1.2, we discuss the current state of these models, near-term improvements, and additional needed development.

5.1.4 Science Requirements for Observations of Terrestrial Planets

The requirements on exozodiacal brightness for a Terrestrial Planet Finder are determined by its impact on the increase in integration time for such a mission. Missions in both the visible (0.5-1 microns) and infrared (6-20 microns) are similarly affected. It is worth reviewing the fundamental noise parameters for these missions to appreciate the effect of a denser extrasolar zodiacal dust cloud. Both calculations below assume that effects from residual starlight such as varying suppression or similar systematics, as well as limitations of detector performance, can be kept below the fundamental Poisson noise from local zodiacal light, exozodiacal light and residual starlight. Similar estimates can be found, for example in Brown (2005) or Beichman et al. (2006).

Impact on an Optical Mission

For an idealized optical mission, the noise in an optical observation is dominated by the Poisson noise associated with background flux from an exozodiacal disk as well as the background flux from local zodiacal dust. The time required to image a planet at optical wavelengths in the presence of background flux from local zodiacal dust, exozodiacal dust, and unsuppressed starlight is given by

$$t_O = \frac{8}{\pi \Delta\lambda F_0} 10^{0.4\left(2\cdot m_p\right)} \frac{SNR^2}{D^4 T}\left[\left(\frac{1}{2}+\mu\right)10^{-0.4z}\pi\lambda^2 206265^2\psi^2 + \zeta D^2 10^{-0.4 m_s}\right]$$

where Ψ is the size of the photometric aperture in units of λ/D, Δλ is the bandwidth, F_0 is the photon flux for zero magnitude, m_s is the stellar magnitude, m_p is the magnitude of the planet, z is the surface brightness of the zodiacal light, λ is the central wavelength of the bandpass, D is the diameter of the telescope aperture, T is the total throughput, SNR is the signal-to-noise, μ is the exozodi brightness in units of zodis, and ζ is the flux in the photometric aperture relative to the unsuppressed stellar image. Typical values for these parameters appear in Table 1. This equation is appropriate for a background-limited observation such as imaging an exo-Earth.

Impact on an IR interferometer mission

For an idealized IR interferometer mission (one not limited by systematic errors or noise associated with chopping or nulling), the calculation is similar to the optical mission. The limiting noise sources are the local zodiacal dust emission, the exozodiacal dust emission, and residual light from the finite size of the star and a floor to the performance of the stellar suppression. The contribution from the exozodiacal emission is slightly different since, for the IR case, the integrated light from the exozodiacal cloud is seen by each element of the interferometer. This effect results in the interferometer's sensitivity to exozodiacal dust being dependent on the element aperture size (D) and the distance to the star, which affects the exozodiacial dust brightness relative to the local zodiacal dust contribution. The resulting time for detection is

$$t_{IR} = \frac{4}{\pi \Delta\lambda F_0} 10^{0.4\left(2\cdot m_p\right)} \frac{SNR^2}{D^4 T}\left[10^{-0.4\cdot z}\pi\lambda^2 206265^2 + \mu 10^{-0.4\cdot ez} D^2 + \left[\left(\zeta + \frac{\pi^2}{16}\frac{s^2}{(\lambda/b)^2}\right) D^2 10^{-0.4 m_s}\cdot 4\right]\right]$$

The first term in the bracket is from local zodiacal dust, the second term from exozody emission (where *ez* is the exozodiacal flux in magnitudes at N band), and the third term is the null leakage from the instrument(ζ) and the star's angular diameter, where *s* is the size of the stellar disc in radians. This calculation assumes the interferometer is a four element design with a nulling baseline of *b* meters. Instrumental parameters in Table 1 are from Lay et al. (2007). The light is combined using two successive stages of beamcombiners, so that the zodiacal and planet light is assumed to be split evenly among four interferometric outputs.

Table 1: Typical parameter values in the exposure time calculation for a direct imaging missions in the visible and the infrared.

Parameter	Visible Value	IR Value	Comment
Ψ	1.5	-	Image "width"
$\Delta\lambda$	0.11 μm	2 μm	
F_0	9.5×10^{10} photons sec^{-1} m^{-2} μm^{-1}	5×10^{7} photons s^{-1} m^{-2} μm^{-1}	
m_s	5	3.5	Sun at 10 pc
m_p	29.9 mag	19.6	Earth at 1 AU from Sun at 10 pc
Z	23 mag $arcsec^{-2}$	14.2 mag $arcsec^{-2}$	Local Zodiacal brightness
Ez	-	14.6 mag	Exozodiacal integrated flux
λ	5.50×10^{-7} m	1.0×10^{-5} m	
D	4 m	2 m	Element size for IR interferometer
T	0.0864, (0.7087)	0.05	Optical: TPF-C (TPF-O)
SNR	10	10	
B	-	20 m	
ζ	5×10^{-11}	1×10^{-5}	
S	-	4.6×10^{-9} radians	Sun's diameter at 10 pc

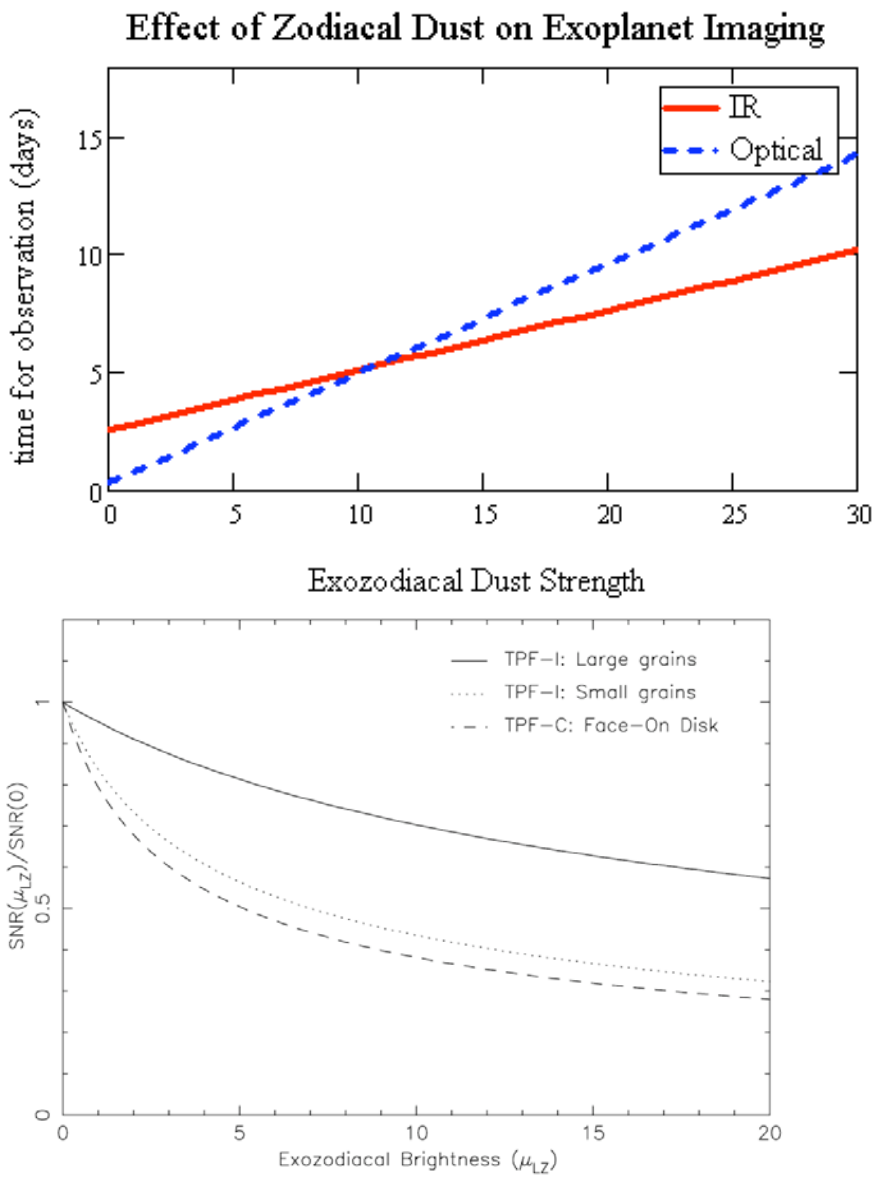

Figure 5-2. Two estimates of the effect of Exozodiacal Dust on detection of an exo-Earth. The left plot shows the effect of exozodiacal dust strength on observing time, based on the equations in the text and using values from Table 1. The right plot shows the estimate of SNR degradation calculated by Beichman et al. (2006).

The time estimates for both cases are necessarily simplistic, not including terms or factors which may refine the actual time needed for a single observation. In this sense the equations may be only approximations of the true time needed. Similarly the values in Table 1 are debatable, and can significantly change the resulting plot in Figure 2. ***The salient point of the calculations is that exozodiacal emission has the ability to significantly increase the time required for a given observation. This has the cascading effect of reducing the sample size for a mission of a fixed duration.*** This effect can be countered, to some extent by using larger apertures or planning for a longer duration mission. However, it is clear that knowledge of average exozodiacal dust strength is a key

input for a robust direct imaging design reference mission , and indeed knowledge of the exozodiacal levels for all candidate TPF or Darwin stars will allow for a greatly optimized mission and characterization strategy (see Wallner et al. 2008).

5.2 Current State of the Field

The next few years will yield significant progress on the abundance, composition, and morphology of exozodiacal material around nearby stars. Using photometry, spectroscopy, direct imaging, and interferometric observations, the formation and evolution of debris disks, their relationship to planetary systems, and their detectability will be explored.

5.2.1 Photometry

Disks are typically first detected by observation of infrared to millimeter-wavelength emission in excess of that expected from the central star. This emission is produced when circumstellar dust absorbs emission from the star and re-emits it at longer wavelengths. Models of the dust emission may be fit to the spectral energy distribution (SED) of the system, providing an estimate of the fractional infrared luminosity (L_{IR}/L_*) and the effective dust temperature, the combination of which can yield the dust mass.

The most important current mission for the detection and characterization of infrared excesses around solar-like stars is the Spitzer Space Telescope. Spitzer is capable of making sensitive measurements of exozodiacal clouds at wavelengths of 24 μm, 70 μm, and 160 μm, spanning typical temperature ranges of 40–200 K and corresponding to distance scales of a few to a few hundred AU from the parent star. The sensitivity to exozodiacal emission is limited by Spitzer's photometric accuracy of a few percent at 24 μm and 7–15% at 70 and 160 μm, allowing Spitzer to detect or set limits on excesses that are greater than 10–50% above the stellar photosphere.

At 24 μm, this limit corresponds to a factor of 100 to 500 times the level of dust emission in our own Solar System in the distance range of 1 to 10 AU, where 100–200 K dust is located for a solar type star (see Figure 3). At longer wavelengths, the photosphere is weaker, and the corresponding limit is 30–100 times the level of dust in our Solar System between 10–100 AU (~50 K dust). Spitzer has already observed or has awarded time for observations of over 200 likely Terrestrial Planet Finder (TPF) target stars (Beichman et al. 2006).

Herschel will be able to search for dust at even cooler temperatures than Spitzer with the PACS instrument. The larger aperture will allow detection of dust at lower optical depths for the outer regions of planetary systems. The expected sensitivity level is equivalent to an optical depth of approximately 10^{-6} for very cold dust(see Figure 5-3).

5.2.2 Disk Imaging

Spectral Energy Distribution (SED) fitting can provide some information on the existence and spatial distribution of the dust (for example, the presence of central holes in the dust disk), but, due to contribution from the star, photometric detection, starting at wavelength shorter than approximately 30 μm, is increasingly difficult for faint levels of dust emission. Imaging of the disk provides two advantages over photometry: separation of unresolved (starlight) and resolved (disk) emission, and determination of the morphology of the debris disk. In principle, imaging should provide fainter levels of detection, compared to photometric limits, particularly for warm dust, within the habitable zone around a star. In

addition, large planetary bodies can create asymmetries in the disk structures that would go unnoticed with photometry alone.

Spitzer

Spitzer has been able to image the thermal emission from dust in debris disks around the closest stars such as Fomalhaut and Vega. The thermal and scattering properties of the disks allow us to place constraints on the amount and size of the dust grains in the disks. But, perhaps more importantly, the presence of asymmetries within the disks may indicate the presence of large planetary bodies orbiting the host stars. For example, in the Spitzer images of Fomalhaut (Stapelfeldt et al. 2004), the disk is asymmetric at both 24 and 70 μm, and in the HST image (Kalas et al. 2006), the disk is found to be off-center from the position of the star. An unseen planet may have given rise to these asymmetries.

Nulling Interferometry

Information on dust in the inner regions of disks will come from the various ground-based nulling interferometers planned to come into operation over the next few years, including the Keck Interferometer and the LBTI. Keck Interferometer observations are currently capable of detecting exozodiacal disks with a 1 sigma noise limit which corresponds to approximately 100 zodis. The LBTI, planned for operation beginning in 2010, has a significantly different architecture than KI which greatly reduces the thermal background and stellar suppression, enabling detection of much fainter disks. LBTI is designed to reach a limit of 10 zodies for a sample of nearby stars (see section 1.3.2 for expected performance). These observations will help determine whether many or all stars have more than 10 times the level of zodiacal dust in our Solar System, which would likely be a complication for efforts to image terrestrial planets in the habitable zones of nearby stars.

Scattered Light Imaging

HST observations of dust disks in scattered light have provided interesting insights into many nearby systems. Detection of disks such as those around Fomalhaut (Kalas et al. 2006) and β Pictoris (Golimowski et al. 2006), has demonstrated the ability to detect material with optical depths of 10^{-4}-10^{-3} (1000-10000x the solar zodiacal level), on scales of 10-1000 AU. The inclination of β Pic's inner disk (Heap et al. 2000) is consistent with a planet sustaining this structure. These observations are typically sensitive to dust in regions comparable to the Sun's Kuiper belt.

In scattered light, about four dozen primordial (protoplanetary) disks have been resolved, plus a similar number of disks seen as silhouettes against bright nebulosity in Orion (so-called proplyds). The census of debris disks resolved in scattered light is much smaller, less than 20 objects. An up-to-date catalog of all these resolved objects may be obtained from http://circumstellardisks.org. The optical depths of these resolved disks range from a high of 3e-3 (e.g. Beta Pic, HD 181327) down to about 10^{-4} (e.g. Fomalhaut, HD 139664). The majority of such disks have been imaged using the Hubble Space Telescope (e.g. Grady et al. 1999, Schneider et al. 1999, Clampin et al. 2003, Krist et al 2005). Adaptive optics imaging has shown increasing promise in recent years, particularly through reducing the residual speckle pattern through either angular differential imaging (e.g. Fitzgerald et al. 2007, Kalas et al. 2007) or simultaneous polarimetry (e.g. Apai et al. 2004, Perrin et al. 2004).

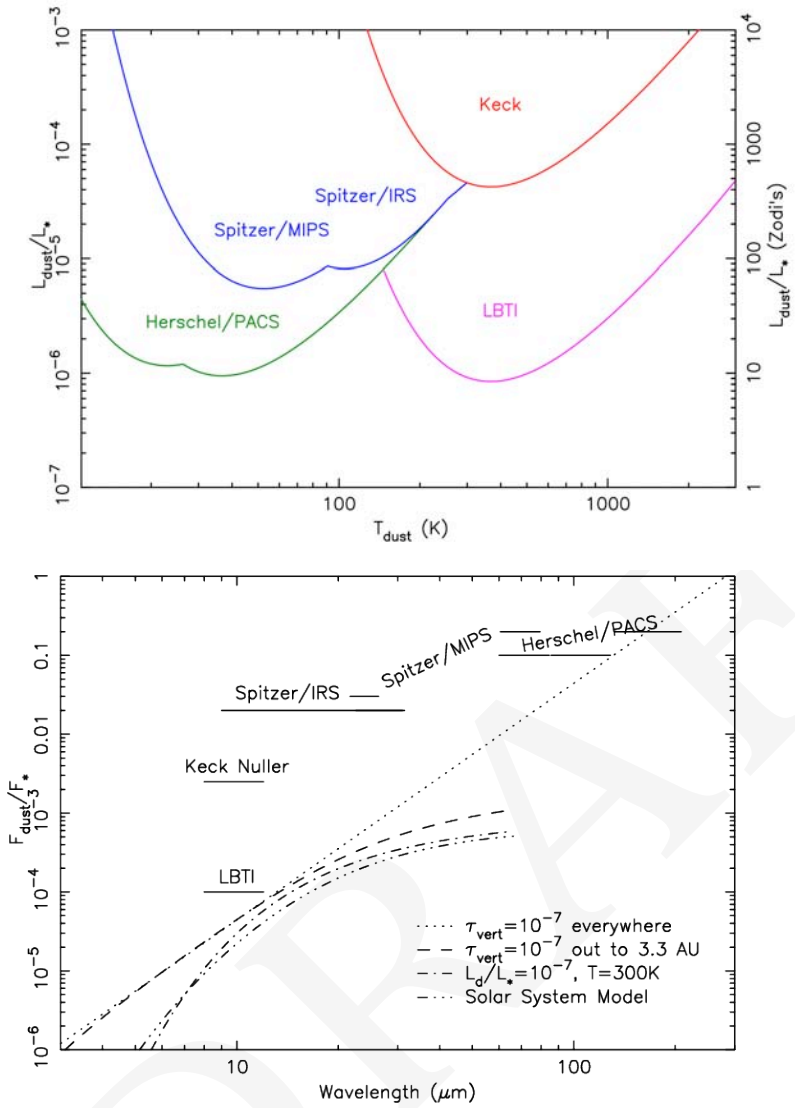

Figure 5-3: Sensitivity limits for detection of dust around nearby solar-type stars. The two plots show the limits in terms of temperature of the dust (left) and detection wavelength (right). Three-sigma detection limits are shown in terms of the dust's fractional luminosity (L_{dust}/L_*, left) or fractional flux (F_{dust}/F_*, right). The assumed 1-sigma accuracies are 20% of the stellar flux for Spitzer/MIPS at 70 μm, 2.5% for Spitzer/IRS at 32 μm, S/N=10 for Herschel/PACS at 100 μm, S/N=2 for Herschel/PACS at 160 μm, 0.5% null for Keck Interferometer at 10 μm, and starlight removal to 0.01% for LBTI at 10 μm. [Figure credit: G. Bryden]

Though not specifically designed for high contrast imaging, HST is extremely stable, allowing for significant reduction of the stellar point spread function by subtracting a reference image of another star or the same star observed at a different orientation. HST has three coronagraphs: in the NICMOS camera (0.9-2.2 microns, multiple filters), in the STIS spectrograph (0.2-1.1 microns, unfiltered), and in the ACS HRC camera (0.2 - 1.1 microns, multiple filters). None of these are optimized, however, and with no wavefront control mechanisms, the bulk of the contrast gain is achieved through PSF subtraction. ACS

and NICMOS have complementary strengths in this area, with ACS offering better overall scattered light rejection, hence greater sensitivity, while NICMOS has a smaller inner working angle. At the moment the STIS and ACS cameras are nonoperational, though they are expected to be repaired during the HST servicing mission scheduled for near the end of 2008.

Observations in scattered light have allowed us to move beyond an initial reconnaissance of disks towards the detailed characterization of their compositions and three-dimensional structures. Multiwavelength and polarimetric imaging has provided significant insights into the detailed properties of the dust grains which comprise these disks, and thus given us better understanding of the physical processes which act upon grains. Because different wavelengths are most sensitive to particles of different sizes, broad wavelength coverage is essential to fully assess the overall dust distributions (e.g. Metchev et al. 2004, Fitzgerald et al. 2007, Pinte et al. 2007). Polarization of light is a fundamental aspect of the scattering process, depending on the properties of the scattering particles and the scattering geometry, and thus polarization is an indispensible diagnostic of grain properties. This is particularly true for edge-on disks, where polarization breaks the degeneracy between dust properties and the radial distribution of dust. In an edge-on disk, without polarization we cannot tell the difference between a disk with constant density and strong forward scattering and a disk with a steep radial density gradient and isotropic scattering. Measurement of linear polarization breaks this degeneracy and allows unambiguous measurement of grain properties such as porosity (Graham et al. 2007). Polarimetric studies of dust grain properties remain currently underway with NICMOS on HST, and will hopefully return with a revitalized ACS in the future as well. We emphasize that together the combination of visible and near-infrared imaging (and mid-infrared, when available) provides significantly greater insight into dust properties than any single wavelength alone. Krist et al. 2007 et al. (2007) suggest that JWST will be no better than HST at the shorter wavelengths (1-2 microns) for imaging debris disks, however, Doyon et al. (2008) have shown that spectral differential coronagaphy using JWST's Tunable Filter Imager will deliver better performance. JWST also offers new coronagraphic capabilities with high performance coronagraphic imaging from 2.5 – 28 microns (Clampin et al. 2007). JWST will offer significant opportunities for imaging the present sample in the mid-infrared where a rich selection of spectral diagnostics of grain properties are available. Over the last few years, new debris disks have been resolved at a rate of 2-4 per year, and the planned repair of ACS this fall is a high priority to enable this trend to continue. The currently resolved disks represent just the tip of the iceberg. Less than a quarter of the debris disks detected by IRAS have since been resolved in scattered light (cf. Figure 4), to say nothing of the much larger sample of debris disks detected by Spitzer. However, the greatest progress in this area will require several orders of magnitude increased contrast compared with present systems. Two orders of magnitude improvement in contrast would allow the entire set of IRAS-detected disks to be imaged in scattered light (though still leaving us unable to image disks less than 100x the solar zodiacal level). Since disks broadly trend to lower optical depths at greater ages, an increased sample size of resolved disks would allow studies across a broader range of ages and evolutionary states than now available.

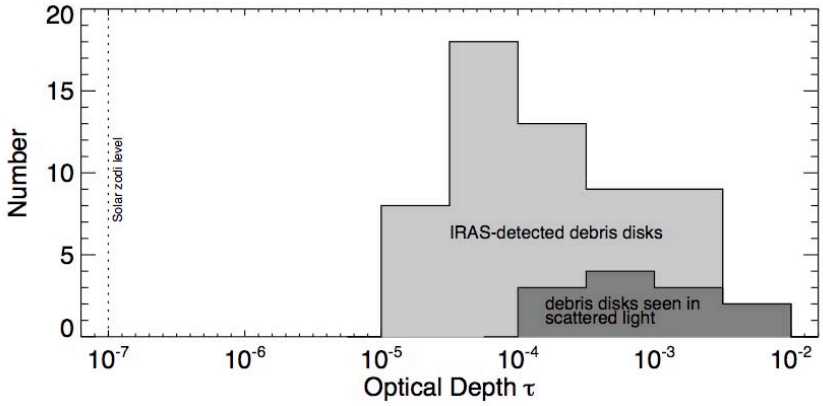

Figure 5-4: Debris Disks detected from thermal emission and scattered light. Currently, only a small fraction of the known debris disks in the solar neighborhood have been resolved in scattered light. This figure shows histograms of the known nearby debris disks detected by IRAS (from Zuckerman & Song, 2004), compared with a histogram of the debris disks which have been resolved in scattered light (data from Paul Kalas and circumstellardisks.org).

In the near term, new high-contrast adaptive optics systems hope to provide at least an order of magnitude contrast over present capabilities. The Gemini Planet Imager (GPI), currently under development for first light at Gemini in early 2011, has a science requirement to image disks down to an optical depth of $3x10^{-5}$, for target stars of I<8 mag. GPI will attain this goal using its high order adaptive optics system with a dual-channel infrared imaging polarimeter that uses a lenslet array to pixellate the image plane prior to polarization beam-splitting, thereby minimizing non-common path errors. Similarly ESO's SPHERE high-contrast AO system will include both near-infrared and visible light dual-channel polarimetry, with comparable contrast goals. The characteristic inner working angles of these systems will be ~0.2 arcsec, and their contrast will decrease outside of the ~1"-wide dark hole created by the AO system. Hence for typical target distances of 20-100 pc, they will be most sensitive to dust on scales of 5-100 AU, comparable in scale to the outer solar system and Kuiper belt. Dust in or near the habitable zone will remain inaccessible to these systems except for the closest targets.

NIR Interferometery

Although most debris disks do not show a clear near-infrared excess in their spectral energy distributions, limits set by spatially unresolved broadband photometry are generally not better than a few to several percent. A small, warm dust component could be present if dust generated by collisions migrated close to the star or was produced by bodies in close orbits. If located within a few AU of the central star, this dust would be at temperatures which would produce near-infrared emission and small grains would produce scattered light. Detection of (or stringent limits on) warm dust will characterize the inner portions of these debris disks. The spatial resolution of infrared interferometry can be exploited to probe for warm dust in these systems. On long baselines (> 100 m) the central star is resolved and the visibility is primarily a measure of the stellar photospheric size. On shorter baselines (< 50 m) the photosphere is mostly unresolved and if the measured visibilities have high accuracy, one can search for emission by looking for deviations from the visibility expected for the stellar photosphere. Any resolved or incoherent emission will decrease the measured visibility from the stellar value.

Obtaining sufficient observational precision currently limits such studies of near-IR excess to the closest and brightest debris systems, and to date, most observations have been of A star systems. Detections have been made of 1-2% near-infrared excesses for the A stars Vega (Ciardi et al 2001, Absil et al 2006), ζ Aql (Absil et al. 2008) and β Leo (Akeson et al 2008) and only 1 lower mass star, τ Ceti (di Folco et al 2007). To be consistent with both the near-infrared excess and the previously known mid to far-infrared excess requires a ring of small, hot dust near the sublimation radius. Given the small number of objects observed so far, it is not clear if these inner hot dust rings are due to transient events or are the product of collisions between larger bodies orbiting close to the star. We discuss the performance of current and near future interferometers in more detail in section 1.3 below.

5.2.3 Spectroscopy of Dust and Gas

Information on the nature (e.g., size and composition) of the dust grains in debris disks is vitally important to our understanding of planetary system formation and evolution. In particular, the composition of the dust grains is likely directly related to the composition of any unseen planetary bodies. For example, Spitzer spectroscopic observations of HD 69830 reveal a rich spectrum of silicates and carbonates similar to that seen on certain classes of asteroids in the Solar System (Beichman et al. 2005; Lisse et al. 2007). The observed dust may be the result of asteroids colliding in a massive belt, producing copious amounts of small grains in the habitable zone around HD 69830.

Interestingly, HD 69830 shows no infrared excess at longer wavelengths (70 μm), indicating that the presence or extent of a debris disk around potential TPF targets cannot be determined unambiguously from single wavelength observations. A Spitzer spectroscopic survey for warm dust around TPF target stars finds only a few stars with silicate emission, for an overall detection rate of just ~1% (Beichman et al. 2006).

Spectroscopy of circumstellar gasses may provide information on the composition of the disk and its constituent bodies that is less readily available from dust observations. In addition, the gas abundance in debris disks is important for modeling of dust structures that have been attributed to the gravitational influence of unseen young planets (e.g., cleared zones, dust rings, and clumps).

Detections of gas in debris disks have been achieved with optical and ultraviolet spectroscopy. Except for one case, observation of resonantly scattered gas emission from β Pic at optical wavelengths (Olofsson et al. 2001; Brandeker et al. 2004), these detections have always involved absorption spectroscopy of edge-on disks. Such observations are sensitive to very small amounts of cold gas. Unfortunately, the geometric constraint that the line of sight to the central star must pass through the disk severely limits the number of disks that may be probed for gas in this way. In the longer-term, an ideal instrument to detect gas in debris disks and also to image new disks uncovered by Spitzer will be the Atacama Large Millimeter Array (ALMA), which is expected to begin operation late in this decade. With 64 antennas of 12-m aperture spread across baselines extending to 10 km, ALMA will achieve a spatial resolution of 30 mas (0.5 AU at β Pictoris; 4 AU in nearby star-forming regions). ALMA will provide detailed maps of the density, kinematic structure, and chemical structure of protoplanetary disks in molecular and atomic line emission, and of the dust continuum emission of nearby debris disks. With no stellar contrast problem at these wavelengths, ALMA should map more disks in greater detail than any prior astronomical facility.

5.2.4 Theory and Modeling

Observations of debris disks often reveal structures (such as rings, clumps, and warps) that are generally attributed to the gravitational influence of unseen planets (e.g., Heap et al. 2000; Holland et al. 2003). Analogous structures in our Solar System are the very narrow rings within Saturn's ring system confined by shepherding satellites and the apparent circumsolar resonant ring structure created by Earth (Dermott et al. 1994). Recognizing these structures in images of exozodiacal clouds and debris disks can allow us to indirectly detect extrasolar planets and measure their masses and orbital parameters. Observations of such structures may be the only way to detect Neptune- and Earth-mass planets located beyond ~10 AU from their host stars, where orbital periods are too long for radial-velocity, transit and astrometric techniques, and where these planets are too faint to detect directly in reflected starlight or thermal emission. In addition, unresolved clumps in an exozodiacal dust disk might initially be mistaken for a terrestrial planet.

Modeling Observed Debris Disks and the Origins of Planetesimal Belts

The most well-studied debris disk is that of our own solar system, which exhibits the zodiacal cloud of dust due to collisions between asteroids and the outgassing of comets, and the Kuiper belt of small icy bodies. The orbital distribution of Kuiper Belt Objects (KBOs) in the outer solar system suggests that a large fraction of planetesimals are scattered outward as a consequence of gravitational perturbation by giant planets, and a significant fraction of KBOs are trapped in mean motion resonances with Neptune. These observations, among others, imply that the Kuiper Belt and the outer planets of our solar system are historically linked. A recent breakthrough in theoretical modeling has produced the first model, known as the Nice Model, which simultaneously explains these features and the orbital distribution of the giant planets, the Trojans of Jupiter and Neptune, and the Late Heavy Bombardment (Tsiganis et al. 2005, Morbidelli et al. 2005, Gomes et al. 2005). The Nice Model reproduces all of these signatures by modeling the outward migration of the giant planets in a planetesimal disk truncated at the current location of Neptune. The Nice Model demonstrates the importance of planetary migration models and gives credence to future models that will attempt to describe the origin and distribution of the residual planetesimals in debris disks.

Models of planetary migration have already been applied to extrasolar debris disks with some success. In currently-observed debris disks, which exhibit optical depths greater than ~100-1000 zodis, collisions dominate the dynamics. Due to the dust grains' short collisional lifetimes, some modelers have interpreted the observed ring structures as tracers of the sources of dust. Models of such disks have focused on capturing planetesimals, the parent bodies of dust particles, into resonances via planet migration (Wyatt 2003, Reche et al. 2008). Simulations which have investigated capture probabilities of planetesimals as a function of planet migration parameters have suggested that we may be able to learn about the migration history of a system from the appearance of a ring structure (Wyatt 2003). Similar migration models have also shown that the eccentricity of the planet's orbit and initial eccentricity of the planetesimals' orbits must be very low (< 0.1) for the resulting ring structure to exhibit any azimuthal asymmetry (Reche et al. 2008).

Other models of collisionally-dominated disks have focused on the size distribution of dust in collisional equilibrium and the outcome of transient collisional avalanche events (Krivov et al. 2007, Grigorieva et al. 2007). We have learned that while collisional avalanches can

lead to brightness asymmetries in an edge-on disk similar to those that may exist due to resonant trapping of dust particles, the probability of witnessing an avalanche event is on the order of a few percent for a disk with as much dust as Beta Pic (Grigorieva et al. 2007).

Several observed collisionally-dominated disks harbor dynamically-significant quantities of gas. Takeuchi and Artymowicz (2001) showed that a relatively modest amount of gas will strongly affect the dynamics of small dust grains, which are the grains most easily seen in optical and near- to mid-infrared disk images, and can lead to the formation of azimuthally symmetric structures, such as cleared zones or dust rings, without the gravitational influence of a planet. This general conclusion is supported by more recent modeling (Klahr and Lin 2006), which also showed that such gas-formed structures can persist after the gas is completely gone. These effects may be a significant source of confusion for young transitional debris disks.

Predictions for Exozodiacal Disks

Other than results from the Keck Interferometer or LBTI, most observations of dust prior to TPF-C and TPF-I will not measure dust emission originating from the habitable zone. In the absence of these measurements, we may be tempted to use observations of dust at larger circumstellar distances to estimate the dust abundance in the habitable zone. However, extrapolating an observed abundance of dust from large circumstellar distances inward to the habitable zone of a given system is a precarious task. Unknown sources and sinks of dust may exist in these systems interior to the regions where these missions will observe. For example, our solar system has many sources of dust interior to the Kuiper belt: comets, main belt asteroids, Trojan asteroids, etc. Exoplanet discoveries have revealed a surprising variety of planetary systems, and we have no reason to believe that the diversity of dust producing bodies will be any less surprising. Understanding the dust in the habitable zones of nearby stars will probably require both observations directly sensitive to habitable-zone dust, and also modeling efforts to interpret these observations.

With future observatories, we expect to directly image exozodiacal disks analogous to our own zodiacal cloud, with optical depths on the order of $\sim 10^{-7}$. Long-term dynamical effects, such as migration due to Poynting-Robertson and corpuscular drag, are important in these tenuous disks. Models have largely ignored collisions altogether and focused on dust capture into a planet's exterior mean motion resonances as the dust migrates inward under the influence of drag (e.g., Jackson & Zook 1989, Dermott et al. 1994, Liou & Zook 1999, Moro-Martin & Malhotra 2002, Wyatt 2006).

Models of these steady state zodiacal clouds structures have come a long way since Dermott et al. (1994) first recognized the leading/trailing asymmetry in the surface brightness of the infrared sky as a circumsolar ring of zodiacal dust trapped in resonance with the Earth. We now more-or-less understand the geometry of resonant signatures from analytical calculations (Kuchner & Holman 2003) and numerical simulations (e.g. Moro-Martin & Malhotra 2002, Deller & Maddison 2005). Figure 5 qualitatively illustrates the basic geometries of resonant structures created by a single planet in a collisionless dust cloud (Kuchner & Holman 2003). Basic numerical models have also revealed that planets on eccentric orbits can trap particles in resonant terms that produce density structures which appear to revolve at mean rates slower than the mean motion of the perturbing planet (Wilner et al. 2002).

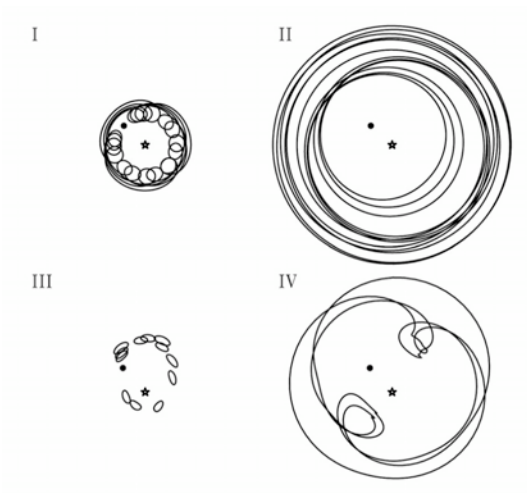

Figure 5-5. Approximate analytic description of the range of resonant structures a single planet can create in a collisionless cloud. Case I, a ring with a corotating gap at the location of the planet is exemplified by Earth's interaction with the solar zodiacal cloud. The other cases have been suggested as models for other debris disks, but not yet verified. [Figure credit: Kuchner & Holman 2003]

Recent advances in collisionless disk models have allowed for a number of quantitative predictions regarding the morphology and contrast of resonant structures formed by terrestrial-mass planets. These models have shown that most resonant structures feature a sharp inner-edge at a circumstellar distance of 83% of the semi-major axis of the planet, a gap in the ring structure at the location of the planet which varies in size linearly with ring brightness (from a few degrees to nearly ninety degrees), and ring widths that vary from a few percent to 1.6 times the semi-major axis of the planet. The same models have shown that a degeneracy exists in particle size, s, and planet semi-major axis, a_p; two exozodiacal ring structures can be geometrically identical for a constant value of ($sa_p^{1/2}$) (Stark & Kuchner 2008).

Models of collisionless exozodiacal clouds of a single grain size estimate that the contrast, defined as the ratio of optical depth within the ring structure to outside of the ring structure, of resonant ring structures created by terrestrial-mass planets can vary from unity to 7:1, as shown in Figure 6. This figure also illustrates that a distribution of particle sizes tends to wash out ring structures, reducing their contrast by up to ~50% (Stark & Kuchner 2008). Figure 7 shows the minimum detectable planet mass that can be indirectly detected via observations of its resonant ring structure, assuming a distribution of particle sizes and a minimum detectable ring contrast of 1.5:1. These estimates assume the dust is produced entirely by a source analogous to our asteroid belt; no highly-inclined or highly-eccentric sources contribute to the production of dust and thus Figure 7 can be thought of as a best-case scenario.

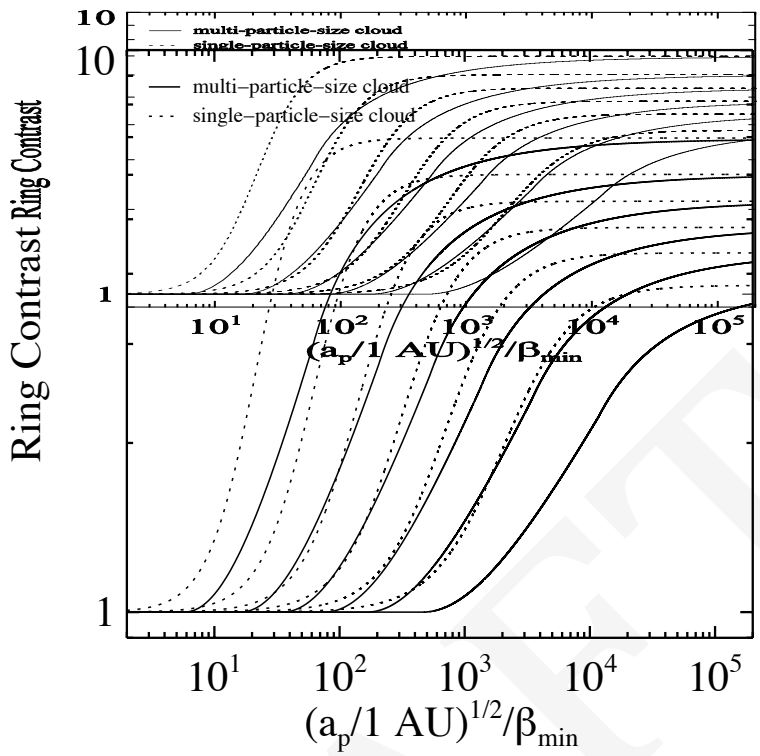

Figure 5-6. Contrast in optical depth for multi-particle-size clouds (solid lines) assuming a Dohnanyi (1969) crushing law compared to single-particle-size clouds (dashed lines). From top to bottom, the six solid lines and six dashed lines correspond to six values of planet mass: 5, 2, 1, 0.25, and 0.1 M_{Earth}. The contributions of the small grains reduce the contrasts of the multi-particle-size clouds compared to single-particle-size clouds with the same minimum value of β, where β is the ratio of the force due to radiation pressure to the gravitational force on a dust grain and is proportional to s^{-1}, the radius of the dust grain. [Figure credit: Stark & Kuchner 2008]

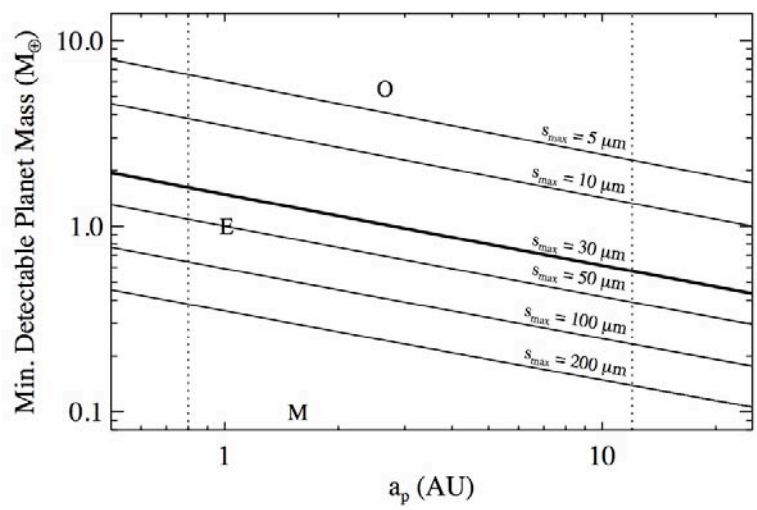

Figure 5-7. Minimum detectable planet mass in a multi-particle-size collisionless cloud as a function of semi-major axis, a_p, and maximum grain size, s_{max}, assuming a Sun-like star, a minimum detectable ring contrast of 1.5:1, and dust produced according to a Dohnanyi (1969) crushing law. Earth-like and Mars-like planets are denoted with an *E* and *M*, respectively. The 5.5 M_{Earth} exoplanet OGLE-

2005-BLG-390Lb is denoted with an *O*. Listed values for maximum dust size in the ring structure assume perfectly absorbing spherical grains with mean density $\rho = 2.0$ gm cm^{-3}. The bold line shows the case of the solar zodiacal cloud, for which the observed emission is dominated by 30 μm grains. The dashed lines show typical inner and outer detection limits for a mission similar to TPF. [Figure credit: Stark & Kuchner 2008]

5.3 Technology Development and Performance Demonstration

The technology development section focuses on the development of nulling interferometry in particular as the key technology needed to advance our knowledge of dust in the habitable zones around nearby stars. This technique has been developed for the Keck Interferometer and the Large Binocular Telescope Interferometer, with prototype testing for LBTI being carried out on the MMT.

5.3.1 Past Accomplishments

Interferometric nulling of thermal emission from stars was demonstrated for the first time in 1998 using the Multiple Mirror Telescope (MMT). By interfering infrared radiation from two of the co-mounted 1.8 m telescopes, the stellar image was suppressed by a factor of order 25 and used to map directly the thermal emission of warm dust surrounding Betelgeuse (Hinz et al. 1998).

The MMT was rebuilt as a single 6.5 m telescope early in the decade and outfitted with an adaptive secondary mirror in 2002. To facilitate testing in preparation for LBTI, a cryogenic nulling interferometer called the Bracewell Infrared Nulling Cryostat (BLINC), was developed (Hinz et al. 2000). The instrument creates a pseudo-interferometer with elliptical 2.5x5 m apertures across a 4 m baseline. Phase variations between the beams are sensed using 2.2 μm light that travels an identical path to the light at 11 μm. A dispersion introduced into the system creates a null which is both achromatic across the science band and creates a suitable phasing signal at 2.2 μm (see Hinz et al. 2000 for more information). The instrument is mated with a Mid-Infrared Array Camera (MIRAC) which measures the amount of flux in the nulled output of the BLINC.

Nulling interferometric techniques have been developed at JPL and are described in detail in the chapter on Interferometry. These techniques have been adapted for use in the Keck Interferometric Nuller (KIN) and are now in regular use at the Keck Interferometer.

The Keck Interferometer combines the two 10 m Keck telescopes as a long baseline interferometer, funded by NASA, as a joint development among the Jet Propulsion Laboratory, the W. M. Keck Observatory, and the Michelson Science Center. The KI nuller (Serabyn et al., 2004, Colavita et al., 2006, 2008) is implemented as a four-beam system operating at a wavelength of 10 μm. The two Keck telescope apertures are split into left ("primary") and right ("secondary") halves at a dual-star module (DSM) at each telescope. Accounting for diffraction and other details, the beam size on the sky at 10 μm is approximately 0.45'' × 0.50''. Two modified Mach-Zehnder beamsplitters combine the light from the left halves and right halves on the long 85 m baseline. The outputs of the two long baselines are combined in a beamsplitter – the cross combiner – with a short 4 m effective baseline. The output of the cross combiner feeds a mid-IR camera, KALI. Modulation on the long baselines is used to chop the central star to detect surrounding extended emission, while modulation on short baseline allows fringe detection in the presence of the strong thermal background. Because of the limited measurement and control bandwidths

achievable in the integration times required to observe faint 10 μm sources, phasing and tilt stabilization rely upon feedforward from two 2 μm fringe trackers (i.e., phase-referencing, or cophasing), as well as tilt feedforward from the KI angle tracker operating at 1.2 or 1.6 μm. Laser metrology and accelerometer feedforward is used to stabilize against non-atmospheric disturbances. A distributed real-time control system controls the various servos and interconnections, aided by high-level sequencers. See Colavita et al (2008 SPIE, Marseille) for more details.

5.3.2 Performance

Keck Interferometer is currently operational and is performing Key Science surveys. The LBTI is being completed with operation anticipated for 2010. The performance, demonstrated and expected for each facility, is described below.

Keck Interferometer

The current observational approach for the Keck Interferometer is to divide the night into three segments, each one dedicated to a single science target. Accounting for overheads, this is well matched to the ±14 m usable contiguous delay range for the nuller delay lines; this range allows for 2 – 3 hour delay tracks on the science targets. The observations goal is for 2 or 3 science scans with interleaved, bracketing calibrators with between 10 and 15 minutes of null/peak data on each target, depending on the source brightness. Including more than one calibrated scan per cluster allows for better estimates of the external errors, rather than relying on formal errors from the internal scatter of a single observation. Repeated observations on subsequent nights provide confidence in the nightly external errors.

A series of performance validation tests were performed between June and Aug. 2007, which revealed a slight, but statistically significant, night-to-night bias. This was ultimately traced to an additive long wavelength leakage term whose impact was flux dependent. The most likely explanation for the bias appears to be radiation from structure at the telescope top end that is diffracting into the beam path and introducing correlated emission into the two halves of each aperture. By changing the adaptive optics rotator offset angle, which changes the orientation of the pupil split on the telescope, and thus the geometry of top-end structure with respect to the cross-combiner baseline, this long wavelength leakage could be substantially reduced, although not completely eliminated. Observationally, more carefully matching target and calibrator fluxes reduced the size of the effect and shifting the broadband null reduction bandpass slightly toward shorter wavelengths also reduced the magnitude of the effect. With these three changes, the biases attributable to this effect have been shown to be much smaller than the external error per cluster based on 21 science clusters measured through April 2008. From analysis of this data set, the KI achieved an external error per cluster computed from the error of the calibrated scans of approximately 0.25% rms in a broadband 8 – 9 μm channel. This value is equivalent to 100 zodi rms (where 1 zodi is the flux produced by the zodiacal dust within our own solar system) after accounting for transmission through the long-baseline fringe pattern.

NASA has allocated a substantial portion of its 2008 Keck time to Key Science projects with the nuller. Three key science teams were selected in Nov. 2007; the PIs of the teams are Phil Hinz, Univ. of Arizona; Marc Kuchner, Goddard Space Flight Center; and Gene Serabyn, JPL. The key science observing program is currently underway and by the time it completes in Feb 2009, will observe roughly 40 nearby main sequence stars which are potential targets for future planet-finding missions and stars with known debris disks. The continued

operation of KI for nulling observations after February 2009 is uncertain; no funding is being planned after this time period.

LBTI

The Large Binocular Telescope is a common mount design interferometer with 8.4 m apertures on a 14.4 m baseline. The common mount design negates the need for long delay lines. Only three warm mirrors, primary, secondary and Nasmyth flat, are used to direct the beams toward the central instrument platform. This is especially important for thermal infrared (>3 μm) observations where telescope emissivity can be the dominant source of noise. The deformable elements of the AO systems of the LBT are integrated into the secondary mirrors of the telescope, which form the aperture stop of the telescope to optimize infrared performance. Extra surfaces in a conventional AO system add a significant amount of background light in the thermal infrared, decreasing the system's sensitivity. These several unique aspects of the LBT allow for efficient high sensitivity beam combination that is well matched to the goals of thermal infrared detection of zodiacal dust.

Very deep stellar suppression can be achieved with nulling interferometry. The fundamental limit to this approach is the angular size of the star compared to the baseline of the interferometer. For a solar type star at 10 pc this limit is below 10^{-4} for the LBT. At the same time the LBT will be sensitive to dust $\lambda/2b$ away or approximately 0.7 AU for a star at 10 pc. This combination of deep stellar suppression achievable, low background in the thermal infrared, and good spatial resolution for nearby stars will enable the LBT to probe nearby stars for zodiacal dust to an unprecedented level.

Performance estimates for the LBTI are based on observational tests being carried out with the Bracewell Infrared Nulling Cryostat (BLINC) on the MMT. Although primarily intended as an engineering prototype, BLINC can probe the very nearest and brightest stars for which the region of emission at 11 μm is comparable to $\lambda/2b$, or 0.25 arcsec. Initial results have been demonstrated by probing for zodiacal dust around Vega (Liu et al. 2004). The 1 σ uncertainty in the null is approximately 7×10^{-3} for observations of Vega, equivalent to an approximately 200 zodi dust disk around Vega. More recent observations (Spring 2008) have reduced this uncertainty to approximately 1×10^{-3} within a specific observation sequence, but with a systematic variation which is three times larger.

The level of the null uncertainty at the MMT is expected to be limited primarily by the performance of the adaptive optics correction. For the parameters of the MMT system, a variation in the characteristic scale of atmospheric turbulence, r_0, by 50% over the time of observation will limit the null to approximately 8×10^{-4}, in agreement with the internal error measured at the MMT. The suspected source of the systematic change is variations in telescope vibration under differing wind conditions and azimuth angles of the telescope. More careful calibration and improvements of the telescope pointing should alleviate this affect in future runs, but it remains to be demonstrated that the systematic variations can be kept below the statistical variations introduced by changes in atmospheric seeing.

To properly estimate limits to detection of zodiacal dust with LBTI it is important to understand photometric detection limitations, and null depth and stability limitations. The former limits the detectable dust for later-type stars and stars further away, and the latter limits dust detection around even the closest, early-type stars. At 11.1 μm a telescope emissivity of 7% for the LBT gives a background flux of 1.6×10^{10} photons/s for a 20% passband. The sky background from a HITRAN model atmosphere (Gillette and Mountain 1998) is expected to be 3.4×10^{9} photons/s. If the total throughput is set at 25%, the 5 σ limit

to sensitivity is 100 μJy per $\sqrt{hour}$ of integration for the LBTI. This photometric uncertainty is sufficient to detect dust disks 0.5, 2, 9, and 100 times solar for a F0, G0, K0, and M0 star at 10 pc respectively. As discussed above, the detection of dust is weighted toward earlier type stars.

For good photometric sensitivity, detection limits are set in practice by the level of null uncertainty. For the AO performance of the LBT, the null uncertainty in a typical observation is expected to be approximately 1.2×10^{-4}. This is nearly six times better than the MMT and is due to two effects: the larger apertures of the LBT, relative to the MMT, and the faster update rate of the LBT AO system (1 kHz, versus 500 Hz for the MMT). This null uncertainty is equivalent to approximately a dust disk which is 3 times solar. At this level confirmation of detection of a signal will be obtained by comparing spectral information of the residual flux. Flux from a dust disk will be reasonable constant in flux across the the 8-13 μm passband, while residuals from poorly suppressed starlight will follow a Rayleigh-Jeans $1/\lambda^2$ spectral slope.

5.3.3 Future Developments and Milestones

Future effort in studying exozodiacal disks will focus on increased sensitivity observations with the LBTI and Herschel, developing improved modeling and theoretical predictions of dust disk-planet interactions, studying the use of ELTs for exozodical detection, and exploring concepts for an exozodiacal precursor mission

LBTI Milestones

The Large Binocular Telescope saw first light with the first primary in October 2005. The telescope is currently in use for astronomical observations using prime focus wide-field imagers. For interferometric operations adaptive secondaries are required. These are planned for delivery in March 2009 and November 2009 for the first and second secondary respectively.

The LBT Interferometer is currently being assembled and tested at Steward Observatory. In summer 2008 it will be shipped to the LBT on Mt Graham to begin integration with the telescope. Initial telescope work will concentrate on vibration and environmental characterization and seeing-limited testing of the LBTI. Once the adaptive secondaries are integrated with the telescope approximately one year of testing and commissioning observations will be required prior to routine exozodiacal observations. On the current schedule this would result in scientific operations beginning in late 2010 to early 2011. Operation of LBTI is currently uncertain, since current NASA funding plans only cover completion of the instrument.

The LBTI is being developed specifically to carry out a Nulling Infra-Red Extrasolar Survey for TPF (NIREST, as in the "nearest" stars). This will involve observations of a comprehensive sample (60-80) of nearby, main sequence stars. In addition to characterizing candidate systems for TPF, the survey will provide useful insights into the prevalence of exozodiacal dust with various stellar parameters.

The sample, as currently composed, has approximately 15 stars in each spectral type bin A, F, G, and K, with 8 M spectral type stars. Age determination will be an additional factor that will factor into our final source selection. Each star is anticipated to require four hours to achieve a reasonable signal to noise level. The total survey will then require on the order of 40-60 nights. A sample with approximately equal number of stars in three age bins of 0-1, 1-

2, and 2-3 Gyr, will be constructed to allow a rough determination of zodiacal dust with both spectral type and age of a star.

Theory Development

There is much more numerical and analytical work to be done to provide a sound framework to understand the possible range of long-lived structures that may persist in an exozodiacal cloud. Future models must focus on disks for which both collisions and long-term dynamical evolution are important. Understanding collisional effects is crucial to understanding the dynamics of most currently known debris disks, which have optical depths 100-10,000 times that of the solar zodiacal cloud. The number of observed collisional disks is expected to grow significantly in the next few years with the observations of JWST, Keck, ALMA, and LBTI. Interpreting these images hinges on improved models of collisional dust clouds (e.g. Wyatt 2005, Krivov et al. 2007). At present, the only example of a system where a known planet creates an observed structure in a debris disk is the solar zodiacal cloud. Observations of other known planet-disk interactions will provide a direct test for the predictions made by our models.

A number of models have attempted to include collisions in dynamical calculations (e.g. Kenyon & Bromley 2005, Thébault & Augereau 2007), but few have been able to treat both collisional effects and resonant trapping simultaneously. This problem will likely yield to a statistical treatment of collisions (e.g. Thébault et al. 2003, Krivov et al. 2007). Several recent codes show promise in solving this issue (e.g. Grigorieva et al. 2007) and dynamical disk models which self-consistently treat collisions are expected to emerge in the next few years.

Extremely Large Telescopes

The next generation of telescopes, including the TMT, GMT, and E-ELT, potentially can reach much fainter photometric sensitivity limits than KI and LBTI by having significantly more collecting area, and suitable diameter to resolve the habitable zones of most stars likely to be in an exo-Earth samples. If the telescopes are optimized for performance in the thermal infrared, it is possible that many lower mass stars could be searched for debris disks than will be possible with KI and LBTI. For example, the GMT expected photometric sensitivity at N band in 1 hour is approximately 20 μJy. If the AO performance is similar to LBTI this is sufficient to detect dust down to 3 times solar level for all stars within 10 pc earlier than K4V.

Scattered light imaging will also be a focus of ELTs with similar high-contrast AO systems to GPI and SPHERE (e.g. the Planet Formation Imager for the Thirty Meter Telescope; Macintosh et al. 2006). Based on current design studies, PFI will reach similar or very slightly greater contrast than GPI (an optical depth of 3×10^{-5}), but its improved inner working angle (0.03") will allow imaging inwards toward the habitable zone for many targets, and to scales comparable to our own asteroid belt (near the "snow line") for young systems as distant as Taurus.

A TPF Precursor Mission for Exozodiacal Dust

Given the challenging nature of detecting exozodiacal dust from the ground, and the importance of it for direct imaging, a mission to characterize exozodiacal dust explicitly is an attractive option. Such a mission might be carried out in the infrared, via detection of thermal emission, or in the visible via scattered light. In either case it will be critical to measure dust in the habitable zone, which requires observing dust at 1 AU or equivalent for

stars of different luminosity. To do so likely requires a significant mission, on the scale of an Exoplanet Exploration Probe, rather than a SMEX scope mission, but the scope of such a mission should be further explored as a first step toward assessing its feasibility.

Several coronagraphic missions are currently under study as possible Probe class Exoplanet missions, including ACCESS and the Visible Light Nulling Coronagraph. A 2-m class coronagraph (Stapelfeldt et al. 2007) provides the 0.1 spatial resolution needed to resolve the rings, warps, and asymmetries driven by planetary perturbations in these disks. With contrast improved ~ 1000 times over HST, it also will be sensitive enough to detect zodiacal disks at approximately solar level, enabling comparative studies of dust inventory and properties across stellar ages and spectral types.

An infrared mission which can observe all the nearby stars of interest to the flagship Darwin and TPF missions has been under study for many years, and is called the Fourier-Kelvin Stellar Interferometer (FKSI) mission (Danchi et al. 2003). The present design is a passively cooled structurally connected interferometer, operating at 60K, from 3-8 (or 10) microns, with two 50 cm apertures separated by 12.5 m on a boom. This system has been extensively studied in the context of detecting and characterizing debris disks (see Defrere et al. 2008) and has been shown to be able to detect, within a few minutes, 1 solar system zodi disks in the habitable zone of any star within 30 pc that is accessible within its field of regard (FoR). With a sunshade having a +/- 20 degree FoR a survey of 443 stars (28 F, 74 G, 164 K and 177 M stars), and this number goes up to >900 stars if the FoR is increased to +/- 40 degrees. Thus an infrared space interferometer is not limited in spectral types or the number of stars that can be surveyed, except by its sunshade configuration. Further details on a small structurally connected interferometer are discussed in Chapter 4 in this volume.

5.4 Research and Analysis Goals

Furthering knowledge of the existence, prevalence, and strength of eoxozodiacal dust disks is critical for planning of future direct imaging missions for exo-Earths. The development of a Design Reference Mission for any of the direct imaging missions under consideration, including TPF-C, TPF-O, or TPF-I, requires information about the average zodiacal dust density around target stars. The information gleaned from detection of exozodiacal dust may also enhance our understanding of exoplanetary systems, as has already happened with observations from HST and Spitzer. The prevalence of dust in the habitable zones, and the structure of this dust, can provide important clues to the architectures of exoplanetary systems. The pivotal nature of this information leads us to the following three recommendations.

- Since information about dust in the habitable zone is crucial to planning future direct detection missions, the continued support of KI, LBTI, as well as any additional efforts that can address this question is needed to maintain momentum in this area.
- Exoplanet Probe class missions that can address the density and distribution of dust in other planetary systems should be further studied in order to optimize their scientific return and cost and technical feasibility. An Exoplanet Probe mission to detect and characterize debris disks and circumstellar material around all TPF and Darwin target stars, and to detect and characterize the atmospheres of super-earth to giants will reduce scientific and technical risk for later flagship missions.

- A robust theory program and development of collisional debris disk models will aid in decoding the resonant structures induced by planets in observed debris disks. These models will give insight into dust transport and the detectability of exoplanets via observations of disk structure.

5.5 Contributors

Olivier Absil, LAOG

Rachel Akeson, MSC/Caltech

David Ardila, Spitzer Science Center

James Breckenridge, JPL

Geoffry Bryden, JPL

Christine Chen, STScI

David Ciardi, MSC/Caltech

Mark Clampin, NASA GSFC

Vincent Coude du Foresto, Observatoire de Paris

William Danchi, NASA GSFC

Denis Defrère, Université de Liège

Dennis Ebbets, Ball Aerospace

Sally Heap, NASA GSFC

John Krist, JPL

Marc Kuchner, NASA GSFC

Charles Lillie, Northrop Grumman

Patrick Lowrance, Spitzer Science Center

Stanimir Metchev, UCLA

Rafael Millan-Gabet, MSC/Caltech

Marshall Perrin, UCLA

Meyer Pesenson, Caltech

Peter Plavchan, MSC/Caltech

Sam Ragland, Keck Observatory

Stephen Rinehart, NASA GSFC

Aki Roberge, NASA GSFC

Chris Stark, University of Maryland

Karl Stapelfeldt, JPL

Motohide Tamura, NAOJ

Angelle Tanner, JPL

Neal Turner, JPL/Caltech

DRAFT

Bruce Woodgate, NASA GSFC

5.6 References

Absil, O. et al. 2008, in press

Absil, O., et al. 2006, A&A, 452, 237

Akeson, R., et al, 2008, ApJ, submitted

Apai et al. "NACO polarimetric differential imaging of TW Hya. A sharp look at the closest T Tauri disk." A&A 415, 671 (2004)

Beichman, C. A.; Bryden, G.; Stapelfeldt, K. R, et al. "New Debris Disks around Nearby Main-Sequence Stars: Impact on the Direct Detection of Planets" *ApJ* 652, 1774 (2006)

Beichman, C. A.; Bryden, G.; Gautier, T. N, et al. "An Excess Due to Small Grains around the Nearby K0 V Star HD 69830: Asteroid or Cometary Debris?" *ApJ* 626, 1061 (2005)

Brandeker, A.; Liseau, R.; Olofsson, G., et al. "The spatial structure of the β Pictoris gas disk" *A&A* 413, 681 (2004)

Brown, R.A., "Single-Visit Photometric and Obscurational Completeness" *ApJ* 624, 1010 (2005).

Bulter, R. P., Vogt, S. S., Marcy, G. W., et al. "A Neptune-Mass Planet Orbiting the Nearby M Dwarf GJ 436." *ApJ*, 617, 580-588 (2004)

Chauvin, G., Lagrange, A.-M., Dumas, C., et al. "A giant planet candidate near a young brown dwarf. Direct VLT/NACO observations using IR wavefront sensing." A&A, 425, L29-L32 (2004)

Clampin et al. "Hubble Space Telescope ACS Coronagraphic Imaging of the Circumstellar Disk around HD 141569A." AJ 126, 385 (2003)

Ciardi, D.R., van Belle, G.T., Akeson, R.L., Thompson, R.R., Lada, E.A., & Howell, S.B. 2001, ApJ, 559, 1147

Colavita, M. Mark; Serabyn, Gene; Wizinowich, Peter L., et al. "Nulling at the Keck Interferometer" *Proc. SPIE* 6268, 3 (2006)

Danchi, William C.; Deming, Drake; Kuchner, Marc J., et al. "Detection of Close-In Extrasolar Giant Planets Using theFourier-Kelvin Stellar Interferometer" *ApJ* 597, 57 (2003).

Defrere, D., Absil, O., et al. 2008, A&A, in press

Deller, A.T., & Maddison, S.T., "Numerical modelling of dusty debris disks," *ApJ*, 625, 398-413 (2005).

Dermott, S. F., Jayaraman, S., Xu, Y. L., et al., "A circumsolar ring of asteroidal dust in resonant lock with the Earth" *Nature*, 369, 719-723 (1994).

di Folco, E., et al. 2007, A&A 475, 243

Fitzgerald et al. "The AU Microscopii Debris Disk: Multiwavelength Imaging and Modeling". ApJ 670, 536 (2007)

Golimowski et al. "Hubble Space Telescope ACS Multiband Coronagraphic Imaging of the Debris Disk around B Pictoris". AJ 131, 3109 (2006)

Gomes, R., Levison, H. F., Tsiganis, K., et al., "Origin of the cataclysmic Late Heavy Bombardment period of the terrestrial planets," *Nature*, 435, 466-469 (2005).

Grady et al. "Hubble Space Telescope Space Telescope Imaging Spectrograph Coronagraphic Imaging of the Herbig AE star AB Aurigae." =ApJ 523, L151 (1999)

Graham et al. "The Signature of Primordial Grain Growth in the Polarized Light of the AU Mic Debris Disk". ApJ 654, 595 (2007)

Grigorieva, A., Artymowicz, P., & Thébault, Ph., "Collisional dust avalanches in debris discs," *A&A*, 461, 537-549 (2007).

Heap, S. R., Lindler, D. J., Lanz, T. M., et al., "Space Telescope Imaging Spectrograph coronagraphic observations of β Pictoris," *ApJ*, 539, 435–444 (2000).

Hinz, Philip M.; Angel, James Roger P.; Woolf, Neville J, et al. "BLINC: a testbed for nulling interferometry in the thermal infrared" *Proc. SPIE* 4006, 349 (2000)

Hinz, Philip M.; Angel, J. Roger P.; Hoffmann, William F., et al. "Imaging circumstellar environments with a nulling interferometer" *Nature* 395, 251 (1998)

Holland, W. S., Greaves, J. S., Dent, W. R. F., et al., "Submillimeter observations of an asymmetric dust disk around Fomalhaut," *ApJ*, 582, 1141–1146 (2003).

Holweger, H., Hempel, M., van Thiel, T., et al., "The surface composition of β Pictoris," *A&A*, 320, L49–L52 (1997).

Jackson, A. A., & Zook, H. A., "A solar system dust ring with earth as its shepherd," *Nature*, 337, 629-631 (1989).

Johnson, J. A., Fischer, D. A, Marcy, G. W., et al. "Retired A Stars and Their Companions: Exoplanets Orbiting Three Intermediate-Mass Subgiants." *ApJ*, 665, 785-793 (2007)

Kalas, Paul; Graham, James R.; Clampin, Mark "A planetary system as the origin of structure in Fomalhaut's dust belt" *Nature* 435, 1067 (2005).

Kalas et al. "First Scattered Light Images of Debris Disks around HD 53143 and HD 139664." ApJ 637, L57 (2006)

Kalas et al. "Discovery of Extreme Asymmetry in the Debris Disk Surrounding HD 15115". ApJ 661, L85 (2007)

Kenyon, S. J., & Bromley, B. C., "Prospects for Detection of Catastrophic Collisions in Debris Disks," *AJ*, 130, 269-279 (2005).

Klahr, H., and Lin, D. N. C., "Dust distribution around HR4796A and HD141569: a self induced ring formation through a clumping instability," in Protostars and Planets V, Reipurth, B., Jewitt, D., and Keil, K., editors, (University of Arizona Press, Tucson, 2006).

Krist et al. *Proc. SPIE* 6693, 16 (2007).

Krist et al. "Hubble Space Telescope Advanced Camera for Surveys Coronagraphic Imaging of the AU Microscopii Debris Disk." AJ 129, 1008 (2005)

Krivov, A.V., Queck, M., Lohne, T., et al., "On the nature of clumps in debris disks," *A&A*, 462, 199-210 (2007).

Kuchner, M. J. & Holman, M. J., "The Geometry of Resonant Signatures in Debris Disks with Planets," 588, 1110-1120 (2003).

Liou, J. C., & Zook, H. A., "Signatures of the Giant Planets Imprinted on the Edgeworth-Kuiper Belt Dust Disk," *AJ*, 118, 580-590 (1999).

Lisse, C. M.; Beichman, C. A.; Bryden, G., et al. "On the Nature of the Dust in the Debris Disk around HD 69830" *ApJ* 658, 584 (2007)

Liu, Wilson M.; Hinz, Philip M.; Hoffmann, William F., et al. "Adaptive Optics Nulling Interferometric Constraints on the Mid-Infrared Exozodiacal Dust Emission around Vega" *ApJ* 610, 125 (2004)

Macintosh et al. "The Gemini Planet Imager." Proceedings of SPIE (2006)

Metchev et al. "Adaptive Optics Imaging of the AU Microscopii Circumstellar Disk: Evidence for Dynamical Evolution", ApJ 622, 451-462. (2005)

Morbidelli, A., Levison, H. F., Tsiganis, K., et al., "Chaotic capture of Jupiter's Trojan asteroids in the early Solar System," *Nature*, 435, 462-465 (2005).

Morbidelli, A., Chambers, J., Lunine, J. I., et al. "Source regions and time scales for the delivery of water to Earth." *Meteoritics and Planetary Science*, 35, 1309-1320 (2000)

Moro-Martín, A., & Malhotra, R., "A Study of the Dynamics of Dust from the Kuiper Belt: Spatial Distribution and Spectral Energy Distribution," *AJ*, 124, 2305-2321 (2002).

Olofsson, Göran; Liseau, René; Brandeker, Alexis, "Widespread Atomic Gas Emission Reveals the Rotation of the β Pictoris Disk" *ApJ* 563, 770 (2001)

Perrin et al. "Laser Guide Star Adaptive Optics Imaging Polarimetry of Herbig Ae/Be Stars." Science 303, 1345 (2004)

Pinte et al. "On the stratified dust distribution of the GG Tau circumbinary ring." A&A, 469, 963 (2007)

Reche, R., Beust, H., Augereau, J.-C., et al. "On the observability of resonant structures in planetesimal disks due to planetary migration," *A&A*, 480, 551-561 (2008).

Roberge, A., Feldman, P. D., Weinberger, A. J., et al., "Stabilization of the disk around β Pictoris by extremely carbon-rich gas," *Nature*, 441, 724–726 (2006).

Schneider et al. "NICMOS Imaging of the HR 4796A Circumstellar Disk." ApJ513, L127-L130 (1999)

Serabyn, Eugene; Booth, Andrew J.; Colavita, M. M. "The Keck interferometer nuller: system architecture and laboratory performance" *Proc. SPIE* 5491, 806 (2004)

Stark, C. & Kuchner, M. J., "The Detectability of Exo-Earths and Super-Earths Via Resonant Signatures in Exozodiacal Clouds," *ApJ* in press(2008).

Takeuchi, T., & Artymowicz, P., "Dust migration and morphology in optically thin circumstellar disks," *ApJ*, 557, 990–1006 (2001).

Thebault, P., & Augereau, J.-C., "Collisional Processes and Size Distribution in Spatially Extended Debris Discs," *A&A*, 472, 169-185 (2007).

Thébault, P., Augereau, J. C., & Beust, H., "Dust production from collisions in extrasolar planetary systems. The inner beta Pictoris disc," *A&A*, 408, 775-788 (2003).

Thi, W.-F., van Dishoeck, E. F., Blake, G. A., et al. "H2 and CO Emission from Disks around T Tauri and Herbig Ae Pre-Main-Sequence Stars and from Debris Disks around Young Stars: Warm and Cold Circumstellar Gas." *ApJ*, 561, 1074-1094 (2000)

Tsiganis, K., Gomes, R., Morbidelli, A., et al., "Origin of the orbital architecture of the giant planets of the Solar System," *Nature*, 435, 459-461 (2005).

Wallner, Oswald; Ergenzinger, Klaus, Johann, Ulrich "Terrestrial exo-planet science by nulling interferometry: instrument design and scientific performance" *Proc. SPIE* 7013, 70132O (2008)

Wilner, D. J., Holman, M. J, Kuchner, M. J., et al. "Structure in the Dusty Debris around Vega," *ApJ*, 569, L115-L119 (2002).

Wolszczan, A., & Frail, D. A. "A Planetary System around the Millisecond Pulsar PSR 1257+12." *Nature*, 355, 145-147 (1992)

Wyatt, M. C. "Resonant Trapping of Planetesimals by Planet Migration: Debris Disk Clumps and Vega's Similarity to the Solar System," *ApJ*, 598, 1321-1340 (2003).

Wyatt, M.C., "The insignificance of P-R drag in detectable extrasolar planetesimal belts," *A&A*, 433, 1007-1012 (2005).

Wyatt, M.C., "Dust in Resonant Extrasolar Kuiper Belts: Grain Size and Wavelength Dependence of Disk Structure," *ApJ*, 639, 1153-1165 (2006).

DRAFT

6 Microlensing

Chair: B. Scott Gaudi, The Ohio State University

LOC: Andy Boden, Michelson Science Center

6.1 Introduction

Microlensing is a relative newcomer among planet detection methods. To date only eight planets have been detected with microlensing (Bond et al. 2004, Udalski et al. 2005, Beaulieu et al. 2006, Gould et al. 2006, Gaudi et al. 2008, Bennett et al. 2008, Dong et al. 2008), but these detections have already provided important constraints on planet formation theories. The detection of two cool, "Super Earth" planets among the first four planets suggest that these planets are common (Beaulieu et al. 2006; Gould et al. 2006). The detection of a Jupiter/Saturn analog also suggests that solar system analogs are probably not rare (Gaudi et al. 2008). The detection of a low-mass planetary companion to a brown-dwarf star suggests that such objects can form planetary systems similar to those around

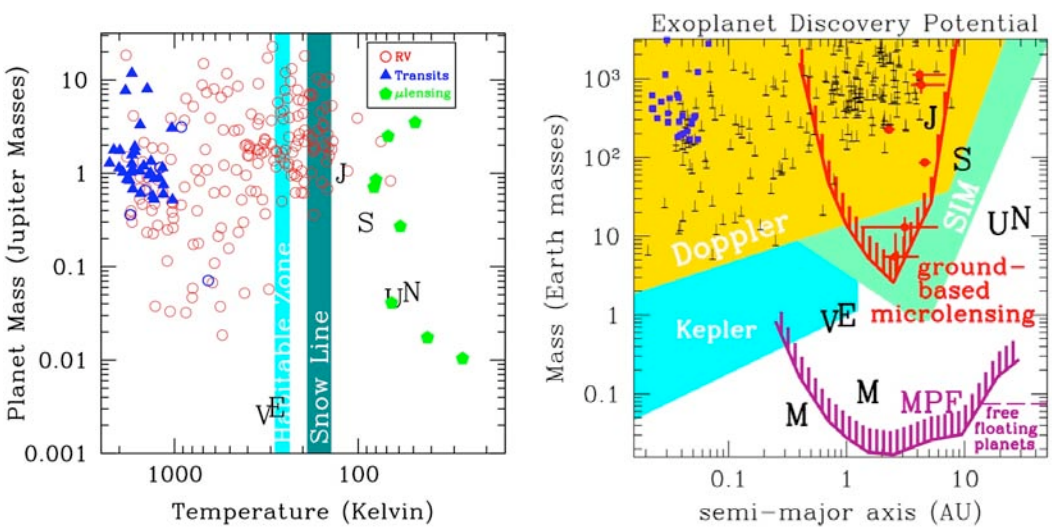

Figure 6-1: (left) Extrasolar planets detected via transits (triangles), RV (circles), and microlensing (hexagons), as a function of their mass and equilibrium temperature. Blue circles are planets found via RV that were subsequently found to be transiting. Also shown are the approximate locations of the habitable zone (e.g., Kasting et al. 1993) and the snow line (e.g., Kennedy & Kenyon 2008; Lecar et al. 2006). (right) Ground-based (red) and space-based (purple) microlensing surveys are sensitive to planets above the curve in the mass vs. semi-major axis plane. The gold, green and cyan regions indicate the sensitivities of radial velocity surveys, SIM and *Kepler*, respectively. The location of our Solar System's planets and many extrasolar planets are indicated, with microlensing discoveries in red.

solar-type main-sequence stars (Bennett et al. 2008).

Microlensing's disproportionately large contribution stems from its ability to probe regions of parameter space that are current inaccessible to other methods. In particular, microlensing is most sensitive to planets in the cold, outer regions of systems beyond the snow line, the point in the protoplanetary disk exterior to which the temperature is less than the condensation temperature of water (Lecar et al. 2006; Kennedy & Kenyon 2008). Giant planets are thought to form in the region immediately beyond this line, where the surface density of solids is highest and thus planet formation is most efficient. It is also thought that this region is likely to be the ultimate source of the water for habitable planets. In addition, microlensing is sensitive to very low-mass planets, potentially down to the mass of Mars. Finally, microlensing is the only method capable of detecting old, free-floating planets, hypothesized to be a common by-product of planet formation and evolution.

Microlensing planet searches have likely saturated their planet detection rate in their current form. On the other hand, they have far from saturated their potential. Realizing this potential, however, will require a fundamentally new, next-generation approach to ground-based searches, and ultimately will require a space-based mission. In this Chapter we review how the microlensing planet-search method works, and then outline the science goals for a next-generation ground-based survey and space mission and the requirements that must be met to achieve these goals. We propose several observatory concepts that could meet these requirements, and finally we discuss the relatively few technology developments that are needed to realize these concepts. Our final recommendations echo those made by the Exoplanet Task Force.

Summary of Recommendations

1. In the next 1-5 years, construct a small aperture (1-2m) wide FOV (2-4 deg^2) telescope in Southern Africa in order to complete a network of similar telescopes in the southern hemisphere and so allow a next-generation microlensing survey. This survey would determine the frequency of planets beyond the snow line, and detect ~10 Earth-mass planets if every main-sequence star in the Galactic disk and bulge has such a planet in the range 1.5 – 4 AU.
2. In the next 5-10 years, build and launch a 1-m class wide field-of-view space telescope that can image the central Galactic bulge in the near-IR or optical almost continuously for periods of at least several months at a time, for at least four years. Such a space-based satellite may be realized as an independent, stand-alone exoplanet mission, or a joint exoplanet/dark energy mission. This survey would determine the demographics of planets with $0.5\mathrm{AU}$ - ∞, and $m_p \gtrsim M_{\mathrm{Mars}}$, determine the frequency of free-floating, Earth-mass planets, and determine the frequency of Earth-mass in the outer habitable zone of solar-type stars in the Galactic disk and bulge.

6.1.1 How Microlensing Finds Planets.

A microlensing event occurs when a foreground "lens" happen to pass very close to our line of sight to a more distant background "source." The lens is a typically main-sequence star or stellar remnant in the foreground Galactic disk or bulge, whereas the source is a main-sequence star or giant typically in the bulge. The lens splits the source into two images which have a separation near the time of closest alignment of $\sim 2\theta_E$, where the Einstein ring radius is defined by $\theta_E = \sqrt{\kappa M \pi_{rel}}$, where M is the mass of the lens, $\pi_{rel} = \mathrm{AU}(d_l^{-1} - d_s^{-1})$ is

the lens-source relative parallax, d_l and d_s are the distances to the lens and source, and $\kappa = 4G/c^2\mathrm{AU}$. For typical lens masses and lens and source distances, $\theta_E \sim 500\mu\mathrm{as}$, and so the images are not resolved. However, the source is magnified by an amount that depends only on the angular separation of the lens and source in units of θ_E.

The transverse motion of the lens, source, and observer results in a time-variable magnification and gives rise to a smooth, symmetric microlensing event with a characteristic form. Typically, observations of a microlensing event caused by an isolated lens can fit by a simple five-parameter model. Three specify the magnification as a function of time: the minimum angular separation of the lens and source in units of θ_E (the impact parameter, which also specifies the maximum magnification), the time of maximum magnification, and finally the Einstein timescale, $t_E = \theta_E / \mu$, where μ is the relative lens-source proper motion. The typical timescales for events toward the Galactic bulge are of order a month. Only t_E contains any information about the physical properties of the lens, and then only in a degenerate combination of the lens mass, distance, and transverse velocity. However, as mentioned below, it has proven to be the case that it is often possible to obtain additional information, which partially or totally breaks this degeneracy. The remaining two parameters required to fit a single-lens event are the flux of the source, and the flux of any unresolved light that is not being lensed. The latter can include light from a companion to the source, light from unrelated nearby stars, light from a companion to the lens, and (most interestingly) light from the lens itself. In those cases where it is possible to isolate the lens light, this measurement can be used to constrain the lens mass (Bennett et al. 2007).

If the lens star happens to have a planetary companion, the companion can perturb the images created by the primary, resulting in a short-timescale deviation from the smooth, symmetric primary microlensing event (Mao & Paczynski 1991; Gould & Loeb 1992). The durations of these perturbations range from a few hours for an Earth-mass planet to a day for Jovian-mass planets. Since the planet must perturb one the two primary images in order to yield a detectable deviation, and these images are always located near the Einstein ring radius when the source is significantly magnified, the sensitivity of the microlensing method peaks for planet-star separations of $\theta_E d_l \sim 2.5\mathrm{AU}(M/0.3M_\odot)^{1/2}$. Given a planet located within 0.6-1.6 of this optimal separation, also called the "lensing zone," the detection probabilities range from tens of percent for Jovian planets to a few percent for Earth-mass planets (Gould & Loeb 1992; Bennett & Rhie 1996). The perturbed light curves yield unambiguous planet parameters: for the great majority of events, the basic planet parameters that describe the perturbation, the planet/star mass ratio, and the planet-star separation, can be "read off" the planetary deviation (Gould & Loeb 1992; Bennett & Rhie 1996). Possible ambiguities in the interpretation of planetary microlensing events have been studied in detail (Gaudi & Gould 1997; Gaudi 1998), and these can be resolved with good quality, continuous light curves.

The unique way in which microlensing finds planets leads to some useful features, most of which can be understood simply as a result of the fact that planet detection relies on the direct perturbation of images by the gravitational field of the planet, rather than on light from the planet, or the indirect effect of the planet on the parent star.

Peak Sensitivity Beyond the Snow Line. The sensitivity of microlensing peaks at equilibrium temperatures of

$$T_{eq} = 278\mathrm{K}\left(\frac{L}{L_\odot}\right)^{1/4}\left(\frac{\theta_E d_l}{\mathrm{AU}}\right)^{-1/2} \sim 70\mathrm{K}\left(\frac{M}{M_\odot}\right)$$

where for the last relation we have assumed $L \propto M^5$, $d_l = 4$ kpc, and $d_s = 8$ kpc. Thus microlensing is most sensitive to planets in the cool, outer regions beyond the snow line.

Microlensing is not sensitive to planets with separations very much smaller than the Einstein ring radius, as these can only perturbed highly demagnified images. Thus microlensing is much less sensitive to planets in the habitable zones of their parent stars (Park et al. 2006). Nevertheless, a space-based microlensing survey would still detect dozens of planets in the habitable zones of their parent stars, provided such planets are common (see § x.2.2.2 and Figure x.6)

Sensitivity to Low-mass Planets. The amplitudes of the perturbations caused by planets are typically large, > 10%, Furthermore, although the durations of the perturbations get shorter with planet mass (as $m_p^{1/2}$) and the probability of detection decreases (also roughly as $m_p^{1/2}$), the amplitude of the perturbations are independent of the planet mass. This holds until the zone of influence of the planet, which has a size of order the Einstein ring radius of the planet θ_p, is smaller than the angular size of the source θ_*. When this happens, the perturbation is smoothed over the source size. For typical parameters, $\theta_p \sim \mu\mathrm{as}(m_p / M_\oplus)^{1/2}$, and for a turn-off star in the bulge $\theta_* \sim \mu\mathrm{as}$, so this finite-source suppression begins to become important for planets with the mass of the Earth, but does not completely suppress the perturbations until masses below that of Mars, for main-sequence sources (Bennett & Rhie 1996).

Sensitivity to Long-Period and Free-Floating Planets. Since microlensing can 'instantaneously' detect planets without waiting for a full orbital period, it is sensitive to planets with very long periods. Although the probability of detecting a planet decreases for planets with separations larger than the Einstein ring radius because the magnifications of the images decline, it does not drop to zero. Indeed since microlensing is directly sensitive to the planet mass, planets can be detected even without a primary microlensing event. Even free-floating planets that are not bound to any host star are detectable in this way. Microlensing is the only method that can detect old, free-floating planets. A significant population of such planets is a generic prediction of most planet formation models (e.g., Goldreich et al. 2004), particularly those that invoke strong dynamical interactions to explain the observed eccentricity distribution of planets (e.g., Juric & Tremaine 2008).

Sensitivity to Planets Throughout the Galaxy. Because microlensing does not rely on light from the planet or host star, planets can be detecting orbiting stars with distances of several kiloparsecs. The host stars probed by microlensing are simply representative of the population of massive objects along the line of sight to the bulge sources, weighted by the lensing probability. The lensing probability peaks for lens distances about halfway to the sources in the Galactic bulge, but remains substantial for lens distances in the range $d_l = 1 - 8$ kpc.

Sensitivity to Planets Orbiting a Wide Range of Host Stars. The sensitivity of microlensing is weakly dependent on the host star mass, and has essentially no dependence on the host star luminosity. Thus microlensing is about equally sensitive to planets orbiting stars all along the main sequence, from brown dwarfs to the main-sequence turn-off, as well as planets orbiting white dwarfs, neutron stars, and black holes.

Sensitivity to Multiple-Planet Systems. Microlensing is also sensitive to multiple-planet systems, particularly in high-magnification events (Gaudi et al. 1998). This, along with the fact that high-magnification events are potentially sensitive to very low-mass planets, makes microlensing an excellent probe of planetary systems.

6.1.2 Science Goals

Ground-based microlensing planet surveys, in their current incarnation, have basically saturated their detection rate at roughly half a dozen planets per year. At this rate, these surveys will be able to test the robustness of the preliminary results by indicated by the first eight detections, and push the lower mass limit of microlensing detections down to roughly the mass of the Earth for a handful of rare, very high-magnification events (Griest & Safizadeh 1998; Rattenbury et al. 2002; Dong et al. 2006). However, these surveys are unlikely to realize the full potential of the microlensing method, and are unlikely to provide enough detections to accurately determine the statistics of Earth-mass planets beyond the snow line, at least in the next ten years. Rather, what is needed is a survey that is sensitive enough to detect tens of cool, Earth-mass planets over the next ~5 years, assuming such planets are common. This requires a fundamentally new approach.

Next generation ground-based microlensing planet searches will operate in a very different mode than the current model, in which a large area of the bulge is monitored by survey groups to identify ongoing microlensing events, which are then individually monitored by follow-up collaborations to search for planetary perturbations. With a sufficiently large field-of-view (FOV) of 2-4 deg^2 , it becomes possible to monitor tens of millions of stars every 10–20 minutes, and so discover thousands of microlensing events per year. Furthermore, these would be simultaneously monitored to search for planetary perturbations. In order to obtain round-the-clock coverage and so catch all of the perturbations, several such telescopes would be needed, located on 3-4 continents roughly evenly spread in longitude. Detailed simulations of such a next-generation microlensing survey indicate that, if Earth-mass planets with semimajor axes of several AU are common around main-sequence stars, it should detect several such planets per year.

Ultimately, with a space-based survey, microlensing is capable of detecting planets with mass as small as that of Mars, with all separations greater than ~0.5 AU, orbiting main sequence stars with distances between 1 - 8 kpc. Thus, in combination with *Kepler*, microlensing can provide a nearly complete determination of the demographics of planets throughout the Galaxy. This dataset would provide a stringent test planet formation models.

The exoplanet demographics that a space-based microlensing survey provides will also yield a unique insight into the planetary habitability. The suitability of a planet for life depends on a number of factors, such as the average surface temperature, which determines if the planet resides in the habitable zone. However, there are many other factors that also may be important, such as the presence of sufficient water and other volatile compounds necessary for life (Raymond et al. 2004; Lissauer 2007). Thus, a reasonable understanding of planet formation is an important foundation for the search for nearby habitable planets and life. Although not in its optimal regime of sensitivity, a space-based microlensing is also capable of probing the outer habitable zone for G and K stars.

The particular capabilities of the microlensing method, when compared to the current sample of known exoplanets, the expected yield of extrasolar planets using current and future detection methods, and when taken in consideration with current ideas about the

formation of planetary systems, lead to the following science goals for future microlensing planet search experiments. We divide these in the 'ground-based' and 'space-based' goals, as future ground and space-based experiments are distinct in both the timeline for their completion, as well as their intrinsic capabilities.

Summary of Science Goals

3. Ground-based Survey Science Goals (1-5 years):
    a. Determine the frequency of planets beyond the snow line. If every main-sequence star in the Galactic disk and bulge has a planet in the range 1.5 – 4 AU, over the next 5 years detect 10 with $m_p = M_\oplus$, 100 with $m_p = M_{\rm Nep}$, and 500 with $m_p = M_{\rm Jup}$.
    b. Estimate the frequency of free-floating, Jupiter-mass planets. If there exists one free-floating planet per main-sequence star, detect at least 200 of them.
4. Space-based Survey Science Goals (5-10 years):
    a. Determine the demographics of planets with $0.5\,\mathrm{AU}$ - ∞, and $m_p \gtrsim M_{\rm Mars}$. If every star has an analog to our solar system, detect 150 terrestrial planets (Earth/Venus/Mars), 5000 Jupiters, 1000 Saturns, and 130 ice giants (Uranus/Neptune).
    b. Estimate the frequency of free-floating, Earth-mass planets. If there exist one free-floating planet per main-sequence star, detect at least 60 of them.
    c. Determine the frequency of Earth-mass habitable planets ($\eta_\oplus$). Find 30 habitable Earth-mass planets if there is an average of one planet per star in the habitable zone.
    d. Characterize host star masses and distances, and measure star-planet separations and planet masses to <20% for most detected planetary events.

6.1.3 Science Requirements

Planet detection via microlensing has several general requirements. First, the microlensing events due to the primary stars must first be discovered. Microlensing is an intrinsically rare phenomenon, and thus detecting microlensing events at a substantial rate practically requires monitoring stars in the Galactic bulge, where the density of source and lens stars is high. Toward the Galactic bulge, the microlensing event rate is $\Gamma \sim 10^{-5}$ per star per year. Next, these events must be monitored with sufficient precision and cadence such that the perturbations due to the planets (i.e., Earth-mass planets) of interest are detectable. Finally, a sufficient number of such events must be monitored in order to detect the planets of interest. Since the detection probability decreases with decreasing planet mass, this implies that more events must be monitored for smaller planets.

If n_* stars are monitored with a given cadence and precision, the number of planet detections per year is approximately

$$N \approx n_* \Gamma P \approx 10\ \mathrm{yr}^{-1} \left(\frac{n_*}{10^8}\right)\left(\frac{\Gamma}{10^{-5}\,\mathrm{yr}^{-1}}\right)\left(\frac{P}{1\%}\right).$$

For an Earth-mass planet and a main-sequence source, detection probabilities of $P \sim 1\%$ can be achieved with cadences of 20 minutes and ~2% photometry (Bennett & Rhie 1996).

Thus, to detect Earth-mass planets, roughly 10^8 planets must be monitored on timescales of 20 minutes with ~1% photometry. Detecting smaller planets requires monitoring a larger number of smaller stars with higher cadence and better photometric precision.

There are approximately 10 deg^2 in the Galactic bulge for which the microlensing event rate is $\geq 10^{-5}$ yr^{-1} and the reddening is not extraordinarily high. In this region, there are on average 10^7 stars per square degree down to $I \sim 21$, and so the required 10^8 main-sequence sources in the usable 10 deg^2. Achieving a few percent photometry on stars with $I \sim 21$ requires apertures (or equivalent apertures) of 1-2m. Finally, wide field-of-views of ~2 deg^2 are needed in order to simultaneously monitor a sufficient number of stars per pointing to achieve the required ~20 minute cadence. We note there is considerably flexibility in these requirements. For example, it is possible to achieve the same planet detection rate by going deeper on a smaller field of view, provided that the requisite photometry can be achieved on the fainter target stars.

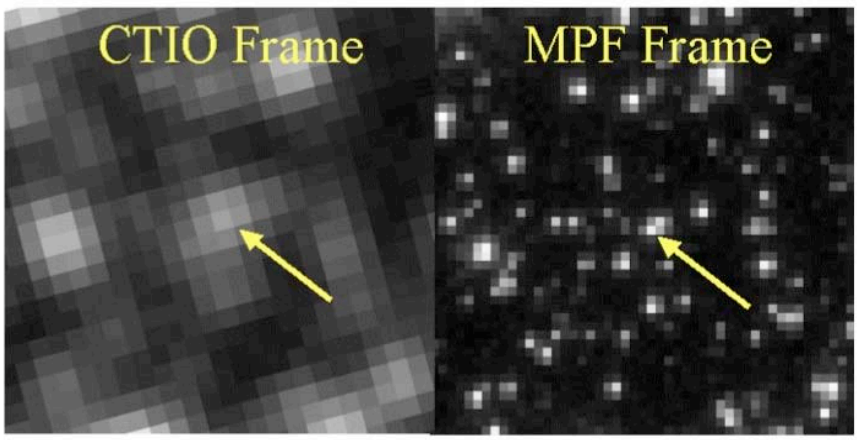

Figure 6-2: A comparison between an image of the same star field in the Galactic bulge from CTIO in 1" seeing and a simulated MPF frame (based on an HST image). The indicated star is a microlensed main sequence source star.

The full potential of the microlensing technique can only be achieved from a space mission. Ground-based microlensing surveys are inherently limited in the mass and separations of the planets they can detect. Because of the high density of stars in the Galactic bulge, main sequence source stars are not generally resolved in ground-based images, as Figure 6-2 demonstrates. As a result, the photometry needed to detect Earth-mass planets can generally only be obtained when the source is significantly magnified. This, in turn, implies that ground-based microlensing is typically only sensitive to terrestrial planets located close to the Einstein ring (at ~1.5-5 AU). Furthermore, obtaining accurate photometry of the smaller and fainter main-sequence stars that is required to detect planets with mass much smaller than the Earth is effectively impossible from the ground.

Ground-based microlensing surveys also suffer losses in data coverage and quality due to poor weather and seeing. As a result, a significant fraction of the planetary deviations seen in a ground-based microlensing survey will have poorly constrained poor light curve coverage (Peale 2003).

For all but a small fraction of planetary microlensing events, the detection of light from the host star is necessary to allow the star and planet masses and separation in physical units to be determined. This can be accomplished with HST or ground-based adaptive optics observations for a small number of planetary microlensing events (Bennett et al. 2007), but

space-based survey data will be needed for the detection of host stars for hundreds or thousands of planetary microlensing events.

Sensitivity to terrestrial planets in all orbits from 0.5 AU to ∞, sensitivity to Mars-mass planets, and full characterization of detected planets, only come from a space-based survey.

Summary of Science Requirements

1. Ground-based Survey: Monitor 100 million main-sequence stars with radius $\sim R_\odot$ in the Galactic bulge with 2% precision and 20 minute cadence continuously (weather permitting) during the 8 months/year during which the Galactic bulge is visible for five years.
2. Space-based Survey: Monitor 500 million main-sequence stars with radius $\sim$0.5-1$R_\odot$ with 1% precision and 15 minute cadence continuously during the 9 months/year during which the Galactic bulge is >45° from the Sun for four years. The resolution must be better than 0.3" in order to resolve the brightest main-sequence stars.

6.2 Observatory Concept

We will discuss two basic observatory concepts. The first is a next-generation ground-based survey, which consists of a longitudinally-distributed network of 1-2m class, wide-field telescopes. The second is a space-based 1m-class wide-field imaging satellite. Such a space-based satellite may be realized as an independent, stand-alone exoplanet mission, or a joint exoplanet/dark energy mission.

6.2.1 Architectures

Next-Generation Ground-based Network.

To satisfy science requirement #1 from §x.1.3, a network of 1-2m class telescopes equipped with large-format cameras is required. Cameras with fields-of-view of 2-4 deg^2 are required in order to monitor tens of millions of stars spread out over ~10 deg^2 in the bulge with cadences of 10-20 minutes. In order to obtain round-the-clock coverage and so catch all planetary perturbations, several such telescopes would be needed, located on 3-4 continents roughly evenly spread in longitude. With this higher cadence and larger field-of-view, these telescopes will find 6000 events per year instead of the 600 found in current surveys. Furthermore these events will be automatically monitored for planets. These two changes will yield more than a 10-fold increase in the number of events probed and so in the number of planetary detections.

A next-generation ground-based microlensing planet search network is being 'spontaneously' assembled step by step. The Japanese/New Zealand group MOA already has a 2.2 deg^2 camera in place on their 1.8m telescope in New Zealand, and currently monitors about 4 deg^2 every 10 minutes, while covering a much wider area every hour. The OGLE team has funds from the Polish government to replace their current 0.4 deg^2 camera on their 1.3m telescope in Chile with a 1.7 deg^2 camera. When finished, they will also densely monitor several deg^2 while monitoring a much larger area once per night.

Once OGLE has upgraded their camera, a network that will be able to satisfy the science requirements for a next-generation ground-based survey will be nearly in place, save a third telescope to fill in the gap in longitudinal coverage between Chile and New Zealand. Indeed,

astronomers from Korea, Germany and China have considered initiatives, or have made comprehensive proposals to their governments, to acquire funding for a 1-2m class telescope with a wide FOV in southern Africa or Antarctica. To date, none of these initiatives have secured guaranteed funding for such a project. By funding a third leg of the network in southern Africa, the US has an excellent opportunity to play a pivotal role in the development of a burgeoning field of exoplanet studies, a field in which they will otherwise be left behind. The Exoplanet Task Force recognized the importance of completing the next-generation ground-based network, and one if its recommendations over the next five years was to fund this third facility.

Space-Based Microlensing Mission.

The key mission requirements for a space-based microlensing mission are summarized in Table 1. The basic requirements are a 1-m class wide field-of-view space telescope that can image the central Galactic bulge in the near-IR or optical almost continuously for periods of at least several months at a time. The wide field-of-view is required in order to monitor a sufficient number of stars with a sufficient cadence to detect the short-timescale perturbations from low-mass planets, whereas the aperture is required both to achieve the photometric precision of $\sim$1% on $\sim 0.5 R_{\odot}$ source stars in the bulge required to detect Mars-mass planets, as well as in order to obtain the angular resolution needed to resolve the crowded bulge fields.

The proposed Microlensing Planet Finder (MPF) mission is an example of a space-based microlensing survey that can accomplish these objectives, essentially entirely with proven technology, and at a cost of ~$300M without the launch vehicle. MPF uses a 1.1m Three-Mirror Anastigmat (TMA) telescope feeding a 145 Mpixel HgCdTe focal plane residing on a standard spacecraft bus as shown in Figure 6-3. The MPF design leverages existing hardware and design concepts, many of which are already demonstrated on-orbit and/or flight qualified. We describe the basics of MPF here. The expected performance of a four-year mission with observing seasons of 9 months each is described in § x.2.2.2

Property	Value	Units
Launch Vehicle	7920-9.5	Delta II
Orbit	Inclined GEO 28.7	degrees
Mission Lifetime	4.0	years
Telescope Aperture	1.1	meters (diam.)
Field of View	0.95x0.68	degrees
Spatial Resolution	0.240	arcsec/pixel
Pointing Stability	0.048	arcsec
Focal Plane Format	145	Megapixels
Spectral Range	600-1700	nm in 3 bands
Quantum Efficiency	>75% >55%	900-1400 nm 700-1600 nm
Dark Current	<1	e-/pixel/sec
Readout Noise	<30	e-/read
Photometric Accuracy	1% or better	at J=20.5
Data Rate	50.1	Mbits/sec

Table 1: Key Space Mission Requirements

Orbit: MPF will continuously observe two 1.3 sq. degree fields in the central Galactic bulge with a sampling interval of 15 minutes for each field. Thus MPF requires an orbit allowing nearly continuous monitoring of its Galactic bulge target fields,

interrupted only as necessary, such as a 3-month period every year to avoid the Sun. The optimal orbit is a geosynchronous orbit inclined by 28.7° to the Equator and 52° to the Ecliptic. This allows a continuous view of the Galactic bulge for all but 1-2 days per month plus continuous data downlink to a dedicated ground station in White Sands, NM. The orientation of the telescope is kept fixed for the first 4.5 months of the 9-month observing season, and then, the spacecraft is rolled by 180° about the telescope bore-sight. This prevents sunlight from falling on the "dark site" of the telescope where the thermal radiators are mounted, since the MPF field is only ~5° from the Ecliptic plane.

Focal Plane Array (FPA): The MPF focal plane consists of 35 HgCdTe sensor chip assemblies (SCAs). Each SCA is a 2048^2 array of 18 μm pixels, and so the total FPA is 147 megapixels. The 140 million pixels result in a peak raw data rate of 76 Mbits/s before compression. The MPF detectors allow for non-destructive readouts, which require no dead time between exposures at the same pointing, and no shutter. The pixel size of 0.24" corresponds to the diffraction limit FWHM at a wavelength of ~1.3 μm and is sufficient to resolve most of the bulge main sequence stars.

The plate scale is 0.24"/pixel, so the FPA will cover a continuous region of 0.95°x0.68°, or 0.65 sq. degrees. Four pointings yield a total survey area of 2.6 sq. degrees. These fields will be selected to maximize the microlensing event rate and extrasolar planet detection sensitivity. To achieve the required cadence, MPF will take five 33.67-sec integrations at each pointing in a 6×6 dither pattern spanning 2×2 pixels for each subfield, spending about 3 minutes at each subfield location. This dither pattern is required to order to provide relative photometry with better than 1% precision as well as accurate astrometry. Allowing for slewing to the next subfield and spacecraft settling, the four-subfield sampling rate for microlensing events would be about 15 min.

The bandpass and the sensors are chosen to maximize the sensitivity to MPF's target stars, which are reddened main sequence stars in the Galactic bulge. In order to achieve the desired precision on the target stars, >75% QE is required in the wavelength regime 900-1400 nm and >55% QE is required for 700-1600 nm. This requirement has already been achieved with current-generation detectors, e.g., for the IR detectors developed for HST/WPC3. The QE curves for these detectors exhibit high QE across the full MPF-required bandpass. The QE operability is typically better than 99%, far exceeding the 90% requirement. These detectors also satisfy the requirements for the dark current and readout noise. Most images will be taken with the high throughput "clear" filter which spans 600–1700 nm, but at least once a day, images are taken through the "visible" (600–900 nm) and "IR" (1300–1700 nm) filters for color determination. Color measurements will help to identify the stellar type

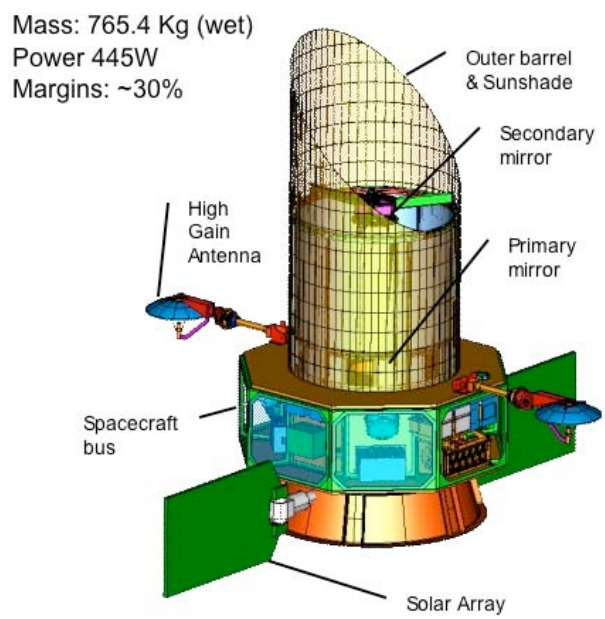

Figure 6-3: MPF On-Orbit Configuration.

of both the source and lens stars and aid in determining their properties.

Optical Telescope Assembly (OTA):

The OTA optical design of MPF is a 1.1-m aperture consisting of a three-mirror anastigmat all-reflective telescope configuration, providing a large field-of-view (FOV), and delivering diffraction limited optical performance over MPF's wide wavelength range. Starlight entering the OTA is collected by the primary mirror and reflected off the secondary mirror through the center-hole of the primary mirror assembly into the aft optics assembly, where the image is redirected and focused onto the FPA.

Microlensing/Dark Energy Mission Synergy

The requirements for a space-based microlensing mission can be accomplished by a standalone mission at a cost of about $400M (including the launch vehicle), as the example of the MPF mission shows, however the telescope requirements are very similar to the requirements for a number of the proposed dark energy missions. Thus, it seems likely that a combined dark energy/planet finding mission could be accomplished at a substantial savings compared to doing each mission separately. Thus, we expect that there may be a substantial benefit to NASA if a joint dark energy, microlensing planet search mission were considered. Although detailed simulations of the expected planet detection sensitivity of the various proposed joint dark energy missions (JDEM) have not been done, several space microlensing planet search simulation codes are available (Bennett & Rhie 2002; Gaudi, unpublished) that could be easily adapted to accomplish this.

The technical requirements of a space-based microlensing mission can be compared to those of the three JDEM concepts currently under study, ADEPT, Destiny, and SNAP, as well as the two dark energy missions under study by ESA, DUNE and SPACE. Since MPF is a well-explored example of a space mission whose technical specifications can accomplish the science objective of a space-based microlensing mission, it serves as a useful point of reference. All of these JDEM missions are wide field-of-view space telescopes with an aperture larger than MPF's 1.1m, and all include near-IR observations, although some also have an optical imaging capability. As far as we know, these missions have pointing and stability requirements that are at least as stringent as those for MPF, and most also require higher angular resolution than MPF. They all propose an Earth-Sun L2 orbit, which permits continuous viewing of the MPF Galactic bulge field, although as we explain in the next section, MPF's inclined geosynchronous orbit might be better for both applications.

The DUNE mission, which is now under study for ESA's Cosmic Visions program, is probably the most similar to MPF. In fact, it is so similar that it satisfies all of the science requirements for a space-based mission and so can meet all of the science goals, without modification to the instrument, telescope or spacecraft, provided that the planet search program is given a similar time allocation as the MPF mission. The DUNE mission is now being combined with SPACE to form a new mission called Euclid, but Euclid is expected to maintain the same capabilities for a microlensing planet search as DUNE.

While the hardware requirements for a space-based microlensing planet search mission and a dark energy mission are similar, there are a number of differences in the precise requirements for each program. In most cases, accommodating both missions will necessitate additional requirements beyond what is needed for each alone, and this implies that the cost will necessarily be higher. We have not performed a detailed trade study in order to design a mission that is optimized for both science applications, but we list here the major issues that such a trade study would address:

1. **Observing time.** The planet search mission must observe very dense fields in the Galactic bulge, which are not useful for dark energy science. Thus, the same observing fields cannot be used for both missions, so a joint mission would need to be designed for a longer lifetime than would be required for only the dark energy science. Although some progress could be made with a small amount of telescope time, detecting habitable planets will require a time commitment at the level envisioned for a dedicated space-based survey, of order four 9-month seasons. Since the detector requirements for a microlensing survey are generally less stringent than that for dark energy missions, it may be possible to perform the microlensing survey after the detectors have degraded to below the requirements for the dark energy component of the mission.
2. **Pass Bands.** The microlensing planet search program benefits from detecting as many photons from as many Galactic bulge stars as possible. Due to the extinction by dust in the foreground of the bulge, the microlens target stars are brightest in the near infrared, at wavelengths of 1- 1.5 μm. Thus, the microlensing planet search program prefers that most observations be made with an extremely wide passband centered in the near-IR. There is also a requirement that a few percent of the microlensing observations be made in narrower passbands, although the precise bassbands to be used are not critical. The desire for a very wide passband is not a hard and fast requirement, as the losses from using a narrower passband can be made up with a larger (> 1.1m) aperture telescope, or more observing time.
3. **Telescope Field-of-View and Detectors.** The proposed MPF telescope can image a field of 0.65 deg^2 with 35 2048^2 HgCdTe detectors in a single exposure. Some of the proposed JDEM missions have a smaller field-of-view. However, the dark current and QE requirements for the microlensing planet search mission are probably less stringent than for JDEM, so it might be possible to add some lower grade detectors to the focal plane.
4. **Orbit.** Most JDEM missions propose an Earth-Sun L2 orbit, whereas the proposed orbit for MPF is an inclined geosynchronous orbit. The latter orbit has the advantage of a continuous ground-link to a dedicated ground station, which makes data transmission much easier and less expensive. Our preliminary studies for the MPF mission indicate that the adverse effects of the trapped electron radiation in this orbit can be removed by a careful shielding design. If the effects of scattered Earth-shine can also be minimized by a careful baffle design, it might be possible to use this orbit for the combined mission.
5. **Data Downlink.** The data downlink requirements for a microlensing planet search mission are likely larger for the microlensing planet search program than for JDEM, the due to shorter exposures and/or a larger focal plane. If the inclined geosynchronous orbit proposed for MPF proves to be unsuitable for the dark energy mission, using a cosmic ray removal and compression scheme could reduce the data rate for the planet search observations.
6. **Telescope Aperture, PSF Sharpness, Pointing Stability.** It is expected that the dark energy science will impose tighter requirements on these parameters than the planet search program.

6.2.2 Performance

Ground-based Next-Generation Network.

Detailed simulations of ground-based next-generation microlensing survey have been performed by several groups (Bennett 2004; Gaudi, unpublished). These simulations include models for the Galactic population of lenses and sources that match all constraints, and account for real-world effects such as weather, variable seeing, photometry systematics, moon and sky background, and crowded fields. While these two independent simulations differ in detail, they reach similar conclusions. Such a survey would increase the planet detection rate at fixed mass by at least an order of magnitude over current surveys. Figure 6-4 shows the predictions of one of these simulations for the detection rate of planets of various masses, assuming every main-sequence stars has a planet within the specified range of separations. In particular, if Earth-mass planets with semimajor axes of 1.5-5AU are common around main-sequence stars, a next generation microlensing survey should detect several such planets per year. In four years, such a survey would detect Jupiter-mass free-floating planets at a rate of hundreds per year if every star has ejected Jupiter-mass planet.

As mentioned previously, microlensing lightcurves routinely yield the planet/star mass ratio and projected separation in units of θ_E. Space-based imaging or adaptive optics is needed to detect the flux of the planetary host stars, which allows the star and planet masses and separation in physical units to be determined (Bennett et al. 2007). This can be accomplished for a small number of the most interesting planetary events with HST or adaptive optics imaging.

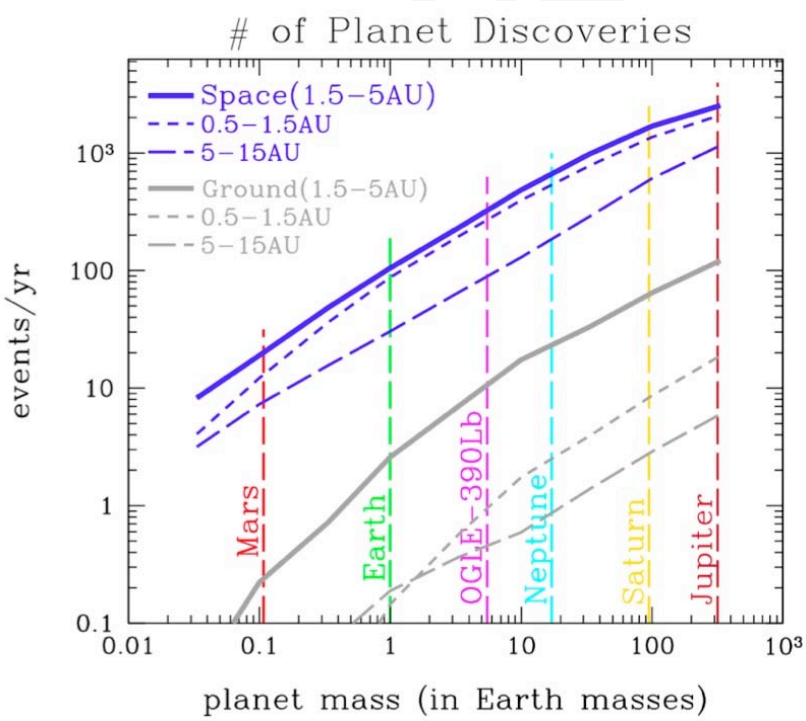

Figure 6-4. The expected number of planet discoveries as a function of the planet mass if every main-sequence stars has a single planet at the specified separation for a next-generation ground-based survey, and a space-based survey. The blue curves indicate the sensitivity of a space-based survey, and the grey curves represent a next-generation ground-based program.

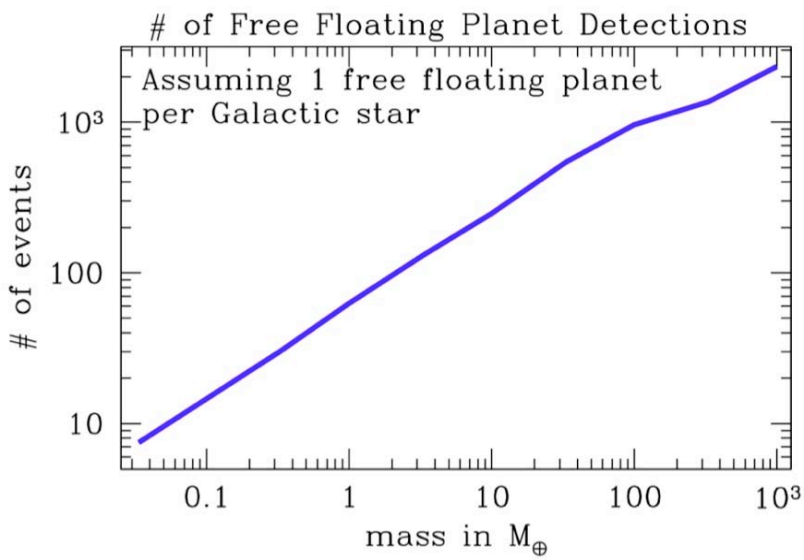

Figure 6-5: The expected number of free-floating planet discoveries for a space-based microlensing survey.

Space-based Mission:

Bennett & Rhie (2002) and Gaudi (unpublished) have independently simulated space-based microlensing surveys. These simulations included variations in the assumed mission capabilities that allow us to explore how changes in the mission design will affect the scientific output, and they form the basis of our predictions in Figs. 6-4 to 6-6. In order to predict the number of planets that will be detected by a space-based microlensing survey, we must make assumptions regarding the frequency of exoplanets. Figures 6-4 and 6-5 show the expected number of planets that MPF would detect at three different ranges of orbital separations, and ∞ (i.e. free-floating planets) assuming one such planet per star.

Figure 6-6 shows the sensitivity of MPF for planets of various masses and fixed equivalent orbital radius $a / L_*^{0.5}$, where *a* is the semimajor axis and L_* is the host star luminosity. This corresponds to a fixed equilibrium temperature for a constant albedo. Thus the boundaries of the habitable zone (HZ), shown as the dashed box, is located at roughly constant values of the equivalent orbital radius for host stars of different mass. As Figure 6-6 shows, while both MPF and *Kepler* have significant sensitivity in the HZ, MPF's sensitivity peaks for planets outsize the HZ, whereas *Kepler* is most sensitive to planets interior to the HZ. Thus by combining the results from these two missions, it will be possible to robustly interpolate the frequency of planets in the HZ, even if this frequency should turn out to be small.

A space-based microlensing survey will provide nearly complete demographics of planetary systems. The sensitivity of the microlensing method extends down to very low mass planets with $< 0.1 M_\oplus$, as shown in Figure 6-4. It is only planets well inside the Einstein ring radius that are missed because the stellar lens images that would be perturbed by these inner planets have very low magnifications and a very small contribution to the total brightness. These features can be seen in Figure 6-1, which compares the sensitivity of the MPF mission with expectations for other planned and current programs. Other ongoing and planned programs can detect, at most, analogs of two of the Solar System's planets, while a space-based microlensing survey can detect seven—all but Mercury. The only method with

comparable sensitivity to MPF is the Kepler space-based transit survey, which complements the microlensing method with sensitivity at semi-major axes < 1 AU.

A space-based survey will also detect the flux from most of the planetary host stars, which generally allows the host star mass, approximate spectral type, and the planetary mass and separation to be determined (Bennett et al. 2007). The distance to the planetary system is determined when the host star is identified, so a space-based microlensing survey will also measure how the properties of exoplanet systems change as a function of distance from the Galactic Center. There is usually some redundancy in the measurements that determine the properties of the host stars, and so the determination is robust to complicating factors, such as a binary companion to the background source star. Figure 6-7 shows the distribution of planetary host star masses and the predicted uncertainties in the masses and separation of the planets and their host stars (Bennett et al. 2007) from simulations of the MPF mission. The host stars with masses determined to better than 20% are indicated by the red histogram in Figure 6-7(a), and these are primarily the host stars that can be detected in MPF images.

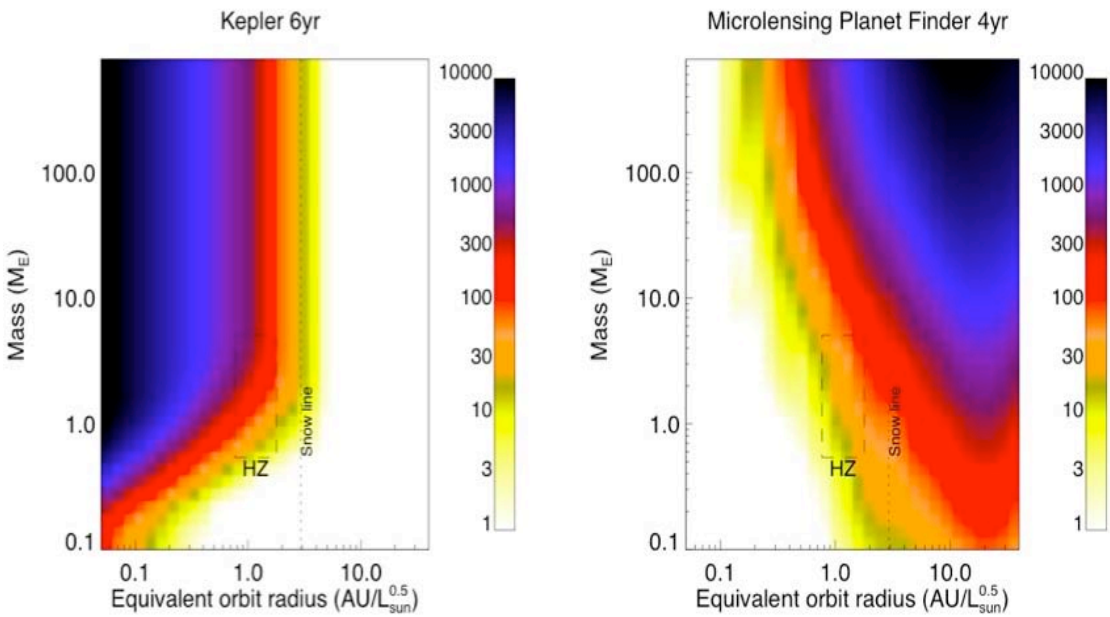

Figure 6-6: MPF sensitivity (on the right) is compared to the sensitivity of *Kepler* (on the left) in the mass vs. equivalent orbital radius plane in two figures taken from the Exoplanet Task Force Report. The equivalent orbital radius is the orbital radius (in AU) normalized to the square root of the stellar luminosity, so the Habitable Zone (HZ) has an equivalent orbital radius of ~1. MPF and *Kepler* are most sensitive to planets exterior and interior to the HZ, respectively, but both MPF and *Kepler* have some sensitivity in the HZ. The *Kepler* plot assumes an extended mission, whereas only the standard mission is assumed for MPF.

Effects of Descopes on Expected Performance

Unlikely most other planet search techniques, microlensing does not rely on flux from the host star, and as a result the expected yields of the ground and spaced-based microlensing experiments are much less sensitive to degradation in the expected performance. For experiments that rely on detecting light from the host, the number of detections is a relatively steep function of signal-to-noise ratio, typically $\propto(S/N)^{-3}$ because the number of objects in the sample is $\propto(\text{flux})^{-3/2}$ whereas the $S/N\propto(\text{flux})^{1/2}$. For microlensing, on the other hand, what matters is the brightness distribution of the sources, which are in the Galactic bulge and so at fixed distance. As a result, the scaling of the number of detections as a function of signal-to-noise ratio is much shallower, typically $\propto(S/N)^{-1}$ (Bennett & Rhie 2002). Thus the expectations for the yields of microlensing experiments are fairly robust to descopes. For a space-based mission such as MPF, detailed simulations indicate that the number of discoveries scales as $A(FOV)^{0.6}(PSF)^{-0.26}$ T, where A is the aperture, FOV is the field of view, PSF is the point spread function size, and T is the observing time (Bennett & Rhie 2002).

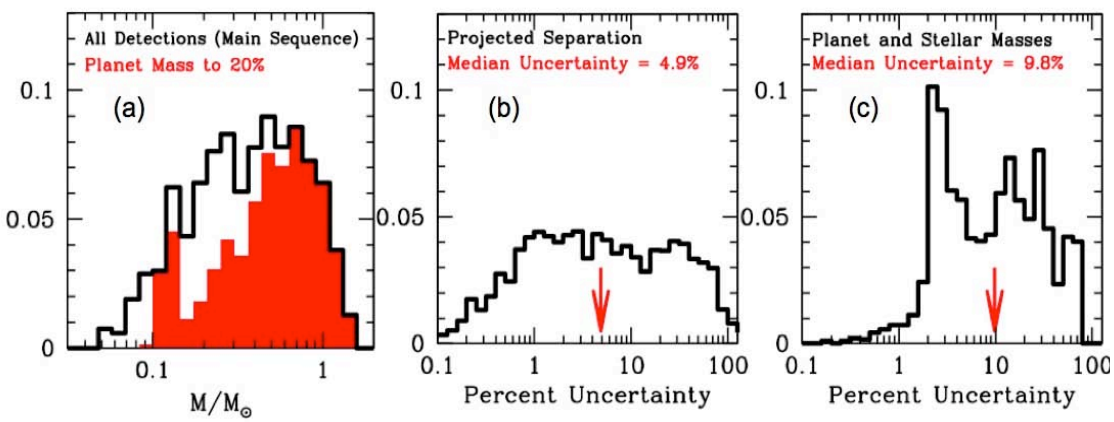

Figure 6-7: (a) The simulated distribution of stellar masses for stars with detected terrestrial planets. The red histogram indicates the subset of this distribution for which the masses can be determined to better than 20%. (b) The distribution of uncertainties in the projected star-planet separation. (c) The distribution of uncertainties in the star and planet masses.

6.3 Technology

Because the microlensing planet search technique is operationally relatively simple, in that is requires only reasonably precise (~1%) relative photometry for a large number of stars over a large field-of-view, next-generation ground and space-based microlensing planet searches require almost no technology development.

A next-generation ground-based survey requires a single, 1-2m class telescope with a wide FOV camera (2-4 deg^2). Such a system, while not trivial to construct, is certainly not unprecedented. Indeed, the MOA-II telescope (1.8m, 2.18 deg^2) has many of the features that are required. This particular design is not suitable for a South African site, however, because the plate scale is too course. The design of the Pan-STARSS-1 telescope is quite well suited for this purpose. Substantial savings over the cost of the PS-1 system could be achieved by using traditional CCD detectors rather than Orthogonal Transfer Arrays.

A space-based microlensing survey offers a few additional minor technological challenges, however these are all manageable. In particular, the MPF design leverages existing

hardware and design concepts, many of which are already demonstrated on-orbit and/or flight qualified. Indeed, essentially all elements are at TRL 6 or better.

Spacecraft:

The Spitzer spacecraft, which was developed by Lockheed Martin and has been in flight since August 2003, forms the architectural basis for the MPF spacecraft design. The Spitzer spacecraft has demonstrated performance that meets the requirements for MPF.

Optical Telescope Assembly:

The 1.1m three-mirror anastigmat OTA design for MPF is similar to that for the NextView program. NextView is a next-generation commercial remote sensing imaging instrument currently under development by ITT as a successor to ITT-built IKONOS, and is sponsored by the National Geospatial-Intelligence Agency (NGA). In fact, much of the NextView design heritage can applied to directly MPF.

Focal Plane Array:

The focal plane array (FPA) is arguably the most challenging technological aspect of a space-based microlensing mission. Fortunately, nearly all the needed technology has been developed for other missions. For example, the MPF mission extensively leverages existing detector and packaging technology developed for JDEM, WPF3, and JWST.

Rockwell Scientific (RSC) has developed infrared HgCdTe detectors, which meet the requirements of a space-based microlensing mission. RSC has delivered over 150 1K and 2K sensor chip assemblies (SCAs), and in particular 1K and 2K class SCAs for space flight missions. Most have detector requirements that are far more stringent than required for MPF. Also, 1.7μm cutoff 2K SCAs of the exact format needed for MPF have been produced for the JDEM/SNAP project evaluation. The 5.0μm cutoff 2K SCAs for NIRSpec on JWST have completed flight qualification (TRL 6). Both the JDEM/SNAP and JWST SCAs meet the MPF requirements for the quantum efficiency and wavelength coverage, dark current, and noise properties (see Table 1).

6.3.1 Future Milestones

As we have just discussed, a space-based microlensing mission requires technology that has been either already been demonstrated in-orbit, or is currently in an advanced state of development for upcoming missions. For the MPF mission specifically, essentially all of the elements of the design are at TRL 6 or better. Thus, no future technology milestones need to be achieved before a space-based microlensing mission can be launched.

The one minor exception to this is the FPA packaging. The key issues to demonstrate here are the cryogenic stability, temperature uniformity, and alignment. The path forward to demonstrating these and achieving TRL 6 is straightforward. Indeed, a pathfinder version of a FPA for the MPF mission has already been assembled in order to demonstrate the assembly methodology, and the primary components have all successfully undergone either flight qualification tests and/or on-orbit flight operations on structures of similar complexity. Similar large mosaic FPAs are currently under development for both ground and space based astronomical instruments.

6.4 Research and Analysis Goals

6.4.1 Detailed Predictions for a Next-Generation Ground-based Survey

Although realistic simulations have been performed to estimate the expected returns of a next-generation ground-based microlensing survey using a network of 'generic' 2m-class wide FOV telescopes, simulations have not been performed which consider the actual characteristics of the MOA-II telescope and upcoming OGLE IV telescopes, which generally have smaller apertures and/or FOV than those adopted in the simulations. Because the expected number of detections degrades gracefully for less capable experiments, it is still expected and some limited simulations indicate that a survey with these instruments will yield interesting scientific returns with the addition of a third telescope in southern Africa. Nevertheless, it is important to carry these simulations through in order to provide a quantitative assessment of this assertion; this will, in turn, help to inform the requirements for the third telescope.

6.4.2 Selection of Candidate Fields for Future Surveys

Although the current microlensing surveys (OGLE and MOA) have made efforts to choose those fields with the highest rate of observable microlensing events, a space-based survey will generally be going much deeper and so will be operating in a somewhat different regime. Therefore, it will be important to characterize the potential survey fields using ground-based observations. OGLE and MOA can monitor candidate fields, in order to select the fields with the highest rate of fainter events. The candidate fields should also be imaged at the highest possible resolution with one of the large telescopes located in Chile, in the optical and near-IR. These images will then provide an accurate map of the stellar populations, deep luminosity function, reddening, etc., with multicolor characterization of each potential microlensing source star. They will also provide accurate multiband photometric calibrations of thousands of relatively uncrowded standard stars in our fields, allowing accurate calibration of the very wide passbands used in the space images with the data from the primary science fields.

6.4.3 Detailed Trade Study for a Joint Dark Energy/Microlensing Mission.

The synergy between a dark energy mission and a space-based microlensing planet survey is quite compelling. A Joint Dark Energy/Microlensing Mission may offer a substantial savings over stand-alone missions, while still allowing both components to achieve their science goals. However, as outlined above, there may be some challenges to joining these missions, and so a detailed trade study needs to be done to assess the potential impacts on the expected performance.

6.5 Contributors

J.P. Beaulieu, Institut d'Astrophysique de Paris

David P. Bennett, University of Notre Dame

Edward Cheng, Conceptual Analytics

Kem Cook, Lawrence Livermore National Laboratory

Andrew Boden, Michelson Science Center

B. Scott Gaudi, The Ohio State University

Andrew Gould, The Ohio State University

John Mather, NASA

Charley Noecker, Ball Aerospace

Domenick Tenerelli, Lockheed

6.6 References

Bennett, D.P., "The Detection of Terrestrial Planets via Gravitational Microlensing: Space vs. Ground-based Surveys," Extrasolar Planets: Today and Tomorrow, ASP Conference Proceedings, Vol. 321, Eds. J.-P. Beaulieu, A. Lecavelier des Etangs and C. Terquem. (2004)

Bennett, D.P., Anderson, J., & Gaudi, B.S., "Characterization of Gravitational Microlensing Planetary Host Stars," ApJ, 660, 781-790 (2007)

Bennett, D.P., Bond, I.A., Udalski, A., et al., "A Low-Mass Planet with a Possible Sub-Stellar-Mass Host in Microlensing Event MOA-2007-BLG-192," ApJ, in press (2008)

Bennett, D.P., & Rhie, S.H., "Detecting Earth-Mass Planets with Gravitational Microlensing," ApJ. 472, 660-664 (1996)

Bennett, D. P., & Rhie, S.H., "Simulation of a Space-Based Microlensing Survey for Terrestrial Extra-Solar Planets," ApJ. 574, 985-1103 (2002)

Beaulieu, J.-P., Bennett, D.P.; Fouqué, P., "Discovery of a cool planet of 5.5 Earth masses through gravitational microlensing," Nature, 439, 437-440 (2006)

Bond, I. A., Udalski, A., Jaroszynski, M., et al., "OGLE 2003-BLG-235/MOA 2003-BLG-53: A Planetary Microlensing Event," ApJL, 606, 155-158 (2004)

Dong, S., Bond, I.A., Gould, A., et al., "Microlensing Event MOA-2007-BLG-400: Exhuming the Buried Signature of a Cool, Jovian-Mass Planet," in preparation

Dong, S., DePoy, D., Gaudi, B.S., et al., "Planetary Detection Efficiency of the Magnification 3000 Microlensing Event OGLE-2004-BLG-343," ApJ, 642, 842-860 (2006)

Gaudi, B.S., "Distinguishing Between Binary-Source and Planetary Microlensing Perturbations," ApJ, 506, 533-539 (1998)

Gaudi, B.S., Bennett, D.P., Udalski, A., et al., "Discovery of a Jupiter/Saturn Analog with Gravitational Microlensing," Science, 319, 927-930 (2008)

Gaudi, B.S., & Gould, A., "Planet Parameters in Microlensing Events," ApJ, 486, 85-99 (1997)

DRAFT

Gaudi. B.S., Naber, R.M., & Sackett, P.D., "Microlensing by Multiple Planets in High-Magnification Events, " ApJL, 502, 33-37 (1998)

Goldreich, P., Lithwich, Y., & Sari, R., "Final Stages of Planet Formation," ApJ, 614, 497-507 (2004)

Gould, A. & Loeb, A., "Discovering planetary systems through gravitational microlenses," ApJ, 396, 104-114 (1992)

Gould, A., Udalski, A., An, J., et al., "Microlens OGLE-2005-BLG-169 Implies That Cool Neptune-like Planets Are Common," ApJL, 644, 37-40 (2006)

Griest, K., & Safizadeh, N., "The Use of High-Magnification Microlensing Events in Discovering Extrasolar Planets," ApJ, 500, 37-50 (1998)

Juric, M., & Tremaine, S., "Dynamical Origin of Extrasolar Planet Eccentricity Distribution," ApJ, submitted (2008)

Kasting, J.F., Whitmire, D.P., & Reynolds, R.T., "Habitable Zones around Main Sequence Stars," Icarus, 101, 108-128 (1993)

Kennedy, G.M., & Kenyon, S.J., "Planet Formation around Stars of Various Masses: The Snow Line and the Frequency of Giant Planets," ApJ, 673, 502-512 (2008)

Lecar, M., Podolak, M., Sasselov, D., et al., "On the Location of the Snow Line in a Protoplanetary Disk," ApJ, 640, 1115-1118 (2006)

Lissauer, J., "Planets Formed in Habitable Zones of M Dwarf Stars Probably Are Deficient in Volatiles," ApJL, 660, 149-152 (2007)

Mao, S. & Paczynski, B., "Gravitational microlensing by double stars and planetary systems", ApJL, 374, 37-40, (1991)

Park, B.-G., Jeon, Y.-B.; Lee, C.-U., et al., "Microlensing Sensitivity to Earth-Mass Planets in the Habitable Zone," ApJ, 643, 1233-1238 (2006)

Peale, S., "Comparison of a Ground-based Microlensing Search for Planets with a Search from Space," AJ, 126, 1595-1603 (2003)

Rattenbury, N.J., Bond, I.A., Skuljan, J., et al., "Planetary microlensing at high magnification," MNRAS, 355, 159-169 (2002)

Raymond, S.N., Quinn, T., & Lunine, J.I., "Making other earths: dynamical simulations of terrestrial planet formation and water delivery," Icarus, 168, 1-17 (2004)

Udalski, A., Jaroszynski, M., Paczynski, B., et al., "A Jovian-Mass Planet in Microlensing Event OGLE-2005-BLG-071," ApJL, 628, 109-112 (2005)

DRAFT

7 Radial Velocity

Guillermo Torres, Harvard-Smithsonian Center for Astrophysics

Dawn M. Gelino, Michelson Science Center, Caltech

7.1 Introduction

High precision stellar radial velocity (RV) measurements have proven to be a spectacularly successful technique for the detection of extrasolar planetary systems. The first major RV search was conducted on the 3.6-m Canada-France-Hawaii Telescope (CFHT) by Campbell and Walker (1979), using a HF gas absorption cell as a velocity metric. This pioneering survey came tantalizingly close to detecting several planets. This CFHT survey, along with several other early searches, was based on the assumption that all planetary systems would have an architecture similar to our own solar system. The inner portions would have rocky terrestrial-mass planets, and gas giants would be found in the outer regions beyond 3–5 AU. Thus, when Mayor and Queloz (1995) found a candidate around a solar-type star, the half Jupiter-mass planet in a 4.2-day orbit around 51 Peg, the discovery was met by considerable astonishment that a Jovian planet could be so close to its parent star. This planet was quickly followed by the discovery of several others orbiting main-sequence stars, some in surprisingly eccentric orbits. These early exoplanets were all discovered by precise radial velocity measurements, and this method is now responsible for the initial detection of over 80% of the nearly 300 exoplanets known today.

Stellar radial velocity measurements detect the reflex orbital motion of a star around the star-planet barycenter. The stellar radial velocity signal K resulting from an exoplanetary system is given by

$$K = 28.4 \frac{M_p \sin i}{(M_* + M_p)^{2/3}} P^{-1/3} \text{ meters/sec,} \qquad (1)$$

where M_p is in Jupiter masses, M_* is in solar masses, and P is in years. From this equation, we see immediately that radial velocity detection gives the largest signal for massive planets in short period orbits. Thus, in retrospect, it should not have been much of a surprise that 51 Peg has a 4.2-day orbital period and $M_p \sin i$ of about half of a Jupiter mass. Its velocity semi-amplitude is $K = 59$ m/s, which is significantly larger than Mayor and Queloz's velocity measurement precision of 13 m/s. In contrast, the radial velocity signal of the Sun due to Jupiter's orbit is only about 13 m/s. We note also that the radial velocity technique is sensitive to $M_p \sin i$, rather than M_p. Thus, RVs allow only to measure a lower limit to the mass of a planet, unless the inclination i of the system can be determined by some independent means. Shortly after the first planets were discovered, this $\sin i$ ambiguity led some to suggest that none of these objects were really planets, but instead

that they were brown dwarfs or even very low mass stars in orbits viewed nearly pole-on. Fortunately, the sheer number of these objects discovered in the late 1990s laid this notion to rest.

Radial velocity measurement precision has continually improved from the initial ~15 m/s regime (Campbell & Walker 1979) to the current state-of-the-art of 1 m/s or better. The attainment of very high measurement precision has mostly been a matter of controlling systematic measurement errors. The use of a gas absorption cell or the continual illumination with a separate reference spectrum measures intrinsic spectrograph drifts. Enclosing the spectrograph in a vacuum and stabilizing the temperature to mK tolerances result in the achievement of residuals to planetary orbit fits as low as 64 cm/s (Lovis *et al.* 2006). Reaching this level of measurement precision opens up new possibilities for planet detection. While the radial velocity signal of an Earth-mass planet in a 1 AU orbit around a solar-mass star is only 9 cm/s, we *do* have the measurement precision to detect habitable Earths around low-mass M stars, and to detect super-Earths (planets of a few Earth masses) in short-period orbits around solar-mass stars. These super-Earths are objects in the transition region between ice-giants like Uranus and Neptune and the rocky terrestrial planets of our inner solar system. An extremely wide variety of compositions of such planets is possible, with mixtures of various fractions of metals (iron and nickel), silicates, "ices" (water, methane, ammonia, etc.) and H_2-He. The detection of these objects, and the measurement of their mass and radius (for those that undergo transits), will open up exciting new areas of planetary astrophysics.

Once a planet is discovered, the interesting science has only just begun. The characterization of planetary systems via RV observations, among other techniques, is becoming just as important as the initial discoveries. Planets often occur in multi-planet systems. The first of these found was the system around υ And. Intensive follow-up observations often reveal the presence of additional planets in the system. Many times, these planets will be gravitationally interacting with each other. The study of such interactions helps us to understand the dynamics of planetary system formation and evolution.

Doppler studies have revealed that approximately 10% of all FGK stars have at least one planet in the mass range 0.3–10 M_{Jup} with periods between 2 and 2000 days (Cumming *et al.* 2008). Extrapolating to longer periods, it is estimated that 17–19% of stars have a gas giant within 20 AU. We have also learned that gas giant formation is much more efficient around stars with super-solar metallicity (see, *e.g.*, Santos *et al.* 2004; Fischer & Valenti 2005).

7.1.1 Relevance to Space Missions

Radial velocities play a key supporting role in at least two types of NASA space missions to detect planets: astrometric missions, and missions to find planets by the transit technique. Additionally, RVs are a cost-effective way to find targets for future missions aimed at the direct detection and characterization of exoplanets. The sin *i* ambiguity of RVs, mentioned above, can be removed with a single image of the system, yielding the true mass of a planet. Foreknowledge of the spectroscopic orbit would maximize the returns of such missions because it enables the targets to be observed at the most favorable times.

The high potential for detecting low mass, even terrestrial, planets via a space-based astrometric mission has been promoted in two Decadal Surveys. NASA's Space Interferometry Mission (SIM/PlanetQuest), ESA's GAIA satellite, and ESA's ground-based PRIMA projects are examples of astrometric missions capable of detecting low mass planets.

The astrometric instrumentation measures the side-to-side reflex motion of a planet-bearing star, as opposed to the line-of-sight motion measured by RV. However RV measurements are key to establishing a reference frame composed of "fixed" stars, since astrometric measurements of greater precision that those missions will obtain are obviously not available to pre-select suitable reference stars.

The solution adopted by SIM is to select distant K giants as reference stars. Astrometric signatures of planetary companions to the K giants would be minimized by the stars' distance compared to nearby dwarfs. However, stellar and brown dwarf companions could still induce astrometric wobbles in the reference stars above SIM's tolerance of 1 microarcsecond. Candidate reference stars orbited by these more massive companions can be detected by precise radial velocity measurements, and removed from consideration.

Companions orbiting close to the K giant are not a concern since they induce small astrometric wobbles. (Note also that the radii of K giants preclude "hot Jupiter" type companions). Companions orbiting at very large radii are also not a concern since the astrometric wobble they induce will have a period longer than the mission lifetime and will appear quasi-linear, and will probably be absorbed into the astrometric solution for proper motion. However, companions at intermediate distances corresponding to periods of a few to a few tens of years are the most problematic for SIM.

Frink *et al.* (2001) have demonstrated empirically that early K giants (K0–K3) are relatively stable in RV, with a typical scatter of ~20 m/s. Their numerical simulations adopting reasonable distributions for the mass and eccentricity of companions to these reference stars based on previous RV work have shown that the expected RV signals of these companions in the period range of interest are not swamped by the intrinsic scatter quoted above, and can therefore be detected efficiently by the Doppler technique. Hence SIM has commenced a program of RV observations for each of the candidate reference stars. SIM requires 4–5 reference stars per target star, each within about 1 degree of the target star, and so RV measurements are needed for about 10 reference stars per target star in order to ensure that 4–5 survive this vetting process. A minimum of three observations is required to determine that a candidate reference star is stable, and the observation schedule typically spans about 5 years. This large-scale effort already underway is one example of the critical importance of the Doppler technique for the success of NASA missions to detect and characterize extrasolar planets.

Beyond establishing a stable reference grid for SIM, precise radial velocity measurements of all potential science targets may be viewed as "cheap insurance". They will help leverage SIM observations, allowing fewer astrometric observations with lower cadence, using RVs to fill in gaps and set constraints that rule out the effects of unknown multiple planets in these systems. An intensive RV study of all nearby potential SIM and Terrestrial Planet Finder (TPF) targets could essentially provide a "treasure map" for space-based missions to follow-up. RVs could identify all nearby systems with Jupiter-mass planets in distant and essentially circular orbits (or with no eccentric Jupiters) where dynamical space is available for habitable Earths to reside for billions of years.

Radial-velocity and spectroscopic follow-up observations are essential for understanding transiting planets, both for confirming that a candidate really is a planet and for deriving the mass and radius of the planet, as well as for characterizing the host star. Both of these steps are critical for enabling the interpretation of the planetary astrophysics that can be learned from transiting planets.

Photometric surveys for transiting planets are plagued by stellar systems that mimic the light curves of true planets (see, *e.g.*, Mandushev *et al*. 2005; Bouchy *et al*. 2005; Pont *et al.* 2005; O'Donovan *et al*. 2006). There are several lines of evidence that can be helpful in fingering the stellar imposters. For example, the discovery light curves may have marginal photometric precision, good enough to see that something interesting is going on, but not good enough to see the details of the light curve accurately. High quality follow-up photometry can sometimes reveal the stellar nature of the companion responsible for the light curve, for example by the detection of shallower secondary eclipses, or subtle light variations out of eclipse due to gravitational distortions of the primary star induced by a massive secondary, or durations of ingress and egress that are too long to be a planet. Another approach is to look for a slight shift of the centroid of light in the stellar image during transit, but this requires very accurate astrometry. Such approaches for sorting out the stellar imposters are helpful, but the ultimate proof that the companion is a planet requires a mass determination. In principle masses can be derived from either astrometric or spectroscopic orbits, but at the present time we only have the technology to do this with radial velocities for the short-period systems that are being discovered.

The role of quantitative spectroscopy in the study of transiting planets should not be overlooked. From a single-lined spectroscopic orbit the mass of the planet can only be determined relative to the host star, so an estimate of the mass of the star is needed. High-quality spectra are essential for such determinations, especially because stellar masses depend on the chemical composition. Indeed, it often turns out that the masses derived for transiting planets are limited by the uncertainty in the mass estimated for the host star (Torres *et al*. 2008). Moreover, the characteristics of the host stars are important for the interpretation of the astrophysics of populations of planets and theories of formation and evolution. Fortunately, some of the same spectra that are obtained for the radial-velocity work can often be used for the characterization of the host stars.

Thus all the NASA missions that are aimed at the study of transiting planets rely on ground-based radial-velocity and spectroscopic follow-up observations. A good example is the Kepler Mission, which is expected to discover hundreds, maybe even thousands of transiting planets. However, the transiting-planet candidates identified by Kepler will be contaminated by an even larger number of stellar imposters. Thus ground-based radial-velocity and spectroscopic follow-up observations are critical for the scientific success of the Kepler Mission. Indeed, the amount of follow-up work is expected to exceed the resources available, both in quantity and in quality. In particular, we do not yet have the technological capability to derive the mass of a transiting Earth-like planet in an Earth-like orbit, especially for the relatively faint and distant systems that Kepler will discover. Similar comments apply to the Transiting Exoplanet Survey Satellite (TESS), an all-sky SMEX project, except that TESS will have the advantage that it will discover the brightest and nearest transiting planets.

The EPOCh mission of opportunity (Deming *et al*. 2007) is another example, only in this case much of the hard work has already been done, because EPOCh is studying known transiting planets for which radial velocities and spectroscopy have already been observed. Nevertheless, given the value of the new data from EPOCh, these systems deserve additional attention, for example to see if radial-velocity monitoring reveals additional planets in the systems. Similar comments apply to the transiting planets being studied by Cold Spitzer now, the Warm Spitzer and the James Webb Space Telescope in the future, and other missions in the next decade.

7.1.2 Science Goals

Perhaps one of the most exciting science goals for NASA in which RVs will play a central role, and one that is of captivating interest to the general public, is the search for Earth-type planets around nearby stars, particularly those that may harbor life. These planets are located in what is called the "habitable zone" (HZ). We define the habitable zone here as the region around the star in which liquid water on the surface of the planet is stable. Because the RV signature on the star depends inversely on the stellar mass (see eq.[1]), late-type dwarfs are much more favorable for detecting smaller, Earth-mass planets by the Doppler technique. These stars also have lower luminosity, so the HZ moves closer to the star and this again results in a larger reflex velocity, making the detection easier. There is a growing emphasis in these searches to focus on M dwarfs to achieve the sensitivity to the lowest mass planets, in the HZ of their parent stars. The discovery of a super-Earth orbiting the M3 dwarf GJ 581 that might support liquid water (Udry *et al.* 2007) and the discovery of a transiting Neptune around GJ 436 (Gillon *et al*. 2007) have increased the focus on M dwarfs. If the sensitivity of near infrared RV measurements can be improved so that they deliver the same precision as now achieved in the optical, that would allow many hundreds of mid- to late-M stars to be studied for the presence of terrestrial planets in the HZ, which would create synergies with space missions such as CoRoT, Kepler, and TPF/Darwin. The crucial role of the RV technique here will be to *characterize* those planets (*i.e.*, to measure their masses). The synergy with CoRoT/Kepler is particularly compelling, since the capability to confirm the radial velocity orbit of planetary candidates detected around low-mass stars, where the transit amplitude and period are most favorable for the detection of terrestrial-mass, habitable-zone planets is especially challenging. CoRoT was successfully launched in December 2006, and Kepler is scheduled to launch in February 2009.

But another compelling question of our time is: How common are Solar System analogs, with Saturn- and Jupiter-mass planets beyond 4 AU in circular orbits? How often are planets in other systems arranged as in our own Solar System? One may argue that when interferometric or direct imaging techniques reach the capability to detect Earth-type planets, it is the Solar System analogs that will hold the most immediate interest. Understanding the architecture of planetary systems around other stars is a key science goal to inform theories of planet formation.

Looking to the future, one of the highest priorities should be to use the RV technique to find nearby bright planetary systems with sufficient dynamical room to allow stable Earth-like planets in the habitable zone, which could then be imaged by space missions in the next decade. A related science goal is to provide the best targets for JWST to study in the IR, such as nearby bright transiting systems with favorable contrast that would allow us access to their physical and atmospheric properties. Knowing the masses of these planets is of crucial importance for interpreting the measurements. For example, the mass for transiting planets will establish whether the object is made primarily of rock, ice, or whether it has a H/He atmosphere. Therefore, measuring the spectroscopic orbits of all potential planetary targets for JWST and the imaging missions is essential.

Another key area that needs a targeted study is measuring the "jitter" of all potential SIM and TPF targets. This is the excess scatter (over and above the measurement errors) that is of astrophysical origin, i.e., that comes from the star itself (see, *e.g.*, Santos *et al.* 2000; Wright 2005). Sources of jitter include p-mode oscillations, stellar granulation, active regions, and magnetic cycles. Stellar radial velocity jitter is not very well understood. Some stars are much quieter than expected from their spectral characteristics, while others are noisier. The most stable stars measured to date show rms dispersions below 1 m/s as

measured by the HARPS instrument on the ESO 3.6-m telescope over several years, but the majority have larger scatter. Given a measurement precision now slightly better than 1 m/s, the conclusion is that we are limited in most cases by the various sources of stellar noise rather than instrumental problems. However, the study of the power spectrum of stellar noise suggests that it may be possible to reduce the impact of jitter significantly by targeting the most stable stars and by binning the observations over timescales sufficiently long to average out these sources of astrophysical noise. This is particularly relevant for the search for terrestrial planets in the HZ, since the periods involved are long enough to allow such binning. The importance of jitter should not be underestimated. Until we understand it better, it may well be that we can only confirm (*i.e.*, measure the masses of) Earth-mass planets around late-type stars that are relatively quiet. Only a fraction of the stars surveyed may fulfill this requirement, making the need for larger samples more pressing.

7.1.3 Science Requirements

The science goals in the preceding section lead to two primary requirements: improved RV precision, and increased availability of telescope time.

In the optical, the precision of the Doppler measurements should be improved to the level of ~10 cm/s, particularly for nearby M dwarfs. This should enable the detection of Earth-like planets in the habitable zone around late-type stars. This is illustrated in Figure 1, which shows the velocity semi-amplitude in cm/s expected from terrestrial-type planets with masses of 1 $M_\oplus$, 2 $M_\oplus$, and 5 $M_\oplus$ located in the habitable zone, as a function of the mass of the parent star. It is seen, for example, that a 1 $M_\oplus$ planet in the HZ around a solar-mass star will induce a wobble on the parent star of the order of 10 cm/s. Since the effect for a given planet is inversely proportional to the 2/3 power of the mass of the star, and the HZ is located closer in for less luminous stars ($r \propto L^{-0.5}$), the same planet in the HZ of a 0.1 $M_\odot$ star produces a 1 m/s effect, which is much more easily detectable.

As identified by the ExoPlanet Task Force (ExoPTF) report, it is attractive to apply this technique in the NIR region of the spectrum where cool M-type stars emit most of their energy. The majority of the Sun's stellar neighbors are cool, low-mass stars. Of the ~150 stars lying within 8 parsecs, there are ~120 M dwarfs but only 15 solar-type G dwarfs. M dwarfs are intrinsically faint at visual wavelengths (15 to 10^6 times fainter than the Sun), but are considerably less faint in the near-infrared. Thus, an M4 dwarf at 20 parsecs has $V \sim 14$, which is beyond the reach of current optical instruments, but with $J \sim 9.5$, it is readily accessible to high-precision infrared RV observations. Although the catalogs of nearby late M dwarfs are not complete over the whole sky, the identification of all the M dwarfs within at least 30 parsecs is expected to be complete in the near future with the combination of 2MASS, proper motion surveys, and synoptic surveys such as Pan-STARRS and LSST. Although much more difficult than in the optical, it is therefore important to push the precision of RV measurements with IR spectrometers to significantly better than 10 m/s, perhaps down to the level of 1 m/s.

In order to characterize the astrophysical limitations to the RV precision generically referred to as "jitter" (stellar oscillations, granulation, etc.) it is essential to observe a sufficiently large sample of stars of different spectral types. These observations will help understand the various components of the jitter, their velocity amplitudes, and their typical timescales.

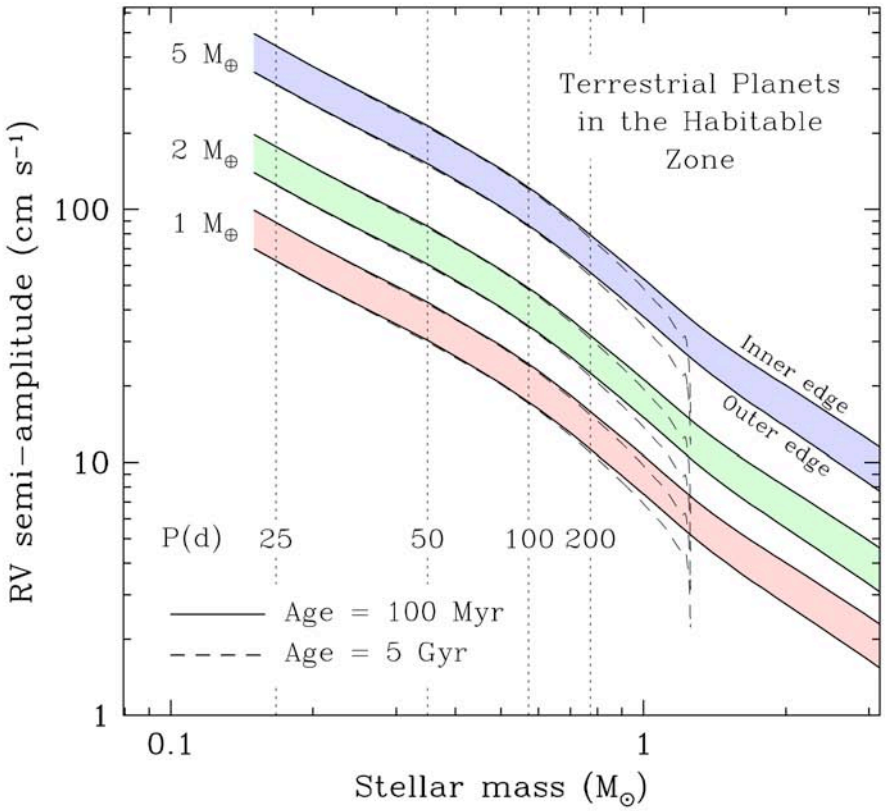

Figure 7-1: Radial velocity semi-amplitude (in cm/s) induced on the parent star by terrestrial planets in the habitable zone, as a function of stellar mass. The HZ is indicated by the different bands, and its definition follows the work by Kasting *et al*. (1993). Three different planet masses are considered, as labeled. The orbital periods of these planets (in days) are indicated by the vertical lines. HZs are shown for two different stellar ages, given that the stellar luminosity depends on age and influences the size and location of the HZ.

Perhaps one of the most important requirements, however, is to have access to significant amounts of telescope time. Present work to survey the latest-type stars (around which lower-mass planets are more likely to be detected; see above) is severely limited by the availability of observing time. The leading RV groups are essentially limited by shot noise and the number of visits they can afford make to a given target. Lengthening the exposure times and/or increasing the number of visits is important to reduce the impact of astrophysical noise, as described earlier. Longer exposures and more telescope nights would immediately bring not only higher precision, but also fainter M dwarfs into reach. The present RV surveys of late-type stars are observing only a few hundred objects. Complete samples down to V = 13 would include thousands of M dwarfs, and extending the brightness limit to V = 14 could bring tens of thousands more within reach. Exposing such faint stars for long enough to avoid being limited by photon noise requires enormous amounts of observing time, which is not presently available.

7.2 Observatory Concepts

The limited availability of telescope time has emerged as one of the most serious challenges for reaching many of the science goals listed in Sect. 1.1.2, as indicated also in the ExoPTF

report. In the area of *detection,* present surveys are collectively observing some 3,000 bright Sun-like stars systematically, mostly of spectral types F, G, and K. It is highly desirable to increase the sample size, and in particular to increase the number of M dwarfs subjected to Doppler monitoring, as those are the ones most likely to allow the detection of the first Earth-mass planet in the habitable zone. The *characterization* of planets, particularly those that undergo transits, is becoming increasingly important for the ground-based photometric surveys, and will move center-stage with the launch of the Kepler mission. The enormous amounts of time required on large telescopes to follow up relatively faint transiting planet candidates and measure their spectroscopic orbits (allowing the mass to be determined) is already the bottleneck for the CoRoT mission (see, *e.g*., Pont *et al*. 2007).

Although gaining access to more telescope time does not in itself require new technology, it is still viewed by the community as a major obstacle and a significant cost item for detecting lower mass planets and characterizing all planets, one that policy makers would be well-advised to pay close attention to, starting now and continuing into the next decade.

There are a number of options for this, including (in rough order of cost):

- Buy more telescope time on existing telescopes equipped with 1 m/s precision RV capability. Examples include the AAT in the southern hemisphere, or Keck in the North.
- Build instruments with 1 m/s precision capability and place them on existing telescopes that have available time or are under-used. This could include a number of 4-m class telescopes.
- Build dedicated ground-based large telescopes equipped with 1 m/s capability. This could be either a North-South pair of 6–8-m class Magellan-style clones, or perhaps a global network of 2–4-m class telescopes with high-precision RV spectrometers. These facilities could be fully automated and remotely operated by experienced radial velocity teams.

7.2.1 Architecture and Performance

Because of the large mass of RV spectrometers, launching high-precision RV planet detection instruments into space is not practical in the immediate future. A much better use of resources is to support space-based missions with cost-effective ground-based RV programs (as described above regarding Kepler and SIM). Furthermore, focused ground-based RV programs can carry out some of NASA's planet detection goals in their own right. A number of designs for ground-based facilities that will address the science requirements described above are already in the construction stages or will soon be tested. They represent valid examples of efforts that should be strongly supported over the next decade, and are described briefly here, beginning with the optical.

- HARPS-NEF (High Accuracy Radial velocity Planet Searcher – New Earths Facility): This is a high-resolution (R = 120,000) fiber-fed optical spectrograph with broad wavelength coverage (3780–6910 Å) designed after the very successful HARPS instrument currently in operation on the 3.6-m ESO telescope at La Silla, Chile. HARPS-NEF is a collaboration between the New Earths Facility (NEF) scientists of the Harvard Origins of Life Initiative and the HARPS team at the Geneva Observatory. It is expected to be a workhorse for follow-up of transit candidates from the Kepler mission, and will be operational in the 2010 observing season. HARPS-NEF is a cross-dispersed echelle spectrograph that will benefit not only from

updates and improvements over the original HARPS instrument, but in addition it will be installed on a larger telescope aperture in the northern hemisphere (the 4.2-m William Herschel Telescope on La Palma, Canary Islands). It is designed for ultra-high stability (10–20 cm/s), and will be placed in a vacuum chamber with careful temperature control. The method chosen for the wavelength calibration is the simultaneous Th-Ar technique, in which light from the comparison lamp is directed to the CCD through an optical fiber, separate from the fiber carrying the light from the star. However, plans also call for the installation of a laser frequency comb with the potential of increasing the measurement precision further.

- Magellan PFS (Planet Finder Spectrograph): The design of this instrument is optimized to achieve 1 m/s RV precision. Relatively few of these instruments exist today. The motivation is to provide more "air time" for high-precision velocity measurements needed to detect and characterize extrasolar planets (particularly in the South), as discussed earlier. The Magellan PFS will be mounted on the Clay 6.5-m telescope at the Las Campanas Observatory, in Chile, and is expected to see first light at the end of 2008 or beginning of 2009. It is a high-resolution (R4 grating, giving $R \sim 38{,}000$/arcsec) high-efficiency double-pass slit echelle spectrograph with passive and active temperature control, designed to enable very high quality flat-fielding and with careful slit and pupil illumination to minimize velocity errors. The wavelength fiducial is an iodine gas absorption cell. The goal is to achieve 2 m/s precision for a single exposure, and 1 m/s by binning 4 exposures over suitable timescales to average out p-mode stellar oscillations.
- MARVELS (Multi-object Apache Point Observatory Radial Velocity Exoplanet Large-area Survey): This is not an actual instrument, but an unprecedented large-scale Doppler survey of ~11,000 stars (compared to the ~3000 stars currently being observed collectively by other surveys in the brightness range V = 8–12. MARVELS uses new-generation fiber-fed multi-object instruments based on a dispersed fixed-delay interferometer (see T-EDI below). These instruments consist of a wide-angle Michelson interferometer followed by a medium-resolution spectrograph. The spectrograph can be thought of as dispersing the light output from the interferometer into a large number of narrow wavelength channels. The interferometer creates interference fringes within each of these channels. A Doppler shift can be measured as a shift in the phase of the fringes. One of the main science motivations is to provide the largest homogeneous giant planet sample for revealing the diversity in giant exoplanet populations, and testing models of the formation, migration, and dynamical evolution of giant planets. The survey, which is slated to start in late 2008, is also expected to find rare planets, transiting planets, as well as signposts for planetary systems with lower-mass or more distant planets, to be detected with follow-up observations.
- Automated Planet Finder Telescope: This is a completely robotic 2.4-m telescope under construction at the Lick Observatory (commissioning expected in June 2009), equipped with a high-resolution spectrograph designed to give a RV precision of 1 m/s to allow the Doppler detection of planets with masses as small as 5 $M_\oplus$. It is optimized for high efficiency, with a small secondary obscuration and protected silver coatings on the secondary and tertiary mirrors. The optical train will include an atmospheric dispersion compensator, as well as an iodine cell to serve as the wavelength reference. It is a *dedicated* telescope that will make intelligent decisions each night about which stars to observe, what data quality is optimal, and whether a

planet can be considered to have been detected. Given sufficient funding support, one could imagine replicating the facility a number of times to build an efficient network of similar dedicated robotic telescopes that would substantially increase the number of nights available to the community for RV work.

Extensive efforts over the last five years have focused on the development of infrared RV capabilities, to extend the reach of high-precision measurements to the lowest mass stars and brown dwarfs. Although these objects are faint in the optical where existing RV spectrometers are capable, they are much brighter in the near infrared and have atmospheres that are rich molecular cocktails with dense forests of lines suitable for precise RV measurements. We describe here only two of the more advanced near-infrared efforts.

- T-EDI (TripleSpec Externally Dispersed Interferometry): The principle on which this instrument operates is a combination of interferometry and multichannel dispersive spectroscopy that dramatically improves the velocity precision of moderate-resolution, high-throughput spectrographs (Edelestein *et al*. 2006). T-EDI is essentially an interferometer coupled with the existing Cornell TripleSpec infrared simultaneous *JHK*-band spectrograph at the Palomar Observatory 200-inch telescope. This scheme effectively multiplies the spectral resolution of the spectrograph by a factor of several to an order of magnitude over its full and simultaneous bandwidth. The interferometer creates a transmission comb that is periodic with wavelength, which multiplies the input spectrum to create moiré fringes. These fringes provide a periodic spectral fiducial comb covering the entire bandwidth of the spectrograph. This comb is analogous to the fiducial lines of an iodine absorption cell, but with lines of exceedingly uniform spacing, shape, and amplitude over the entire bandwidth. The comb, in multiplication with the input spectrum, heterodynes fine spectral features into a lower spatial-frequency moiré pattern that is recorded by the spectrograph detector. The EDI fringing signal provides a precise internal fiducial that can be used to defeat systematic instrumental noise so that the tolerance to blur or pupil changes is improved by orders of magnitude compared to classical high-resolution spectrographs that directly map telescope image quality and pupil stability to spectral performance. A Doppler velocity change induces a phase change in the moiré pattern relative to the moiré pattern of a simultaneously measured calibration spectrum, produced by either a gas absorption cell or an emission lamp that has been simultaneously recorded in the same fringing signal. Tests indicate an expected RV precision of ~5–10 m/s. This instrument was commissioned at the end of 2007, and is presently in the science verification phase at Palomar.
- Precision Radial Velocity Spectrograph Pathfinder (Ramsey *et al*. 2008): This is an in-plane fiber-fed echelle spectrograph that operates across the spectral range of 0.9–1.7 μm at a resolving power of R = 50,000, and uses a liquid nitrogen-cooled HAWAII 1K detector. In its present implementation the wavelength reference is provided by standard Th-Ar, Ar, Kr, Ne, and Xe lamps to achieve a sufficient number of lines. Tests in the laboratory have indicated precisions near 10 m/s over the short term, although the system has yet to be used on stars and longer-term stability at this level has yet to be demonstrated. The instrument is intended for use on the Hobby-Eberly Telescope at the McDonald Observatory.

Over the next decade significant progress will be made in the development of the next generation of giant (20- or 30-m) segmented mirror telescopes (GSMT). If equipped with optimized high-precision RV spectrometers, these facilities would have unique capabilities

to search for habitable Earth-mass planets around nearby stars later than spectral type M3, and brown dwarfs as well. They would also provide the crucial follow-up capability required for determining masses in current and future space-based searches for transiting planets. The larger aperture of a GSMT would also make possible very high signal-to-noise ratio spectroscopy of the atmospheres of hot Jupiters, enabling studies of their atmospheric constituents in transmission (during transits) and in reflection. The following describes briefly an instrument concept designed for a 30-m class telescope (TMT):

- Moderate to High Resolution spectrometer: This concept combines the best advantages of both the VLT's UVES instrument and Keck's HIRES spectrometer (see Sect. 1.3.1). The dual-white-pupil/dual-arm configuration of UVES is used to limit the sizes of the echelle grating, cross disperser, and camera, and a HIRES-style camera is used to allow for a much larger camera as the spectrometer is scaled up to match a TMT's enormous 30-m aperture. Moderate resolution could be used to allow multi-object capability, and the high resolution mode would be used for single objects. The resulting design would work very efficiently on a TMT, already exceeding the throughput (product of slit width and resolution) of any existing spectrometer by about 15%, with even higher throughput possible upon further scaling or using a steeper echelle. This is a large instrument, with a footprint of about 10 × 11 m. The optics are also large and challenging, though well within today's technological capabilities. The echelle gratings themselves are ~1.0 × 3.5 m, and the collimators are 2 m in diameter and are off-axis sections of a 3-m parent paraboloid. To lower costs, they could also be made spherical and warped into off-axis paraboloids by stressing harnesses. Placed on the Nasmyth platform at an f/15 focus, it is anticipated that this queue-scheduled instrument could be available at any time during the night, and could be brought into operation on the sky in as little time as it takes to rotate the tertiary to feed the light onto its slit. It is expected that a precision of 1 m/s could be achieved on a V = 13 mag M dwarf in about 8.3 minutes. Thus, larger samples of late-type stars than presently accessible would be within reach and could be observed in a reasonable amount of time.

7.3 Technology

7.3.1 Past Accomplishments

The last decade has seen tremendous technical progress in achieving high precision in RV measurements to search for and characterize extrasolar planets. In the optical, the two most productive instruments (HIRES on the Keck 10-m telescope, Vogt *et al*. 1994; HARPS on the ESO 3.6-m telescope, Mayor *et al*. 2003) now routinely achieve 1 m/s precision on slowly-rotating solar type as well as late-type stars, and have demonstrated sub-m/s precision in some cases (Lovis *et al*. 2006; Vogt 2008, priv. comm.). HIRES is a cross-dispersed echelle spectrograph in operation since the mid 1990's, typically used with slit widths giving resolving powers of $R \sim 70{,}000$. It makes use of an iodine gas absorption cell to impose a dense forest of I_2 lines on the stellar spectrum, providing a very stable wavelength reference and allowing changes in the instrumental profile to be tracked very accurately (Marcy & Butler 1992; Butler *et al.* 1996). HARPS is a $R \sim 110{,}000$ fiber-fed echelle spectrograph maintained in a temperature-controlled vacuum chamber, which has been in operation since 2003. Instead of using a gas absorption cell, it relies on Thorium-Argon emission lines recorded simultaneously with the star to provide the wavelength reference and track velocity shifts. Both of these instruments have allowed the discovery of super-Earths,

planets with masses a few times larger than our own. Other instruments have achieved precisions of a few m/s, allowing the discovery of Neptune-mass planets (~20 $M_\oplus$; McArthur *et al*. 2004).

Based on the experience in operating these spectrographs, the main factors currently limiting the precision of the RVs, in addition to photon noise, are stellar noise, the wavelength calibration, telescope guiding, stability in the illumination of the spectrograph, and detector-related effects. The only solution to photon noise is more photons. This may come from either larger telescopes equipped with high-precision spectrographs, or more telescope time on existing facilities permitting longer exposures without compromising the size of the samples of stars surveyed for planets. Indications are that the remedy to the problem of stellar noise may be similar. Longer exposures or binning over suitable timescales (again implying access to more telescope time) can reduce astrophysical jitter to some extent by averaging out those intrinsic variations (see, *e.g*., Pepe & Lovis 2007). The instrumental factors are currently estimated to limit the precision of the RVs obtained with HARPS to 30–50 cm/s on both the short term and the long term. Recent progress has been made to improve the wavelength calibrations (*e.g.*, Lovis & Pepe 2007) as well as to stabilize the spectrograph illumination. All in all, from the technological point of view it appears possible to achieve ~10 cm/s precision in the near future with a new-generation instrument designed with the above factors in mind.

Recently a new kind of instrument (the Exoplanet Tracker, or ET) entered the arena of Doppler searches and produced the discovery of a 0.5 Jupiter mass planet around a K0 main-sequence star (Ge *et al*. 2006). This marked the first time that a planet was discovered by a radial-velocity technique other than the echelle technique. The ET is based on a dispersed fixed-delay interferometer (DFDI) for Doppler measurements, described earlier. It combines a moderate-dispersion spectrograph with a two-armed interferometer, adding a graded phase delay perpendicular to the dispersion direction that creates fringes in each resolution element. Doppler shifts cause the fringes in each resolution element to move, allowing a measurement of the radial velocity against the reference provided by an iodine gas absorption cell (Erskine & Ge 2000; Ge 2002; Ge *et al.* 2002). Although the velocity precision demonstrated so far on real stars is limited to 10–20 m/s, improvements are underway. A significant advantage of the DFDI is that the same technique can provide multi-object capability on telescopes with large fields of view, although at the cost of fewer photons per star. Tests have been conducted on a prototype instrument that observed 60 stars simultaneously in the brightness range V = 8–12 with the Sloan Digital Sky Survey 2.5-m telescope at the Apache Point Observatory, in New Mexico. This multiplexing advantage opens the possibility of carrying out large surveys of ~10,000 stars at moderate RV precision (see MARVELS above) that were previously simply not possible due to the limited amount of telescope time available on telescopes equipped with single-object spectrographs.

Efforts to measure precise RVs in the near infrared (0.9–2.5 μm), where M dwarfs are brighter, have so far met with limited success. In the late 1970's and 1980's a rapid scanning Fourier Transform Spectrometer (Hall *et al*. 1979) was operated on the Kitt Peak 4-m telescope to obtain spectra of giant stars in the 2.2–2.5 μm region. Precisions of ~30–50 m/s per measurement were achieved on α Boo using the telluric H_2O lines for the zero-point calibration, and changes of ~200 m/s were measured over a span of several years at the 6–8σ level (Heyer *et al.* 1988). However, the sensitivity of the instrumental setup was rather limited, and the effort has not been continued. More recently Walker *et al*. (2003) used UKIRT's Cooled Grating Spectrometer (CGS4) to measure velocities for GJ 229B, a T6

brown dwarf of magnitude J = 14. The precision they achieved was slightly worse than 1 km/s. Smith *et al*. (2003) used the PHOENIX high-resolution infrared spectrometer on the Gemini South 8-m telescope to obtain radial velocities of Epsilon Indi Ba and Bb. Their resolving power was $R \sim 50{,}000$, and their stated radial velocity precision was only ~700 m/s. Lebzelter *et al*. (2005) used a NICMOSS detector on the 1.9-m Mt. Stromlo coudé spectrograph to perform a radial velocity study of long-period variables in 47 Tuc at J = 7.5–8.5. Their spectral resolving power was $R \sim 37{,}000$, and they achieved a ~400 m/s velocity precision. For the past 4–5 years a group has been attempting to use the state-of-the-art NIRSPEC near-IR spectrometer (R = 25,000) on the Keck 10-m telescope for planet detection around brown dwarfs and very low-mass stars in the K-band (Charbonneau 2004; Wizinowich *et al*. 2007). The technique involves using telluric methane absorption features superimposed on a ^{12}CO R-branch band at 2.3 μm (*c.f.*, Deming *et al*. 2005). The velocity precision reported thus far by this approach (Wizinowich *et al.* 2007; White 2007, priv. comm..) is about 70 m/s for two M3.5V stars (GJ 725A and B), although this has only been demonstrated over a 3-day timescale. A more representative precision obtained over several years for late-type stars is ~200 m/s (Blake 2008, priv. comm.). Stability and calibration issues with the NIRSPEC detector (Raytheon ALADDIN-III InSb 1024×1024) appear to be limiting the precision of these measurements.

7.3.2 Future Milestones

One of the key factors that determine the precision of the RVs is the wavelength reference. Existing technologies in the optical (Th-Ar technique, iodine gas absorption cell) have already achieved sub-m/s precision in some cases, but further improvements are needed if the Doppler technique is to reach cm/s precisions. A new technology that has emerged in the last few years and that holds great promise for providing a very stable reference is that of laser "frequency combs". As the name suggests, a frequency comb generated from mode-locked femtosecond-pulsed lasers provides a spectrum of very narrow emission lines with a constant frequency separation given by the pulse repetition frequency, typically 1 GHz for this application. This frequency can be synchronized with an extremely precise reference such as an atomic clock. For example, using the generally available Global Positioning System (GPS), the frequencies of comb lines have long-term fractional stability and accuracy of better than 10^{-12}. This is more than enough to measure velocity variations at a photon-limited precision level of 1 cm/s in astronomical objects (see, e.g., Murphy *et al.* 2007). This direct link with GPS as the reference allows the comparison of measurements not only between different instruments, but potentially also over long periods of time. To provide lines with separations that are well matched to the resolving powers of commonly used echelle spectrographs, a recent improvement incorporates a Fabry-Pérot filtering cavity that increases the comb line spacing to ~40 GHz over a range greater than 1000 Å (Li *et al*. 2008). Prototypes using a titanium-doped sapphire solid-state laser have been built that provide a reference centered around 8500 Å.

In practice, Doppler measurements will also be affected by other instrumental problems as described earlier, so that the value of this new technology for highly precise RV measurements is still to be demonstrated. For example, it is unclear to what degree the different paths of the laser light and the star light into the spectrograph might affect the velocity measurements. Laser comb systems have many optical components (lenses, Fabry-Pérot elements, mirrors, etc.) whose long-term stability could affect the resultant RV precision. Anti-reflection coatings tend to age, and group-delay dispersion changes in the coatings could affect the stability of the system. Non-linear effects involving power and

system efficiency variations over time, as well as detector non-linearities over the much larger dynamic range involved, could also potentially compromise the velocity precision.

For the laser comb approach to be practical, these issues will need to be worked out. As of this writing, tests of this "astro-comb" are scheduled to begin in late 2008 on telescopes operated by the Harvard-Smithsonian Center for Astrophysics on Mt. Hopkins (Arizona), and elsewhere. If successful, plans call for the deployment of an astro-comb at the ultra-stable HARPS-NEF spectrograph being built by the Harvard Origins of Life Initiative for the 4.2m William Herschel telescope on La Palma (Canary Islands). Achieving this milestone would bring us a step closer to being able to routinely measure the masses of Earth-mass planets in the habitable zones of nearby stars, even solar-type stars, a capability that is central to the success of the Kepler mission.

The lack of a suitable wavelength fiducial redward of 1 μm is considered one of the major factors limiting the precision of RV measurements with IR spectrometers. The current reliance by some projects on telluric methane absorption features that are naturally superimposed on the stellar lines has so far not produced precisions anywhere near those obtained even on late-type stars in the optical. Effects such as wind currents in the Earth's atmosphere are expected to limit the precision attainable with this technique to 10–30 m/s. Gas absorption cells that have worked so well in the optical have the potential to overcome this problem if a suitable species can be found that has sufficient line density and wavelength coverage in the IR. Some promising candidates have been identified that produce rich absorption features in the *J* and *H* bands, including the molecules CH_3I, C_2H_2, NH_3, and HCN (Guelachvili & Rao 1993; Vander Auwera *et al*. 2002). Other species such as CH_3, CO, HCCN, H_2S, and HF have also been proposed. A practical demonstration that any of these species provide a useful and stable wavelength reference would be a crucial step toward achieving a RV precision of m/s in the IR. Alternatively, it may be possible to extend the laser comb technique to the IR, for example using a different type of laser. Either implementation of a stable wavelength fiducial would be a major step forward in our ability to measure the masses of Earth-type planets orbiting late-type stars.

An additional difficulty in the IR is the lack of high-resolution IR spectrographs with $R \sim$ 60,000 or higher and a large wavelength coverage. The lack of wavelength coverage in current instruments is largely due to the lack of large-format IR detectors and the coarse echelle gratings fabricated with commercially available grating ruling technology. The most obvious way to increase the IR dispersion is to increase the grating size by placing multiple gratings in a phased mosaic, similar to what was done with HIRES on the Keck telescope. A significant disadvantage is that the collimated beam size is large and the overall instrument becomes very bulky and costly. It is also impractical to cool and maintain very large IR high-resolution spectrographs. Another way of increasing the grating dispersion without increasing the grating size is to use immersion diffraction gratings. Silicon immersion gratings are of special interest for increasing the dispersion power of IR spectroscopy because silicon has one of the highest refractive indices, $n = 3.4$, and has good transmission over the range 1.05–6 μm at cryogenic temperatures (*e.g.,* MacFarlane *et al.* 1958; Jorce 2005, priv. comm.). Demonstrating this technology would be another important step forward toward achieving m/s precision in the IR.

7.4 Research and Analysis Goals

The following is a list of research and analysis activities that should be supported in order to enable progress in the detection and characterization of extrasolar planets with the RV technique. Many of these provide indirect support to space missions such as SIM or TPF by either helping to improve the precision of the Doppler measurements or allowing more access to telescope time so that targets of interest for those missions can be identified.

- Support research to significantly improve the stability of the wavelength reference used for Doppler measurements in the optical, and to extend it to the IR. One avenue would be the implementation of femtosecond laser frequency combs, both in the optical and the IR. Another would be to extend the applicability of gas-absorption cells already used in the optical to longer wavelengths. Examples include a "hot" iodine cell (~200 ºC) that could provide a stable wavelength reference in the 8000–9000 Å range. Recent studies show that there are a number of other promising candidate chemicals (CH_3I, C_2H_2, NH_3, and HCN; Guelachvili & Rao 1993; Vander Auwera *et al.* 2002) that produce absorption bands in the *J* and *H* bands and can be potentially used for providing an accurate wavelength reference in the IR.
- Support the development of multi-object high-precision optical and IR Doppler instruments for wide field telescopes (such as the SDSS 2.5m telescope with a 7 square degree field of view, or China's LAMOST 4m wide-field telescope with a 20 square degree field of view). These instruments would have an enormous multiplexing advantage, and would be a much more efficient way of increasing the number of stars observed compared to simply adding more telescopes with single-object RV instruments. As an example of this advantage, there are ~50 solar type stars with $V < 10$ within a ~20 square degree of field of view that could be observed *simultaneously* with such instruments. Multi-object high precision Doppler instruments with $R \sim 20{,}000$ and 4000–6000 Å wavelength coverage should be able to reach a photon-limited precision of ~1 m/s in ~0.5 hour integrations at $V = 10$.
- Support efforts to design Doppler measurement instruments for 20–30m class telescopes, intended for high precision.
- Support efforts to obtain the observations needed to understand stellar jitter. This will require a focused and dedicated effort run by teams that have demonstrated sub-m/s precision capability.

7.5 Contributors

Paul Butler, Carnegie Institution of Washington, Department of Terrestrial Magnetism

William Cochran, University of Texas at Austin

Debra Fischer, San Francisco State University

Jian Ge, University of Florida

Dawn M. Gelino, Michelson Science Center, Caltech

Nader Haghighipour, Institute for Astronomy, University of Hawaii

Scott Horner, Lockheed Martin

Stephen Kane, Michelson Science Center, Caltech

David Latham, Harvard-Smithsonian Center for Astrophysics

Gregory Laughlin, UCO/Lick Observatory

James Lloyd, Cornell University

Christophe Lovis, Geneva University

Geoff Marcy, University of California, Berkeley

Michel Mayor, Geneva University

Chris McCarthy, San Francisco State University

Francesco Pepe, Geneva University

Didier Queloz, Geneva University

Jean Schneider, CNRS-Paris Observatory

Guillermo Torres, Harvard-Smithsonian Center for Astrophysics

Stephane Udry, Geneva University

Steven Vogt, UCO/Lick Observatory

Kaspar von Braun, Michelson Science Center, Caltech

7.6 References

Butler, R. P., Marcy, G. W., Williams, E. *et al.* 1996, *Attaining Doppler Precision of 3 m/s*, PASP, 108, 500

Bouchy, F., Pont, F., Melo, C. *et al*. 2005, *Doppler follow-up of OGLE transiting companions in the Galactic bulge*, A&A, 431, 1105

Campbell, B. & Walker, G. A. H. 1979, *Precision Radial Velocities with an Absorption Cell*, PASP, 91, 540

Charbonneau, D. 2004, Bok Prize Lecture (shared), *The Brown Dwarf Radial Velocity Survey*, CfA Colloquium Lecture Series Talk

Cumming, A., Butler, R. P., Marcy, G. W. *et al*. 2008, *The Keck Planet Search: Detectability and the Minimum Mass and Orbital Period Distribution of Extrasolar Planets,* PASP, 120, 531

Deming, D., A'Hearn, M. F., Charbonneau, D. *et al*. 2007, *The EPOXI/EPOCh Investigation of Transiting Extrasolar Planets*, American Astronomical Society, DPS Meeting #39, #22.02

Deming, D., Brown, T., Charbonneau, D. *et al.* 2005, *A New Search for Carbon Monoxide Absorption in the Transmission Spectrum of the Extrasolar Planet HD 209458b*, ApJ., 622, 1149

Edelstein, J., Erskine, D. J., Lloyd, J. *et al.* 2006, *The TEDI Instrument for Near-IR Radial Velocity Studies*, SPIE, 6269, p. 46

Erskine, D.J., & Ge, J. 2000, in Proc. *Imaging the Universe in Three Dimensions*, Edited by W. van Breugel and J. Bland-Hawthorn ASP Conference Series, 195, 501

Fischer, D., & Valenti, J. 2005, *The Planet-Metallicity Correlation*, ApJ, 622, 1102

DRAFT

Frink, S., Quirrenbach, A., & Fischer, D. A. *et al*. 2001, *A Strategy for Identifying the Grid Stars for the Space Interferometry Mission*, PASP, 113, 173

Ge, J. 2002, *Fixed Delay Interferometry for Doppler Extrasolar Planet Detection*, ApJ, 571, L165

Ge, J., Erskine, D. J., & Rushford, M. 2002, *An Externally Dispersed Interferometer for Sensitive Doppler Extrasolar Planet Searches*, PASP, 114, 1016

Ge, J., Van Eyken, J., Mahadevan, S. *et al.* 2006, *The First Extrasolar Planet Disovered with a New-Generation High-Throughput Doppler Instrument*, ApJ, 648, 683

Gillon, M., Pont, F., Demory, B.-O. *et al*. 2007, *Detection of transits of the nearby hot Neptune GJ 436b*, A&A, 472, L13

Guelachvili, G. & Rao, K.N. 1993, *Handbook of Infrared Standards – II* (Harcourt Brace & Company, Boston)

Hall, D. N., Ridgway, S., Bell, E. A. *et al.* 1979, *A 1.4 meter Fourier Transform Spectrometer for Astronomical Observation,* SPIE 172, p. 121

Heyer, I., Hall, D. N. B., & Hinkle, K. 1988, *Search for Dark Companions of K and M Giants. Preliminary Results for α Boo*, Vistas in Astronomy, Vol. 31, p. 317

Kasting, J. F., Witmire, D. P., & Reynolds, R. T. 1993, *Habitable Zones around Main Sequence Stars,* Icarus, 101, 108

Lebzelter, T., Wood, P., Hinkle, K. H. *et al.* 2005, *Long period variables in the globular cluster 47 Tuc: Radial velocity variations*, A&A, 432, 207

Li, Ch-H., Benedick, A. J., Fendel, P. *et al*. 2008, *A laser frequency comb that enables radial velocity measurements with a precision of 1 cm/s*, Nature, 452, 610

Lovis, C., Mayor, M., Pepe, F. *et al*. 2006, *An extrasolar planetary system with three Neptune-mass planets,* Nature, 441, 305

Lovis, C., & Pepe, F. 2007, *A new list of thorium and argon spectral lines in the visible*, A&A, 468, 1115

MacFarlane *et al*. 1958 Phys. Rev., 111, 1245

Mandushev, G., Torres, G., Latham, D. W. *et al*. 2005, *The Challenge of Wide-Field Transit Surveys: The Case of GSC 01944-02289*, ApJ, 621, 1061

Marcy, G.W. & Butler, R.P 1992, *Precision radial velocities with an iodine cell*, PASP, 104, 270

Mayor, M., Pepe, F., Queloz, D. *et al.* 2003, *Setting New Standards with HARPS*, ESO Messenger, 114, 20

Mayor, M. & Queloz, D. 1995, A *Jupiter-Mass Companion to a Solar-Type Star*, Nature, 378, 355

McArthur, B. E., Endl, M., Cochran, W. D. *et al.* 2004, *Detection of a Neptune-Mass planet in the* ρ^1 *Cancri System Using the Hobby-Eberly Telescope*, ApJ, 614, 81

Murphy, M. T., Udem, Th., Holzwarth, R. *et al*. 2007, *High-precision wavelength calibration of astronomical spectrographs with laser frequency combs*, MNRAS, 380, 839

DRAFT

O'Donovan, F., T., Charbonneau, D., Torres, G. *et al.* 2006, *Rejecting Astrophysical False Positives from the TrES Transiting Planet Survey: The Example of GSC 03885-00829*, ApJ, 640, 1237

Pepe, F. A., & Lovis, C. 2007, *From HARPS to CODEX: Exploring the limits of Doppler measurements,* Proceedings of the Nobel Symposium 2007, in press

Pont, F., Bouchy, F., Melo, C. *et al*. 2005, *Doppler follow-up of OGLE planetary transit candidates in Carina*, A&A, 438, 1123

Pont, F., Tamuz, O., Udalski, A. *et al*. 2007, *A transiting planet among 23 new near-threshold candidates from the OGLE survey – OGLE-TR-182*, A&A, submitted (arXiv:0710.5278)

Ramsey, L. W., Barnes, J., Redman, S. L. *et al*. 2008, *A Pathfinder Instrument for Precision Radial Velocities in the Near-Infrared*, in press (arXiv:0806.3749)

Santos, N. C., Israelian, G., & Mayor, M. 2004, *Spectroscopic [Fe/H] for 98 extra-solar planet-host stars. Exploring the probability of planet formation*, A&A, 415, 1153

Santos, N. C., Mayor, M., Naef, D. *et al.* 2000, *The CORALIE survey for Southern extra-solar planets. IV. Intrinsic stellar limitations to planet searches with radial-velocity techniques,* A&A, 361, 265

Smith, V., Tsuji, T., Hinkle, K. H. *et al*. 2003, *High-Resolution Infrared Spectroscopy of the Brown Dwarf ε Indi Ba*, ApJ**,** 599, L107.

Torres, G., Winn, J. N., & Holman, M. J. 2008, *Improved parameters for extrasolar transiting planets*, ApJ, 677, 1324

Udry, S., Bonfils, X., Delfosse, X. *et al*. 2007, *The HARPS search for southern extra-solar planets. XI. Super-Earths (5 and 8 $M_{\oplus}$) in a 3-planet system*, A&A, 469, L43

Vander Auwera, J. *et al.* 2002, Mol. Phys., 100, 3563.

Vogt, S. S., Allen, S. L., Bigelow, B. C. *et al*. 1994, *HIRES: the high-resolution echelle spectrometer on the Keck 10-m telescope*, SPIE, 2198, p. 362

Walker, G.A.H., *et al*. 2003. Proceedings of the Conference on "Towards Other Planets: DARWIN/TPF and The Search for Extrasolar Terrestrial Planets", 22–25 April 2003, Heidelberg, Germany, eds. M. Friedlund and T. Henning, ESA SP-539, Noordwijk, Netherlands, p. 647

Wizinowich, P., Armandroff, T., Marcy, G., *et al.* 2007, *W. M. Keck Observatory's Role in ExoPlanet Research,* (priv. comm.), submitted as a White Paper to the Exoplanet Task Force, March 22, 2007

Wright, J. T. 2005, *Radial Velocity Jitter in Stars from the California and Carnegie Planet Search at Keck Observatory*, PASP, 117, 657

DRAFT

8 Transits

Chair: Drake Deming (Goddard Space Flight Center)

LOC: Mark Swain (JPL)

8.1 Introduction

Transits provide enormous astrophysical leverage to reveal the physical nature of extrasolar planets. The transit itself, supplemented by high precision radial velocity observations, gives us the *mass* and *radius* of the planet. This in turn constrains the planet's bulk composition. Absorption of starlight passing through the planet's atmosphere during transit (Figure 8-1) tells us the composition and scale height of the exoplanet atmosphere e.g., (Charbonneau et al. 2002, Swain et al. 2008b). Modulation of the combined light of the system during secondary eclipse provides a direct detection of the planet's emergent spectrum (Figure 1, and Charbonneau et al. 2005, Deming et al. 2005, 2006, Grillmair et al. 2007, Richardson et al. 2007, Swain et al. 2008a). Since the planet's emergent radiation peaks in the infrared (IR) spectral region, secondary eclipse measurements have been primarily focused on the IR.

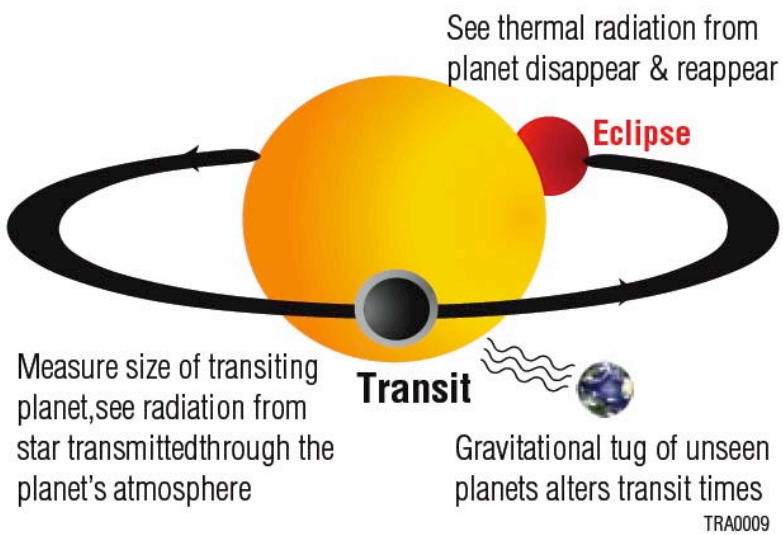

Figure 8-1. Transit geometry provides the astrophysical leverage that allows direct detection and in-depth characterization of close-in extrasolar planets.

Figure 8-2 shows one aspect of recent scientific results from transit measurements, namely the empirical mass-radius relation for exoplanets down to the size of Neptune (GJ 436b, Gillon et al. 2007, Deming et al. 2007). As noted on Figure 1, the nature and origin of giant planets with radii too large for their mass is currently a major open question in exoplanetary science.

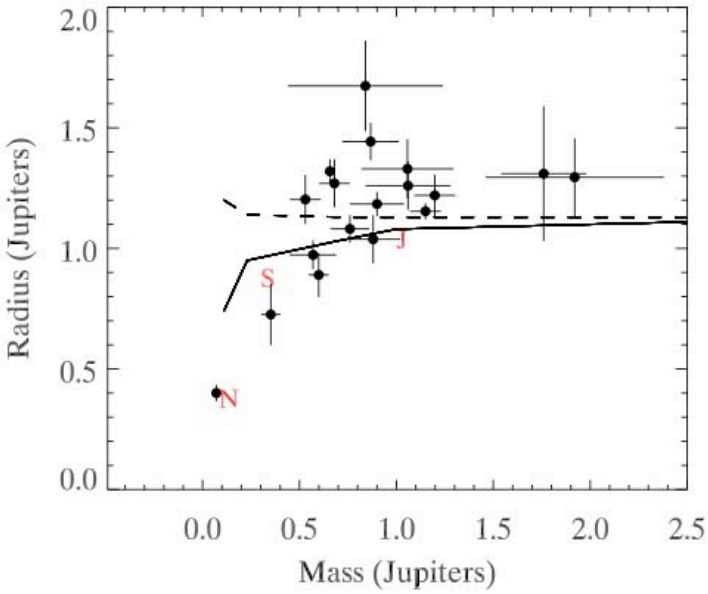

Figure 8-2. Mass-radius relation for transiting exoplanets to date. The solid and dashed lines are theoretical relations from Bodenheimer et al. (2003), for planets with (solid line), and without (dashed line) a heavy element core. Note that several giant planets have radii that exceed even the coreless models by substantially more than the observational errors.

The different geometries of transit and secondary eclipse allow localization of atmospheric knowledge: transit spectroscopy probes the atmospheric interface between the day and night hemispheres of a tidally locked planet (Swain et al. 2008b), whereas secondary eclipse measurements probe the emergent spectrum of the dayside. Moreover, measurements of transiting systems have been extended well beyond the times of transit and eclipse, to include observations in the combined light of star and planet at a large range of orbital phases. In instances where the planet's rotation is tidally locked to its orbit, these measurements can be inverted to yield the distribution of emergent intensity versus longitude on the planet (Knutson et al. 2007).

The observational techniques used for transiting systems can also be extended to non-transiting systems, so it is valuable to consider a generalization of the transit technique, namely exoplanet characterization in combined light. Without a transit, the planet radius cannot be measured directly, and that is a significant limitation. Nevertheless, much can be learned, for example from observing fluctuations in IR intensity that are phased to the planet's known radial velocity orbit (e.g., Harrington et al. 2006).

8.1.1 Science Enabled by Transits

The science enabled by transit measurements can be concisely summarized in Table 1. The quantity of results obtained by the transit technique is large, and growing rapidly (and will soon make this Chapter obsolete!) **Virtually everything we know about the physical nature of exoplanets has come from a combination of radial velocity and transit measurements.**

Table 1. Science enabled by transits.

Orbital Phase	*Science Enabled*
Transit (primary eclipse)	Radius measurement Mass measurements (when combined with radial velocity) Bulk composition inferred from mass & radius Atmospheric absorption spectroscopy Detection of unseen planets via timing variations Measurement of the relative inclination of stellar spin angular momentum versus planetary orbital angular momentum, via the Rossiter-McLaughlin effect
Secondary eclipse	Measurement of the emergent spectrum of the planet Measurement of orbit eccentricity (or limits thereon) Ultra-high spatial resolution, mapping the disk of the planet (in longitude, expected to be achieved by JWST)
Other orbit phases	Longitudinal temperature maps and inferences concerning zonal winds Spectroscopy of the planet at all longitudinal aspects (in principle, but not yet achieved)

8.1.2 Measurement Requirements

The principal requirement of transit measurements is high photometric and spectrophotometric precision, on relatively bright stars. This need for precision derives from the fact that transit measurements are made in the combined light of the star plus planet. Hence the planet signal is greatly diluted by the stellar photons, and the measurement precision must be as high as possible. Moreover, the time scale of the photometric noise is crucial. Since transits are typically a few hours in duration, the precision of individual measurements should improve as the inverse square-root of the measurement time, for times exceeding several hours. Since a photometric baseline is required before and after transit, a reasonable time scale for the required stability is ~ 20 hours. Since both visible and IR measurements are important for transits (Figure 8-1), the instrumentation should be designed to reach the fundamental limits determined by the stellar photon noise (primarily important in the visible) and the background noise caused by the thermal emission of the instrument, telescope, and zodiacal dust (primarily important in the IR).

For more extended ("around-the-orbit") science, the phenomena being measured have time scales of several days, so ~ 20 day stability is needed. Since there is also scientific motivation to study much longer-term changes on exoplanets, due for example to seasonal effects for transiting planets in longer period orbits, then eventually there may be motivation to extend the stability time to ~ 20 months.

Ground-based photometry has made great strides, and is achieving sub-milli-magnitude precision in favorable cases (Hartman et al. 2005). However, for most exoplanet characterization science, space-borne observations will be necessary. The best location for a space-borne transit mission is heliocentric orbit, or placement at a Lagrangian point. Although significant transit science can be done from near-Earth orbit, those orbits have two principal limitations: 1) long uninterrupted observing times, such as are needed for exoplanet around-the-orbit observations, are generally not possible from a near-Earth location, and 2) proximity to the Earth results in time-variable scattered light and thermal radiation that can interfere with achieving the necessary precision.

1.1.3 Previous and Planned Transit Missions

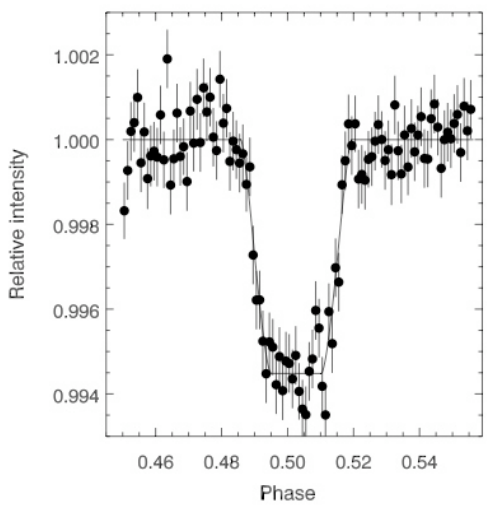

Figure 3. Example of a Spitzer exoplanet detection, the secondary eclipse of HD 189733b (Deming et al. 2006). By detecting the eclipse Spitzer is able to make a direct measurement of the IR flux from the planet.

Major advances in our knowledge of the physical nature of exoplanets have come from the Great Observatories, principally Hubble and Spitzer. HST observations yielded the first detection on an exoplanet atmosphere (Charbonneau et al. 2002), and Spitzer observations gave us "first light" for exoplanet emission (Charbonneau et al. 2005, Deming et al. 2005). Many follow-up results are summarized below in the description of a new combined light mission, and in reviews by Charbonneau et al. (2007), and Deming (2008), and one particular result is illustrated in Figure 8-3. Although the Great Observatories were not specifically designed for exoplanet observations, their general capabilities are sufficient to deeply exploit the transit geometry, and produce abundant cutting edge science.

Several NASA and ESA missions have been dedicated to exoplanet transits in large part or in total. The Kepler mission (Borucki et al. 2003) aims to determine the frequency of occurrence of Earth analogs, by monitoring ~ 100,000 solar-type stars (a field in Cygnus) for four years. The CoRoT mission is similarly monitoring numerous solar-type stars to determine the frequency of occurrence of super-Earths, and to find and characterize exoplanets ranging in size from giant planets, down to super-Earths. CoRoT has already

identified new giant transiting planets (e.g., Barge et al. 2008), and the CoRoT team is currently working to extend the detections to much smaller planets.

In addition to search missions such as CoRoT and Kepler, several missions have focused on follow-up of bright transiting systems. The MOST missions has observed transits of giant planets orbiting bright stars, and has been particularly successful at placing very stringent limits on the magnitude of reflected light from HD 209458b, a very low albedo planet. Similarly, the EPOXI mission is concentrating on the properties of giant planets transiting bright stars, and is searching these systems for additional planets down to the size of Earth (Christiansen et al. 2008, Ballard et al. 2008).

8.2 Observatory Concepts

Transit missions fall into two general categories: search and characterization. We here describe an all-sky transit search mission, and two examples of transit characterization. In the case of the characterization missions, we first describe a combined-light mission that is quite general, and can make inferences about the emergent spectra of close-in exoplanets in combined light, even for systems that do not transit. We also describe a characterization mission that extends transit spectroscopy into the ultraviolet spectral region, where the transit absorption signatures can be quite large.

An All-sky Transit Survey: The purpose of missions like Kepler is to identify exoplanets as small as Earth in size, both in order to find individual planets and to get statistical data on the population and distribution of such planets. This information can then be used to guide follow-up studies of the individual exoplanets and to assist in designing efficient finding or characterization missions based on techniques other than transit observations. Although Kepler looks for transiting exoplanets out to considerable distance, about 1000 parsecs, it has the limitation of looking towards only one direction in the galaxy, along the Orion arm in the constellations of Cygnus and Lyra. It is possible that terrestrial exoplanet statistics could be somewhat different in other regions of the galaxy, and some very interesting individual planets could be discovered by looking toward those regions.

We are most interested in finding planets relatively nearby to our solar system, because the consequent greater observed brightnesses of the star and planet permit more detailed characterization to be achieved, so an all-sky survey, albeit less deep than Kepler, is needed. Kepler observes stars typically of magnitudes 10 to 14 in a field just over 100 square degrees in size (about 1/400 of the sky). An all-sky survey merely out to magnitude 12 should find at least eight times as many planets as Kepler does, and the ones found would, on average, be four times closer than the Kepler planets. The recent inference that superEarths are common around solar-type and lower main sequence stars (Mayor et al. 2008) adds greatly to the motivation for an all-sky survey. An all-sky survey would find the closest transiting superEarth or transiting Earth analog. The Mayor et al. (2008) results imply that there will be a large number of transiting superEarth orbiting nearby solar-type stars, and the closest example is likely to be the planet that can be characterized to the highest signal-to-noise ratio.

As an example of such a potential search mission, MIT scientists, with Google's support, are designing a satellite-based observatory to provide a sensitive survey of the entire sky to search for transiting exoplanets. The Transiting Exoplanet Survey Satellite (TESS) could potentially be launched in 2012 to discover new planetary systems that are nearby and bright. TESS was recently selected by NASA for a Phase-A study under the SMEX program. TESS could rapidly discover hundreds of planets with radii similar to the Earth. The

satellite will be equipped with six high-resolution, wide-field digital cameras, now under development. The cameras--which have a total resolution of 192 megapixels--will cover the whole sky by the end of two years, observing about two million stars. Since the amount of data collected will be enormous, only selected portions will be transmitted back to Earth. But remaining data will be stored on the satellite for about three months, so astronomers could check images of an unexpected event. The Harvard-Smithsonian Center for Astrophysics and the Origins of Life Initiative, NASA Goddard and NASA Ames, and the Las Cumbres Observatory Global Telescope Network are already scientific participants with MIT on the TESS program.

A Combined-Light Characterization Mission (CLM): Dramatic measurements made with the Spitzer and Hubble space telescopes have redefined the field of exoplanet characterization (e.g., Barman 2007, Beaulieu et al. 2008, Charbonneau et al. 2002, 2005, Deming et al. 2005, 2006, 2007, Demory et al. 2007, Gillon et al. 2007, Grillmair et al. 2007, Harrington et al. 2006, 2007, Knutson et al. 2007, 2008, Richardson et al. 2007, Swain et al. 2008a,b); collectively, this work has decisively established that detailed characterization of exoplanet atmospheres is feasible. Today, due to the extraordinary and unforeseen success of the Spitzer and Hubble space telescopes, we can discuss the observational signatures of exoplanet atmospheres including weather, vertical and longitudinal temperature profiles, molecular abundances (including prebiotic molecules), dayside to night side atmospheric chemistry changes, and the role of photochemistry. Of equal significance to this scientific advance is the method by which the breakthroughs were made wherein the *combined light* star-planet system is measured. Spitzer and Hubble space telescope measurements do not spatially resolve the exoplanets; rather, information about the exoplanet is extracted from precise measurements in the "light curve" or changes in the spectrophotometric intensity arising from the planet during its orbit. Further, observations of different portions of the light curve have demonstrated the ability to **localize molecular abundances** to specific regions of the exoplanet atmosphere and explore, for example, how the differences of dayside and nightside atmospheric chemistry. The Spitzer and Hubble results demonstrate that we have, today, the flight-proven technology required to study prebiotic chemistry of organic molecules in habitable zone exoplanets and to localize this knowledge to specific regions of the atmosphere. This is a completely unexpected yet extraordinary accomplishment for the Spitzer and Hubble Space Telescopes and it will be an important part of their legacy.

Building on the extraordinary successes of Spitzer and Hubble, we advocate strongly that NASA consider a combine-light exoplanet characterization mission. This mission would focus on the detection of molecules in exoplanet atmospheres. By detecting and determining the molecular abundance of molecules, the principal goal of a combined-light mission would **determine the conditions, composition, and chemistry** of exoplanet atmospheres. A high priority for the combined-light mission is observing habitable zone planets for (1) the detection of prebiotic molecules and (2) characterization of the nature of photochemical and thermochemical contributions to atmospheric carbon chemistry. Given an appropriate target, such as an exoplanet in a 15 to 25 day orbit around a nearby M star, a combined-light mission could determine a detailed picture of the atmospheric chemistry of a planet where life could exist. A combined-light mission could also characterize the surfaces of rocky planets.

Determining the conditions, composition, and chemistry of exoplanet atmospheres would be accomplished by interpreting the observed spectra using retrieval methods (Tinetti et al. 2007) to extract molecular abundances and the pressure-temperature profiles; this

knowledge would be localized by repeating the retrieval for different portions of the planet's orbit. Examples of important target molecules are H_2O, CH_4, CO, CO_2, and NH_3; all these species have strong absorption bands in the 2–5-μm wavelength range. Each of these molecules probes the atmospheres in different ways. CO and CH_4 are primary reservoirs of carbon; the CO/CH_4 ratio is sensitive to temperature. CO_2 probes the vertical temperature profile and the vertical mixing ratio (potentially a diagnostic of photochemistry) using the v=13–15 bands. CO_2 also serves as a proxy for CO, while CO and CH_4 abundances differing from thermochemical equilibrium might indicate photochemistry. For tidally locked, hot-Jovian planets, the chemistry of the atmosphere is expected to change, particularly the $[CO]/[CH_4]$ ratio, as a function of orbital phase and, in some cases, a dayside hot stratosphere might form (Burrows et al. 2007, Fortney et al. 2008, Knutson et al. 2007); the $[CO]/[CH_4]$ ratio at the terminator is also a potential diagnostic of variability, possibly associated with large scale eddies generated by zonal winds. Although atmospheric heating will be characterized by Spitzer photometry, spectroscopy is required to probe how the atmosphere chemistry changes from the dayside to the night side. The targets accessible to a combined-light mission cover a range of exoplanet sizes, temperatures, and stellar spectral types and will reveal the influences of the stellar primary on the exoplanet atmosphere. Thus, a combined-light mission would enable us to understand the effect of radiation forcing from the stellar primary on photochemistry and stratosphere formation.

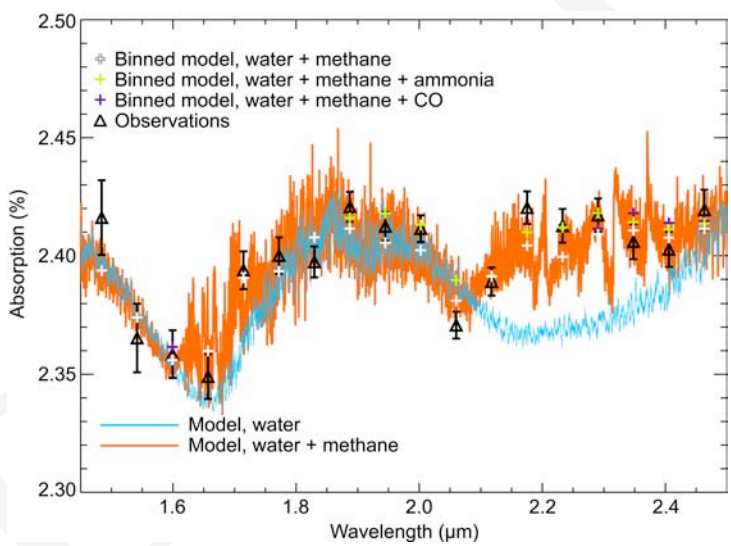

Figure 8-4. A comparison of observations (black triangles) with a model of water (blue) and water + methane in an absorption spectrum of the planet HD 189733b (Swain et al. 2008b). These data constitute the first detection of an organic molecule in an exoplanet atmosphere and were obtained with the Hubble Space Telescope using the NICMOS instrument. A combined-light exoplanet characterization mission could deliver data of similar quality for the many exoplanets and would extend the spectral coverage into the thermal infrared.

Architecture

The architecture of a Combined-Light Mission can be very conventional. CLM is envisioned as a 1.2- to 1.4-m telescope in an Earth-trailing or L2 orbit. This type of orbit is probably essential for achieving instrument stability. The telescope would be passively cooled, and mechanical coolers would be used to cool the focal plane. The baseline mission length would be 5 years, but with no stored cryogens, an extended mission is possible. The science instrument would be a spectrometer with selectable dispersion. The baseline wavelength range is 2-15 μm although missions with reduced mid-IR coverage are still valuable. The 2–15 μm wavelength range would be split between two focal-plane arrays (FPA), one for 2-5 μm and one for 5-15 μm. Each FPA would have dispersive optics matched for that band. The dispersion is selected such that the FPA is photon noise limited in every pixel for solar-type stars up to some distance (~100 pc). In this regime, the spectrum can be averaged to the desired spectral resolution to achieve greater SNR. This configuration also has the advantage that there are no moving components required to change spectral resolution. Thus, the instrument could be designed to only have one observing mode (full spectral resolution). This increases the instrument stability and simplifies the calibration process. Calibration of CLM would be accomplished by monitoring of a calibrator network throughout the mission life and, possibly, by relying on an on-board calibration source. The data rate is low. The CLM would probably incorporate a fast-steering mirror in the science instrument for fine guidance and for precision placement of the science and calibration targets. The fast-steering mirror control would use visible light imaging with a CCD. At the shortest wavelengths and the lowest spectral resolutions, the CLM has the potential to achieve a measurement dynamic range of ~10^5. Photometry with a dynamic range of ~5000:1 at 2 μm is possible for a 12th magnitude G star, making the photometric study of exoplanets in the Kepler field an important part of the CLS mission.

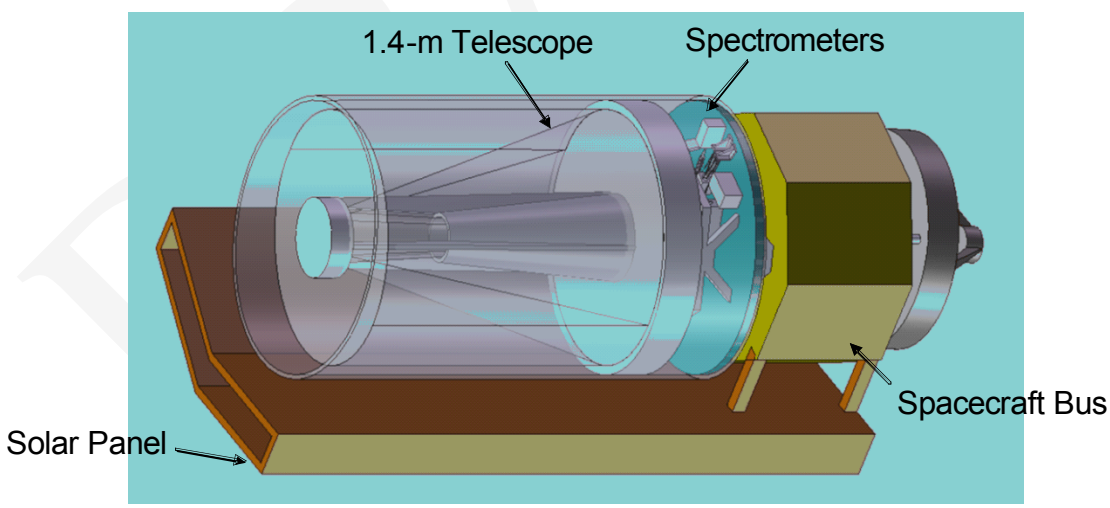

Figure 8-5. The combined-light mission concept is an intuitively straightforward, low-risk design. A 1.4 m-diameter passively cooled telescope provides light collection for two actively cooled spectrometers, one covering 2-5 μm (SWIR) and the other 5-12 μm (MWIR). Readily available spacecraft cores possess the power, bus-level pointing and other capabilities required by a combined-light mission. A Spitzer-like solar panel/thermal shield combination makes efficient use of mass and volume resources.

Performance

The performance of all transit missions, and the CLM in particular, should be specifically designed to approach the fundamental limits imposed by stellar photon noise and intrinsic stellar variability noise. On the time scales of transits, the stellar variability will be dominated by the photon noise. Spitzer, for example, routinely achieves ~ 70- to 80-percent of the photon noise limit for transit and eclipse photometry (e.g., Harrington et al. 2007, Deming et al. 2007), so designing the mission to specifically achieve this goal will give even greater consistency of performance.

Aside from the performance of the mission *per se*, it is instructive to consider how a given level of performance (in terms of signal-to-noise for a given brightness) can be used optimally by insightful choice among different transiting systems. Since the light emergent from a transiting exoplanet is measured using a secondary eclipse technique, consider how the amplitude of the eclipse scales with different planet-star combinations. In the Rayleigh-Jeans (long wavelength) limit, the depth of a secondary eclipse, in units of the stellar flux, is given as $A_\lambda = (R_p/R_s)^2\ (T_p/T_s)$, where R is radius and T is brightness temperature, and the planet and star are indexed by p and s, respectively. In thermal equilibrium the brightness temperature of the planet is related to the stellar temperature as $T_p = \alpha\ T_s\ \theta^{1/2}$, where α is a constant that contains the planet's albedo, circulation properties, etc., and θ is the angular diameter of the star as seen from the planet. As we proceed down the main sequence, the smaller sizes of the stars causes the $(R_p/R_s)^2$ to dominate over $\theta^{1/2}$. So planets orbiting small stars will have more prominent eclipses, and this is one basis for much of the recent interest in super-Earths orbiting M-dwarfs. The CLM and other transit missions would have a large focus on M-dwarf planets for this reason.

An Ultraviolet Transit Mission: Transiting exoplanets have all been discovered at optical wavelengths and the majority of characterization studies have been performed at optical and infrared wavelengths. Optical and infrared wavelengths yield information about the atmospheric albedo (e.g., Rowe et al. 2006), atomic abundances (e.g., Redfield et al. 2007), molecular abundances (e.g., Tinetti et al. 2008) and thermal radiation of the planet (e.g., Knutson et al. 2007), and shorter wavelengths can yield information about haze, atomic species, and condensed particles in the atmosphere and the interaction of the planet with the stars.

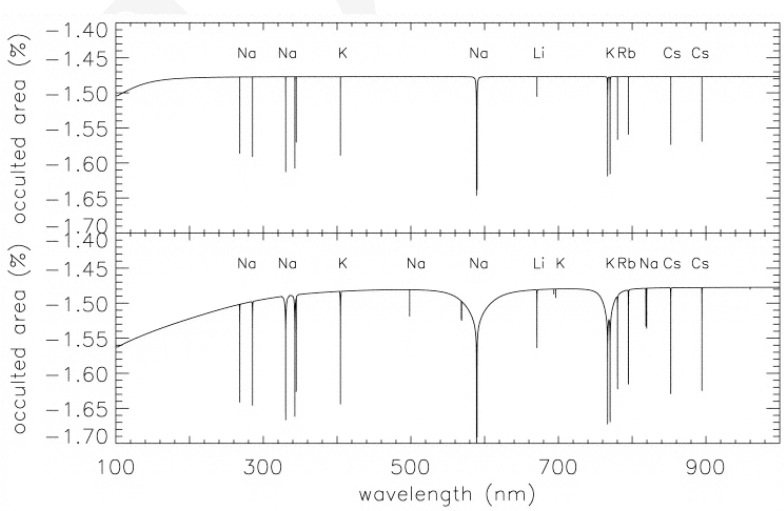

Figure 6. Model for the normalized in-transit minus out-of-transit spectra displaying some of the prominent atomic species in the UV and visible. Adopted from Seager & Sasselov (2000).

The first detection of an atomic species was made by observing the Na II doublet in absorption against the stellar host HD 209458 (Charbonneau et al. 2002). However, at ultraviolet wavelengths, absorption line studies of other species can provide information about the atomic and ionic species content of the planetary atmosphere. Various atomic species are visible in the stellar spectra including Na, K, and Li (Figure 8-6) and can probe different layers and physical conditions of the planetary atmosphere (Seager & Sasselov 2000).

For giant planets in short orbital periods (i.e., the hot Jupiters), the observed atmosphere transitions from being dominated by the planetary thermal emission to being dominated by reflected emission from the star (Figure 7). By studying the emission at shorter wavelengths, where reflectance dominates the exoplanetary emission, studies of the planetary haze and cloud content can be performed. The scattering and polarization signatures become less diluted by thermal emission as the observation wavelengths grow shorter.

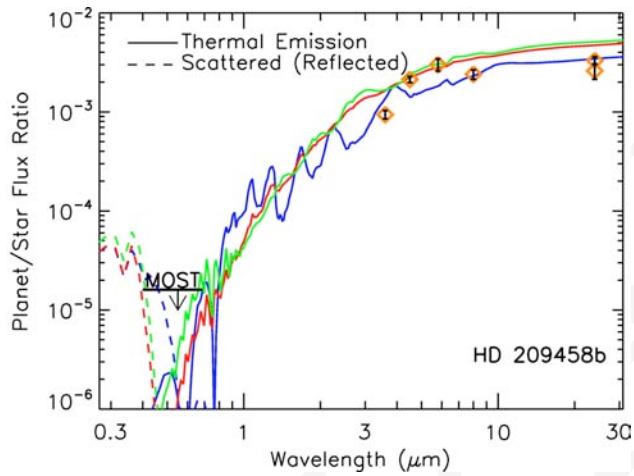

Figure 8-7. Predicted spectrum for HD209458b from 0.3 – 30 μm, along with observational data from Spitzer and MOST. Solid lines are thermal emission while dashed lines are reflected stellar flux. The colored lines represent models with differing opacity sources. Adopted from Figure 12 in Fortney et al. 2008.

High precision polarization studies can yield detailed information about the cloud particulate content, sizes, and cloud layer distributions (e.g., Seager, Whitney, & Sasselov 2000; Hough et al. 2006). For example, below 0.2 μm, Rayleigh scattering from H_2 is important. In general, photometric and polarization light curves are a function of the atmospheric opacity and the observational viewing angle and can, in principle, yield details about the day/night variations of the cloud layers and particulates (e.g., Seager, Whitney, & Sasselov 2000). The first polarization detection of a planetary atmosphere was recently claimed by Berdyugina et al. (2008) where they concluded that HD 189733b at (~0.4 μm) may have a radius that is 30% larger than the optically opaque planetary disk, indicating that scattering material may fill the Roche lobe, possibly escaping from the planetary atmosphere.

Absorption line studies of Lyman-α suggest that HD 209458b contains a large exo-sphere of hydrogen (Figure 8-8). Interpretations of this phenomenon include evaporation of the planetary atmosphere, where the particles are accelerated by radiation pressure (Vidal-Madjar et al. 2008). Other interpretations require an interaction with the stellar wind to achieve the observed velocities (Holmstrom et al. 2007). In either case, it seems clear that the planet and the star may be interacting, and UV spectroscopy has enabled the discovery (and a better understanding) of the process.

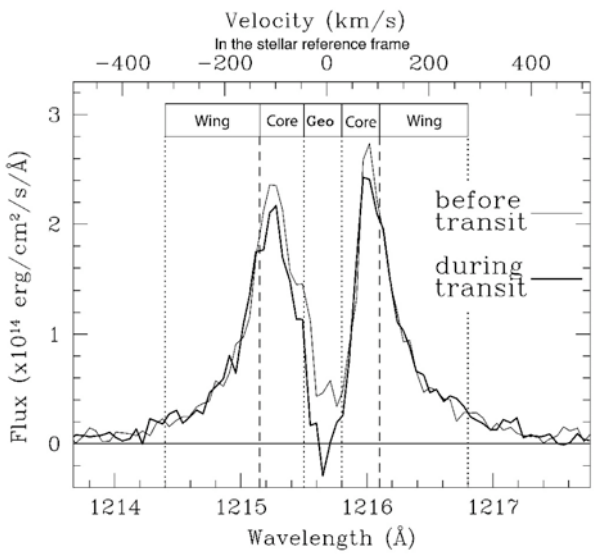

Figure 8-8. Observed HD 209458 Ly-α profiles in and out of transit, as observed by Vidal-Madjar et al. 2003 - suggesting that hydrogen is evaporating from the planetary atmosphere. Adopted from Vidal-Madjar et al. 2008.

The interaction between the planet and the star may have important consequences for the both the stellar host and the exoplanet. Recent observations of Tau Boo with MOST suggest that stellar surface activity may be correlated with the planetary orbit, indicating that the planet may be inducing stellar activity on the surface of the star (Matthews, private communication). Further, Penz et al. (2008) suggests high energy stellar flux (X-ray and UV) may be strong enough evaporate the planets at a rate large enough for the giant planets to turn evolve into hot Neptunes (Penz et al. 2008). Detailed studies of the exoplanetary exosphere at the short wavelengths may be crucial to our understanding of how planets interact with their stars and evolve on geological timescales.

8.3 Technology

The combined-light characterization mission is the most technologically demanding of the three mission concepts described above. Nonetheless, it does not require daunting technology development to deliver high-impact exoplanet characterization science; in this way, it is strongly differentiated from exoplanet characterization missions using other techniques such as high-contrast imaging. Over periods of several hours, combined-light spectroscopy measurements have been demonstrated with a dynamic range of 40,000:1 in the visible (Pont et al. 2007) and 20,000:1 in the near-IR (Swain et al. 2008b), while mid-IR broad-band photometry has demonstrated ~30,000:1 dynamic range (Knutson et al. 2007). The near-IR and mid-IR measurements are achieving performance that is approaching the photon noise limit. Moreover, this level of performance has been achieved by missions that have not been specifically designed for stability on bright stars. Rather, these missions (e.g., HST and Spitzer) were designed to optimize the sensitivity for faint sources. Thus, meeting the 100,000:1 dynamic range goal for a combined-light exoplanet characterization mission - that would be specifically designed for that application - seems quite feasible using careful application of existing technology. However, there are a few simple technology improvement tasks that would result in better instrument performance.

The primary requirement common to all transit missions is a stable observatory/instrument configuration (no moving spectral dispersion elements). Determining the stability of the spectral response function (as set by variable thermal conditions) in low Earth orbit vs. orbits with better thermal stability (Earth trailing or L2)

could have an important impact on mission design. The design of such a mission should also pay particular attention to:

- FPA characterization for modeling effects such as long-term responsivity changes, charge-trapping, and effects such as intra-pixel variations in detector quantum efficiency and charge transfer efficiency.
- Incorporation of a fine steering mirror (FSM) in the instrument for precise placement of the target star in the spectrometer entrance slit. Since the target stars are relatively bright, the FSM error signal could be generated by a visible light CCD.
- A high-stability, on-board, calibration source. Although not essential, the availability of on-board calibration could relax the requirements on a calibrator star network and improve observing efficiency.

Past Accomplishments

Two current transit missions have specifically developed technology that will likely be very beneficial to future transit missions. For transit measurements, mathematical techniques to perform high precision data analysis (e.g., decorrelation techniques), and techniques to execute observations in an optimal manner, carry an importance on a par with, or exceeding, the development of new hardware. The Kepler mission has pioneered measurement techniques to obtain very high precision CCD photometry. These techniques include differential spatial and temporal photometry, and decorrelation methods to compensate for the effects of image motion. Kepler implemented a photometry test bed (Koch et al. 2000) and demonstrated a photometric precision of 10^{-5} for CCD photometry in the laboratory prior to designing and building their flight hardware.

The MOST mission (Matthews et al. 1999) has also used specific measurement techniques to obtain very high photometric precision. These techniques include imaging of the pupil at the focal plane to reduce the sensitivity of the photometric signal to spacecraft pointing jitter. Advanced transit spectroscopy missions such as the CLM (described above) will benefit from similar pupil imaging, but in a dispersed mode for spectroscopy.

Future Technology Development: Milestones?

The success of HST and Spitzer for transit science shows in the first place that current technology and careful attention to mission and instrument design go a long way toward achieving excellent transit science. The success of MOST, and the (so far) successful development of Kepler, further suggest that innovative optical design and detector test-bed development are appropriate vehicles for achieving transit mission science goals. This type of mission-specific technology development is the best model for transit and combined-light mission science, as opposed to a program having technology-development milestones that might be more broadly applicable. This would, in our opinion, remain true for transit mission development up to the "Probe Class" , which is in fact not far removed in fiscal terms from the development of Kepler.

8.4 Research and Analysis Goals

To extract maximum science from transit studies, it will be necessary to implement a vigorous Research and Analysis program to:

- Support the Spitzer warm mission and extensive Hubble exoplanet observations, thereby extending the current progress in exoplanet characterization, and thus refine the science case for a combined-light exoplanet characterization mission. Examples of direct scientific support for these missions include ground-based telescopic detections of secondary eclipses (e.g., at 2 microns), and ground-based transmission spectroscopy (e.g., Redfield et al. 2007).
- Support ongoing transit and radial velocity surveys that find giant transiting planets from the ground, and support extensions of these surveys to lower main sequence stars such as M-dwarfs (Nutzman and Charbonneau 2008).
- Support precursor projects (such as a balloon-borne instrument) that would demonstrate important aspects of the technology and science case for a combined-light exoplanet characterization mission.
- Support the modest technology development efforts (FPA characterization and fine steering mirror technology) which are beneficial for a combined-light exoplanet characterization mission.
- Support a detailed study of the complementary roles of JWST and a dedicated, combined-light exoplanet characterization mission.

8.5 Contributors

Drake Deming, NASA's Goddard Space Flight Center

Mark Swain, Jet Propulsion Laboratory

Charles Beichman, Jet Propulsion Laboratory

Joseph Harrington, University of Central Florida

Steve Kilston, Ball Aerospace Corporation

David Ciardi, Michelson Science Center, Caltech

8.6 References

Ballard, S., Charbonneau, D., A'Hearn, M., et al., 2008 "Preliminary Results on HAT-P-4, TrES-3, XO-2, and GJ436 from the NASA EPOXI Mission," proceedings of IAU Symposium 253, in press, astro-ph/0807.2803"

Barge, P., Baglin, A., Auvergne, M., et al. 2008, "Transiting Exoplanets from the CoRoT Space Mission, I. CoRoT-Exo-1b: a low-density, short period planet around a G0V star."

Barman, T., 2007, "Identification of Absorption Features in an Extrasolar Planet Atmosphere", ApJ **661**, L191-L194.

Beaulieu, J. P., Carey, S., Ribas, I., & Tinetti, G., 2008, "Primary Transit of the Planet HD 189733b at 3.6 and 5.8 Microns", ApJ **677**, 1343-1347.

Berdyugina, S. V., Berdyugin, A. V., Fluri, D. M., & Piirola, V. 2008, "First Detection of Polarized Scattered Light from an Exoplanet Atmosphere", ApJ **673**, L83-L86.

Bodenheimer, P., Laughlin, G., & Lin, D., 2003, "On the Radii of Extrasolar Giant Planets", ApJ **592**, 555-563.

Borucki, W. J. & 14 co-authors 2003, "The Kepler Mission", ASP Conf. Ser. **294**, 427.

Burrows, A., Hubeny, I., Budaj, J., Knutson, H. A., and Charbonneau, D., 2007, "Theoretical Spectral Models of the Planet HD 209458b with a Thermal Inversion and Water Emission Bands" ApJ **668**, L171-L174.

Charbonneau, D., Brown, T. M., Noyes, R. W., & Gilliland, R. L. 2002, "Detection of an Extrasolar Planet Atmosphere", ApJ **568**, 377-384.

Charbonneau, D., Allen, L. E., Megeath, S. T., et al. 2005, "Detection of Thermal Emission from an Extrasolar Planet", ApJ **568**, 377-384.

Charbonneau, D., Brown, T. M., Burrows, A., & Laughlin, G. 2007, "When Extrasolar Planets Transit Their Parent Stars," in Protostars and Planets V, Univ. Arizona Press.

Christiansen, S., Charbonneau, D., A'Hearn, M., et al., 2008, "The NASA EPOXI Mission of Opportunity to Gather UltraPrecise Photometry of Known Transiting Exoplanets," proceedings of IAU Symposium 253, in press, astro-ph/0807.2852

Cowan, N., Agol, E., and Charbonneau, D. 2007, "Hot Nights on Extrasolar Planets: Mid-infrared Phase Variations of Hot Jupiters", MNRAS **379**, 641-646.

Deming, D. 2008, "Emergent Exoplanet Flux: Review of the Spitzer Results," Proceeding of IAU Symposium 253, in press.

Deming, D., Seager, S., Richardson, L. J., and Harrington, J. 2005, "Infrared Radiation from an Extrasolar Planet," Nature **434**, 740-743.

Deming, D., Harrington, J., Seager, S., and Richardson, L. J. 2006, "Strong Infrared Emission from the Extrasolar Planet HD 189733b." ApJ **644**, 560-564.

Deming, D., Harrington, J., Laughlin, G., et al. 2007, "Transit and Secondary Eclipse Photometry of GJ436b," ApJ **667**, L199-L202.

Demory, B.-O., Gillon, M., Barman, T., et al. 2007, "Characterization of the Hot Neptune GJ 436b with Spitzer and Ground-based Observations," A&A **475**, 1125-1129.

Ehrenreich, D., Hebrard, G., des Estangs, L., et al. 2007, "A Spitzer Search for Water in the Transiting Exoplanet HD 189733b," ApJ **668**, L179-L182.

Fortney, J. J., Lodders, K., Marley, M. S. & Freedman, R. S. 2008, " A Unified Theory for the Atmospheres of the Hot and Very Hot Jupiters: Two Classes of Irradiated Atmospheres", ApJ **678**, 1419-1435.

Gillon, M., Demory, B. O., Barman, T., et al. 2007, "Accurate Spitzer Infrared Radius Measurement for the Hot Neptune GJ 436b," A&A **471**, L51-L54.

Grillmair, C. J., Charbonneau, D., Burrows, A., et al. 2007, "A Spitzer Spectrum of the Exoplanet HD 189733b," ApJ **658**, L115-L118.

Harrington, J., Hansen, B. M., Luszcz, S., et al., 2006, "The Phase-Dependent Infrared Brightness of the Extrasolar Planet Upsilon Andromedae b," Science, **314**, 623.

Harrington, J., Luszcz, S., Seager, S., et al. 2007, "The Hottest Planet", Nature **447**, 691-693.

DRAFT

Hartman, J. D., Stanek, K. Z., Gaudi, B. S., et al. 2005, "Pushing the Limits of Ground- based Photometric Precision: Sub-milli-magnitude Time-Series Photometry of the Open Cluster NGC 6791", AJ, **130**, 2241-2251.

Holmstrom, M., Ekenback, A., Selsis, F., 2007, "Energetic Neutral Atoms Around the Extrasolar Planet HD 209458b", AGU Fall Meeting, #SH12A-0857.

Knutson, H. A., Charbonneau, D., Allen, L. E., et al. 2007, " A Map of the Day-Night Contrast of the Extrasolar Planet HD 189733b," Nature **447**, 183-186.

Knutson, H. A., Charbonneau, D., Allen, L. E., et al. 2008, "The 3.6-8.0 Broadband Emission Spectrum of HD209458b: Evidence for an Atmospheric Temperature Inversion", ApJ **673**, 526.

Koch, D. G., Borucki, W. J., Dunham, E. W., et al. 2000, "CCD Photometry Tests for a Mission to Detect Earth-sized Planets in the Extended Solar Neighborhood", SPIE **4013**, 508.

Matthews, J., Kuschnig, R., Walker, G., et al. 1999, "The MOST Space Mission: a 15-cm Telescope in the 8-m Class Era", J. Astron. Soc. Can., **93**, 183.

Mayor, M., Udry, S., Lovis, C., et al. 2008, "The HARPS Search for Southern Extrasolar Planets. XIII. A Planetary System with Three SuperEarths," A&A, in press, astro-ph/0806.4587.

Nutzman, P., & Charbonneau, D. 2008, "Design Considerations for a Ground-Based Transit Search for Habitable Planets Orbiting M-Dwarfs", PASP, in press, astro-ph/0709.2879.

Penz, T., Erkaev, N. V., Kulikov, Yu. N., et al., 2008, "Mass Loss from Hot Jupiters - Implications for CoRoT Discoveries, II. Long Time Thermal Atmospheric Evaporation Modeling," Plan. Space Sci. **56**, 1260.

Pont, F., Gilliland, R. L., Moutou, C., et al. 2007, "Hubble Space Telescope Time-Series Photometry of the Planetary Transit of HD 189733: No Moon, no Rings, Starspots", A&A **476**, 1347-1355.

Redfield, S., Endl, M., Cochran, W. D., et al. 2007, "Sodium Absorption from the Exoplanetary Atmosphere of HD189733b Detected in the Optical Transmission Spectrum", ApJ (Letters), in press. astro-ph/0712.0761.

Richardson, L. J., Deming, D., Horning, K., Seager, S., & Harrington, J., 2007, "A Spectrum of an Extrasolar Planet" Nature, **445**, 892-895.

Rowe, J. F., Matthews, J. M., Seager, S., et al. 2006, " An Upper Limit on the Albedo of HD 209458b: Direct Imaging Photometry with the MOST Satellite," ApJ **646**, 1241-1251.

Seager, S., & Sasselov, D. D. 2000, "Theoretical Transmission Spectra during Extrasolar Giant Planet Transits," ApJ, **537**, 916-921.

Seager, S., Whitney, B. A., & Sasselov, D. D. 2000, "Photometric Light Curves and Polarization of Close-in Extrasolar Giant Planets", ApJ **540**, 504-520.

Swain, M. R., Bouwman, J., Akeson, R. L. et al., 2008a, "The Mid-Infrared Spectrum of the Transiting Exoplanet HD 209458b", ApJ **674**, 482-497.

Swain, M. R., Vasisht, G., & Tinetti, G., 2008b "The Presence of Methane in the Atmosphere of an Extrasolar Planet," Nature **452**, 329-331.

Tinetti, G., Vidal-Madjar, A., Liang, M.-C., et al. 2007, "Water Vapor in the Atmosphere of a Transiting Extrasolar Planet", Nature **448**, 169-171.

DRAFT

Vidal-Madjar, A., Lecavelier des Etangs, A., Desert, J. M., et al. 2003, "An Extended Upper Atmosphere Around the Extrasolar Planet HD209458b," Nature **422**, 143-146.

Vidal-Madjar, A., Lecavelier des Etangs, A., Desert, J. M., et al. 2008, "Exoplanet HD 209458b (Osiris): Evaporation Strengthened," ApJ **676**, L57-L60.

DRAFT

9 Magnetospheric Emission

Chair: J. Lazio (Naval Research Laboratory)

LOC: D. Winterhalter (Jet Propulsion Laboratory)

9.1 Introduction

All of the solar system giant planets and the Earth produce radio wavelength emissions as a result of an interaction between their magnetic fields and the solar wind. In the case of the Earth, its magnetic field may contribute to its habitability by protecting its atmosphere from solar wind erosion and by preventing energetic particles from reaching its surface. Indirect evidence for at least some extrasolar giant planets also having magnetic fields includes the modulation of calcium emission lines of their host stars phased with the planetary orbits likely due to magnetic reconnection events between the stellar and planetary fields. If magnetic fields are a generic property of giant planets, then extrasolar giant planets should emit at radio wavelengths allowing for their *direct* detection. In the case of terrestrial-mass planets, if magnetized, they should also emit at radio wavelengths, and detecting this radiation may be a means of assessing their habitability. Existing radio wavelength observations place limits comparable to the flux densities expected from the strongest emissions. Future radio wavelength facilities, currently under design & development or construction, will offer more than one order of magnitude improvement.

9.1.1 Science Goals

Search for and exploit extrasolar planetary magnetospheric emissions as a means of directly detecting and characterizing those planets.

Planetary Magnetospheric Emission

The Earth and gas giants of our solar system are described commonly as "magnetic planets" because they contain internal dynamo currents that generate planetary-scale magnetic fields. These magnetic fields are immersed in the solar wind, a high speed magnetized plasma. The solar wind deforms a planetary magnetic field, compressing the field on the front side and elongating it on the back, forming a "tear-dropped"–shaped magnetosphere aligned with the solar wind flow (Figure 9-1) The magnetopause forms the boundary between the magnetosphere, in which the planet's magnetic field is dominant, and the solar wind. The stellar wind incident on the magnetopause is an energy source to the planetary magnetosphere.

All of the solar system's magnetic planets generate electron cyclotron masers within their magnetospheres via a coupling between it and the incident solar wind. The magnetosphere-solar wind interaction produces energetic (keV) electrons that then propagate along magnetic field lines into auroral regions, where an electron cyclotron maser is produced.

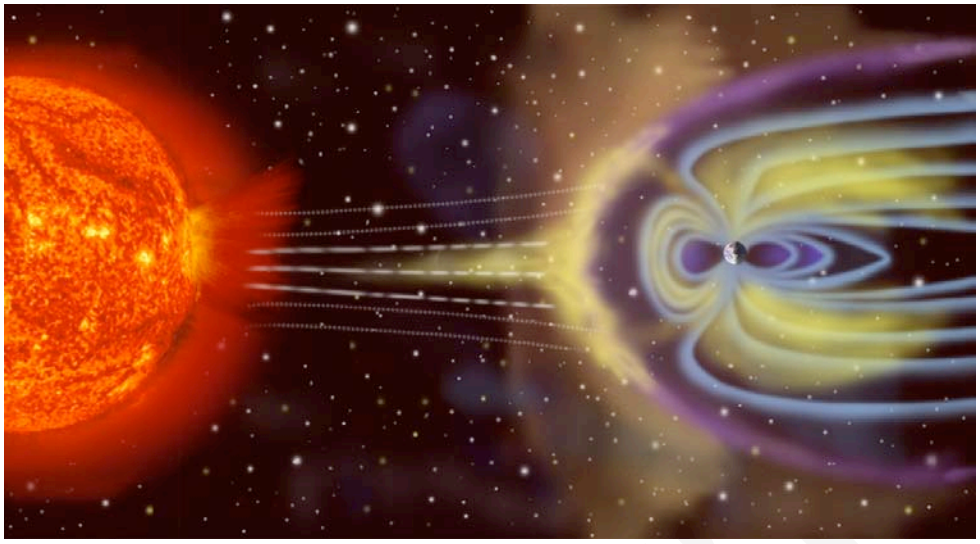

Figure 9-1. An illustration of the Earth's magnetosphere (not to scale). Credit: NASA

Specific details of the electron cyclotron maser emission vary from planet to planet, depending upon such secondary effects as the planet's magnetic field topology. Nonetheless, applicable to all of the magnetic planets is a macroscopic relation relating the incident solar wind power P_{sw}, the planet's magnetic field strength, and the median radio luminosity L_{rad} (Figure 9-2). Various investigators (e.g., Millon & Goertz 1988) find

$$L_{rad} = \varepsilon P_{sw}^{x},$$

with ε the efficiency at which the solar wind power is converted to radio luminosity, and $x \approx 1$. The value for ε depends on whether one considers the magnetic energy or kinetic energy, respectively, carried by the stellar wind. The strong solar wind dependence is reflected in the fact that the luminosity of the Earth is larger than that of either Uranus or Neptune, even though their magnetic fields are 10–50 times stronger than that of the Earth.

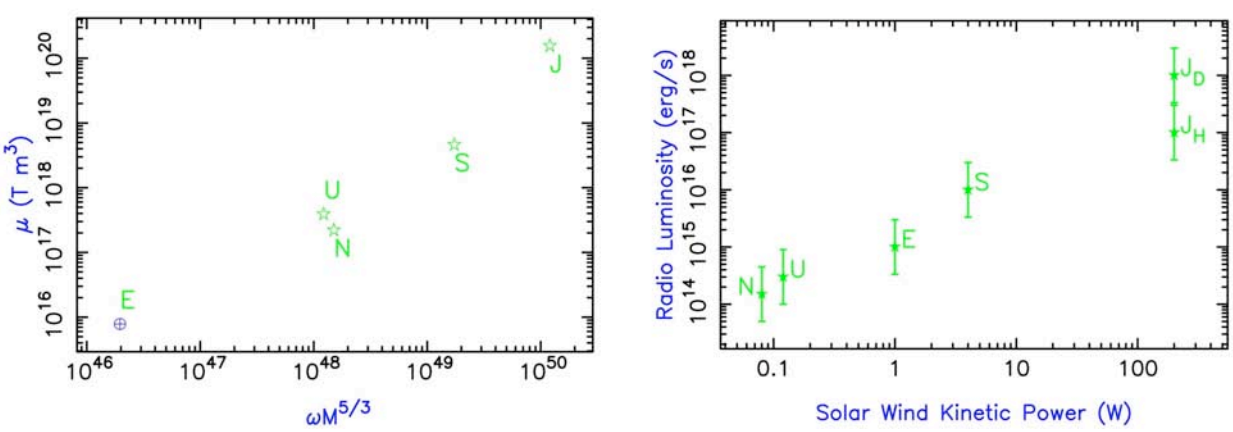

Figure 9-2 (*Left*) Magnetic field strengths of solar system planets as a function of the rotation rate ω and mass M. (*Right*) Radio luminosities of solar system planets as a function of the incident solar wind kinetic power. Even though the magnetic field strength of Earth is less than that of Uranus or Neptune, it is more luminous because it is closer to the Sun and a larger solar wind power is incident. (Adapted from Zarka et al. 2001.)

The incident solar wind power depends upon the ram pressure of the solar wind and the cross-sectional area of the magnetosphere. In general, the magnetopause has a dynamic configuration determined by the instantaneous solar wind flow, and the electron cyclotron maser is an exponential amplifier so that modest changes in solar wind density or velocity or both (e.g., factor of a few) can change planetary magnetospheric emissions by large factors (> 100). However, the average cross-sectional area depends upon the strength of the planet's magnetic field, which can be estimated from various planetary parameters, and on the average stellar wind conditions.

The electron cyclotron maser occurs below a characteristic emission frequency determined by the cyclotron frequency in the magnetic polar region, which in turn depends upon the planet's magnetic moment or magnetic field strength. Using similar scaling laws based on the solar system planets, one can predict this characteristic frequency. For reference, the characteristic frequency of Jupiter is approximately 40 MHz (≈ 7 m wavelength). Above the characteristic frequency, a planet's luminosity drops by several orders of magnitude to levels of incoherent synchrotron emission.

These scaling relations are not only descriptive but also *predictive*. Before *Voyager 2* reached both Uranus and Neptune, their luminosities were predicted (Desch & Kaiser 1984; Desch 1988; Millon & Goertz 1988). For both planets, the predictions were in excellent agreement with the measurements.

Indirect evidence for extrasolar planetary magnetic fields is found in modulations of the Ca II H and K lines of the stars HD 179949 and υ And—modulations in phase with planetary orbital periods (Shkolnik et al. 2005, 2008). Photometric observations by the MOST space telescope of several hot-Jupiter systems, including HD 179949 and τ Boo, also suggest that the giant planet can induce stellar surface activity in the form of active spots (Walker et al. 2008). In addition, while the Ca II lines of τ Boo do not clearly vary with its close-in giant planet, Catala et al. (2007) find an apparently complex magnetic field topology for the star itself, while Donati et al. (2008) report a polarity switch on τ Boo in an unusually shortened stellar activity cycle. Both results are consistent with a possible interaction with the planet's magnetic field.

These solar system scaling laws enable quantitative predictions for an extrasolar planet's radio emission (Zarka et al. 1997; Farrell et al. 1999; Zarka et al. 2001; Lazio et al. 2004; Stevens 2005; Zarka 2006; Griessmeier et al. 2007; Zarka 2007). In the case of a known planet, these estimates depend either upon measured parameters—the planet's mass and orbital semi-major axis—or upon parameters that can be estimated reasonably—for example, the rotation period can be assumed to be of order 10 hr., or for hot Jupiters taken to be orbital period under the assumption that the planet is tidally locked to its host star. Combined with the distance of the star from the Sun, one can predict the planet's average flux density. In the case of stars not yet known to have planetary companions, any radio limits can be inverted to obtain constraints on the presence of planets, especially useful for active stars for which the popular radial velocity method is limited.

Implicit in some of the early predictions for extrasolar planetary radio emission is that the stellar winds of other stars are comparable to the solar wind. As noted above, changes in the stellar wind parameters can produce significant changes in the planet's flux density (Griessmeier et al. 2005, 2007). From measurements of the sizes of astropauses (i.e., the boundary between the stellar wind and the local interstellar medium), Wood et al. (2002, 2005) find the mass loss rate as a function of age, $dM/dt \propto t^x$, with $x \approx -2$. Thus, the stellar wind around a 1 Gyr old star may be 25 times as intense as the solar wind.

Accordingly, planets around young or "adolescent" stars are likely to have stronger cyclotron maser emissions than the planets in our solar system. Young stars are often not observed in radial velocity surveys because the high stellar activity levels (which are in turn related to their stellar wind strengths) make it problematic to isolate a planetary signal. Thus, a blind survey for

magnetospheric emissions presents a search methodology that could mitigate a selection bias in the current extrasolar planet census. If iron-rich "super-Earths" exist, they may also have sufficiently strong magnetic fields to power radio emissions detectable over interstellar distances.

As a specific illustration of the effect of stronger stellar winds, early predictions for the flux density of the planet orbiting τ Boo were of order 1–3 mJy at wavelengths around 10 meters (Farrell et al. 1999; Lazio et al. 2004). More recent estimates, that attempt to take into account the likely stellar wind strength of τ Boo, predict flux densities potentially as high as 300 mJy (Stevens 2005; Griessmeier et al. 2008). The former prediction (1–3 mJy) is below the sensitivity of current instrumentation; the latter is not.

Magnetic Fields and Planetary Characterization

The dynamo currents generating the planetary magnetic field arise from differential rotation, convection, compositional dynamics, or a combination of these in the planet's interior. In any case, for a planetary magnetic field to be sustained, there must be an interior region of the planet that is both conducting and fluid. Consequently, knowledge of the planetary magnetic field places constraints on the thermal state, composition, and dynamics of the planetary interior, all of which will be difficult to determine reliably by other means.

Planetary Interiors: For the solar system planets, the composition of the conducting fluid ranges from liquid iron in the Earth's core to metallic hydrogen in Jupiter and Saturn to perhaps a salty ocean in Uranus and Neptune. The high-frequency cutoff of Jovian emissions (≈ 40 MHz) allowed an estimate for the strength of the Jovian magnetic field 20 yr prior to *in situ* observations. Likewise, radio detection of the magnetic field of an extrasolar planet would provide an indication of the planet's internal composition, insofar as it would require the planet to have a partially conducting interior. Combined with an estimate of the planet's mass, one could infer the composition of the fluid by analogy to the solar system planets.

Planetary rotation: The rotation of a planet can impose a periodic modulation on the radio emission. For all of the gas giant planets in the solar system, this modulation *defines* the rotation periods. As the magnetic field is presumed to be tied to the interior of the planet, it provides a more accurate measure of the planet's rotation rate than atmospheric phenomena such as clouds. For instance, the rotation period of Neptune was determined initially by observations of differentially rotating cloud tops but then was redefined after detection of its radio emission (Lecacheux et al. 1993).

Planetary Satellites: In addition to being modulated by its rotation, Jupiter's radio emission is affected strongly by the presence of its satellite Io, and more weakly by Callisto and Ganyemede. As the Jovian magnetic field sweeps over a moon, a potential is established across the moon by its $\mathbf{v} \times \mathbf{B}$ motion in the strong Jovian magnetic field. This potential drives currents along the magnetic field lines, connecting the moon to the Jovian polar regions, where the currents modulate the radio emission. Modulations of planetary radio emission may thus also reveal the presence of a satellite.

Atmospheric retention: A common and simple means of estimating whether a planet can retain its atmosphere over geological time is to compare the thermal velocity of atmospheric molecules with the planet's escape velocity. If the thermal velocity is a substantial fraction of the escape velocity, the planet will lose its atmosphere. For a planet immersed in a stellar wind, *nonthermal* atmospheric loss mechanisms can be important (Shizgal & Arkos 1996). These are varied (sputtering, mass loading), but all result from the typical stellar wind particle having a *supra-thermal* velocity relative to the planet's atmosphere. If directly exposed to a stellar wind, a planet's atmosphere can erode more quickly than a thermal-only estimate would suggest. Based on the Mars Global Surveyor observations of the remnant Martian magnetic field, this erosion process is

thought to have been important for Mars' atmosphere and oceans (Mitchell et al. 2001; Lundin et al. 2004).

Planetary albedo: Cosmic rays can induce nucleation in water vapor–saturated air and stimulate cloud formation. Larger cosmic ray fluxes can produce more cloud cover and an increased albedo. This effect has already been seen for Galactic cosmic rays (Svensmark 2000), but stellar wind particles may be an important secondary effect.

Habitability: Depending upon its ability to deflect cosmic rays, high-energy charged particles, or stellar wind particles, the magnetic field may influence the habitability of a planet (e.g., Griessmeier et al. 2005). In addition to its effect on the atmosphere, if the cosmic ray flux at the surface of an otherwise habitable planet is too large, it could cause severe cellular damage and disruption of genetic material to any life on its surface or frustrate its origin altogether.

9.1.2 Science Requirements

The exploitation of extrasolar planetary magnetospheric emissions will require sensitive, long-wavelength radio observations.

Table 2 summarizes key requirements on observations aimed at detecting and exploiting extrasolar planetary magnetospheric emissions. In the rest of this section we motivate these requirements.

The characteristic wavelength (frequency) above which magnetospheric emissions are no longer generated is determined by the strength of the planet's magnetic field. For reference, at the cloud tops, the Jovian magnetic field strength is approximately 4 Gauss, leading to a characteristic (cutoff) frequency of approximately 40 MHz (~ 7 m wavelength). A planet's magnetic field strength is likely to be correlated by its mass, as suggested by the "magnetic planets" in the solar system. Allowing for the fact that planets more massive than Jupiter are known, we consider it likely that observations below 100 MHz (longward of 3 m) will be required for extrasolar planetary magnetospheric studies.

Table 2. Scientific Requirements for Extrasolar Planetary Magnetospheric Observations

Parameter	Value	Comment
Wavelength (Frequency)	>~ 3 m (<~ 100 MHz)	Determined by planetary magnetic field; Recent brown dwarf observations suggest shorter wavelengths/higher frequencies possible.
Sensitivity	< 25 mJy	Extrapolations from solar system relations; Constrained by existing radio observations.

The sensitivity requirement is motivated both by extrapolations of magnetospheric emissions from solar system planets as well as current observational limits (§1.3.1). The sensitivity requirement is both somewhat frequency/wavelength dependent as well as influenced by the planet targeted. Broadly, extrapolations from solar system planets suggest that at longer wavelengths, planetary magnetospheric emissions are stronger so that a somewhat less stringent requirement suffices.

Also, because magnetospheric emissions are driven by the stellar wind, planets closer to their host star are likely to be brighter.

9.2 Observatory Concept

Planetary magnetospheric emissions are most likely to be detected with a long-wavelength radio interferometer, a concept with which the radio astronomy community has a long heritage (50+ yr) of experience and for which there are multiple telescopes currently in the design and development or construction phases.

9.2.1 Architecture

The recognition that the Universe could be observed at wavelengths other than those in the visual spectrum began with the discovery of celestial radio emission at a wavelength of 14.6 m (20.5 MHz, Jansky 1935). Given the fundamental limitation of λ/D for angular resolution, the large wavelengths implied single apertures too large to be practical and spurred the development, at 7.9-m wavelength (38 MHz), of aperture synthesis interferometry (Ryle & Vonberg 1946; M. Ryle was awarded a Nobel Prizes in Physics for his efforts toward the development of aperture synthesis). Subsequent work at the relevant wavelengths has been almost exclusively via interferometers, and this is the concept envisioned for all future long-wavelength telescopes.

A high-level description of a radio interferometer is that it consists of the following subsystems:

Antennas/receptors: At the relevant wavelengths, dipole antennas are usually used as individual parabolic antennas are often impractically large. Dipoles have further advantages. Their collecting area scales as λ^2 while the temperature of the Galactic background scales approximately as $\lambda^{2.6}$, so that to first order they provide approximate wavelength-independent sensitivity. Moreover, dipoles are intrinsically low cost, suggesting that a substantial collecting area can be obtained relatively inexpensively. However, the standard thin dipole provides only a relatively narrow frequency response, so various techniques including making the dipoles have a finite width or placing various electronics at the dipole itself are used to help broaden the frequency response. The spectral dynamic range of modern dipoles is at least an octave in frequency and potentially a factor of 3.5:1.

Station: Even with modern computing, the requisite number of dipoles required to produce the required sensitivity (§1.2.2) is often too large to handle individually. Thus, modern radio interferometers group the dipoles into stations. The signals from all of the dipoles in a station are combined together to produce a single output, conceptually equivalent to the output from a single parabolic dish for radio interferometers at shorter wavelengths.

Signal Transmission: Signals from the multiple stations are transmitted to a central processing facility. Modern interferometers implement or plan to implement this transmission over fiber optic links.

Central processing facility/correlator: The unique pairs of stations in an interferometer sample the Fourier transform of the sky brightness distribution. A central processing facility, dominated by a correlator, multiples and integrates the signals from unique pairs of stations, thereby forming the sampled transform (or visibility) function. An alternate approach is to add together, in phase, the signals from the individual stations, effectively forming a single pencil-beam response in the desired pointing direction.

Post-processing: Offline post-processing typically is used to invert the measured visibility function and make an image of a part of the sky defined by the beamwidth of a station, as well as apply various calibration factors.

9.2.2 Performance

The effective performance of a ground-based long-wavelength radio telescope is determined by a combination of two design parameters (its collecting area and angular resolution), the calibration of the telescope, and the identification and excision of radio frequency interference (RFI). Modern long-wavelength radio telescope aim for order-of-magnitude performance improvements by improving angular resolution, calibration, or RFI handling.

The radiometer equation indicates that the theoretical sensitivity of a radio telescope is determined by its collecting area A_{eff}, its system temperature T_{sys}, the observation bandwidth $\Delta\nu$, and integration time Δt. The magnetospheric emission from solar system planets is broadband, with a bandwidth comparable to the emission frequency, and modern radio astronomical systems can or will be able to process bandwidths $\Delta\nu$ that are a large fraction of the observing frequency. At wavelengths longward of 3 meters (< 100 MHz), the nonthermal emission from the Galaxy makes a significant, if not entirely dominant, contribution to the system temperature T_{sys}. Finally, the standard procedure in radio astronomy is to obtain high sensitivity, in part, via long integration times (Δt). However, magnetospheric emission from solar system planets is quite "bursty," so that long integrations are not necessarily useful, as a long integration may average together times when the planet is emitting with times when it is not.

Consequently, for long-wavelength radio telescopes, the only parameter from the radiometer equation available for increasing the sensitivity of the telescope is to increase the collecting area A_{eff}. Also determining the effective sensitivity, however, is the angular resolution, which determines the confusion limit of the telescope. Past generations of long-wavelength radio telescopes have had large collecting areas (as large as $A_{eff} = 10^5$ m^2). These collecting areas have been concentrated in relatively small areas, though, so that the angular resolution was poor and the confusion limit was quite large, well above the value that would be suggested by a straightforward application of the radiometer equation. As an indication of the importance of the angular resolution in determining the sensitivity of long-wavelength radio telescopes, the 4-m wavelength (74-MHz) system on the Very Large Array, with its sub-arcminute angular resolution, has obtained flux densities some 1–2 orders of magnitude lower than those of previous generations of long-wavelength radio telescopes even though the collecting area of the VLA is comparable to or smaller than previous long-wavelength radio telescopes.

Many of the modern long-wavelength radio telescopes under development or in construction couple a significant collecting area with relatively high angular resolution. The goal is to approach or exceed a sensitivity of approximately 1 mJy at wavelengths around 5 m (60 MHz); viz. Table 2.

The primary impediment to angular resolution at long wavelengths was the limited maximum baselines of the available instruments. In all cases, the maximum baselines was no more than about 5 km, which in turn was limited by the phase distortion imposed by the Earth's ionosphere over the intrinsically wide fields of view and the lack of suitable algorithms to compensate for these ionospherically-imposed distortions. On baselines longer than a few kilometers, without a calibration algorithm, phase distortions are severe enough to cause decorrelation, making higher-resolution imaging difficult to impossible. In the past decade, new calibration schemes have been developed for the ionospheric phase corruptions at radio wavelengths, often bearing at least a conceptual similarity to adaptive optics techniques for tropospheric phase corruptions at visible wavelengths.

Modern long-wavelength radio telescopes plan both to exploit these new algorithms as well as develop new algorithms in order to reach the theoretical noise limit implied by the radiometer equation. Indeed, in many cases, extraction and understanding of ionospheric physics from the

radio astronomical data is a key part of the science case for the next-generation of long-wavelength radio telescopes.

The final impact on performance of long-wavelength radio telescopes is radio frequency interference (RFI) produced by civil or military transmitters operating at similar wavelengths. These transmitters are often orders of magnitude stronger than the desired signal from extrasolar planets. In the most moderate case, RFI simply restricts the available bandwidth by limiting the range of available frequencies (and having a concomitant effect on the telescope's sensitivity). In worst cases, RFI can be strong enough to cause non-linear effects in the electronics and render the data useless. (In even more extreme cases, extremely strong RFI can damage the electronics.)

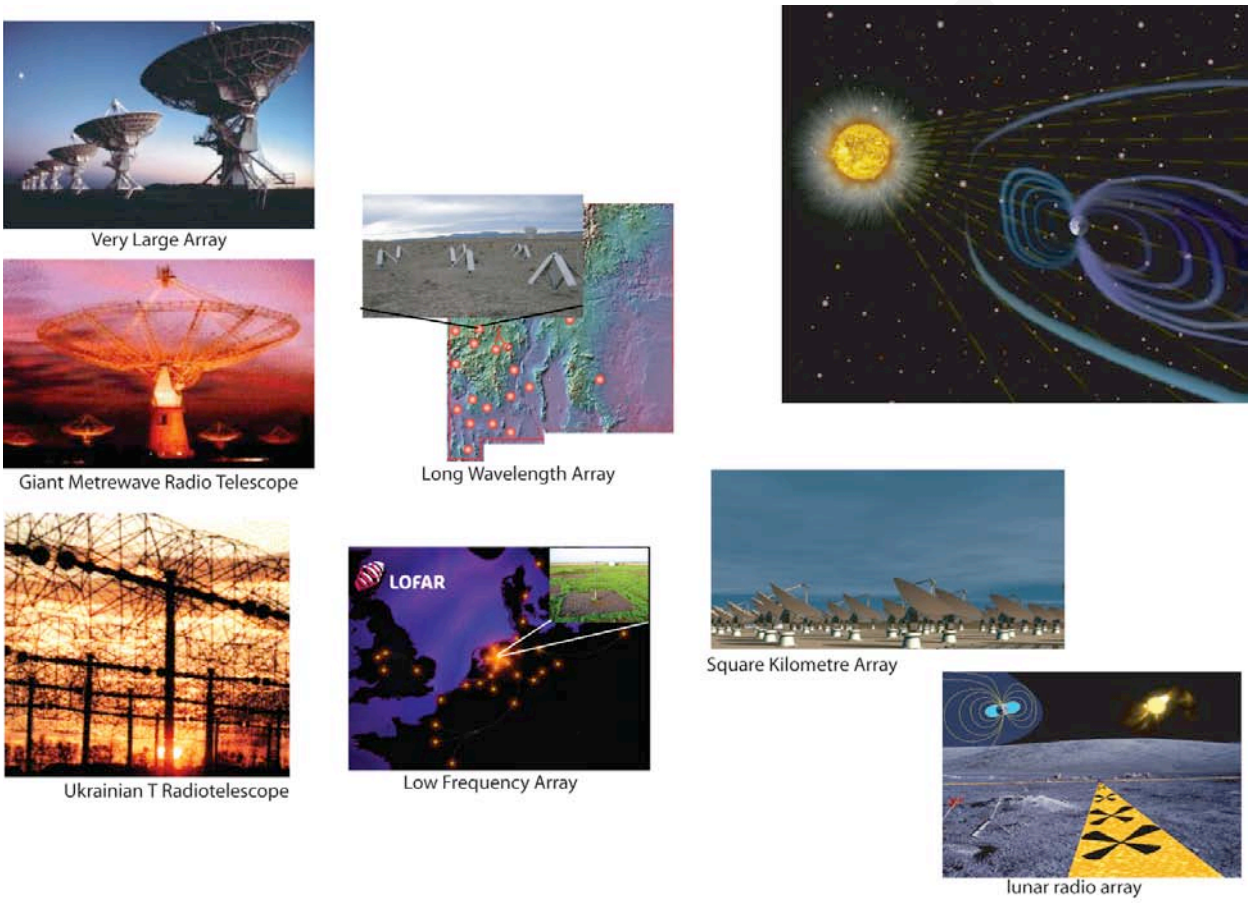

Image credits: JPL; NRAO; NCRA; IRA; UNM/ONR/NRL; ASTRON; SKA; NASA/GSFC

The identification and excision of RFI remains a significant challenge for the next-generation radio telescopes, particularly for their utility for extrasolar planets. RFI that is not properly identified and excised effectively serves as an additional noise source, limiting the sensitivity of the telescope. Moreover, using Jupiter's magnetospheric emission as an exemplar of planetary radio emission, there can be considerable structure in the time-frequency behavior of a planet's emission. Current RFI identification and excision techniques are relatively crude, largely consisting only of blanking the signal either in time or frequency. Further, RFI identification and excision often remains a laborious task, conducted by an individual examining the data. More sophisticated algorithms for

the identification of RFI, e.g., by employing better statistical tests, is among the key development aspects for the next-generation of radio telescopes.

9.3 Technology

A number of long-wavelength radio telescopes are in development or construction. Key technical developments required relate to algorithm and software development (§1.2.2), rather than hardware.

9.3.1 Past Accomplishments

The magnetospheric emissions of the solar system planets motivated searches for analogous emissions prior to the discovery of extrasolar planets (Yantis et al. 1977; Winglee et al. 1986). The two significant changes in the past decade have been the discovery of extrasolar planets and the long-wavelength telescopes with an order of magnitude more sensitivity than historical telescopes. (See also Zarka et al. 1997.)

The scaling relations developed from solar system planets predict that the relevant frequencies are below 1000 MHz (λ > 30 cm). The premier instruments in this range are the Very Large Array (VLA), with its 74 MHz system, and the Giant Metrewave Radio Telescope (GMRT), with its 150 MHz system, and the Ukranian T-shaped Radiotelescope (UTR-2), which observes at 25 MHz. The UTR-2 observes at low enough frequencies that it can detect Jovian emissions, and the 74-MHz VLA observes at a frequency that is within a factor of two of the highest frequency Jovian emissions (40 MHz or 7.5 m wavelength). There have been a handful of searches at all three telescopes, targeting known extrasolar planets, with many of these searches still in progress. Sensitivities achieved range from a few milliJanskys at the GMRT to a few tens or hundreds of milliJanskys at the VLA to a few Janskys at the UTR-2.

Perhaps the most effort has been directed toward the planet orbiting τ Boo (Bastian et al. 2000; Farrell et al. 2003; Lazio & Farrell 2008; see also George & Stevens 2007), as various authors predict that its flux density is comparable to or greater than what can be obtained in a modest duration (few hours) observation (Farrell et al. 1999; Lazio et al. 2004; Stevens 2005; Griessmeier et al. 2008). Lazio & Farrell (2008) have obtained multi-epoch VLA observations, as magnetospheric emissions are expected to be "bursty" and the predicted flux densities are just comparable to the current sensitivity limits. A single observation might occur at an inopportune time when the stellar wind flux was below average. The observational limits now constrain this planet's luminosity to be less than 10^{23} erg s^{-1}, unless its radiation is highly beamed into a solid angle $\Omega << 1$, which would be much smaller than that for any of the solar system planets. Presuming that the radiation is not highly beamed, this luminosity limit is lower than some, but not all, recent predictions. Although higher sensitivity observations are likely required, the non-detection may also be hinting that the magnetic fields, and internal compositions, of extrasolar planets are as varied as the planets themselves.

9.3.2 Future Milestones

Future Ground-based Telescopes

There are a number of long-wavelength telescopes, in various stages of development, which will have sensitivities potentially as much as two orders of magnitude better than current facilities. For some facilities, searching for the radio emission from extrasolar planets is recognized explicitly as part of the science case.

In the initial construction phases are the Long Wavelength Array (LWA, in New Mexico) and the Low Frequency Array (LOFAR, in the Netherlands). The LWA will operate in the 20–80 MHz band (3.75–15 m wavelength); LOFAR will operate in the 30–80 MHz and 110–240 MHz bands (1.25–2.7 m wavelength). Both instruments cover the frequency range expected for emission from Jovian-mass to several Jovian mass planets. Expected initial operational phases for both instruments are the next few years.

The Square Kilometer Array (SKA) is a next-generation telescope that is expected to operate above 100 MHz. Located either in Australia or South Africa, its design goals are such that it should be easily capable of detecting the radio emissions from the most massive extrasolar planets, for those that cutoff frequencies above 100 MHz. The SKA is currently in the design and development phase, with considerable international activity, funded by entities including the NSF, the European Commission, various European governments, the Australian government, and the South African government.

Future Space Facilities

A significant constraint to all ground-based facilities is the Earth's ionosphere. While the value changes with time (e.g., day vs. night), the ionosphere generally is opaque below about 10 MHz ($\lambda >$ 30 m). Jupiter produces the most intense and highest frequency emissions of the solar system planets, but even these cut off above 40 MHz. The Earth's magnetosphere emits auroral kilometric radiation (AKR) below 1 MHz. Thus, the detection of AKR from extrasolar terrestrial-mass planets—and assessments of their habitability—can only be accomplished from space. The most promising location for a telescope designed to detect AKR from extrasolar terrestrial-mass planets is the far side of the Moon. Not only is the far side always shielded from the Earth, for half of the Moon's orbit, an array on the far side would be shielded from solar radio emissions as well.

NASA plans a return to the Moon in the next decade (~ 2019) and is funding concept studies for a lunar radio telescope under both the Lunar Sortie Science Opportunities and Astrophysics Strategic Mission Concept Studies programs. In Europe, ESA, the aerospace company EADS, and various European institutes have been investigating the deployment of a lunar radio array. The key science driver for a large lunar radio telescope is cosmological studies. However, in all cases, extrasolar planetary emission is recognized as an important secondary science goal.

Developments required for a lunar radio array include a number of technologies with broad applicability. These include ultra-low power electronics, high energy density-low mass batteries, autonomous or semi-autonomous robotics (including rovers), and high bandwidth data downlinks. Research and Analysis Goals

The construction of the next-generation radio telescopes offers an opportunity to leverage investments to characterize extrasolar planets.

The radio telescopes under development and construction (the LWA, LOFAR, and the SKA) are being developed by a variety of institutes and funding agencies. Thus, searches for extrasolar planetary radio emission can leverage the investments for little or no marginal cost, and extrasolar planetary radio emission is recognized as a potential science result from many of these telescopes. Exploiting their full potential for extrasolar planetary work will likely require additional algorithm development or observations.

- Key algorithm development includes more sophisticated RFI identification and excision and processing of the time-frequency nature of the radio signals (§1.2.2). In particular, pattern-matching algorithms that could use Jovian radio emission as a template for higher significance detection of extrasolar planetary radio emission are unlikely to be developed by any of these projects.

- Support for coordinated multi-wavelength observations with space missions, such as the European COROT mission. Some preliminary work has already been done with COROT and GMRT observations, which will make further coordination more feasible.
- Continued polarimetric observations of the host stars to detect and characterize additional phenomena related to star-planet interactions (§1.1.1.1). These observations will allow fundamental planetary characteristics to be extracted, particularly when combined with modeling efforts, some of which are underway already (e.g., Lanza et al. 2008; Kitiashvili et al. 2008, Preusse et al. 2006; McIvor et al. 2006).
- Exploitation of the existing ground-based arrays (the VLA, GMRT, and UTR-2, §1.3.1) as testbeds for development of new algorithms as well as improving limits on known extrasolar planets, when possible.
- Development of algorithms that may be deployed in firmware to carry out active adaptive nulling of bright sources in antenna primary beams. The adaptation of such techniques in routine observations are currently prohibitively expensive in terms of computing cycles, but with the advent of FPGA technologies may be feasible for future instruments.

Finally, the development of a future lunar radio array would benefit from a number of technologies with broad applicability. These include ultra-low power electronics, high energy density-low mass batteries, autonomous or semi-autonomous robotics (including rovers), and high bandwidth data downlinks.

9.4 Contributors

J. Lazio, Naval Research Laboratory

D. Winterhalter, Jet Propulsion Laboratory

T. Bastian, National Radio Astronomy Observatory

G. Bryden, Jet Propulsion Laboratory

W. M. Farrell, NASA/GSFC

J.-M. Griessmeier, ASTRON

J. Kasper, Smithsonian Astrophysical Observatory

T. Kuiper, Jet Propulsion Laboratory

A. Lecacheux, Observatoire de Paris

W. Majid, Jet Propulsion Laboratory

R. Osten, STScI

E. Shkolnik, Carnegie Institute of Washington

P. Zarka, Observatoire de Paris

9.5 References

Bastian, T. S., Dulk, G. A., & Leblanc, Y. 2000, ApJ, 545, 1058

Catala, C., Donati, J.-F., Shkolnik, E., Bohlender, D., & Alecian, E. 2007, MNRAS, 374, L42

Donati, J. F., Moutou, C., Farés, R., et al. 2008, MNRAS, 385, 1179

DRAFT

Farrell, W. M., Lazio, T. J. W., Desch, M. D., Bastian, T., & Zarka, P. 2003, in Bioastronomy 2002: Life Among the Stars, eds. R. Norris et al. (ASP: San Francisco) p. 73

Farrell, W. M., Desch, M. D., & Zarka, P. 1999, J. Geophys. Res., 104, 14025

George, S. J., & Stevens, I. R. 2007, MNRAS, 382, 455

Griessmeier, J.-M., Zarka, P., & Spreeuw, H. 2007, A&A, 475, 359

Griessmeier, J.-M., Preusse, S., Khodachenko, M., Motschmann, U., Mann, G., & Rucker, H. O. 2007, Planetary & Space Sci., 55, 618

Grießmeier, J.-M., Motschmann, U., Mann, G., & Rucker, H. O. 2005, A&A, 437, 717

Griessmeier, J.-M., Stadelmann, A., Motschmann, U., et al. 2005, Astrobiology, 5, 587

Jansky, K. G. 1935, Proc. I. R. E., 23, 1158

Kitiashvili, I. N., & Gusev, A, 2008, Celestial Mech. & Dynamical Astron., 100, 121

Lanza, A. F. 2008, arXiv:0805.3010

Lazio, T. J. W., & Farrell, W. M. 2008, ApJ, 668, 1182

Lazio, T. J. W., Farrell, W. M., et al. 2004, ApJ, 612, 511

Lecacheux, A., Zarka, P., Desch, M. D., & Evans, D. R. 1993, Geophys. Res. Lett., 20, 2711

Lundin, R., Barabash, S., Andersson, H., et al. 2004, Science, 305, 1933

McIvor, T., Jardine, M., & Holzwarth, V. 2006, MNRAS, 367, 1

Millon, M. A., & Goertz, C. K. 1988, Geophys. Res. Lett., 15, 111

Mitchell, D. L., Lin, R. P., Mazelle, C., et al. 2001, J. Geophys. Res., 106, 23419

Preusse, S., Kopp, A., Büchner, J., & Motschmann, U. 2006, A&A, 460, 317

Ryle, M., & Vonberg, D. D. 1946, Nature, 158, 339

Shkolnik, E., Walker, G. A. H., Bohlender, D. A., Gu, P.-G., & Kuerster, M. 2005, ApJ, 622, 1075

Shkolnik, E., Bohlender, D. A., Walker, G. A. H., & Collier Cameron, A. 2008, ApJ, 676, 628

Shizgal, B. D., & Arkos, G. G. 1996, Rev. Geophys., 34, 483

Stevens, I. R. 2005, MNRAS, 356, 1053

Svensmark, H. 2000, Space Sci. Rev., 93, 155

Walker, G.A.H., Croll, B., Matthews, J., et al. 2008, A&A, 482, 691

Winglee, R. M., Dulk, G. A., & Bastian, T. S. 1986, ApJ, 309, L59

Wood, B. E., Müller, H.-R., Zank, G. P., Linsky, J. L., & Redfield, S. 2005, ApJ, 628, L143

Wood, B. E., Müller, H.-R., Zank, G. P., & Linsky, J. L. 2002, ApJ, 574, 412

Yantis, W. F., Sullivan, W. T., III, & Erickson, W. C. 1977, Bull. Amer. Astron. Soc., 9, 453

Zarka, P. 2007, Planet. Space Sci., 55, 598

Zarka, P. 2006, in Planetary Radio Emission VI, eds. H. O. Rucker et al. (Austrian Acad.: Vienna) p. 543

Zarka, P., Treumann, R. A., Ryabov, B. P., & Ryabov, V. B. 2001, Astrophys. & Space Sci., 277, 293

DRAFT

Zarka, P., Queinnec, J., Ryabov, B. P., et al. 1997, in Planetary Radio Emission VI, eds. H. O. Rucker et al. (Austrian Acad.: Vienna) p. 101

DRAFT